Carbene ligand and complex design directed towards application in synthesis and homogeneous catalysis

by

ELZET STANDER-GROBLER

Dissertation for the degree

of

DOCTOR in PHILOSOPHY

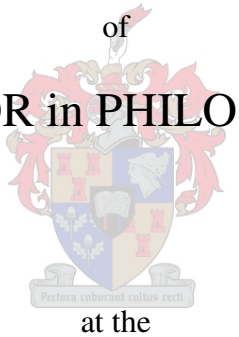

at the

UNIVERSITY of STELLENBOSCH

Department of Chemistry and Polymer Science
Faculty of Natural Sciences

Promotor: Prof. H. G. Raubenheimer
Co-promotor: Dr. S. Cronje

December 2008

DECLARATION

By submitting this dissertation electronically, I declare that the entirety of the work contained therein is my own, original work, that I am the owner of the copyright thereof (unless to the extent explicitly otherwise stated) and that I have not previously in its entirety or in part submitted it for obtaining any qualification.

Date: 28 October 2008

SUMMARY

In general this study describes the preparation and characterisation of new carbene complexes which could be useful as precatalysts in homogeneous catalysis or as synthons in stoichiometric methodology.

Alkylated acetonitrile that forms during the synthesis of the sulfonium salt, $[(Me_3)_2(MeS)S][BF_4]$, is involved in the formation of new α,β-unsaturated Fischer-type carbene complexes from $(CO)_5M{=}C(OMe)CH_2Li$ (M = Cr, W). Metal migration observed when the substitution product obtained from the reaction of the anionic carbene complexes $(CO)_5M{=}C(NMe_2)C{\equiv}C^-$ (M = Cr, W) with Ph_3PAu^+ was left in solution, was also kinetically and theoretically investigated. ^{1}H NMR and quantum mechanical (at the B3LYP level of theory) data indicated a complicated mechanism.

The α,β-unsaturated Fischer-type carbene complex, $(CO)_5Cr{=}C(OMe)CH{=}C(Me)NH(Me)$, obtained from the reaction of $(CO)_5M{=}C(OMe)CH_2^-$ with alkylated acetonitrile, was transformed into the new *remote* one-N, six-membered, carbene ligand (rN^{1}HC^6) complex, $(CO)_5Cr{=}\overline{C(CH{=}C(Me)N(Me)CH{=}C(n\text{Bu})}$. The carbene ligand unprecedentedly preferred the softer $Rh(CO)_2Cl$ moiety to the $Cr(CO)_5$ metal fragment and transferred readily.

A new series of *remote* and *abnormal* square planar compounds $[r/a(NHC)(PPh_3)_2MCl]CF_3SO_3$ (M = Pd or Ni) was prepared by oxidative substitution. The various positions for metal-carbon bond formation on a pyridine ring to furnish various ligand types *i.e.* C2 for nN^{1}HC^6, C3 for aN^{1}HC^6 or C4 for rN^{1}HC^6 received attention. The ligands were arranged in increasing order of carbene character, aNHC < nNHC < rNHC and *trans* influence, nN^{2}HC^5 ~ aN^{1}HC^6 ~ nN^{1}HC^6 < rN^{1}HC^6.

In competitive situations, oxidative substitution occurred selectively at C4 of the pyridine ring rather than at C2 and on the aromatic ring containing the heteroatom (C4), rather than on an annealed aromatic ring (C7). Crystal and molecular structure determinations confirmed the preferred coordination sites. Quantum mechanical calculations (at the RI-BP86/SV level of theory) indicated that the chosen carbene ligand has a much larger influence than the metal on the BDE of the M-$C_{carbene}$ bond; the farther away the N-atom is from the carbene carbon, the stronger the bond.

In complexes that also contain additional external nitrogen atoms, *e.g.* *trans*-chloro(*N*-methyl-1,2,4-trihydro-2-dimethylaminepyrid-4-ylidene)bis(triphenylphosphine)palladium(II) triflate and *trans*-chloro(*N*-methyl-1,2,4-trihydro-2-dimethylaminepyrid-4-ylidene)bis(triphenylphosphine)nickel(II) triflate, stabilisation originates from both the nitrogens. 2-Chloro-1-methyl-1*H*-pyrid-4-

ylidenephenylammonium triflate afforded complexes with both *remote* as well as *normal* nitrogen atoms. New azole complexes of palladium and nickel with remote heteroatoms were also prepared from *N*-methyl-4',4'-dimethyl-2'-thiophen-3-chloro-2-yl-4,5-dihydro-oxazole. Employing the compound 1,5-dichloroanthraquinone, the product of a double oxidative substitution on two Pd centra could be isolated but not alkylated.

The fact that the chemical shift of the metal bonded carbon in the ^{13}C NMR spectrum can not be used as absolute measure of carbene character, was emphasised in a compound where the heteroatom was situated seven bonds away from the carbon donor.

In efforts to synthesise a sulphur-bridged complex that contains carbene ligands, crystals of *trans*-di-iodobis(1,3-dimethyl-imidazoline-2-ylidene)palladium were obtained. Bridged thiolato complexes with N^1HC^6 ligands were unexpectedly found in the attempt to substitute the halogen on chosen square planar carbene complexes of palladium, widening the application possibilities of N^1HC^6 ligands in organometallic chemistry beyond that of catalysis. A trinuclear cluster, $[(PdPPh_3)_3(\mu\text{-}SMe)_3]BF_4$ was isolated as a by-product of these reactions.

A series *normal* and *abnormal* thiazolylidene complexes of nickel and palladium were prepared by oxidative substitution of the respective 2-, 4- and 5-bromothiazolium salts with $M(PPh_3)_4$ (M = Pd or Ni), and unequivocally characterised. In a preliminary catalytic investigation, all the thiazolinium and simple pyridinium derived palladium complexes showed activity in the Suzuki-Miyaura coupling reaction. Little variation in activity in the order *a* (N next to carbon donor) > *n* > *a* (S next to carbon donor) was found for the former series, whereas decreased activity was exhibited in the sequence *r* > *a* > *n* of the latter group. The pyridinium derived complexes showed superior activity to the thiazolinium ones. The *r*NHC complex, *trans*-chloro(*N*-methyl-1,2,4-trihydro-2-dimethylaminepyrid-4-ylidene)bis(triphenylphosphine)palladium(II) triflate, showed similar Suzuki-Miyaura activity to the standard N^2HC^5 carbene complex precatalyst, *trans*-chloro[(1,3-dimethyl-imidazol-2-ylidene)triphenylphosphine]palladium(II) triflate.

OPSOMMING

Hierdie studie behels die sintese en karakterisering van nuwe karbeenkomplekse wat moontlik nuttig kan wees as prekatalisatore in homogene katalise of as sintons in stoichiometriese metodologie.

Ge-alkileerde asetonitriel wat vorm tydens die sintese van die sulfonium sout, $[(Me_3)_2(MeS)S][BF_4]$, is betrokke by die vorming van nuwe α,β-onversadigde Fischer-tipe karbeen komplekse uit $(CO)_5M{=}C(OMe)CH_2Li$ (M = Cr, W). Die metaalmigrasie wat waargeneem word wanneer die substitusieproduk, wat verkry word wanneer die anioniese karbeenkomplekse $(CO)_5M{=}C(NMe_2)C{\equiv}C^-$ (M = Cr, W) met Ph_3PAu^+ reageer, in oplossing gelaat word, is kineties en teoreties ondersoek. ^{1}H-KMR en kwantummeganiese (B3LYP vlak van teorie) data dui op 'n gekompliseerde meganisme.

Die α,β-onversadige Fischer-tipe karbeenkompleks, $(CO)_5Cr{=}C(OMe)CH{=}C(Me)NH(Me)$, wat verkry word vanaf die reaksie van $(CO)_5M{=}C(OMe)CH_2^-$ met ge-alkileerde asetonitriel is omgeskakel na 'n nuwe *verwyderde*, een-N, seslid, heterosikliese karbeenkompleks (*r*N^{1}HC^6), $(CO)_5Cr{=}\overline{C(CH{=}C(Me)N(Me)CH{=}C(n\text{Bu})}$. Die karbeenligand verkies ongekend die sagter $Rh(CO)_2Cl$-eenheid tot die $Cr(CO)_5$-eenheid en dra geredelik oor.

'n Nuwe reeks van v*erwyderde* en *abnormale* vierkantigvlak verbindings $[r/a(NHC)(PPh_3)_2MCl]CF_3SO_3$ (M = Pd or Ni), is berei deur middel van oksidatiewe substitusie. Die verskeie posisies vir metaal-koolstof bindings vorming aan 'n piridienring om verskeie ligandtipes te lewer nl. C2 vir *n*N^{1}HC^6, C3 vir *a*N^{1}HC^6 of C4 vir *r*N^{1}HC^6 het aandag ontvang. Die ligande is volgens toenemende orde van karbeenkarakter gerangskik, *a*NHC < *n*NHC < *r*NHC en volgens toenemende *trans*-invloed, *n*N^{2}HC^5 ~ *a*N^{1}HC^6 ~ *n*N^{1}HC^6 < *r*N^{1}HC^6.

In mededingende omstandighede, vind oksidatiewe substitusie selektief by C4 van die piridienring plaas, eerder as by C2 en aan die aromatiese ring wat die heteroatoom bevat (C4), eerder as aan die aangeslote aromatiese ring (C7). Kristal- en molekulêre struktuurbepalings het die voorkeur koördinasie setels bevestig. Kwantummeganiese berekeninge (B3LYP vlak van teorie) het aangedui dat die gekose karbeenligand 'n groter invloed het op die BDE (binding dissosiasie energie) van die $M\text{-}C_{karbeen}$ binding as die metaal; hoe verder die N-atoom verwyder is van die karbeenkoolstof, hoe sterker is die binding.

In komplekse wat ook addisionele eksterne stikstofatome bevat, bv. *trans*-chloro(*N*-metiel-1,2,4-trihidro-2-dimetielamienpirid-4-ilidene)bis(trifenielfosfien)palladium(II) triflaat en *trans*-chloro(*N*-metiel-1,2,4-trihidro-2-dimetielamienpirid-4-ilidene)bis(trifenielfosfien)nikkel(II) triflaat, kom die stabilisering van beide stikstowwe. 2-Chloro-1-metiel-1*H*-pirid-4-ilidenefenielammonium triflaat lewer komplekse met beide verwyderde asook normale stikstofatome. Nuwe asool-komplekse van palladium en nikkel is vanaf *N*-metiel-4',4'-dimetiel-2'-tiofeen-3-chloro-2-il-4,5-dihidro-oksasool berei. Deur gebruik te maak van die verbinding 1,5-dichloroantrakinoon, is die produk van 'n dubbele oksidatiewe substitusie aan twee Pd kerne, geïsoleer maar nie gealkileer nie.

Die feit dat die chemiese verskuiwing van die metaalgebonde koolstof in die ^{13}C KMR spektrum nie as absolute maatstaf van karbeenkarakter gebruik kan word nie, is beklemtoon in 'n verbinding waar die heteroatoom sewe bindings verwyderd is van die koolstofdonor.

Tydens pogings om swawel-gebrugde komplekse wat karbeenligande bevat te sintetiseer, is kristalle van *trans*-di-iodobis(1,3-dimethyl-imidazoline-2-ylidene)palladium verkry. Gebrugde tiolato-komplekse met N^1HC^6 ligande is onverwags verkry tydens die poging om die halogeen van die piridinium afgeleide karbeenkomplekse van palladium te verplaas en gevolglik is die toepassings moontlikhede van N^1HC^6 ligande in organometalliese chemie verbreed buite die grense van katalise. 'n Trikernige trosverbinding, $[(PdPPh_3)_3(\mu\text{-}SMe)_3]BF_4$ is as byproduk van die reaksies geïsoleer.

'n Reeks *normale* en *abnormale* tiasolilidene komplekse van nikkel en palladium is gesintetiseer deur oksidatiewe substitusie van die onderskeie 2-, 4- en 5-bromotiasolium soute met $M(PPh_3)_4$ (M = Pd of Ni) en eenduidig gekarakteriseer. Tydens 'n inleidende katalitiese ondersoek, het al die tiasolium en eenvoudige piridien afgeleide komplekse van palladium aktiwiteit vertoon in die Suzuki-Miyaura koppelingsreaksie. Min afwisseling in aktiwiteit in die volgorde *a* (N langs koolstofdonor) > *n* > *a* (S langs koolstofdonor) is gevind vir die eersgenoemde reeks, terwyl afnemende aktiwiteit in die volgorde *r* > *a* > *n* vertoon is vir die laasgenoemde groep. Die piridinium afgeleide komplekse het beter aktiwiteit as die tiasolium komplekse getoon. Die *r*NHC kompleks, *trans*-chloro(*N*-metiel-1,2,4-trihidro-2-dimetielamienpirid-4-ilidene)bis(trifenielfosfien)-palladium(II) triflaat, het eenderse Suzuki-Miyaura aktiwiteit getoon as die standaard N^2HC^5 karbeenkompleks prekatalisator, *trans*-chloro[(1,3-dimetiel-imidasool-2-ilidene)trifenielfosfien]-palladium(II) triflaat.

TO MY PARENTS, BROTHER AND HUSBAND JEAN

The greatest gift anyone can receive is to be loved unconditionally

ACKNOWLEGDEMENTS

There are a few people I would like to thank and acknowledge for their great contribution to my study:

Prof Raubenheimer, for being an excellent study leader, being always available and also for being a great mentor.

Dr Stephanie Cronje, thank you for all your support, care, assistance and motivation through my studies. Thanks for being my "chemistry mother".

Elsa Malherbe and Jean McKenzie for your excellent service and friendliness with the NMR spectroscopy. Dr Catherine Esterhuysen for executing computational calculations on some of the complexes. My gratitude to Mr Ward, for being an excellent glass blower and always being friendly and having a little chat. Mr Allen, Tommie and Johnny, without you, things would not be able to run so smoothly.

Stefan Nogai, Oliver Schuster, Liliana Dobrzanska and Christoph Strasser, for not only the X-Ray crystallographic measurements and help with solving some of the tough structures, but also for your wonderful friendship.

Jacorien Coetzee and Anneke Kruger, thank you for your wonderful friendship and all the good times we had. I really missed you guys in Lab 1006 during my last year of study.

Gerrit Julius and William Gabrielli, for being friends and teachers, I'll never forget what you taught me about chemistry and life.

To the rest of my co-workers, Ulrike Horvath, Magda Barwiolek, Adelé le Roux, Leigh-Anne de Jongh, Tesfamarium Kifle Hagos and Julia Even, thank you for making the working environment a great place to do chemistry.

Prof Martin Albrecht for the two months that I spent with him at the Fribourg University, Switzerland. Thank you for going out of your way to make me feel welcome, share a bit of Switzerland with the group and teaching me new techniques.

Arno Neveling, my mentor at Sasol, thank you for your interest in my work and visiting me so regularly to see if I am really coping. Thanks for organising a visit to Sasol R&D to do some research.

Sasol for the student sponsorship and financial support to attend conferences.

My parents and brother, for all your sacrifices, love, support and prayers.

My husband Jean, thank you for being a rock of support during the writing of this thesis, both at home and in the laboratory. Thank you for hours of help with the melting points of my samples. Your unconditional love made the path much smoother.

To my heavenly Father, thank you for all the oppurtunities and grace in my life.

ABBREVIATIONS

n.a.	not applicable
n.o.	not observed
NHC	N-heterocyclic carbene
*r*NHC	remote N-heterocyclic carbene
Å	Ångström (10^{-10} m)
R	alkyl- of aryl-
Me	methyl
Et	ethyl
Bu	buthyl
Ph	phenyl
Ad	adamantyl
LDA	lithium di-isopropylamide
COD	η-cyclooctadiene-1,5
dppe	bis(diphenylphosphino)ethane
rt	room temperature
L	ligand
M	metal
HUMO	highest occupied molecular orbital
LUMO	lowest unoccupied molecular orbital
THF	tetrahydrofuran
tht	tetrahydrothiofene
MS	mass spectrometry
EIMS	electron impact mass spectrometry
ESMS	electron spray ionisation mass spectrometry
FAB	fast atom bombardment mass spectrometry
m/z	mass/charge
M^+	molecular ion
%I	intensity relative to base peak
IR	infra red
m	medium
sh	shoulder
st	strong
w	weak
NMR	nuclear magnetic resonance

TMS	trimethylsilyl
ppm	parts per million
δ	chemical shift in ppm
Δ	difference between two values
ghsqc	gradient heteronuclear single quantum coherence
ghmqc	gradient heteronuclear multiple quantum coherence
s	singlet
d	doublet
t	triplet
x	sextet
m	multiplet
dd	doublet of doublets
J	coupling constant (Hz)
DFT	density functional theory
NBO	natural bond orbital
EDA	energy decomposition analysis

PUBLICATIONS

Parts of this dissertation have been accepted for publication:

E. Stander, S. Cronje and H. G. Raubenheimer, "Preparing α,β-unsaturated Fischer-type carbene complexes *via* an unforeseen route", *Dalton Trans*., 2007, 424.

E. Stander, C. Esterhuysen, J. M. McKenzie, S. Cronje and H. G. Raubenheimer, "Reaction and subsequent transformation of anionic acetylide–carbene complexes using the Ph_3PAu^+ fragment" *Dalton Trans.,* 2007, 5684.

POSTER PRESENTATIONS

Pushing and testing the boundaries of remote N-heterocyclic carbene complex formation, E. Stander, O. B. Schuster and H. G. Raubenheimer

- Cape Organometallic Symposium, Organometallics and their applications, Breakwater Lodge, Cape Town, South Africa, 9 – 11 August 2006
- International Conference on Coordination Chemistry, Cape Town, South Africa, 13-18 August, 2006.
- 15th International Symposium on Homogeneous Catalysis, Sun City, South Africa, 20-25 August 2006.

N-heterocyclic carbene complexes with remote heteroatoms (rNHCs) with possible application in C-C coupling catalysis, A. Krüger, E. Stander, S. Cronje and H. G. Raubenheimer

- Cape Organometallic Symposium, Organometallics and their applications, Breakwater Lodge, Cape Town, South Africa, 9 – 11 August 2006.
- 15th International Symposium on Homogeneous Catalysis, Sun City, South Africa, 20-25 August 2006.

Discriminating between normal, abnormal and remote N^1HC^6 complexes, E. Stander-Grobler, O. B. Schuster, S.Cronje, M. Albrecht and H. G.Raubenheimer

- 16th International Symposium on Homogeneous Catalysis, Florence, Italy, 6-11 July 2008.

Highly variable remote N-heterocyclic carbenes: Pyridylidenes in cross coupling reactions, O. B. Schuster, E. Stander-Grobler, E. Tosh, A. Krüger and H. G. Raubenheimer

- 16th International Symposium on Homogeneous Catalysis, Florence, Italy, 6-11 July 2008.

ORAL PRESENTATIONS

Unexpected products from anionic Fischer-type carbene complexes and the Ph_3PAu^+-moiety, Elzet Stander, S. Cronje and H. G. Raubenheimer, Cape Organometallic Symposium, Organometallics and their applications, Breakwater Lodge, Cape Town, South Africa, 21 October 2005

Chemistry within the 'Ligand design' theme, Elzet Stander and H. G. Raubenheimer
Sasol Research and Development, Sasol, Sasolburg, South Africa, May 2006

Carbene chemistry within the ligand design theme, Elzet Stander, S. Cronje and H. G. Raubenheimer, FIGIPAS Inorganic, Vienna, Austria 4-7 July 2007

TABLE OF CONTENTS

Chapter 3 – Extending the remote heteroatom carbene complex theme 45

Chapter 4 – Complications with S- and O-atoms in the synthesis of heterocyclic carbene complexes 166

1 INTRODUCTION AND AIMS

1.1 Introduction

The discovery of truly new reactions is likely to be limited to the realm of transition-metal organic chemistry, which will almost certainly provide us with additional "miracle reagents" in the years to come"

Dieter Seebach[1]

Despite the fact that organometallic chemistry has made a huge impact on homogeneous catalysis in industrial process technology in the past decades, heterogeneous catalysis still strongly dominates the scene. The success of homogenous catalysis can be largely attributed to the development of a diverse range of tailor made ligand frameworks that have been used to tune the behaviour of a variety of systems. In contrast to this are the disadvantages of low thermal stability and difficulties in catalyst-product separation. The strengths of organometallic catalysts namely particular activity, regio-, chemo- and stereoselectivity result from a simple concept: the catalytic metal is kept in a low-nuclearity while at the same time the metal complexes participate in dissociation equilibria, promoting the reactivity at the metal center by making appropriate coordination sites available.[2]

For a catalyst to successfully enter the industrial scene, the reagent should have a proper ligand outfit allowing it to (re)enter a catalytic cycle. Ligand modification around the active transition metal is therefore of paramount importance.

The recent realization of more active catalyst systems can be attributed to an increased focus on ligand design. Presently it is often the price of a more or less sophisticated ligand that dictates the economics of a new process, whereas the cost of the metals themselves (even rhodium, palladium and platinum!) are of less importance in this respect. Recently, spectacular achievements have been made using cyclic diaminocarbenes, usually called N-heterocyclic carbenes, as ligands for transition-metal-based catalysts. Reactions in which carbene complexes have found application

[1] D. Seebach, *Angew. Chem. Int. Ed. Engl.,* 1990, **29**, 1320.
[2] W. A. Herrmann and B. Cornils, *Angew. Chem. Int. Ed. Engl.,* 1997, **36**, 1048.

include furan synthesis (Ru),[3] olefin methathesis (Ru),[4] hydrosilylation and hydroformylation (Rh),[5] co-polymerisation (Pd)[6] and C-C coupling reactions (Pd, Ni).[7]

The first definition of a carbene[8] was "a bitumen soluble in carbon disulfide, but insoluble in carbon tetrachloride." Till 1956 the word carbene appeared only 15 times in *Chemical Abstracts*.[9] One can say, things became more complicated over the years...

Since Fischer and Maasböl[10] have reported the existence of a transition metal complex possessing a carbene ligand more than four decades ago. At that time these complexes must have appeared as exotic curiosities. The chemistry of the so called Fischer-type complexes (**I**) has since then developed rapidly with extensive studies of their structure and reactivity,[11] their usefulness as a synthetic tool in organic and organometallic chemistry as well as application in catalysis. For example, in olefin metathesis and the cyclopropanation of olefins, both of which are employed in industry, metal carbenes are involved as the reactive intermediates.[12]

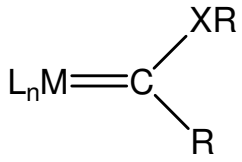

R = alkyl, aryl
X = O, N, S

I

Carbenes are uncharged, reactive compounds containing a divalent carbon atom and two unshared electrons, which can be assigned to two nonbonding orbitals in different ways. For this reason, the chemistry of carbenes, nitrenes and arynes are similar in many respects.[13] If the carbene has a

[3] H. Kücükbay, B. Cetinkaya, G. Salaheddine and P. H. Dixneuf, *Organometallics,* 1996, **15**, 2434.
[4] T. Weskamp, W. C. Schattenmann, M. Spiegler and W. A. Herrmann, *Angew. Chem. Int. Ed. Engl.,* 1998, **37**, 2490; L. Jafarpour, H.-J. Schanz, E. D. Stevens and S. P. Nolan, *Organometallics,* 1999, **18**, 5416.
[5] M. F. Lappert and R. K. Maskell, *J. Organomet. Chem.,* 1984, **264**, 217.
[6] M. G. Gardiner, W. A. Herrmann, C.-P. Reisinger, J. Schwarz and M. Spiegler, *J. Organomet. Chem.,* 1999, **572**, 239.
[7] W. A. Herrmann, M. Elison, J. Fischer, C. Köcher and G. R. Artus, *Angew. Chem. Int. Ed. Engl.,* 1995, **34**, 2371; D. S. McGuinness, M. J. Green, K. J. Cavell, B. W. Skelton and A. H. White, *J. Organomet. Chem.,* 1998, **565**, 165; E. Peris, J. A. Loch, J. Mata and R. H. Crabtree, *Chem. Commun.,* 2001, 201.
[8] *Webster's New International Dictionary*, 2nd Ed., G. & C. Merriman Co., Springfield, Massachusetts, 1952, p.402.
[9] W. von E. Doering and L. H. Knox, *J. Am. Chem. Soc.,* 1956, **78**, 4947.
[10] E. O. Fischer and A. Maasböl, *Angew. Chem. Int. Ed. Engl.,* 1964, **3**, 580.
[11] J. Barluenga, M. A. Fernández-Rodríguez and E. Aguilar, *J. Organomet. Chem.,* 2005, **690**, 539.
[12] Some reviews: K. H. Dötz, H. Fischer, P. Hofmann, F. R. Kreissl, U. Schubert and K. Weiss, *Transition Metal Carbene Complexes,* VCH, Weinheim, 1983; W.D. Wulff in *Comprehensive Organometallic Chemistry II;* E. W. Abel, F. G. A. Stone and G. Wilkonson, Eds., Pergamon Press, Oxford, 1995, vol. 12, p 469; R. Aumann and H. Nienaber, *Adv. Organomet. Chem.,* 1997, **41**, 163; J. Barluenga, A. L. Suárez-Sobrino, M. Tomás, S. García-Granda and R. Santiago-García, *J. Am. Chem. Soc.,* 2001, **123**, 10494.
[13] W. A. Herrmann and C. Köcher, *Angew. Chem. Int. Ed. Engl.* 1997, **36**, 2162.

nonlinear structure with an sp^2-hybridized carbon atom, the structure of a singlet ground state compares to that of a carbenium ion $(CR_3)^+$ and a triplet state to a free radical $^{\bullet}CR_3$.

These versatile organometallic reagents, Fischer-type carbene complexes, have an extensive chemistry. They have been used to for the synthesis of various heterocycles[14] and a number of natural products such as peptides, antibiotics, vitamins, steroids and alkaloids[15] as well as for the preparation of dendritic molecules[16] and helical chiral frameworks.[17] In these instances, readily accessible aryl- or vinylcarbene chromium complexes serve as starting materials for the [3 + 2 + 1]-benzannulation reaction with alkynes, providing an undemanding approach to densely functionalized benzenoids and fused arenes and additionally regioselectively labelled with a $Cr(CO)_3$ fragment.

Fischer-type carbene complexes are probably one of the few families that can undergo cycloadditions of almost any kind, for instance [1 + 2], [2 + 2], [3 + 2], [3 + 3], [4 + 1], [4 + 2], [4 + 3] and [6 + 3] cycloadditions. Even multicomponent cycloadditions such as [1 + 1 + 2], [1 + 2 + 2], [3 + 2 + 1],[18] [3 + 2 + 2],[19] [4 + 2 + 1], or even [4 + 2 + 1 – 2] and [2 + 2 + 1 + 1] to Fischer carbene complexes have been reported.[20]

Fischer-type carbene complexes have been effectively immobilized on polymer-based resins[21] by diphenylphosphine/carbon monoxide ligand exchange or bonding through the heteroatom. An even better strategy was developed by Barluenga *et al.*[22] synthesising isocyanide alkoxycarbene complexes on solid support following the standard Fischer procedure. This method excludes the drawback of decreased activity on the metal-carbene reactivity when a CO is replaced with a phosphine. This method is advantageous in terms of recycling and reusing the stoichiometric amounts of metal reagent which are routinely being discarded after utilization in organic synthesis. The reactivity of group 6 alkoxy- and aminocarbene complexes can be increased by using Pd-catalysts. Transmetallation from Cr or W centra to Pd enhances the reactivity of chromium(0) or

[14] J. Barluenga, J. Santamaría and M. Tomás, *Chem. Rev*., 2004, **104**, 2259.
[15] K. H. Dötz, *Angew. Chem. Int. Ed. Engl.,* 1984, **23**, 587.
[16] L. Quast , M. Nieger and K. H. Dötz, *Organometallics*, 2000, **19**, 2179.
[17] J. F. Schneider, M. Nieger, K. Nättinen and K. H. Dötz, *Synthesis*, 2005, 1109.
[18] K. S. Chan and W. D. Wulff, *J. Am. Chem. Soc.,* 1986, **108**, 5229.
[19] K. Kamikawa, Y. Shimizu, H. Matsuzaka and M. Uemura, *J. Organomet. Chem.,* 2005, **690**, 5922.
[20] H. –G. Schmalz, *Angew. Chem. Int. Ed. Engl.,* 1994, **33**, 303; H. –W. Frühauf, *Chem. Rev.,* 1997, **97**, 523; J. Barluenga, S. Martínez, A. L. Suárez-Sobrino, M. Tomás, *J. Am. Chem. Soc.,* 2001, **123**, 11113; J. Barluenga, M. Tomás, E. Rubio, J. A. López-Pelegrin, S. García-Granda and M. P. Priede, *J. Am. Chem. Soc.,* 1999, **121**, 3065.
[21] S. Maiorana, P. Seneci, T. Rossi, C. Baldoli, M. Ciraco, E. De Magistris, E. Licandro, A. Papagni and S. Provera, *Tetrahedron Lett.,* 1999, **40**, 3635; S. Klapdohr, K. H. Dötz, W. Assenmacher, W. Hoffbauer, N. Husing, M. Nieger, J. Pfeiffer, M. Popall, U. Schubert and G. Trimmel, *Chem. Eur. J.,* 2000, **6**, 3006.
[22] J. Barluenga, A. de Prado, J. Santamaría and M. Tomás, *Organometallics*, 2005, **24**, 3614.

tungsten(0) Fischer carbene complexes in reactions such as dimerisation and CH-insertion.[23] It is also able to promote previously unknown processes by decreasing the ability of the metal center to accept electrons.[24]

The great interest that was awakened in the scientific community over the years since the first discovery of carbenes has shifted to N-heterocyclic carbenes (NHCs). After their first introduction by Öfele[25] and Wanzlick,[26] NHCs (**II**, **III**) have been become universally accepted ligands in organometallic and inorganic coordination chemistries.

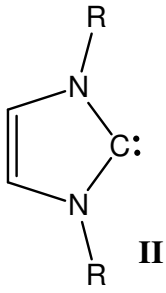

II

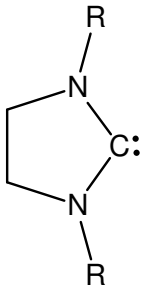

III

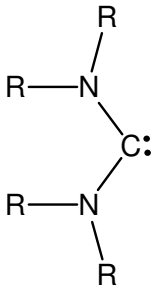

IV

Hundred years after Nef[27] announced that the isolation of methylene would be his next challenge (which he and many others failed to accomplish), Arduengo first isolated the "impossible" free carbenes.[28] Since then, NHCs have attracted increasing attention as ancillary ligands in homogeneous catalysis. In 1996 Alder *et al.* synthesised the first stable acyclic carbene, bis(diisopropylamino)carbene (**IV**).[29] These compounds have been demonstrated to be even stronger σ-donor ligands than their cyclic counterparts.[30] Furthermore they are extremely useful ligands for Pd-catalysed Suzuki-Miyaura, Sonogashira and Heck cross-coupling reactions of aryl/alkenyl bromides and chlorides.[31]

[23] M. A. Sierra, M. J. Mancheño, E. Sáez and J. C. del Amo, *J. Am. Chem. Soc.,* 1998, **120**, 6812; M. A. Sierra, J. C. del Amo, M. J. Mancheño and M. Gómez-Gallego, *J. Am. Chem. Soc.,* 2001, **123**, 851.
[24] M. A. Sierra, J. C. del Amo, M. J. Mancheño, M. Gómez-Gallego and M. Rosario Torres, *Chem. Commun.,* 2002, 1842.
[25] K. J. Öfele, *J. Organomet. Chem.,* 1968, **12**, 42.
[26] H. W. Wanzlick and H. J. Schönherr, *Angew. Chem. Int. Ed. Engl.,* 1968, **7**, 141.
[27] J. V. Nef, *Justus Liebigs Ann. Chem.,* 1895, **287**, 359.
[28] A. J. Arduengo, R. L. Harlow and M. Kline, *J. Am. Chem. Soc.,* 1991, **113**, 361.
[29] R. W. Alder, P. R. Allen, M. Murray and A. G. Orpen, *Angew. Chem. Int. Ed. Engl.,* 1996, **35**, 1121.
[30] K. Denk, P. Sirsch and W. A. Herrmann, *J. Organomet. Chem.,* 2002, **649**, 219.
[31] B. Dhudshia and A. N. Thadani, *Chem. Commun.,* 2006, 668.

The tuning of the NHCs' stereo electronic properties has been achieved by slight modifications of the ring framework, as exemplified by **V**,[32] **VI**[33] and **VII**.[34] Even a sterically hindered free amino-aryl-carbene (**VIII**) has been isolated.[35]

V

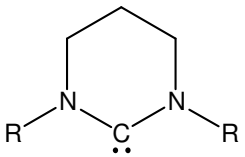

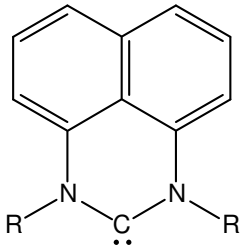

VI

VII

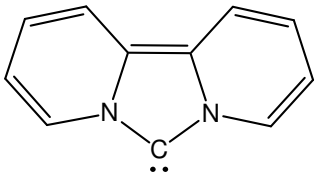

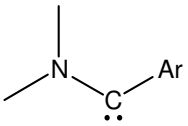

VIII

Since the 4-, 5- and 6-membered ligands have a nearly planar heterocyclic framework which places constraints on the spatial arrangement; a new class of seven-membered NHCs have been targeted and prepared successfully in coordinated form (**XX**).[36] These molecules could possibly undergo a torsional twist to alleviate ring strain. So far it has been impossible to isolate examples of such a free carbene.[37]

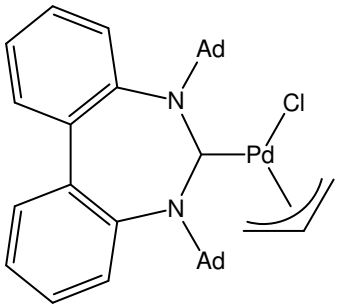

XX

In the light of the wide application of NHCs, many synthetic approaches have been developed to generate these heterocycles. The procedures utilised includes cyclocondensation[38] and cyclization

[32] R. W. Alder, M. E. Blake, C. Bortolotti, S. Bufali, C. P. Butts, E. Linehan, J. M. Olivia, A. G. Orpen and M. J. Quayle, *Chem. Commun.,* 1999, 241.
[33] P. Bazinet, G. P. A. Yap and D. S. Richeson, *J. Am. Chem. Soc.,* 2003, **125**, 13314.
[34] R. Weiss, S. Reichel, M. Handke and F. Hampel, *Angew. Chem. Int. Ed. Engl.,* 1998, **37**, 344.
[35] S. Solé, H. Gornitzka, W. W. Schoeller, D. Bourissou and G. Bertrand, *Science,* 2001, **292**, 1901.
[36] C. C. Scarborough, M. J. W. Grady, I. A. Guzei, B. A. Gandhi, E. E. Bunel and S. S. Stahl, *Angew. Chem. Int. Ed. Engl.,* 2005, **44**, 5269.
[37] C. C. Scarborough, B. V. Popp, I. A. Guzei, B. A. Gandhi and S. S. Stahl, *J. Organomet. Chem.,* 2005, **690**, 6143.
[38] M. R. Grimmett, in *Comprehensive Heterocyclic Chemistry II,* A. R. Katritzky, C. W. Ress and E. F. Schriven, Eds., Pergamon Press, Oxford, 1996.

methods.[39] Imidazoles can be synthesised by a one-step Pd-catalysed coupling of imines and acid chlorides.[40] Many efforts have been made in the design of compounds containing NHC ligands exhibiting different topologies, including bis- and triscarbenes[41] with a wide range of coordination modes like bischelate, pincer[41] and tripodal.[42] Despite the popularity of NHC-derived complexes, relatively few methods have been reported for their preparation. Current methods include the deprotonation[43] or oxidative addition[44] of imidazolium salts, thermolysis of 2-(trichloromethyl)-imidazolidine complexes, [45] bridge-cleaving reactions of binuclear and/or ligand substitution reactions of mononuclear metal compounds with electron-rich olefins,[46] oxidative addition of 2-chloroimidazolium salts, [47] transmetalation of Ag-NHC complexes, [48] sodium reduction of imidazolidin-2-thiones,[49] and the use of *N,N'*-dialkylimidazolium-2-carboxylates as precursors with the concomitant release of CO_2.[50] Recently Grubbs and co-workers[51] have described a simple, base-free method involving the decomposition of 2-(pentafluorophenyl)imidazolidines under mild thermolytic conditions. Carbene complexes with O-, N-, and P-heteroatom functionalized side arms, chiral carbenes, water-soluble and polymer-supported carbenes have also been prepared.[52]

NHCs have been used as ligands for transition-metal-based catalysts[53,54,55] and even as catalysts in their own right.[56,57] The improvement in these catalytic systems have been attributed to the robust nature of late transition metal-NHC bond properties. In contrast, NHC complexes of early transition metals are less developed mainly due to the ease of dissociation of the NHC ligand from the

[39] S. Saman, K. Mitsuru and A. D. Abell, *Org. Lett.,* 2005, **7**, 609; M. T. Bilodeau and A. M. Cunningham, *J. Org. Chem.,* 1998, **63**, 2800.
[40] A. R. Siamaki and B. A. Arndtsen, *J. Am. Chem. Soc.,* 2006, **128**, 6050.
[41] E. Peris and R. H. Crabtree, *Coord. Chem. Rev.,* 2004, **248**, 2239.
[42] E. Mas-Marza, M. Poyatos, M. Sanau and E. Peris, *Inorg. Chem.,* 2004, **43**, 2213.
[43] K. J. Öfele, *J. Organomet. Chem.,* 1968, **12**, 42; D. Méry, J. R. Aranzaes and D. Astruc, *J. Am. Chem. Soc.,* 2006, **128**, 5602.
[44] D. S. McGuinness, K. J. Cavell, B. W. Skelton and A. H. White, *Organometallics*, 1999, **18**, 1596; S. Gründemann, M. Albrecht, A. Kovacevic, J. W. Faller and R. H. Crabtree, *Dalton Trans.,* 2002, 2163.
[45] T. M. Trnka, J. P. Morgan, M. S. Sanford, T. E. Wilhelm, M. Scholl, T.-L. Choi, S. Ding, M. W. Day and R. H. Grubbs, *J. Am. Chem. Soc.,* 2003, **125**, 2546.
[46] M. F. Lappert, *J. Organomet. Chem.,* 1975, **100**, 139.
[47] A. Fürstner, G. Seidel, D. Kremzow and C. W. Lehmann, *Organometallics*, 2003, **22**, 907.
[48] J. C. Garrison and W. J. Youngs, *Chem. Rev.,* 2005, **105**, 3978.
[49] F. E. Hahn, M. Paas, D. le Van and T. Lügger, *Angew. Chem. Int. Ed. Engl.,* 2003, **42**, 5243.
[50] A. M. Voutchkova, L. N. Appelhans, A. R. Chianese and R. H. Crabtree, *J. Am. Chem. Soc.,* 2005, **127**, 17624.
[51] A. P. Blum, T. Ritter and R. H. Grubbs, *Organometallics*, 2007, **26**, 2122.
[52] W. A. Herrmann, C. Köcher, L. Gooßen and G. R. J. Artus, *J. Eur. Chem.,* 1996, **2**, 1627.
[53] W. A. Herrmann, *Angew. Chem. Int. Ed.,* 2002, **41**, 1290.
[54] L. Jafarpour and S. P. Nolan, *Adv. Organomet. Chem.,* 2001, **46**, 181.
[55] T. M. Trnka and R. H. Grubbs, *Acc. Chem. Res.,* 2001, **34**, 18.
[56] D. Enders and T. Balensiefer, *Acc. Chem. Res.,* 2004, **37**, 534.
[57] G. A. Grasa, R. Singh and S. P. Nolan, *Synthesis,* 2004, 971.

electron deficient metal center.[58] Thermally stable zirconium complexes of the tridentate bis(aryloxide)-NHC ligand have recently been prepared by a group in Japan.[59]

NHC ligands are an extreme case of the traditional Fischer-type complexes because the π-donation from the nitrogen lone pairs into the carbon p orbital is so extensive that many free NHCs are stable without metal coordination. In fact, NHCs behave like typical σ-donor ligands that can substitute classical two electron donor ligands such as amides and ethers in metal coordination chemistry. Due to them being strong σ-donors and relatively weak π-acceptors, therefore resembling organophosphines, these ligands have been seen as phosphine replacements.[60] Infrared studies performed by Nolan *et al.*[61] confirmed that NHC-ligands are better σ donors than the most basic tertiary phosphine ligands. They bond more strongly to metal centers than phosphines, thus avoiding the necessity for the use of excess ligand. They considerably increase the electron density at metal centers, and therefore, the most effective catalysts generally combine carbene and phosphine ligands. NHC-based catalysts are also less sensitive to air and moisture, and have proven remarkably resistant to oxidation.[62] In addition to this, these ligands are non-toxic and they exhibit high thermal stability when compared with phophines.[63] NHCs are perceived to be less likely to participate in rearrangements within the metal coordination sphere. However, several recent reports show that NHC-metal bonds are not inert, and NHC ligands are able to take part in various inter- and intramolecular reactions. This includes migration of a methyl group to a coordinated NHC ligand,[64] the reductive elimination of alkylimidazolium salts from NHC alkyl complexes,[65] and substitutions of NHC ligands by trialkylphosphines.[66]

Triazole (**IX**) as well as thiazole (**X**) derived carbenes also fall in the classical NHC group. Enders *et al.* reported the first synthesis of the crystalline triazole-derived carbene by thermal decomposition of the 5-methoxytriazole.[67]

[58] P. L. Arnold, S. A. Mungur, A. J. Blake and C. Wilson, *Angew. Chem. Int. Ed. Engl.,* 2003, **42**, 5981.
[59] D. Zhang, H. Aihara, T. Watanabe, T. Matsuo and H. Kawaguchi, *J. Organomet. Chem.,* 2007, **692**, 234.
[60] W. A. Herrmann, K. Öfele, M. Elison, F. E. Kühn and P. W. Roesky, *J. Organomet. Chem.,* 1994, **480**, C7.
[61] R. Dorta, E. D. Stevens, N. M. Scott, C. Costabile, L. Cavello, C. D. Hoff and S. P. Nolan, *J. Am. Chem. Soc.,* 2005, **127**, 2485; R. Dorta, E. D. Stevens, C. D. Hoff and S. P. Nolan, *J. Am. Chem. Soc.,* 2003, **125**, 10490.
[62] E. Peris and R. H. Crabtree, *Chim.,* 2003, **6**, 33.
[63] T. Weskamp, F. J. Kohl, W. Hieringer, D. Gleich and W. A. Herrmann, *Angew. Chem. Int. Ed.,* 1999, **38**, 2416.
[64] A. A. Danopoulos, N. Tsoureas, J. C. Green and M. B. Hursthouse, *Chem. Commun.,* 2003, 756.
[65] D. S. McGuiness, N. Saendig, B. F. Yates and K. Cavell, *J. Am. Chem. Soc.,* 2001, **123**, 4029.
[66] L. R. Titcomb, S. Caddick, F. G. N. Cloke, D. J. Wilson and D. McKerrecher, *Chem. Commun.,* 2001, 1388.
[67] D. Enders, K. Breuer, J. Raabe, J. Runsink, J. H. Teles, J.-P. Melder and S. Brode, *Angew. Chem. Int. Ed. Engl.,* 1995, **34**, 1021.

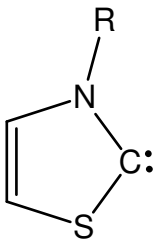

IX

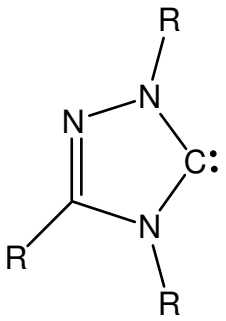

X

Lithiated azoles and imidazoles have also been used in the synthesis of Fischer-carbene complexes and Öfele-Wanzlick-type complexes.[68]

Ionic liquids of N-containing imidazolium salts have created the possibility for the *in situ* generation of metal catalysts by activating the ionic liquid to form metal-carbene species. The formation of a Pd carbene specie in the Mizoroki-Heck (M-H) reaction performed in an ionic liquid has been reported by Xiao and co-workers.[69] Ionic liquids have also been used successfully in *eg.* nickel catalysed olefin dimerisation reactions.[70] McGuinness and Cavell suggested that the decomposition of Pd-carbene complexes through reductive elimination can be limited by using an ionic liquid as solvent in Pd-catalysed reactions. The excess imidazolium ions force the reaction in the opposite direction towards oxidative addition.[71]

For a long time carbenes were considered as prototypical reactive intermediates, their instability being due to their six-valence-electron shell that defies the octet rule.[72] The unusual stability of NHCs results from the ability of nitrogen to act as a π-donor, which decreases the electron deficiency at the adjacent carbene center in the same way stabilisation occurs in Fischer-carbene complexes. This electronic stabilisation produces the strong σ-donor and weak π-acceptor properties that qualitatively explain their efficiency as ligands for transition-metal-based catalysts.

More recently, an interesting ligand candidate to compete and/or compliment NHCs, has been reported, called the P-heterocyclic carbenes (PHCs).[73] They exhibit however an inferior donor ability owing to difficulty in achieving the optimum planar configuration. Recently, a stable PHC (**I**) has been prepared, employing 2,4,6-tri-*tert*-butylphenyl substituents to enforce planarisation of

[68] H. G Raubenheimer and S. Cronje, *J. Organomet. Chem.,* 2001, **617**, 170.
[69] L. Xu, W. Chen and J. Xiao, *Organometallics,* 2000, **19**, 1123.
[70] Y. Chauvin, S. Einloft and H. Olivier, *Ind. Eng. Chem. Res.,* 1995, **34**, 1149.
[71] D. S. McGuiness, N. Saendig, B. F. Yates and K. J. Cavell, *J. Am. Chem. Soc.,* 2001, **123**, 4029.
[72] Eds. M. Jones and R. A. Moss, *Reactive Intermediate Chemistry,* Wiley-Interscience, Hoboken, 2004.
[73] T. Cantat, N. Mezailles, N. Maigrot, L. Ricard and P. Le Floch, *Chem. Commun.,* 2004, 1274.

the phosphorus centers. This PHC also successfully coordinates to Rh(I).[74] Also acyclic P-N, O-N and S-N carbenes (**II**) have been successfully synthesised by substitution reactions at a carbene center.[75]

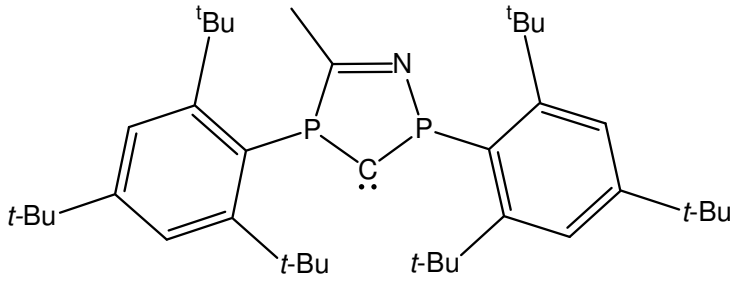

I

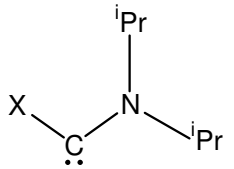

II
X = 2,6-$Me_2C_6H_3$,
2-$^tBuC_6H_4O$,
Ph_2P

Recent results indicate that N-heterocyclic carbenes as ligands in the pre-catalyst complexes[76] lead to increased stability but this advantage is accompanied by loss of activity, especially in olefin polymerization. The problem might be solved by the use of functionalized bidentate or polydentate NHC ligands, which can control the stability and reactivity of active centra more efficiently as has been done in olefin polymerisations. This led to the development of pyridine functionalised bidentate and polydentate NHC ligands as versatile ancillary ligands in catalysis.[77] In recent publications, it has alternatively been proposed that the above mentioned problem could possibly be overcome by introducing a new type of one-N, six-membered carbene ligand, derived form simple pyridine based frameworks and modifications thereof.[78] Pyridinium-derived N-heterocyclic carbene complexes are not only available by oxidative substitution, but also by cyclometalation (**III**).[79]

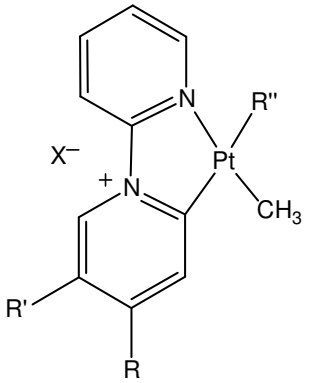

III
R = H, CMe_2, NMe_2
R' = H, NMe_2
R'' = SMe_2, CO
X^- = OTf, BPh_4

[74] D. Martin, A. Baceiredo, H. Gornitzka, W. W. Schoeller and G. Bertrand, *Angew. Chem. Int. Ed.,* 2005, **44**, 1700.
[75] N. Merceron-Saffon, A. Baceiredo, H. Gornitzka and G. Bertrand, *Science,* 2003, **301**, 1223.
[76] W. A. Herrmann, K. Öfele, D. v. Preysing and S. K. Schneider, *J. Organomet. Chem.,* 2003, **687**, 229, and references cited therein; P. W. N. van Leeuwen, *Homogeneous Catalysis – Understanding the Art,* Kluwer Academic Publishers, Dordrecht, 2005.
[77] G. Chelucci, *Chem. Soc. Rev.,* 2006, **35**, 1230.
[78] H. G. Raubenheimer and S. Cronje, *Dalton Trans.,* 2008, 1265.
[79] J. S. Owen, J. A. Labinger and J. E. Bercaw, *J. Am. Chem. Soc.,* 2004, **126**, 8247.

Since these complexes are only stabilised by one mesomeric nitrogen, they should be even better σ-donors than their two-N counterparts (*n*N^{2}HC^5).[80] The halogenated ligand precursor, a pyridinium salt, can oxidatively add to a low-valent metal center of Group 10 to form carbene complexes *via* C-X (X = halogen) activation as was first reported for classical NHC ligands by Stone and co-workers[81] and more recently by Fürstner *et al*.[82] Cavell and co-workers[83] reported the synthesis of the first stable metal carbene hydride complexes of Ni and Pd by "insertion" of the metal center into the C2-H bond of imidazolium salts while being formally oxidised - not yet reported for pyridine derived carbene ligands. For application in catalysis it is worth remembering that metal insertion into an alkyl halide bond (oxidative addition) occurs *via* an S_N2-type mechanism and is enhanced by an electron-rich palladium center.[84] Effective reductive elimination is dependent on the catalyst's steric environment.[85] The easy synthesis of the six-membered carbene ligands based on cheap and commercially available starting materials, make them by far superior when compared to the mixed (NHC)(phosphine) catalysts known thus far.

The classic NHC-ligand bonds through C^2 of the original imidazole ring, but in 2001 Crabtree and co-workers[86] isolated and characterised the first C^5 bound carbene complex, a so-called "abnormal" carbene complex. Theoretical DFT calculations indicated that C^4/C^5-bonding is much less thermodynamically favoured than the C^2-bonded complex,[87] but the C^5-bonded carbene was found to be more stable than its C^2 counterpart. It is now believed that the lower steric hindrance around the metal center is advantageous for C^5-bonding.[88] Infrared studies that have been performed on carbonyl derivatives of C^2- and C^5-bonded NHC complexes, indicate that the latter are significantly stronger electron donors.[89]

The vast majority of group 10 heterocyclic carbene complexes, as well as those of manganese, contain at least one heteroatom situated adjacent (α) to the carbene carbon (normal NHC – *n*NHC). In the Stellenbosch research group we have started to synthesise abnormal NHCs (*a*NHCs) where the heteroatom necessary for stabilisation is situated in a position from where it is not available for

[80] R. Gleiter and R. Hoffmann, *J. Am. Chem. Soc.,* 1968, **90**, 5457.
[81] P. J. Fraser, W. R. Roper and F. G. A. Stone, *J. Chem. Soc., Dalton Trans.,* 1974, **102**; P. J. Fraser, W. R. Roper and F. G. A. Stone, *J. Chem. Soc., Dalton Trans.,* 1974, 760.
[82] A. Fürstner, G. Seidel, D. Kremzow and C. W. Lehmann, *Organometallics,* 2003, **22**, 907.
[83] N. D. Clement, K. J. Cavell, C. Jones and C. J. Elsevier, *Angew. Chem. Int. Ed. Engl.,* 2004, **43**, 1277.
[84] I. D. Hills, M. R. Netherton and G. C. Fu, *Angew. Chem. Int Ed. Engl.,* 2003, **42**, 5749.
[85] N. Hadei, E. A. B. Kantchev, C. J. O'Brien, and M. G. Organ, *Org. Lett.,* 2005, **7**, 1991.
[86] S. Gründemann, A. Kovacevic, M. Albrecht, J. W. Faller and R. H. Crabtree, *Chem. Commun.,* 2001, 2274.
[87] G. Sini, O. Eisenstein and R. H. Crabtree, *Inorg. Chem.,* 2002, **41**, 602.
[88] S. Gründemann, A. Kovacevic, M. Albrecht, J. W. Faller and R. H. Crabtree, *J. Am. Chem. Soc.,* 2002, **124**, 10473.
[89] A. R. Chianese, A. Kovacevic, B. M. Zeglis, J. W. Faller and R. H. Crabtree, *Organometallics,* 2004, **23**, 2461.

the delocalisation of the electron pair onto the metal, **IV**[90] (more on this in Chapters 3 and 5) as well as so-called remote NHCs (*r*N^{1}HCs) where the N is situated outside the coordinated ring system or separated from the coordinated carbon by several bonds, **V**.[91] Au(I) complexes of this latter type have also been prepared.[92] More recently Rouke and co-workers made and utilised a dimeric platinum complex that contains two *r*N^{1}HC^6 ligands.[93,94]

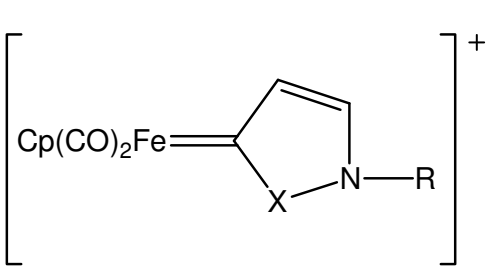

IV

X = S, NPh
R = H, Me

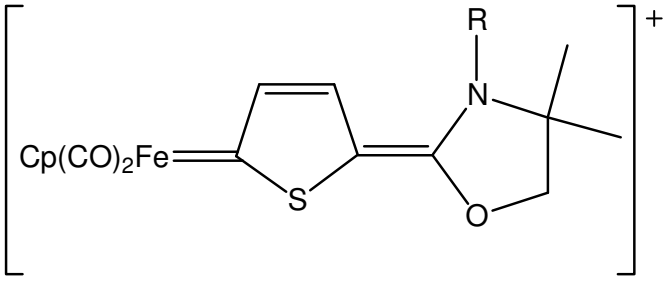

V

The dogma that carbenes are only transient species has disappeared, and synthetic organic chemistry has gained a new and exciting field of research…

1.2 Aims and chapter content

Linking to the theme of research in our Stellenbosch laboratories that is directed towards design of new types of carbene containing transition metal complexes, the main aim of the research described in this dissertation is the preparation and characterisation of new carbene complexes which could be useful as precatalysts in homogeneous catalysis or as synthons in stoichiometric methodology. The particular goals of each investigation are addressed in detail in the various chapters that consider different aspects of the work.

The recent utilisation of anionic Fischer-type carbene complexes as ligands towards a second metal is considered and extended in **Chapter 2**. The introduction of the soft donor atom, sulphur, in the organic side chain as well as the reaction of β-deprotonated carbene complexes with a Au(I) fragment yielded some unexpected initial discoveries.[95] We set out to perform a further, in depth, investigation into the formation of these unanticipated compounds.

---

[90] H. G. Raubenheimer and M. Desmet, *J. Chem. Res. (S),* 1995, 30.
[91] J. G. Toerien, M. Desmet, G. J. Kruger and H. G. Raubenheimer, *J. Organomet. Chem.,* 1994, **479**, C12.
[92] M. Desmet, H. G. Raubenheimer and G. J. Kruger, *Organometallics,* 1997, **16**, 3324.
[93] G. W. V. Cave, A. J. Hallett, W. Errington and J. P. Rourke, *Angew. Chem. Int. Ed. Engl.,* 1998, **37**, 3270.
[94] C. P. Newman, G. J. Clarkson, N. W. Alcock and J. P. Rourke, *Dalton Trans.,* 2006, 3321.
[95] E. Stander, *M. Sc. Thesis,* University of Stellenbosch, April 2005.

The synthesis of a group 6 metal pyridylidene complex from a Fischer-type carbene complex and whether this carbene ligand can be transferred to Rh(I) is investigated in **Chapter 3**. A comparison of pyridine derived complexes, synthesised by oxidative substitution to Pd(0) and Ni(0), in which the coordinated metal is situated in various positions (C2/C6 – *n*NHC; C3/C5 – *a*NHC; C4 - *r*NHC) will be examined spectroscopically and computationally. The use of unusual pyridine derived compounds in the synthesis of new carbene complexes bearing one or two remote nitrogens as well as other functional groups also comes under the spotlight.

The focus of the investigation reported in **Chapter 4** is whether these results can be extended to utilisation of heteroatoms other than nitrogen in the generation of carbene complexes as well as if the halide ligands on selected pyridylidene metal complexes can be functionalised.

The synthesis and characterisation of thiazole derived carbene complexes of Pd and Ni bonded through C^2, C^4 and C^5 of the heterocyclic ring will be attempted in **Chapter 5**. In conclusion, some of the carbene complexes described in this dissertation will be screened as possible pre-catalysts in coupling reactions.

2 REACTIONS OF ANIONIC FISCHER-TYPE CARBENE COMPLEXES AND SUBSEQUENT REARRANGEMENTS

2.1 Introduction and Aims

2.1.1 Background

As mentioned in Chapter 1, the chemistry of metal carbene complexes has provided chemists with exceptionally fertile ground for designing and developing new bond construction for application in organic synthesis. It is well known that the traditional Fischer way of preparing carbene complexes involves the formation of anionic (**VI**) or acyl complexes (**VII**). Fischer carbene complexes are considered similar to esters, in regard to their reactivity [1].

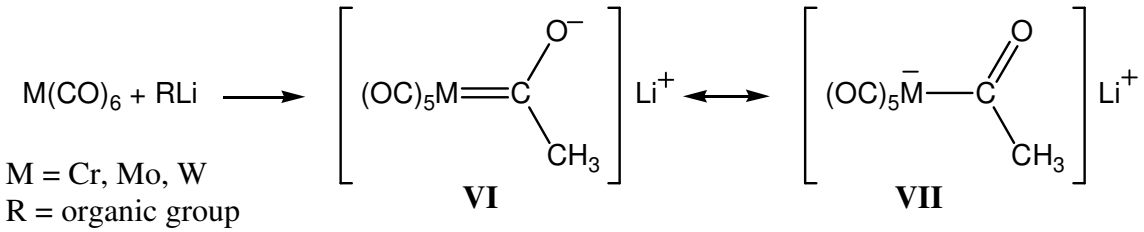

VI **VII**

Scheme 2.1

Recently it has been discovered that complexes obtained by reacting the metal fragment Cp_2ZrCl^+ with the carbene anions are active pre-catalysts for α-olefin oligomerisation and co-polymerisation with ethylene in the presence of a large excess of MAO.[2] Detailed mechanistic studies are complicated by decomposition of the precatalyst, but solid phase analysis suggest that effective ion-pair formation during catalysis occurs, explaining the higher activity these complexes display when compared to $Cp_2Zr(Cl)OMe$ in di-, tri- and tetramerisations of longer chain α-olefins.[3]

---

[1] W. D. Wulff and D. C. Yang, *J. Am. Chem. Soc.,* 1984, **106**, 7565.
[2] R. Brull, A. Kgosane, A. Neveling, H. Pasch, H. G. Raubenheimer, R. Sanderson and U. M. Wahner, *Macromol. Symp.,* 2001, **165**, 11.
[3] N. Luruli, L.-C. Heinz, V. Grumel, R. Bruell, H. Pasch, H. G. Raubenheimer, *Polymer*, 2006, **47**, 56.

Anionic Fischer-type carbene complexes containing a second donor atom with ligating ability towards hard metal centra have been investigated.[4] Some examples are shown in Scheme 2.2. Although Fischer-type carbene complexes as bidentate ligands have not been used in catalytic applications, they pose a possibility to extend the N^O ligand types for use in certain catalytic processes. The first transition metal complexes with anionic Fischer-type carbene complexes as ligands were reported in the early seventies.[5]

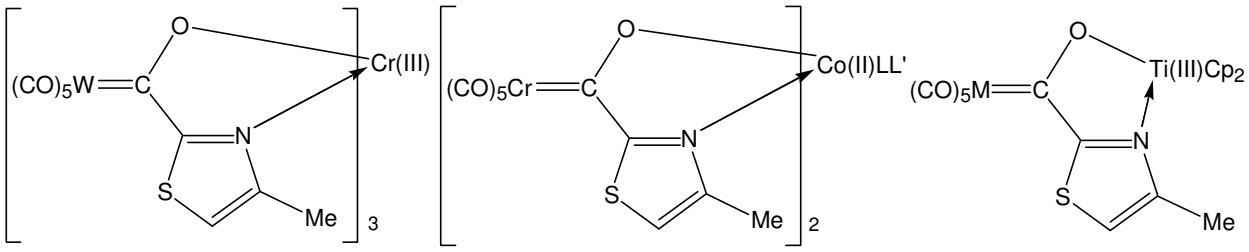

L = THF
L'= 4-methylthiazole

Scheme 2.2

In a neutral Fischer-type carbene complex, the carbon bonded to the metal is the electrophilic centre and the metal pentacarbonyl moiety takes the place of the carbonylic oxygen when compared with an ester. The electron withdrawing nature of the pentacarbonyl group is reflected in the strong acidity of the hydrogens in the position α to the carbenic carbon.[6] Despite the extensive use of Fischer carbene complexes in organic synthesis, reactions in which α-deprotonated carbene complexes (affording 'enolate' anions) participate, are rather more limited.[7] As part of our ongoing studies on new reactions of anionic carbene complexes,[4,8] we recently reported the incorporation of the soft donor atoms, S and P, β to the carbene carbon.[9] In principle such complexes could act as ligands towards soft metals or internally substitute ligands on the parent metal by chelate ring formation. Deprotonation of Fischer-type aminocarbene complexes, $(CO)_5M{=}C[N(CH_3)_2]CH_3$ (M = Cr or W), and subsequent sulfenylation with $[(CH_3)_2(CH_3S)S][BF_4]$, indeed yielded a range of cyclic, acyclic and bridged complexes.[9]

[4] H. G. Raubenheimer, A. du Toit, M. du Toit, J. An, L. van Niekerk, S. Cronje, C. Esterhuysen and A. M. Crouch, *Dalton Trans.,* 2004, 1173.
[5] E. O. Fischer and S. Fontana, *J. Organomet. Chem.,* 1972, **40**, 159; H. G. Raubenheimer and E. O. Fischer, *J. Organomet. Chem.,* 1975, **91**, C23.
[6] C. G. Kreiter, *Angew. Chem.,* 1968, **7**, 390
[7] K. H. Dötz and J. Pheifer, in *Transition Metals for Organic Synthesis,* Ed. M. Beller, C. Bolm, Vol. 1, Wiley-VCH, Weinheim, 1998, p.335.
[8] H. G. Raubenheimer, G. J. Kruger, H. W. Viljoen and S. Lotz, *J. Organomet. Chem*., 1986, **314**, 281.
[9] S. Cronje, G. R. Julius, E. Stander, C. Esterhuysen and H. G. Raubenheimer, *Inorg. Chim. Acta.,* 2005, **358,** 1581.

The same reaction with deprotonated methoxycarbene complexes, $(CO)_5M=C(OCH_3)CH_3$ (M = Cr or W), lead unexpectedly to a very easy route for the preparation of α,β-unsaturated carbene complexes.[10] α,β-Unsaturated carbene complexes with the general formula, $(CO)_5M=C(OCH_2CH_3)CH=C(NR^1R^2)Ph$ (M = Cr or W; R^1 = H, CH_2Ph, Ph, R^2 = alkyl, aryl), have previously been prepared by the Michael addition of an amine, HNR^1R^2, to the alkynyl group of (1-alkynyl)carbene complexes. This addition is highly regio- and stereoselective: secondary alkyl amines yield 4-amino-1-metalla-1,3-dienes with an *E*-configuration at the C=C(N) double bond, while primary aryl amines afford only the *Z*-isomers, since the product is stabilised by an intramolecular hydrogen bond.[11,12,13] Condensation of ethoxy(methyl)carbene complexes with aldehydes, ketones, acid chlorides, acid amides[14] or α,β-unsaturated tertiary acid amides, *e.g.* $PhCH=CHC(=O)NR_2$,[15] also affords similar product types. These complexes contain an NH functional group and can readily be modified by substitution of the hydrogen to have synthetic application. The Dötz reaction of 4-(NH-amino)-1-metalla-1,3-diene carbene complexes, $(CO)_5M=C(OCH_2CH_3)CH=C(NHR^1)R^2$ (R^1, R^2 *e.g.* Ph, CH_3, *i*-Pr), with alkynes, $R^3C\equiv CH$ (R^3 = *n*Bu, Ph or CH_2OCH_3), regioselectively affords 4-1*H*-pyridinylidene complexes, $(CO)_5M=C(CR^3=CH)CH=C(NR^1)R^2$.[16,17] Protonation of the latter with HBF_4 yields pyridinium salts by regioselective substitution of the metal fragment with a proton.[18] Certain reactions of the α,β-unsaturated Fischer-type carbene complexes (group 6 metals) and nucleophiles are similar to those of related organic esters and amides, again confirming the validity of this analogy. In some instances however, the presence of the metal fragment leads to more sophisticated products than expected from standard 1,2- or 1,4-additions of a nucleophile.[19,20] Alkenylcarbene complexes undergo numerous transformations, *e.g.* Diels-Alder reactions,[21] cyclohexadienone annulations,[22] polymerisations[23] and transmetallations.[24]

---

[10] E. Stander, S. Cronje and H. G Raubenheimer, *Dalton Trans.,* 2007, 424.
[11] R. Aumann, K. B. Roths, M. Kössmeier and R. Fröhlich, *J. Organomet. Chem.,* 1998, **556**, 119.
[12] A. de Meijere, *Pure & Appl. Chem.,* 1996, **68**, 61.
[13] R. Polo, J. M. Moretó, U. Schick and S. Ricart, *Organometallics,* 1998, **17**, 2135.
[14] R. Aumann and P. Hinterding, *Chem. Ber.*, 1990, **123**, 2047; R. Aumann and P. Hinterding, *Chem. Ber.*, 1990, **123**, 611.
[15] R. Aumann, X. Fu, D. Vogt, R. Fröhlich and O. Kataeva, *Organometallics,* 2002, **21**, 2736.
[16] K. H. Dötz, *Angew. Chem.,* 1984, **96**, 573.
[17] Y.-T. Wu, B. Flynn, H. Schirmer, F. Funke, S. Müller, T. Labahn, M. Nötzel and A. de Meijere, *Eur. J. Org. Chem.,* 2004, 724.
[18] R. Aumann and P. Hinterding, *Chem. Ber.*, 1992, **125**, 2765.
[19] M. A. Sierra, M. J. Mancheno, J. C. Del Amo, I. Fernandez, M. G. Gallego and M. R. Torres, *Organometallics,* 2003, **22**, 384.
[20] S. Ünaldi, R. Aumann and R. Fröhlich, *Chem. Eur. J.,* 2003, **9**, 3300.
[21] W. D. Wulff and D. C. Yang, *J. Am. Chem. Soc*., 1983, **105**, 6726.
[22] P. C. Tang and W. D. Wulff, *J. Am. Chem. Soc*., 1984, **106**, 1132.
[23] D. W. Macomber, M. H. Hung, M. Liang, A. G. Verma and P. Madhukar, *Macromolecules*, 1998, **21**, 1187.
[24] R. Aumann, H. Heinen, C. Kruger and R. Goddard, *Chem. Ber.*, 1986, **119**, 401.

Deprotonation of the carbene complexes (**1**) and treatment with the sulfonium salt mixture of $[(CH_3)_2(CH_3S)S][BF_4]$ prepared in CH_3CN, have afforded, in a preliminary investigation, after column chromatographic separation, compounds **2** and **3** (Scheme 2.3).[10] The compounds **3** that contain bidentately coordinated carbene-thioether ligands, represent new members of the 4-membered heterometallacyclic ring family that are also α,β-unsaturated relative to the carbene carbon and are related to the thioether complexes obtained from the aminocarbene complexes.[9] All the compounds are stabilised by intramolecular H-bonds thus forming pseudo 6-membered heteroatomic rings (fused to the heterometallacyclic ring in products **3**).

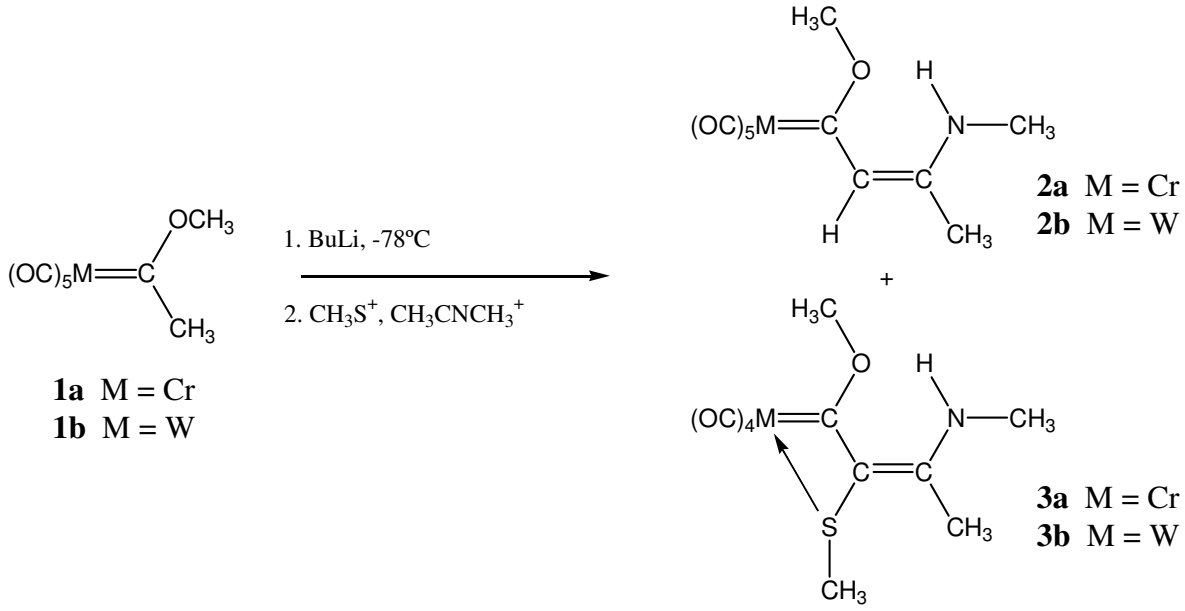

1a M = Cr
1b M = W

Scheme 2.3

In Figure 2.1 the molecular structures of complexes **2b** and **3b** are shown to illustrate the spatial arrangement, H-bonding and carbene-thioether 4-membered chelates.

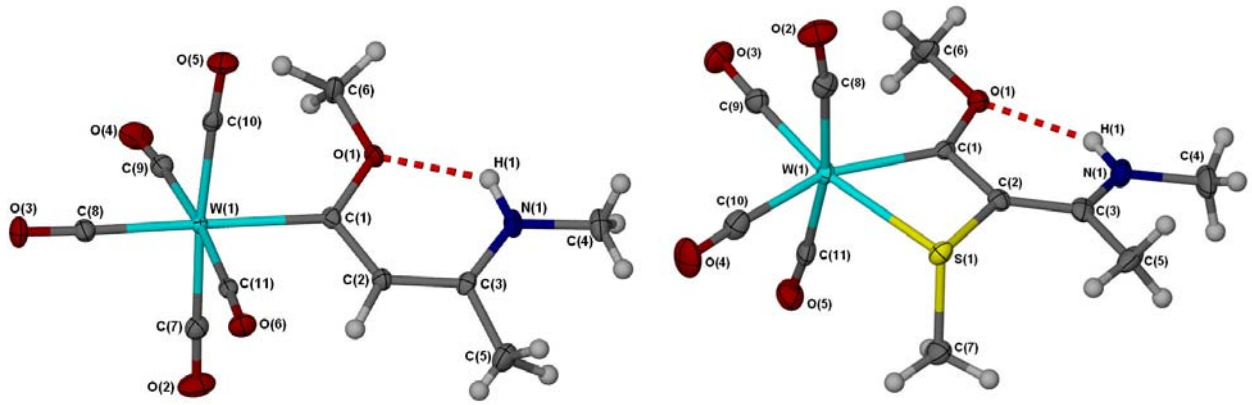

Figure 2.1 Molecular structures of complexes **2b** and **3b**

Synthetic methods relying on gold complexes as catalysts have recently been the focus of intense development and they have been employed in a plethora of organic transformations. Relativistic effects provide a theoretical framework for rationalizing the observed reactivity – the contracted 6*s* orbital and expanded 5*d* orbitals account for the attributes of Au(I) catalysts (the 5*d* electrons remain too low in energy to engage in meaningful backbonding to anti-bonding orbitals but are able to delocalize into lower-energy, empty, non-bonding orbitals).[25] Many of the investigations directed towards the catalytic activity of Au, exploit the propensity of both Au(III) and cationic Au(I) complexes towards activated alkynes regarding nucleophilic addition.[26] R_3PAuX compounds (X = $^-$OTf or weakly coordinating counter ions) have been shown to be superb catalysts for a series of C-C bond-forming reactions, including Conia-ene[27] and hydroarylation[28] as well as several carbon-heteroatom bond formations.[29] Intermediates possessing carbenoid character have recently been postulated in a number of gold-catalysed rearrangements.[30] The activity of Au in catalysis is ascribed to its excellent Lewis acid capability.[25] As for all catalyst systems in homogeneous catalysis, ligand effects can influence the outcome of catalyst reactivity. For example NHC-ligands are optimal for an indene synthesis.[31] Although both phosphines and NHCs exhibit strong σ-donation, and coordination of such ligands results in good stability of Au(I) complexes towards air, moisture and thermolysis, gold has a stronger affinity for NHC ligands than for phosphine and other Fischer acyclic carbenes.[32]

We have recently described[33,34] a number of rearrangements that occur upon treatment of anionic Fischer-type carbene complexes with the metal fragment isolobal to the proton, Ph_3PAu^+. Without exception the gold atom is found attached to the original carbene carbon atom, with the ligand functioning formally as an anionic entity, *e.g.* substituted vinyl, acyl or imodoyl. When starting with N-deprotonated aminocarbene complexes, the expelled $(CO)_5M$ unit is firmly N-coordinated.[35] In particular, the results for the α-deprotonated carbene complexes, $(CO)_5M{=}C(NMe_2)CH_2Li$ (M = Cr or W), which afford bimetallic η^2-coordinated group 6 metal carbonyls, {(dialkylaminovinyl)

[25] D. J. Gorin and F. D. Toste, *Nature,* 2007, **446**, 395.
[26] A. S. K. Hashimi, *Gold Bull.,* 2004, **37**, 51; A. S. K. Hashimi, *Gold Bull.,* 2003, **36**, 3.
[27] J. J. Kennedy-Smith, S. T. Staben and F. D. Toste, *J. Am. Chem. Soc.,* 2004, **126**, 4526.
[28] M. T. Reetz and K. Sommer, *Eur. J. Org. Chem.,* 2003, 3485.
[29] A. Buzas and F. Gagosz, *Org. Lett.,* 2006, **8**, 515.
[30] M. J. Johansson, D. J. Gorin, S. T. Staben and F. D. Toste, *J. Am. Chem. Soc.,* 2005, **127**, 18002.
[31] N. Marion, S. Díez-González, P. de Frémont, A. R. Noble and S. P. Nolan, *Angew. Chem. Int. Ed. Engl.,* 2006, **45**, 3647.
[32] F. Bonati, A. Burini, B. R. Pietroni and B. Bovio, *J. Organomet. Chem.,* 1991, **408** 271.
[33] H. G. Raubenheimer, M. W. Esterhuysen, A. Y. Timoshkin, Y. Chen and G. Frenking, *Organometallics,* 2002, **21**, 3173.
[34] H. G. Raubenheimer, M. W. Esterhuysen, G. Frenking, A. Y. Timoshkin, C. Esterhuysen and U. E. I. Horvath, *Dalton Trans.,* 2006, 4580.
[35] H. G. Raubenheimer, M. W. Esterhuysen and C. Esterhuysen, *Inorg. Chim. Acta,* 2005, **358**, 4217.

$AuPPh_3\}M(CO)_5$, are of interest in this specific chapter (as seen later). Calculations on these conversions have been performed and it comes down to the fact that the group 6 metal unit is prepared to be terminally coordinated, where gold only has a preference for the internal carbon atom.[34] Although the mechanism of this metal fragment substitution reaction is not known, one could assume an electrophilic attack by the cationic gold fragment on the carbanionic carbon atom, located next to the carbene carbon, before metal exchange and further rearrangement occur. To fully explain this mechanism, more work is needed. The potential wealth of unknown organometallic products obtained by employing such rearrangements remains unexplored. Integration of the theoretical and synthetic studies of Au(I) illuminates further avenues for study.

In a somewhat related example preferential C-bonding versus N-bonding has been observed when Ph_3PAuCl is reacted with a C2-bound Mn-NHC complex, as shown in Scheme 2.4.[36] DFT calculations involving deprotonated imidazol have illustrated that preferential C-bonding versus N-bonding depends on the particular metal fragment involved, and that in general *N*-imidazole is the most likely tautomer for first row elements while for second- and third-row elements, *C*-imidazole becomes a viable option.[37]

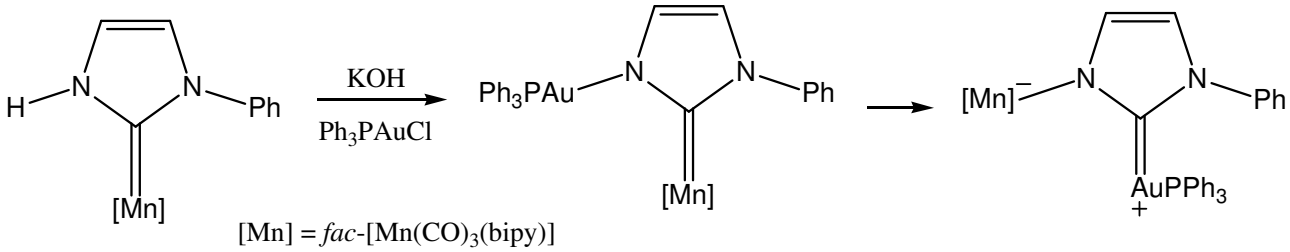

[Mn] = *fac*-[Mn(CO)$_3$(bipy)]

Scheme 2.4

Conversions of N-stabilised amino(ethynyl)carbene complexes, $(CO)_5M^1{=}C(NMe_2)C{\equiv}CH$, into metal complexes of the type $(CO)_5M^1{=}C(NMe_2)C{\equiv}CM^2L_n$ [M^1 = Cr, W; M^2L_n = $Ni(PPh_3)_2Cp$, $Rh(CO)(PPh_3)_2$, $Fe(CO)_2Cp$, *etc.*] have been well studied.[38] In the case where the NMe_2 is replaced by an NH_2 group and then deprotonated and reacted with $Fe(CO)_2CpI$, two binuclear compounds in a ratio of approximately 1:1 are obtained: a C(carbene)-C≡C bridged complex and a C(carbene)-N bridged complex.[39] Such compounds could be important in the context of non-linear optics, electronic bridges in molecular wires and liquid crystallinity.[40,41] Begging an answer, was the

[36] J. Ruiz and B. F. Perandones, *J. Am. Chem. Soc.,* 2007, **129**, 9298.
[37] G. Sini, O. Eisenstein and R. H. Crabtree, *Inorg. Chem.,* 2002, **41**, 602.
[38] C. Hartbaum, G. Roth and H. Fischer, *Chem. Ber.,* 1997, **130**, 479.
[39] H. Fischer, C. Hartbaum, C. Wespel and M. Dede, *Z. Anorg. Allg. Chem.,* 2004, **630**, 1863.
[40] C. Hartbaum, G. Roth and H. Fischer, *Eur. J. Inorg. Chem.,* 1998, 191.

question whether consecutive β-deprotonation and Ph_3PAu^+ addition would then also effect a related group 6 metal substitution reaction? And furthermore, whether both dinuclear species would be isolable?

It has been shown in an MSc investigation, that consecutive treatment of compounds **4**[38] with *n*-BuLi and Ph_3PAuNO_3 in diethylether affords the dinuclear products **5** as orange-red crystals (Scheme 2.5).[42] Spectroscopic characterisation and single crystal structure determinations confirmed that transmetallation affords a gold acetylide product and that no further immediate metal fragment exchange, as when $(CO)_5M{=}C(NMe_2)CH_2^-$ reacts with the Ph_3PAu^+-moiety,[35] takes place.

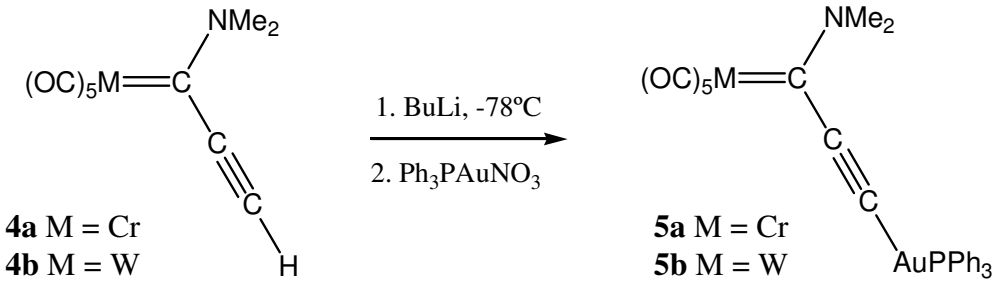

Scheme 2.5

Surprisingly, when left in solution, compounds **5a** and **5b** convert into linkage isomers **6a** and **6b** in which the two metal fragments present in each system has exchanged places. Scheme 2.6 shows a formal exchange between $M(CO)_5$ and Ph_3PAu^+ utilising the most applicable resonance structure of compounds **5**. The final products (although now obtained *via* a stable first intermediate after transmetallation and at a much slower rate) are similar in many respects – at least in terms of the gold coordination sphere – to the complexes obtained when an α-deprotonated carbene complex is treated with Ph_3PAu^+.[33,34,35]

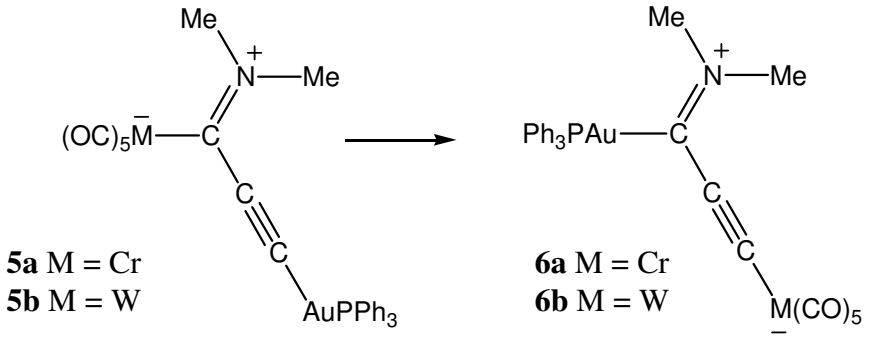

Scheme 2.6

[41] A.-M. Giroud-Godquin and P. M. Maitlis, *Angew. Chem., Int. Ed. Engl.,* 1996, **35**, 969; W. Beck, B. Niemer and M. Wieser, *Angew. Chem. Int. Ed. Engl.,* 1993, **32**, 923.
[42] E. Stander, C. Esterhuysen, J. M. McKenzie, S. Cronje and H. G. Raubenheimer, *Dalton Trans.,* 2007, 5684.

2.1.2 Aims

The work presented in this chapter was inspired by unexpected products obtained from the reaction of deprotonated Fischer-type carbene complexes with electrophiles. In this particular section of the study we aimed at:

1. investigating the mechanistic aspects in the formation of the α,β-unsaturated carbene complexes from α-deprotonated carbene complexes in the presence of acetonitrile;
2. a further, in depth investigation of the unusual reaction of anionic carbene complex $(CO)_5Cr{=}C(NMe_2)C{\equiv}C^-$ with Ph_3PAu^+ and possible isolation of the missing chromium(0) product formed by metal migration of the substitution product;
3. a kinetic investigation, quantum mechanical calculation of the relative energies of the isomers involved and a proposal of a plausible mechanism for this unique transformation.

2.2 Results and discussion

2.2.1 Formation of *α,β*-unsaturated carbene complexes

We proposed the working mechanism in Scheme 2.7 for the formation of the carbene complex. It involves initial nucleophilic attack (Step **A**) by the carbanion on alkylated acetonitrile (formation inevitable during the reaction of acetonitrile with $[(CH_3)_3O][BF_4]$ in the synthesis of the sulfonium salt) then followed by H-migration (imine-enamine tautomerism, Step **B**). The $CH_3CNCH_3^+$ electrophile is equivalent to a carbocationic acetyl group and is expected to react in a similar fashion with other anionic centra.

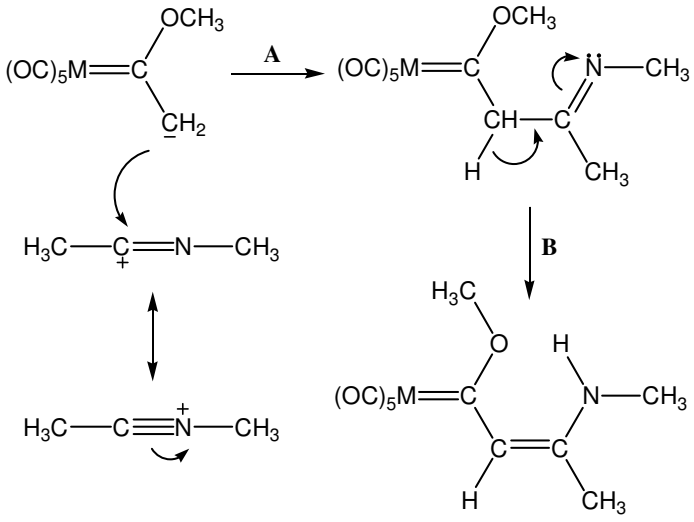

Scheme 2.7

It is well known that nitrilium salts ($[R^1CNR^2]X$) are useful reagents for the synthesis of aromatic ketimines and ketones, benzimidazoles, benzoxazoles, benzothiazoles, quinazolinones and triazolium salts.[43] They also react with phosphorus ylides to form enaminophosphonium salts[44] which are unattainable *via* the methods described earlier. Very few examples of reactions with nitrilium salts within the organometallic field are known. Their reaction with vanadocene to form η^2-iminoacyl complexes,[45] the [2 + 2] cycloaddition with the aminocarbyne complex $Cp^*(CO)_2W{\equiv}CN(CH_2CH_3)_2$ to form an iminocarbene complex[46] and the synthesis of ionic iridium(III) carbene complexes[47] have been reported.

The proposed steps in Scheme 2.7 were confirmed by first alkylating acetonitrile with Meerwein's salt[48] and subsequently reacting the product with an equal mole quantity of deprotonated **1b** to afford complex **2b** in high (70%) yield. An earlier proposal that the deprotonated carbene complex reacts with unmethylated acetonitrile and is then subsequently alkylated[49] to form **2** was flawed by the fact that unmethylated acetonitrile is not a strong enough electrophile to attack the carbanion. We may now extrapolate that complex **3** presumably forms *via* a second deprotonation and sulfenylation, followed by the substitution of one carbonyl group on the group 6 metal by the sulphur atom. Such a second deprotonation and reaction with an electrophile is not uncommon for methoxycarbene complexes.[50,51] We recently reported a similar double deprotonation during a sulfenylation carried out with $[(CH_3)_2(CH_3S)S][BF_4]$ on C-deprotonated aminocarbene complexes.[9] Alternatively, it is possible that a direct attack occurs α to the carbene carbon of **2** or across the α-β double bond to yield a thiiranium-cation which is then deprotonated. The positive charge of this intermediate may contribute to the lability of the departing carbonyl. Non-alkylated acetonitrile is unreactive when reacted with the same deprotonated Fischer-type carbene complexes. To circumvent formation of $[CH_3CNCH_3][BF_4]$, CH_3NO_2 can be used instead of CH_3CN as solvent as described by Smallcombe in the synthesis of the sulfonium salt.[52]

---

[43] B. L. Booth, K. O. Jibodu and M. F. Proença, *J. Chem. Soc., Chem. Commun.,* 1980, 1151; B. L. Booth and M. F. Proença, *J. Chem. Soc., Chem. Commun.,* 1981, 788; B. L. Booth, R. D. Coster, M. Fernanda and J. R. P. Proença, *J. Chem. Soc., Perkin Trans. I,* 1987, 1521

[44] M. I. K. Amer, B. L. Booth and P. Britus, *J. Chem. Soc., Perkin Trans. I,* 1991, 1673.

[45] A. M. Carrier, J. G. Davidson, E. K. Barefield and D. G. Van Derveer, *Organometallics,* 1987, **6**, 454.

[46] A. C. Filippou, B. Lungwitz, C. Völkl and E. Herdtweck, *J. Organomet. Chem.,* 1995, **502**, 131.

[47] B. L. Booth and A. C. Wickens, *J. Organomet. Chem.,* 1993, **445**, 283; M. Barber, B. L. Booth, P. J. Bowers and L. Tetler, *J. Organomet. Chem.,* 1987, **328**, C25.

[48] S. C. Eyley, R. G. Giles and H. Heaney, *Tetrahedron Lett.,* 1985, **26**, 4649.

[49] E. Stander, *M. Sc. Thesis,* University of Stellenbosch, 2005, Chapter 3.

[50] C. P. Casey and R. L. Anderson, *J. Organomet. Chem.,* 1974, **73**, C28.

[51] C. P. Casey and W. R. Brunsvold, *J. Organomet. Chem.,* 1976, **118**, 309.

[52] H. Smallcombe and M. C. Caserio, *J. Am. Chem. Soc.,* 1971, **93**, 5826.

Of note is that the deprotonated aminocarbene complexes, that are stronger bases than the present alkoxycarbene anions, do not form analogues of complexes **2** and **3** although the same acetonitrilium-containing sulfonium salt mixture and experimental procedures were used. Instead, the reaction yielded three different compound classes as mentioned above and all of them only involve sulfenylation.[10] The formation of similar products, with deprotonated methoxycarbene complexes, albeit in very low yields, could also clearly be observed in ^{1}H and ^{13}C NMR spectra, but the yields were insufficient for isolation in pure form. The thioether complexes, $(CO)_5MS(CH_3)_2$, also formed in low yields as in the instance of the aminocarbene complexes.

Since we could not obtain the same α,β-unsaturated complex when starting with the aminocarbene complexes, we attempted to aminolise complex **2**. This reaction was unsuccessful probably due to the stabilising effect of the hydrogen bond between the oxygen and the NHMe. It is however possible to aminolise the complex *2H*-pyran-2-ylidenetungsten (**VIII**) to afford amino-1-tungsta-1,3,5-hexatrienes.[53]

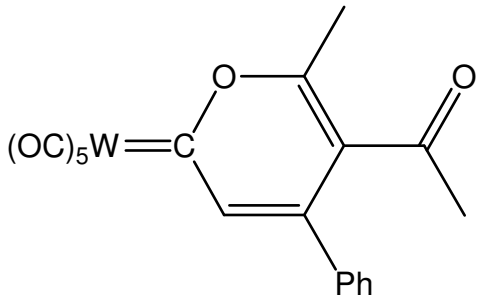

VIII

2.2.2 The mechanism of metal group substitution in dinuclear acetylide carbene complexes

2.2.2.1 Synthesis and characterisation

Since the complete physical characterisation of complexes **5a**, **5b** and **6b** have previously been discussed in detail,[54] only the newly isolated complex **6a** is described here. For comparative purposes, the data of complex **5a** are listed alongside those of complex **6a**.

Despite its relatively slow isomerisation, clean separation of the complex **5a** by column chromatography at low temperatures could not be achieved. This complex was therefore isolated by keeping the reaction mixture cold during the synthesis and crystallisation at low temperature.

[53] R. Aumann, K. Roths, B. Jasper and R. Fröhlich, *Organometallics,* 1996, **15**, 1257.
[54] E. Stander, *M. Sc. Thesis,* University of Stellenbosch, 2005, Chapter 4.

Complex **6a** was now isolated by column chromatography after the solution was kept at room temperature for 24 hours. However, it could not in bulk be obtained in analytically pure form and was always contaminated by small amounts of **5a**. For the discussion of the physical characterisation, the following possible resonance structures for complex **5a** (Scheme 2.8) and **6a** (Scheme 2.9) should be considered.

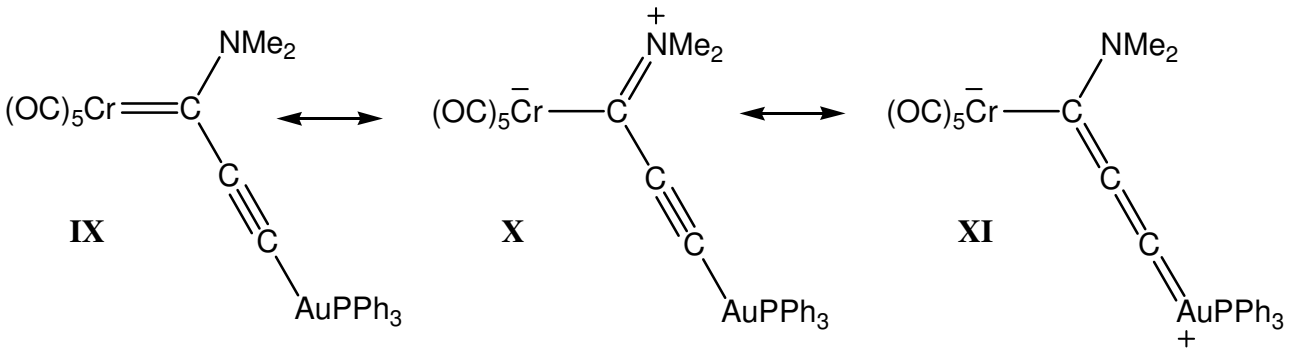

Scheme 2.8

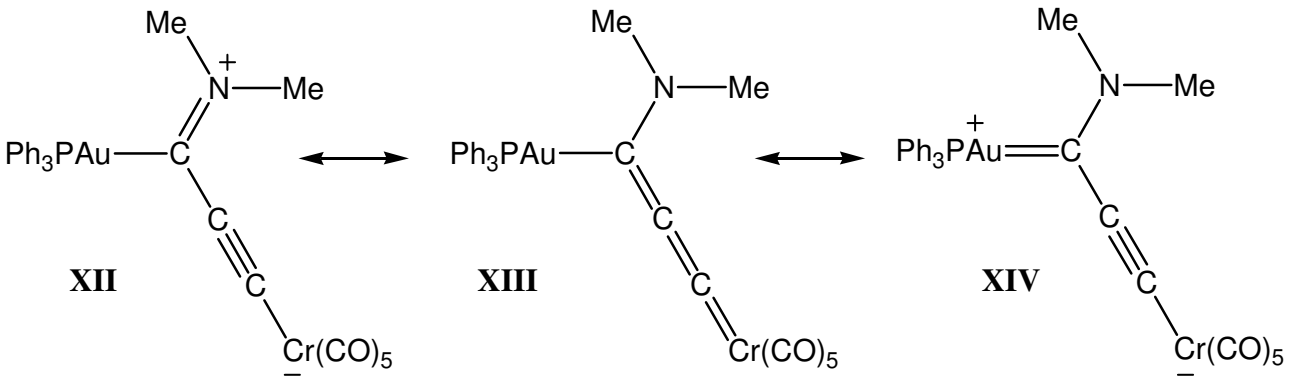

Scheme 2.9

It is clear that the conversion **5a** → **6a** involves an isolobal exchange of $(CO)_5Cr$ for Ph_3PAu^+ (or $(CO)_5Cr^-$ for Ph_3PAu).

NMR spectroscopy

The NMR data for complexes **5a** and **6a** are summarised in Table 2.1. Restricted rotation about the C(carbene)-N bond is apparent from the NMR data for the NMe_2 groups of both complexes indicating important contributions by the canonical structures **X** (Scheme 2.8) for **5a** and **XII** (Scheme 2.9) for **6a**.

Table 2.1 ^{1}H, ^{13}C and ^{31}P NMR data of complexes **5a** and **6a** in CD_2Cl_2

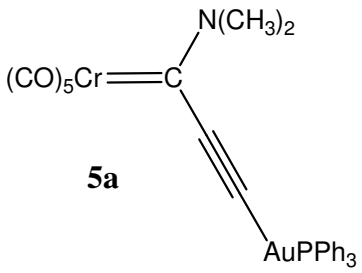

5a

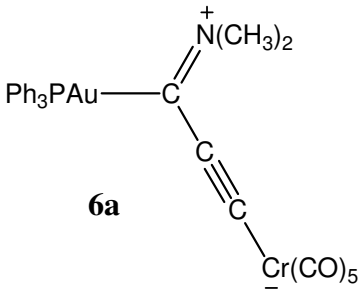

6a

Assignment	δ / ppm*	
	5a	**6a**
^{1}H NMR		
Ph	7.53 (15H, m)	7.54 (15H, m)
NMe	3.77 (3H, s)	3.68 (3H, s)
NMe	3.64 (3H, s)	3.55 (3H, s)
^{13}C NMR		
$C_{carbene}$	248.7 (s)	n.a.
CO_{trans}	225.3 (s)	225.3 (s)
CO_{cis}	218.7 (s)	219.3 (s)
C≡*C*Cr	n.a.	213.4 (s)
AuCN	n.a.	212.4 (s)
C≡*C*Au	181.4 (s)	n.a.
Ph^{ortho}	134.7 (d, $^{2}J_{C-P}$ = 13.9 Hz)	134.6 (d, $^{2}J_{C-P}$ = 13.4 Hz)
Ph^{para}	132.1 (d, $^{4}J_{C-P}$ = 1.9 Hz)	132.2 (d, $^{4}J_{C-P}$ = 1.9 Hz)
Ph^{ipso}	129.8 (d, $^{1}J_{C-P}$ = 53.9 Hz)	129.6 (d, $^{1}J_{C-P}$ = 55.5 Hz)
Ph^{meta}	129.7 (d, $^{3}J_{C-P}$ = 11.1 Hz)	129.7 (d, $^{3}J_{C-P}$ = 11.5 Hz)
C≡CCr	n.a.	125.1 (s)
C≡CAu	106.3 (s)	n.a.
NMe	49.4 (s)	48.9 (s)
NMe	47.2 (s)	43.3 (s)
^{31}P NMR		
PPh_3	42.2 (s)	40.3 (s)

The resonance for the C(carbene) of **5a** appears at somewhat higher field strength (δ 248.7, when compared to that in **4a** with δ 253.3),[42] while the signals for C_α and C_β appear significantly downfield (δ 181.4 and 106.3 in **5a**, when compared to δ 117.3 and 85.3 in **4a**) upon gold(I) complexation. Similar tendencies have been observed for **5b**[42] and also for the complexes $(CO)_5M^1{=}C(NMe_2)C{\equiv}CM^2L_n$,[38] mentioned earlier.

No dramatic changes are observed for compound **6a** compared to **5a** after the exchange in coordination sites of the metal fragments; even the chemical shifts of the amino groups are similar indicating that the C(coordinated)-N partial double bond is retained (**XII** in Scheme 2.9). The most obvious difference between compounds **5** and **6** becomes apparent by comparison of the chemical shifts of metal-bonded carbons in the central ligand backbone. The $Cr(CO)_5$ unit effects a larger downfield chemical shift on its coordinated carbon than Ph_3PAu. The C(carbene) in **5a** resonates at δ 248.7 whereas the gold coordinated carbon in **6a** only has a chemical shift of 212.4 ppm, rather typical of carbene carbons in known gold compounds[55] – compare contributing structure **XIV**, Scheme 2.9.

The signals of the carbonyls for both complexes are also typical for metal pentacarbonyl complexes. The P atom resonates at 42.2 in compound **5a** in the ^{31}P NMR spectrum, whereas in the metal fragment exchanged product **6a**, it appears at δ 40.3. No coupling between the P-atom and alkynyl C-atoms is observed, probably due to the low intensity of the broad resonances.

Similar resonances and tendencies have been observed for the tungsten analogue,[42] reflecting the greater shielding effect that W has on the attached carbon atoms compared to Cr.

Infrared spectroscopy

The number and intensities of CO frequencies (Table 2.2) observed for these complexes are consistent for what is expected from a complex of which the local C_{4v} symmetry has been reduced to either C_s or C_1. The B_1 band is actually Raman active and IR-inactive, but since the complexes do not have true, rigorous C_{4v}, symmetry, it is observed.[56] The lower value of the $A_1^{(1)}$ bands in the IR spectra at *ca.* 1988 cm^{-1} for **6a** compared to 2052.4 cm^{-1} for **5a** can be ascribed to more partial negative charge transferred onto the group 6 metal atom in the former complexes (indicating the importance of **XII** in Scheme 2.9) than in compound **5a** (despite the important contribution of **X**, Scheme 2.8). More electron density is then placed in the π^*-orbital of the carbonyl group (stronger π-basic capacity of the metal), with a concomitant decrease in C-O bond strength and hence the lower frequency. The band for ν(C≡C) is observed at 2312.7 cm^{-1} for **5a** and at 2306.6 cm^{-1} for **6a**, both with medium intensity.

[55] H. G. Raubenheimer, J. G. Toerien, G. J. Kruger, R. Otte, W. van Zyl and P. Olivier, *J. Organomet. Chem.,* 1994, **466**, 291.
[56] F. A. Cotton and C. S. Kraihanzel, *J. Am. Chem. Soc.,* 1962, **84**, 4432.

Tabel 2.2 IR data of complexes **5a** and **6a** in CH_2Cl_2

ν(CO)/cm^{-1}		
5a	**6a**	**Symmetry assignment**
2052.4 (m)	1988.4 (m)	$A_1^{(1)}$
1974.2 (w)	-	B_1
1926.4 (s)	1924.7 (s)	E
1899.4 (sh)	1899.6 (m)	$A_1^{(2)}$

Mass spectrometry

The predicted isotope pattern for the complex with the formula, $C_{28}H_{21}NO_5PAuCr$, compares well with the peaks obtained from the MS-data. A molecular ion peak is observed for both complexes. The fragmentation pattern is typical of Fischer-type carbene(pentacarbonyl)metal complexes where the sequential fragmentation of CO ligands affords the peaks as indicated in Table 2.3. A very strong peak due to the homoleptically rearranged fragment $(Ph_3P)_2Au^+$, is observed for both complexes.

Table 2.3 ES-MS data of complex **5a** and FAB-MS data of complex **6a**

Complex	*m/z*	Relative intensity (%)	Fragment ion
5a	731	17	$[M]^+$
	703	1	$[M-CO]^+$
	675	51	$[M-2CO]^+$
	647	36	$[M-3CO]^+$
	619	100	$[M-4CO]^+$
	591	55	$[M-5CO]^+$
	540	10	$[M-5CO-Cr+H]^+$
	468	4	$[M-PPh_3-H]^+$
6a	731	3	$[M]^+$
	675	2	$[M-2CO]^+$
	647	4	$[M-3CO]^+$
	619	7	$[M-4CO]^+$
	591	8	$[M-5CO-Cr+H]^+$

2.2.2.2 Crystal and molecular structures of complexes 5a and 6a

A new polymorph of the known complex **5a** has been isolated and is compared to previously obtained crystals which had a CH_2Cl_2 solvent molecule included in the unit cell.[42] The crystal and molecular structures of complexes **5a** and **6a** are shown in Figures 2.2 and 2.3 respectively.

Selected bond lengths and angles for the two isomeric complex types are reported in Table 2.4. When crystallisation did not occur overnight, mixtures of **5b** and **6b** were inevitably obtained. Compounds **5a** and **6a** were always obtained as mixtures. Compounds **5a** and **6a** both crystallised as isostructural orange crystals in the space group *P*-1 compared to $P2_1/n$ for the polymorph of **5a** and **5b**[42] with a CH_2Cl_2 molecule present for each complex molecule. Complex **6b** crystallised in the space group $P2_1/c$.

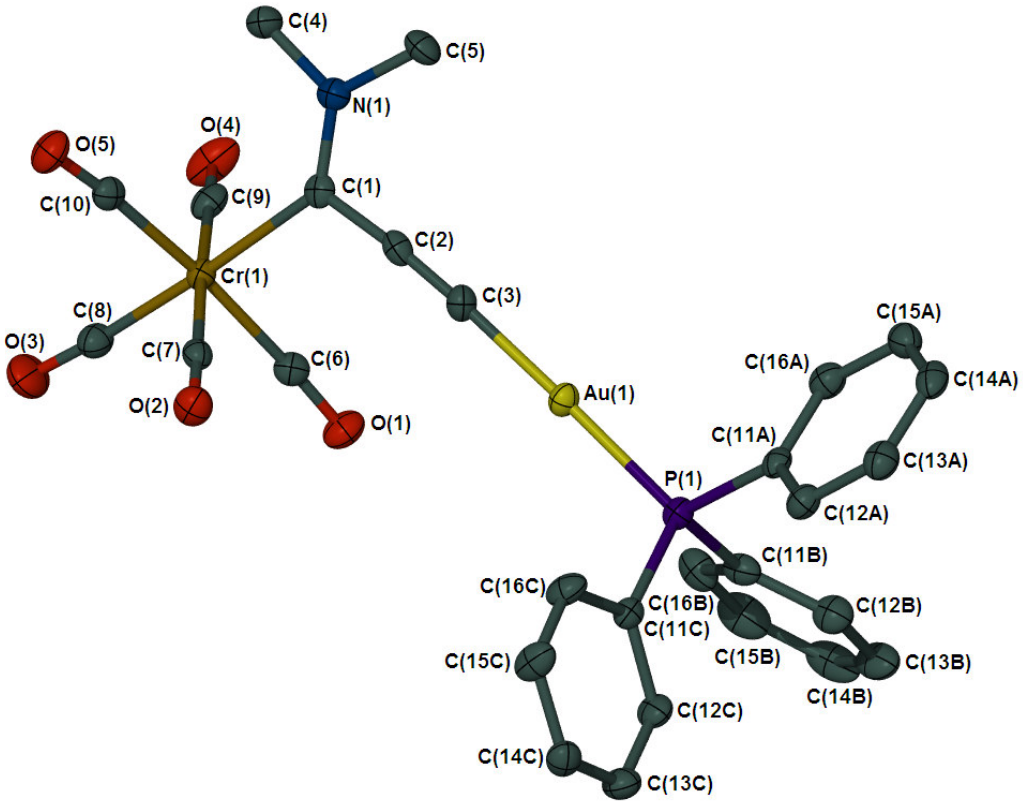

Figure 2.2 Molecular structure of **5a** generated in POV-Ray with ellipsoids at 50% probability showing the numbering scheme; H-atoms are omitted for clarity

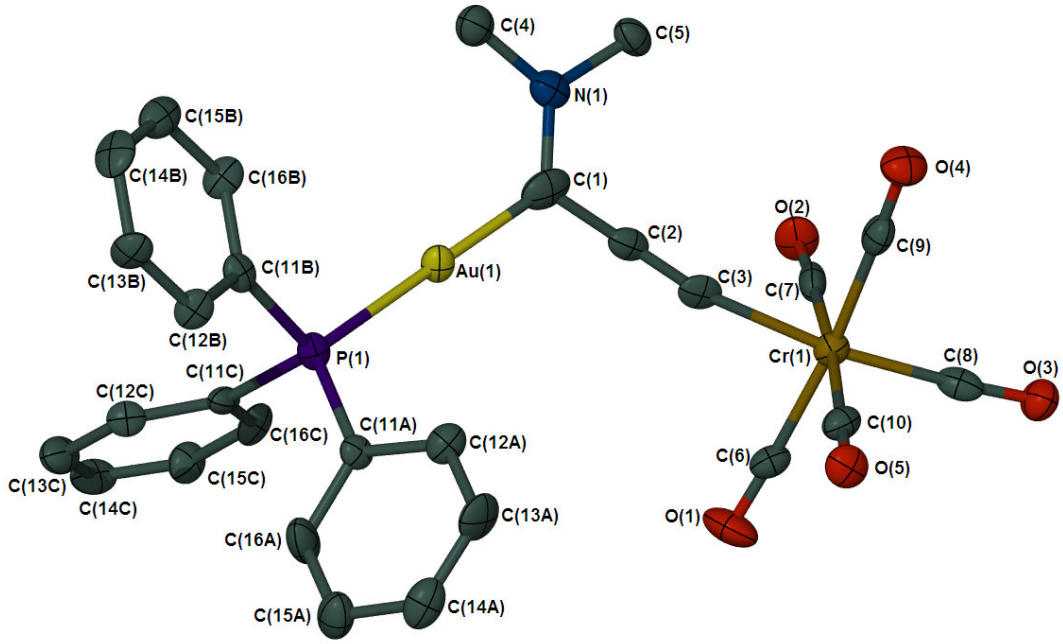

Figure 2. 3 Molecular structure of **6a**, showing the numbering scheme, generated in POV-Ray with ellipsoids at 50% probability; H-atoms are omitted for clarity

Tabel 2.4 Selected bond lengths (Å) and angles (°) for complex **5a**, previously reported polymorph of **5a**[42] and complex **6a**

Bond lengths (Å)	**5a**	Polymorph **5a**	*Bond lengths* (Å)	**6a**
Cr-C(1)	2.121(2)	2.120(2)	Au(1)-C(1)	1.985(17)
Cr-C(8)	1.866(4)	1.870(2)	C(1)-C(2)	1.47(2)
C(1)-C(2)	1.426(5)	1.429(3)	C(2)-C(3)	1.215(19)
C(2)-C(3)	1.209(5)	1.218(3)	C(3)-Cr	2.030(15)
C(3)-Au(1)	1.993(4)	1.990(2)	C(1)-N(1)	1.368(18)
C(1)-N(1)	1.330(5)	1.317(3)	M-C(8)	1.875(16)
Bond angles (°)				
M-C(1)-N(1)	130.6(3)	131.8(2)	Au(1)-C(1)-N(1)	127.1(11)
M-C(1)-C(2)	114.5(3)	113.6(2)	Au-C(1)-C(2)	118.9(10)
C(1)-C(2)-C(3)	174.1(4)	173.6(2)	C(1)-C(2)-C(3)	172.6(14)
C(2)-C(3)-Au(1)	176.9(3)	175.2(2)	C(2)-C(3)-M	170.1(12)
C(3)-Au(1)-P(1)	178.2(1)	179.63(7)	C(1)-Au(1)-P(1)	179.5(4)
C(8)-M-C(1)	176.2(2)	174.05(9)	C(8)-M-C(3)	172.0(6)

The chromium atom resides in a distorted octahedral environment for both **5a** and **6a**. Crystals of both **5a** and **6a** are solvent free and indicate efficient packing of the molecule (Figure 2.4 and Figure 2.5) with no evidence of any aurophilic interactions. It should be noted that the spatial requirement if triphenylphosphine allows room for solvents, as seen for the polymorph of **5a** and in

the tungsten analogue complexes **5b** and **6b**.[42] Comparing the bond lengths of the two polymorphs of **5a**, it is obvious they are very similar. Very small differences are observed in the bond angles, most probably due to crystal packing forces.

The geometry around the Au metal center is linear [C(3)-Au(1)-P(1) is 178.2(1) ° for **5a** and C(3)-Au(1)-P(1) equals 178.2(1) ° for **6a**] and is consistent with the d^{10} configuration of Au(I).[57]

The preference of a staggered or an ecliped arrangement is determined by the substituents on the carbene ligand as well as by the M-C(carbene) bond distance. For both complexes a staggered arrangement is observed.

The ligand structures of **5a** and **6b**, *i.e.* before and after the metal group exchange, are not compared in detail, since a very poor structure of **6a** has been obtained. The ligand structures of **5b** and **6b** remain essentially identical. The most important changes are a lengthening of the formal triple bond by 0.025 Å and a significant decrease in the N(1)-C(1)-M(1) angle when $W(CO)_5$ is replaced by the isolobal Ph_3PAu^+ fragment - leading to a concomitant decrease in the angle N(1)-C(1)-C(2).

The overwhelming contribution of the zwitterionic form **X** to the resonance hybrid in Scheme 2.8 is again reflected in the short C(1)-N(1) bond length of 1.317(3) Å in **5a** compared to a $C(sp^2)$-$N(sp^3)$ single bond distance of 1.416 Å,[16] the bond angles of *ca.* 120º around N(1) and in the relative short C2-C3 bond length [1.209(8) Å] compared to a relatively long C(1)-C(2) separation [1.426(5) Å]. The same can be said for the corresponding bond lengths in the exchanged product **6a** indicating the importance of resonance structure **XII** in Scheme 2.9. The distance of 2.030(15) Å between Cr(1) and C(3) in **6a** is shorter than Cr(1)-C(1) [2.121(2) Å] in **5a** showing that **XIII** in Scheme 2.9 should also be taken into account. On the other hand, the Au(1)-C(3) separation in **5b** is also shorter than the Au(1)-C(1) distance in **6b**[42] indicating that the better overlap between metal orbitals and those of a coordinating carbon with more *s*-character, is responsible for these consistent differences. Unfortunately the standard deviations for **6a** are too large to further support such a statement.

The C(1)-C(2)-C(3)-Au(1)-P(1) chain in **5a** and **6a** is roughly linear with relevant angles varying between 172.6(14)º and 178.2(1)º which is in line with reported values for the known complexes

[57] F. A. Cotton, G. Wilkonson, C. A. Murillo and M. Bochmann, *Advanced Inorganic Chemistry,* 6th ed., Wiley, New York, 1999, pp. 1085-1094.

$(CO)_5M^1{=}C(NMe_2)C{\equiv}CM_2L_n$[38] and the fact that M_2 = Au(I). The slight distortion is probably due to crystal packing forces and it is known that the bending of C(sp) atoms is a low energy process.[58]

Comparably short C(2)-C(3) bond lengths, rather long C(1)-C(2) bonds and significant π-bond character between the amino group and the C(carbene) (shown in the NMR data and the C(1)-N(1) bond length) imply that a strong mesomeric interaction between the two metal centres is absent.

The carbene ligand exerts a weak *trans* influence in **5a** with the Cr(1)-C(8) distance significantly shorter (on average by 0.032 Å) than the other Cr-C bonds. The same holds true for the polymorph of **5a**. This is not observed in the tungsten analogues and the data for **6a** does not allow a final conclusion in this respect.

The molecular packing of complexes **5a** and **6a** are illustrated in Figure 2.4 and 2.5 respectively. Glancing along the c-axis, alternate layers of PPh_3 and $Cr(CO)_5$ groups are stacked diagonally. No short distance interactions are observed between the phenyl rings. In the molecular packing of the polymorph of **5a** however, short distance interactions were observed between the H-atom on the CH_2Cl_2 and two of the carbonyl oxygens.[59]

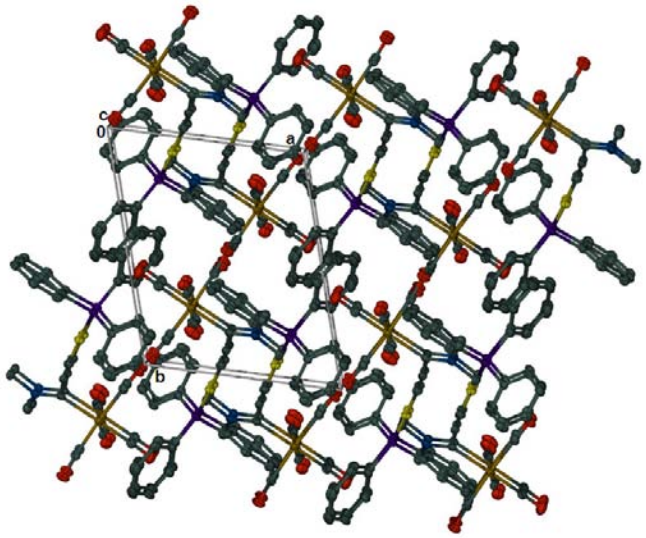

Figure 2.4 Molecular packing of complex **5a** along the c-axis

[58] M. J. Irwin, J. J. Vittal and R. J, Phuddephatt, *Organometallics,* 1997, **16**, 3541.
[59] E. Stander, *M. Sc. Thesis,* University of Stellenbosch, 2005, Chapter 4, p. 137.

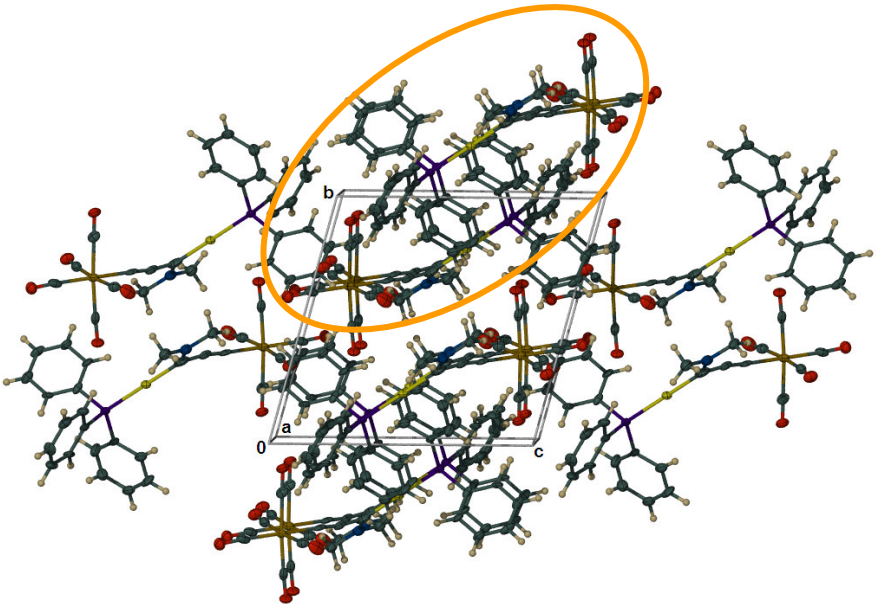

Figure 2.5 Molecular packing of complex **6a** along the c-axis

A view along the a-axis of complex **6a** (Figure 2.5) demonstrates that the molecules pack in units consisting of two columns that are symmetry related through inversion (indicated by orange in Figure 2.5). As for complex **5a**, no short distance interactions are observed.

2.2.2.3 Quantum mechanical calculations

In order to determine which complex is the more stable isomer, DFT calculations were performed on model complexes **5aM**, **5bM**, **6aM** and **6bM**, where triphenylphosphine groups were replaced by PH_3 ligands and the $N(CH_3)_2$ groups replaced by NH_2. The calculated structures, shown in Figure 2.6 and 2.7, agree well with the experimental molecular structures.

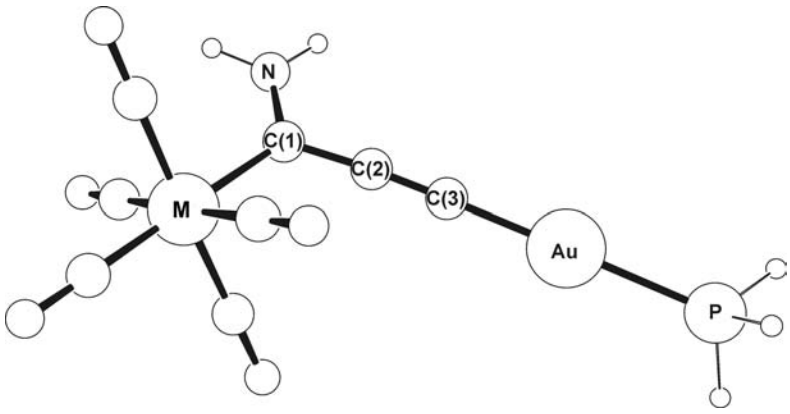

Fig. 2.6 Calculated structure of **5aM** (M = Cr) and **5bM** (M = W) showing the atom numbering scheme.

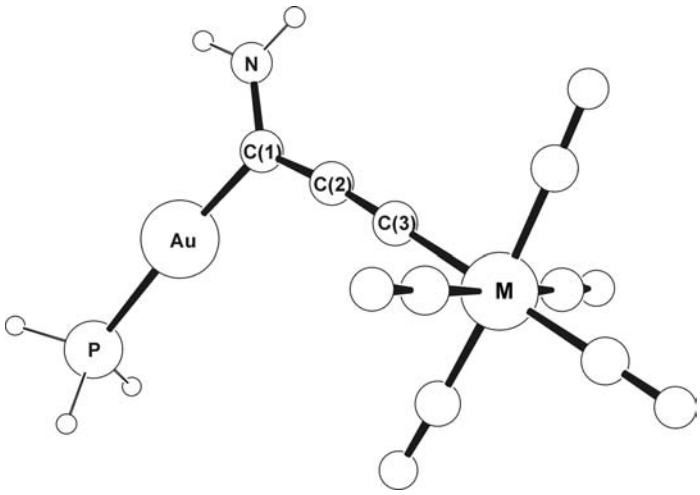

Fig. 2.7 Calculated structure of **6aM** (M = Cr) and **6bM** (M = W) showing the atom numbering scheme.

The greatest differences occur in the Au-P bond lengths, which are overestimated in the calculated structures (0.07 for **5aM** and **5bM** and 0.09 Å for **6aM** and **6bM**, respectively). This could be due to the simplified phosphine ligands in the model compounds - see Table 2.5 for selected bond lengths. M-C bond lengths are slightly shorter than in the experimental structures, although they follow the correct trend. The calculated Au-C bond lengths agree very well with each other, and with the experimental data, with the exception of **6aM**, which is calculated to be 0.06Å longer than found experimentally. This seems to be an artefact of the poor crystal structure determination of **6a**.

Table 2.5 Selected bond lengths calculated for model structures **5aM**, **5bM**, **6aM** and **6bM**

	5aM	**5bM**	**6aM**	**6bM**
Au-C	1.9903	1.9906	2.0506	2.0504
M-C	2.103	2.2273	1.9801	2.1197
C(1)-N	1.3314	1.3338	1.3393	1.3400
C(1)-C(2)	1.4077	1.4090	1.3624	1.3621
C(2)-C(3)	1.223	1.2230	1.2478	1.2482
Au-P	2.3474	2.3476	2.3837	2.3834

Merz-Kollman-Singh charges[60] (Table 2.6) calculated for **5aM** and **5bM** show that the $M(CO)_5$ fragments are negatively charged. The NH_2 groups are almost neutral, however the large negative charges on C(3) suggest a greater correspondence to resonance structure **X** than **XI** in Scheme 2.8.

[60] B. H. Besler, K. M. Merz, Jr. and P. A. Kollman, *J. Comput. Chem.,* 1990, **11**, 431; U. C. Singh and P. A. Kollman, *J. Comput. Chem.,* 1984, **5**, 129.

Table 2.6 Selected Merz-Kollman-Singh charges calculated for model structures **5M** and **6M**

	5aM	**5bM**	**6aM**	**6bM**
Au	0.172	0.153	-0.093	-0.028
M	-2.029	-2.119	-1.958	-2.617
$M(CO)_5$	-0.561	-0.577	-0.478	-0.555
C(1)	0.536	0.163	0.241	-0.023
N(1)	-0.824	-0.808	-0.735	-0.644
NH_2	-0.017	-0.003	0.050	0.108
C(2)	0.135	0.163	-0.301	0.010
C(3)	-0.570	-0.566	0.224	0.144
PH_3	0.304	0.317	0.209	0.343

This also agrees with the conclusion drawn from the experimental molecular structure. In **6aM** and **6bM**, the $M(CO)_5$ groups again have large negative charges, while positive charges are accommodated on the NH_2 groups, again indicating the importance of resonance structure **XII** in Scheme 2.9 and conforming with the experimental data. As mentioned above, the well-known sensitivity of ν(CO) towards charge indicates that in general more negative charge is transferred on to the $M(CO)_5$ moieties in compound **6a** compared to **5a** (also holds for **5b** and **6b**)[42] which is, however, not paralleled by the charge calculations for **5** and **6** in Table 2.6. Calculated NBO charges also do not discriminate clearly between compounds **5** and **6** in this respect.

The two calculated energies show that **5aM** and **5bM** are lower in energy than **6aM** and **6bM** (although only by 2.9 and 1.5 kcal/mol, respectively). This would mean that for a mixture containing **5aM** and **6aM**, only about 1% would be **6aM** (about 8% **6bM** in a mixture with **5bM**). The fact that **6a** does form from **5a** suggests firstly that there is a low energy transition state (that we were unable to determine) in the process described in Scheme 2.6 and that solvent effects could be involved in the conversion. Of course, differences between model and real ligands might also contribute to the discrepancy between relative calculated (**5aM** and **5bM** favoured) and observed (**6a** and **6b** favoured) energies.

2.2.2.4 Mechanism and Kinetics

Kinetic evidence indicated a complicated reaction sequence. The metal exchange was conveniently followed as a function of time at 25ºC by comparison of peak areas of the appropriate well, separated, NMe peaks of **5** and **6** in their ^{1}H-NMR spectra. No new resonances, due to the

formation of by-products or intermediates were observed. The results of a run for the isomerisation of **5a** to **6a** in CD_2Cl_2 are shown graphically in Figure 2.8.

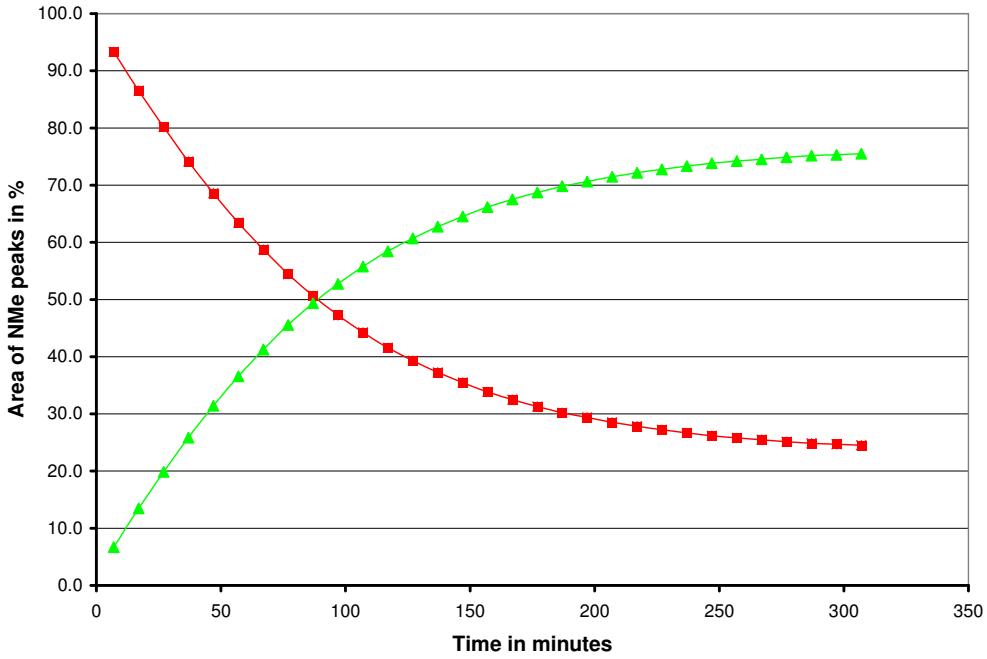

Figure 2.8 Graph showing %**5a** (■) and %**6a** (▲) against time

Although a plot of $1/[\mathbf{5a}]_t$ *versus* time, where $[\mathbf{5a}]_t$ is the concentration of complex **5a** at time *t*, gave a nearly straight line (for 70% of the reaction followed; correlation coefficient 0.9976) in accordance with an initial second-order reaction, the reaction is obviously not trivial since an equilibrium situation is reached after *ca.* 75% conversion. In addition, the kinetics plot has a slight but clearly visible S-shape. Unfortunately neither an analysis for the unexpected first-order (**5** ↔ **6**)[61] nor second-order {2(**5**) ↔ 2(**6**)}[62,63] reversible reactions effected the required straight lines. When starting with **6**, the same equilibrium concentrations were reached as when using **5** as the initial reactant.

The newly discovered isolobal metal fragment exchange is unprecedented in the literature. A few feasible mechanisms present themselves. Interactions between two triple bonds and the gold atom as well as M in a head-to-tail manner, would afford with expulsion of two CO ligands, a transition state that is completely unlikely owing to large losses in configurational entropy as well as being hampered by structural limitations. Considering Stone's association of Ph_3PAu^+ to metal carbene

[61] J. W. Moore and R. G. Pearson, *Kinetics and Mechanism,* 3rd Ed., Wiley Intersience, New York, 1981, p. 304.
[62] J. W. Moore and R. G. Pearson, *Kinetics and Mechanism,* 3rd Ed., Wiley Intersience, New York, 1981, p. 305.
[63] K. L. Laidler, *Chemical Kinetics,* 2nd Ed., McGraw-Hill Book Company, New York, 1965, pp. 21 and 27.

bonds,[64] a more rational explanation would involve a double consecutive metal metathesis – a type of metal fragment (Ph_3PAu^+ for $(CO)_5M$) exchange when two molecules (written as **IX** and **XI** in Scheme 2.8) associate at the metal-carbene bond in head-to-tail fashion to form a dimetallacyclobutane ring and then dissociate with metal exchange. Again, loss and recapture of CO (or even PPh_3) would be necessary. The product Au^+/Au cation and the M/M^- anion may again be written in the forms **IX** and **XI** and the process repeated at the two other ends to produce two molecules of the required product. Considerations counting against such as a mechanism are again steric in origin as well as the fact that **XI** is not an important contributing structure. No worthwhile guiding evidence regarding the transition state could be extracted from theoretical calculations and no evidence was found for the existence of the mentioned intermediates $Ph_3PAu^+=C(NMe_2)C\equiv CAuPPh_3$ or $(CO)_5M=C(NMe_2)C\equiv CCr(CO)_5^-$. The replacement of $W(CO)_5$ in Fischer-type carbene complexes by AuCl reported by Aumann and Fischer seems also relevant to this discussion.[65]

All of the above mentioned ideas therefore pose some problems. Another possibility is that the metal migration occurs *via* metallotropic [1,3]-carbene shift.[66] Stoichiometric metallotropic [1,3]-shifts of alkynyl carbene species with transition metal compounds such as Ti,[67] Cr, Mo and W[68] have been documented and intensively studied.[69] This intriguing, dynamic organic process consists of the carbene center shifting to the remote alkynyl carbon (Eqs. 1 and 2).

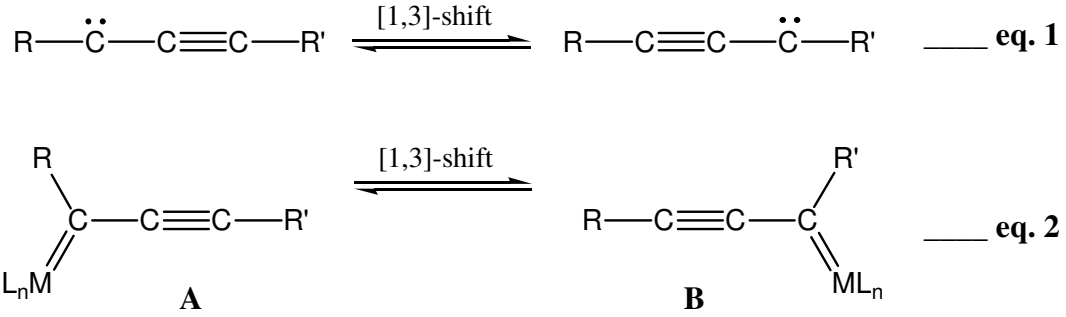

[64] G. A. Carriedo, J. A. K. Howard, F. G. A. Stone and M. J. Went, *J. Chem. Soc., Dalton Trans.,* 1984, 2545, and references therein.
[65] R. Aumann and E. O. Fischer, *Chem. Ber.,* 1981, **114**, 1853.
[66] A. Padwa, D. J. Austin, Y. Gareau, J. M. Kassir and S. L. Xu, *J. Am. Chem. Soc.,* 1993, **115**, 2637.
[67] T. Takeda, M. Ozaki, S. Kuroi and A. Tsubouchi, *J. Org. Chem.,* 2005, **70**, 4233.
[68] J. Barluenga, R. B. de la Rúa, D. de Sáa, A. Ballesteros and M. Tomás, *Angew. Chem. Int. Ed. Engl.,* 2005, **44**, 4981.
[69] C. P. Casey, S. Kraft and M. Kavana, *Organometallics,* 2001, **20**, 3795; C. P. Casey, S. Kraft and R. Powell, *Organometallics,* 2001, **20**, 2651; C. P. Casey and T. L. Dzwiniel, *Organometallics,* 2003, **22**, 5285; C. P. Casey, T. L. Dzwiniel, S. Kraft and I. A. Guzei, *Organometallics,* 2003, **22**, 3915; C. P. Casey, S. Kraft and R. Powell, *J. Am. Chem. Soc.,* 2002, **124**, 2584.

The present reaction mechanism could be formally understood in terms of a [1,3]-metal shift[70] if **B** – eq (2) – becomes

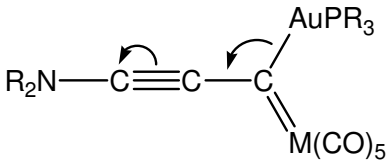

which could then be followed by a $AuPR_3^+$-fragment migration to afford canonical structure **XIII** in Scheme 2.9,

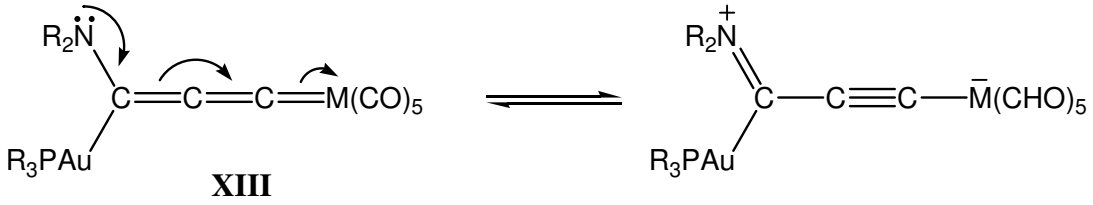

Various other possibilities exist for the mechanism, but such speculations will not be dealt with further. It is clear that the [1,3]-shift has applications not foreseen before.

2.2.3 Increasing the number of C≡C units

An interesting question that arose is whether an increase in the number of acetylide units will also afford this metal migration. Although it is possible to synthesise $(CO)_5W{=}C(NMe_2)C{\equiv}C\text{-}C{\equiv}C\text{-}H$ by using the Sonogashira coupling method, the overall yield is only 4.5%. This complex can be deprotonated and successfully reacted with Bu_3SnCl, $CpRu(CO)_2Cl$ and $CpFe(CO)_2I$ to afford heterobimetallic pentadiynylidene-bridged complexes.[71]

The low yield of the starting complex, combined with the possible difficulty of separation the isomers after reaction with Ph_3PAu^+, makes the planned synthesis unrealistic. We therefore aimed to increase the yield of $(CO)_5W{=}C(NMe_2)C{\equiv}C\text{-}C{\equiv}C\text{-}H$. Reacting $M(CO)_6$ with $LiC{\equiv}C\text{-}C{\equiv}C\text{-}TMS$[72] was unsuccesful. Although a reaction does take place, the formed Li-product is too unstable to last until the alkylation is executed.

Two main ideas were attempted as shown in Schemes 2.10 and 2.11. The number of steps would stay the same but the yield would possibly increase for the proposed synthesis in Scheme 2.10.

[70] C. P. Casey, S. Kraft and R. Powell, *Organometallics,* 2001, **20**, 2651.
[71] C. Hartbaum and H. Fischer, *Chem. Ber./Recueil,* 1997, **130**, 1063.
[72] A. B. Holmes, C. L. D. Jennings-White, A. H. Achulthess, B. Akinde and D. R. M Walton, *J. Chem. Soc., Chem. Commun.,* 1979, 840.

Scheme 2.11 illustrates a possible method that could decrease the amount of steps needed to form the desired product.

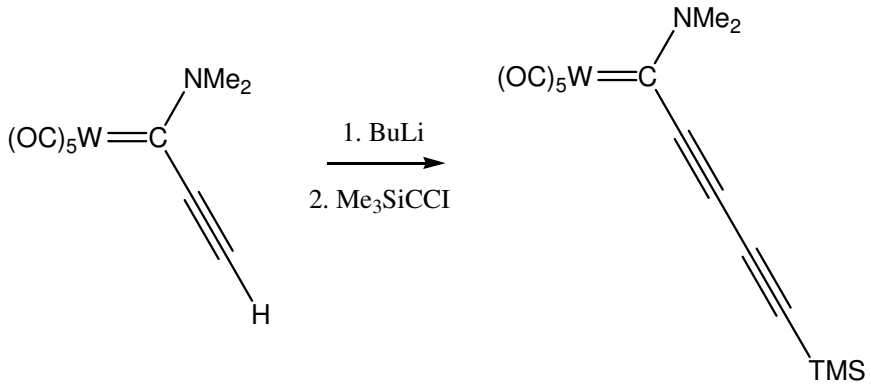

Scheme 2.10

Instead of using the normal Stille coupling with stoichiometric amounts of Cu and complex, a 5 % mole amount of CuI and $(PPh_3)_2PdCl_2$ was used (Sonogashira coupling) since recent research had shown that homocoupling is decreased[73]. However, self-dimerization of alkoxychromium(0) carbene complexes in the presence of catalytic amounts of Pd catalyst, has been reported,[74] which can influence the reaction negatively. In addition to this, NEt_3 was used as solvent and base, to also inhibit possible homocoupling.[75] This reaction led to several products as indicated by TLC and was therefore not pursued further. Cu-free Sonogashira couplings are known, but they require activated arylhalides, high Pd-catalyst loading[76] and elevated temperatures (100 °C)[77] which would probably have lead to decomposition of the Fischer-type carbene complex as well as numerous side reactions.

It is known that the conversion of silyl alkynes to bromoalkynes can be achieved with $AgNO_3$ and NBS in acetone.[78] The first step in Scheme 2.11 to incorporate a Br-atom failed, and therefore the second step was not even attempted. At this stage, time constraints prevented the pursuit of this field of research.

[73] L. Wang, J. Yan, P. Li, M. Wang and C. Su, *J. Chem. Res.*, 2005, **2**, 112.
[74] M. A. Sierra, M. J. Mancheño, E. Sáez and J. C. del Amo, *J. Am. Chem. Soc.,* 1998, **120**, 6812.
[75] L. Wang, J. Yan, P. Li. M. Wang and C. Su, *J. Chem. Res.,* 2005, 112.
[76] A. Soheili, J. Albaneze-Walker, J. A. Murry, P. G. Dormer and D. L. Hughes, *Org. Lett.,* 2003, **5**, 4191.
[77] U. S. Sørensen and E. Pombo-Villar, *Tetrahedron,* 2005, **61**, 2697; N. E. Leadbeater and B. J. Tominack, *Tetrahedron Lett.,* 2003, **44**, 8653.
[78] T. Nishikawa, S. Shibuya, S. Hosokawa and M. Isobe, *Synlett*, 1994, 485.

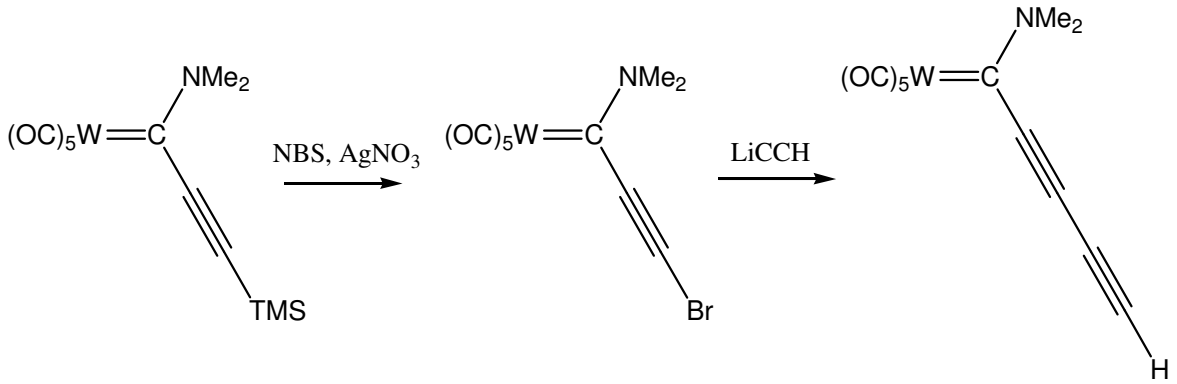

Scheme 2.11

2.3 Conclusions

Cyclic, acyclic and bridged complexes as obtained for deprotonated aminocarbene complexes were expected to form, from the reaction of methyl(methoxy)carbene complexes with the sulfonium salt, $[(CH_3)_2(CH_3S)S][BF_4]$. Instead, the formed anions reacted primarily with alkylated acetonitrile (formed during the synthesis of the sulfonium salt) to yield new examples of α,β-unsaturated Fischer-type carbene complexes. Parallel to this reaction, sulfenylation also occurred to furnish new, unique four-membered carbene-thioether chelates with α,β unsaturation in the carbene organic side chain, thus complementing the series of carbene-heteroatom chelates that now comprises of three to seven membered compounds.

The complex $Ph_3PAuC=(NMe_2)C=C=Cr(CO)_5$ was isolated and characterised. It was shown that the two metal fragments, $M(CO)_5$ and $AuPPh_3$, are labile units when in solution at room temperature and may exchange places through a possible [1,3]-shift type reaction occurring *via* a complicated reaction mechanism. These results should launch the isolation of more dinuclear metal complexes by exchange of the $M(CO)_5$-unit for other organometallic fragments.

2.4 Experimental

2.4.1 General

Reactions were carried out under an inert atmosphere using standard Schlenk techniques.[79] All glassware were dried at 110°C and cooled under vacuum before use. All solvents were freshly

[79] R. J. Errington, *Advanced Practical Inorganic and Metalorganic Chemistry,* Chapman & Hall, London, 1997, pp. 26-52, 97-101.

distilled under an inert atmosphere before use. THF, diethyl ether, pentane and hexane were dried over KOH and distilled over sodium wire. Benzophenone and diethylene glycol dimethyl ether were used as indicators for pentane and hexane and benzophenone for THF and diethyl ether. Dichloromethane was dried over KOH and distilled over CaH_2. Acetonitrile was only distilled over CaH_2. Melting points were determined on a Stuart SMP3 apparatus and are uncorrected. IR spectra were recorded either on a Perkin-Elmer 1600 Series or a Nicolet Avatar 330 FTIR. NMR spectra were determined on a Varian 300 FT or INOVA 600MHz spectrometer (^{1}H NMR at 300/600 MHz, $^{13}C\{^1H\}$ NMR at 75/151 MHz and $^{31}P\{^1H\}$ NMR at 121.5/243 MHz). ^{1}H and ^{13}C chemical shifts refer to δ_{TMS} = 0.00 according to the residual deuterated solvents and are reported in ppm. ^{31}P chemical shifts are reported in ppm relative to an 85% H_3PO_4 external solution. ES-MS determinations were performed on a Micromass Quattro Triple Quadropole instrument and FAB-MS on a VG 70SEQ mass spectrometer in a 2-nitro benzyl alcohol matrix at the University of Witwatersrand, South Africa. Elemental analyses were carried out at the Department of Chemistry, University of Cape Town, South Africa on the complexes after drying the crystals obtained under vacuum for 5 hours.

Flash chromatographic separations[80] were performed with double walled columns that were cooled down to -15° with "flash grade" Florosil (200-300 mesh) or Silica Gel 60 (230-400 mesh) under inert atmosphere.

The Fischer-type carbene complexes $(CO)_5M{=}C(OMe)Me$,[81] $(CO)_5M{=}C(NMe_2)Me$,[82] $(CO)_5M{=}C(NMe_2)C{\equiv}CH$[71] and $[CH_3CNCH_3][BF_4]$[48] were prepared using previously reported procedures. Methyl and *n*-butyl lithium were standardised using 2,5-dimethoxy benzyl alcohol.[83] $[Me_2(MeS)S][BF_4]$ was synthesized using the method described by Meerwein *et al.*[84] The chemicals $Cr(CO)_6$, $W(CO)_6$, $CF_3SO_3CH_3$, HC≡CTMS KF and $HNMe_2$ were purchased and used without further purification.

[80] A. I . Vogel, *Vogel's Textbook of Practical Inorganic Chemistry,* Revised by B. S. Furniss, A. J. Hannoford, P. W. G. Smith and A. R. Tatchell, Harlow, 5th Edition, 1989, Chapter 2, p. 218; W. C. Still, M. Kahn and A. Mitra, *J. Org. Chem.,* 1978, **43**, 2923; K. A. M. Krener and P. Helquist, *Organometallics*, 1984, **3**, 1743.
[81] W. A. Hermann (red.), *Synthetic methods of Organometallic and Inorganic Chemistry, Vol 7, Transition Metals Part 1,* Georg Thieme Verlag, Stuttgart, 1997, p. 127.
[82] E. O. Fischer and M. Leupold, *Chem. Ber.,* 1972, **105**, 599.
[83] M. R. Winkle, J. M. Langsinger and R. C. Ronald, *J. Chem. Soc., Chem. Comm.,* 1980, 87.
[84] H. Meerwein, K.-F. Zenner and R. Gipp, *Justus Liebigs Annalen der Chemie,* 1965, **688**, 67.

2.4.2 Direct synthesis of complex 2a

Complex **1a** (0.44 g, 1.8 mmol) was dissolved in 15 ml THF and cooled to –78 ºC. *n*-BuLi (1.2 ml, 1.5 M, 1.8 mmol) was added dropwise with a syringe. The solution was stirred for 20 min. at -78 ºC and 0.25 g (1.8 mmol) of $[CH_3CNCH_3][BF_4]$ was added. The mixture was stirred for 20 min. at -78 ºC, whereafter it was allowed to reach room temperature over a period of 3 hours. The solvent was removed *in vacuo*, the resulting residue dissolved in CH_2Cl_2, adsorbed onto silica and column chromatographed with hexane/dichloromethane (2:1) as eluant The starting material **1a** was eluted first and then the product was collected as fraction 2 to yield after solvent evaporation, 0.24 g (0.79 mmol, 43.7 % yield) of **2a**.

2.4.3 The direct synthesis of complex 2b

The same procedure was followed as for complex **2a** with 0.13 g (0.33 mmol) of complex **1b**, 0.23 ml *n*-BuLi (1.4 M, 0.33 mmol) and 0.047 g (0.33 mmol) of $[CH_3CNCH_3][BF_4]$ to yield 0.10 g (0.23 mmol, 70 % yield) of **2b**.

2.4.4 Attempt to aminolise complex 2b

Complex **2b** (0.027 g, 0.062 mmol) was dissolved in a small amount of CH_2Cl_2 and pentane was added. Dimethylamine was bubbled through the solution for 3 minutes. No colour change was observed and TLC confirmed that no reaction had occurred. Even when only pentane is used as solvent, there was no reaction.

2.4.5 The reaction of $[CH_3CNCH_3][BF_4]$ with $(CO)_5Cr{=}C(NMe_2)Me$

The dimethylaminocarbene complex (0.17 g, 0.64 mmol) was dissolved in THF and cooled down to -78 °C. BuLi (0.44 ml, 1.4 M, 0.64 mmol) was added and the reaction mixture stirred for 10 minutes at -78 °C after which 0.090 g (0.63 mmol) of $[CH_3CNCH_3][BF_4]$ was added. The solution was allowed to slowly warm up to room temperature. The solvent was evaporated and the resulting precipitate was dissolved in CH_2Cl_2 and filtered through dry silica. NMR spectra indicated that only the starting complex was present.

2.4.6 Synthesis of complex 5a

A solution of **4a** (0.090 g, 0.32 mmol) in diethylether at -78 ºC was treated with 0.21 ml (1.5 M, 0.32 mmol) of *n*-BuLi. The solution was stirred for 30 minutes at -78 ºC and 0.16 g (0.30 mmol) of Ph_3PAuNO_3 added. After 30 minutes at -78 ºC, the reaction mixture was allowed to warm to 0 ºC and filtered through florosil. The filtrate was kept at 0 ºC and concentrated. As soon as a precipitate formed, a minimum amount of CH_2Cl_2 was again added to dissolve it, the solution was layered with pentane and yielded crystals on cooling to -15 ºC.

Table 2.7 Physical data of compound **5a**

Yield		13 %
Colour		orange
Melting point		82 °C with decomposition
Elemental analysis	% calculated	C 45.98, H 2.89, N 1.92
$C_{28}H_{21}NO_5PCrAu$	% found	C 46.22, H 2.79, N 1.85

2.4.7 Synthesis of complex 6a

This complex was obtained in a similar fashion as complex **5a** from **4a** (0.74 g, 1.8 mmol), *n*-BuLi (1.2 ml, 1.5 M, 1.8 mmol) and 0.88 g of Ph_3PAuNO_3 (1.7 mmol). Instead of layering the product mixture with pentane, more CH_2Cl_2 was added. It was kept at room temperature for 24 hours, adsorbed on florosil and chromatographed with the eluant system pentane-ether (2:1) which was gradually changed to 1:4 at -15 °C. Complex **6a** was collected as an intense orange-red band after complex **5a** was eluted as an orange band.

Table 2.8 Physical data of compound **6a**

Yield	22 %
Colour	red-orange
Melting point	129 °C with decomposition

2.4.8 Computational methods

The geometries of the molecules were optimised at the gradient-corrected DFT level using the three parameter fit of the exchange-correlation potential suggested by Becke[85] in conjunction with the LYP[86] exchange potential (B3LYP).[87] A quasi-relativistic small-core ECP with a (341/321/N1) valence basis set for the metal atoms (*N*=4 for Cr and *N*=2 for Au and W)[88] and 6-311+G(d) all-electron basis set[89] for the other atoms were employed in the geometry optimisations. The nature of the stationary points was examined by calculating the Hessian matrix at this level: all four are energy minima on the potential energy surface. Partial charges were estimated with the population analysis of Merz-Kollman-Singh.[60] The calculations were performed with the program package Gaussian 03.[90]

2.4.9 Single crystal analyses

The pertinent crystallographic X-ray data for complexes **5a** and **6a** are listed in Table 2.9. Owing to isomerisation, better crystals of **6a** could not be obtained. Data sets were collected on a Bruker SMART Apex CCD diffractometer[91] with graphite monochromated Mo-K_α radiation (λ = 0.71073 Å) each. Data reduction was carried out with standard methods from the software package Bruker SAINT.[92] Empirical corrections were performed with SADABS.[93] The structures were solved by direct methods (**6a**) or interpretation of Patterson synthesis (**5a**), which yielded the position of the metal atom, and conventional Fourier methods. All non-hydrogen atoms were refined anisotropically by full-matrix least squares calculations on F^2 using SHELXL-97[94] within the X-

[85] A. D. Becke, *J. Chem. Phys.,* 1993, **98**, 5648.
[86] C. Lee, W. Yang and R. G. Parr, *Phys. Rev. B,* 1988, **37**, 785.
[87] P. J. Stevens, F. J. Devlin, C. F. Chablowski and M. J. Frisch, *J. Phys. Chem.,* 1994, **98**, 11623.
[88] P. J. Hay and W. R. Wadt, *J. Chem. Phys.,* 1985, **82**, 299.
[89] R. Ditchfield, W.J. Hehre and J.A. Pople, *J. Chem. Phys.*, 1971, **54**, 724; W.J. Hehre, R. Ditchfield and J.A. Pople, *J. Chem. Phys.*, 1972, **56**, 2257.
[90] M. J. Frisch, G.W. Trucks, H. B. Schlegel, G. E. Scuseria, M. A. Robb, J. R. Cheeseman, J. A. Montgomery, Jr., T. Vreven, K. N. Kudin, J. C. Burant, J.M.Millam, S. S. Iyengar, J. Tomasi, V. Barone, B.Mennucci, M. Cossi, G. Scalmani, N. Rega, G. A. Petersson, H. Nakatsuji, M. Hada, M. Ehara, K. Toyota, R. Fukuda, J. Hasegawa, M. Ishida, T. Nakajima, Y. Honda, O. Kitao, H. Nakai, M. Klene, X. Li, J. E. Knox, H. P. Hratchian, J. B. Cross, V. Bakken, C. Adamo, J. Jaramillo, R. Gomperts, R. E. Stratmann, O. Yazyev, A. J. Austin, R. Cammi, C. Pomelli, J. Ochterski, P. Y. Ayala, K. Morokuma, G. A. Voth, P. Salvador, J. J. Dannenberg, V. G. Zakrzewski, S. Dapprich, A. D. Daniels, M. C. Strain, O. Farkas, D. K. Malick, A. D. Rabuck, K. Raghavachari, J. B. Foresman, J. V. Ortiz, Q. Cui, A. G. Baboul, S. Clifford, J. Cioslowski, B. B. Stefanov, G. Liu, A. Liashenko, P. Piskorz, I. Komaromi, R. L. Martin, D. J. Fox, T. Keith, M. A. Al-Laham, C. Y. Peng, A. Nanayakkara, M. Challacombe, P.M.W. Gill, B. G. Johnson, W. Chen, M. W. Wong, C. Gonzalez and J. A. Pople, *GAUSSIAN 03 (Revision C.02)*, Gaussian, Inc., Wallingford, CT, 2004.
[91] *SMART Data Collection Software (Version 5.629),* Bruker AXS Inc., Madison, WI, 2003.
[92] *SAINT Data Reduction Software (Version 6.45),* Bruker AXS Inc., Madison, WI, 2003.
[93] *SADABS (Version 2.05),* Bruker AXS Inc., Madison, WI, 2002.
[94] G. M. Sheldrick, *SHELX-97. Program for Crystal Structure Analysis,* University of Göttingen, Germany, 1997.

Seed environment.[95] The four structures all have high residual electron densities around their Au(1) atom. The highest peaks of residual electron density are 1.936 at a distance of 0.84 Å from Au(1) for **5a** and 7.00 at 0.94 Å for **6a** The positions of the hydrogen atoms were calculated by assuming ideal geometry and their coordinates were refined together with those of the attached carbon atoms as "riding model". ORTEP-III for Windows[96] was used to generate the various figures of the complexes at the 50% probability level. Additional information regarding these crystal structures is available from Prof H. G. Raubenheimer, Department of Chemistry and Polymer Science, University of Stellenbosch.

[95] L. J. Barbour, *J. Supramol. Chem.,* 2001, **1**, 189.
[96] J. Farrugia, *J. Appl. Crystallogr.,* 1997, **30**, 565.

Table 2.9 Crystal data and structure refinement parameters of complexes **5a** and **6a**

Complex	**5a**	**6a**
Empirical formula	$C_{28}H_{21}NO_5PCrAu$	$C_{28}H_{21}NO_5PCrAu$
Formula weight / g.mol^{-1}	731.39	731.39
Temperature/ K	100(2)	100(2)
Crystal colour and habit	orange prisms	red orange prisms
Space group	*P*-1	*P*-1
a / Å	8.953(1)	10.364(3)
b / Å	11.305(1)	11.566(3)
c / Å	14.623(2)	12.463(4)
α / °	73.960(2)	74.216(14)
β / °	87.532(2)	69.976(5)
γ / °	73.681(2)	82.605(8)
V (Å^3)	1364.1(3)	1349.7(7)
Z	2	2
$D_{calc.}$ / g.cm^{-3}	1.781	1.800
Adsorption coefficient / mm^{-1}	5.866	5.928
F(000)	708	708
θ (min – max) / °	1.95 – 26.37	1.8 – 26.8
Reflections collected	7909 [R_{int} = 0.0153]	14294 [R_{int} = 0.103]
Independent reflections	5432	5629
Data/restraints/parameters	5432/0/336	3999/0/336
Final *R* indices [$I>2\sigma(I)$]	R_1 = 0.0268, wR_2 = 0.0637	R_1 = 0.079, wR_2 = 0.165
R indices (all data)	R_1 = 0.0303, wR_2 = 0.0653	R_1 = 0.116, wR_2 =0.181
Goodness-of-fit on F^2	1.058	1.06
Largest peak / e Å^{-3}	1.936	7.00

3 EXTENDING THE REMOTE HETEROATOM CARBENE COMPLEX THEME

3.1 Introduction and Aims

3.1.1 Background

The metal-mediated (catalytic) activation of strong and typically unreactive bonds under mild conditions requires the development of powerful ligand sets. Metal-NHC (N-heterocyclic carbene) complexes show a favourable profile in synthesis[1] and hydrosilylation.[2] The discovery that substitution of a PCy_3 ligand with an NHC in the Grubbs 1 catalyst[3] results in complexes with improved activity and stability in the application to olefin metathesis,[4] have led to the introduction of Grubbs' 2nd generation catalyst.[5]

The use of palladium compounds has revolutionalised transition-metal-mediated C-C bond formation reactions over the last 30 years,[6] being central to many cross-coupling reactions such as those named after Kumada,[7] Stille,[8] Suzuki[9], Sonogashira[10] and Heck.[11] Palladium compounds are now duly recognized for their catalytic activity in synthetic organic chemistry. The high activity of

---

[1] W. A. Hermann, *Angew. Chem. Int. Ed. Engl.,* 2002, **41**, 1290; W. A. Hermann and C. Köcher, *Angew. Chem. Int. Ed. Engl.,* 1997, **36**, 2162.
[2] L. H. Gade, V. Cósar and S. Bellemin-Laponnaz, *Angew. Chem. Int. Ed. Engl.,* 2004, **43**, 1014.
[3] S. T. Nguyen and T. M. Trnka in *Handbook of Metathesis,Vol. 1,* R. H. Grubbs, Ed., Wiley-VCH, Weinheim Germany, 2003, Chapter 1, pp 61-81.
[4] T. M. Trnka and R. H. Grubbs, *Acc. Chem. Res.,* 2001, **34**, 18; B. F. Straub, *Angew. Chem. Int. Ed. Engl.,* 2005, **44**, 5974.
[5] M. Scholl, S. Ding, C. W. Lee and R. H. Grubbs, *Org. Lett.,* 1999, **1**, 953; J. Huang, E. D. Stevens, S. P. Nolan and J. L. Peterson, *J. Am. Chem. Soc.,* 1999, **121**, 2674.
[6] J. J. Li and G. W. Gribble, *Palladium in Heterocyclic Chemistry : A Guide for the Synthetic Chemist,* Pergamon, Oxford, 2000.
[7] K. Tamao, K. Sumitani and M. Kumada, *J. Am. Chem. Soc.*, 1972, **94**, 4374.
[8] W. A. Herrmann, V. P. W. Böhm, C. W. K. Gstöttmayr, M. Groshe, C.-P. Reisinger and T. Weskamp, *J. Organomet. Chem.,* 2001, **617**, 616.
[9] Some pertinent references: V. P. W. Böhm, C. W. K. Gstöttmayr, T. Weskamp and W. A. Hermann, *J. Organomet. Chem.,* 2000, **595**, 186; D. S. McGuinness and K. J. Cavell, *Organometallics,* 2000, **19**, 741; O. Navarro, R. A. Kelly and S. P. Nolan, *J. Am. Chem. Soc.,* 2003, **125**, 16194.
[10] C. Yang and S. P. Nolan, *Organometallics,* 2002, **21**, 1020.
[11] C. Yang, H. M. Lee and S. P. Nolan, *Org. Lett.,* 2001, **3**, 1511.

Pd-carbene complexes in C-C coupling reactions has been attributed to the high bond dissociation energy of heterocyclic carbenes.[12] During the last decade NHCs have provided a viable alternative to the originally used phosphine-based ligands owing to their better stability to air, moisture and heat.[13] It was however only recently demonstrated that NHC complexes also show high-yielding Negishi alkyl-alkyl cross-coupling reactivity.[14]

The idea that carbene complexes can be synthesised with a *remote* heteroatom (compare Chapter 1) was further developed by preparing Pd(II) and Pt(II) complexes *via* initial oxidative substitution of 4-chloro-N-methylquinolinone as well as related manganese complexes by initial halide displacement followed by consecutive protonation or alkylation of the nucleophilic carbonyl oxygen situated three bonds away from the coordinating carbon to form the respective carbene complexes, **X**. Alternatively, initial alkylation and consecutive oxidative substitution or halide displacement also lead to the respective carbene complexes.[15] Complexes like **XV** containing both *r*NHC and phosphine ligands, combine the stability of NHC carbene complexes with the well-known activity of phosphine complexes in C-C coupling reactions.

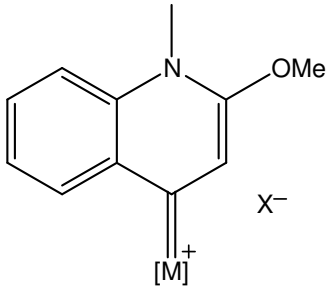

X = BF_4, CF_3SO_3
[M] = $Pd(PPh_3)_2Cl$, $Pt(PPh_3)_2Cl$, $Mn(CO)_5$

XV

The ability to obtain these complexes from a carbene precursor ligand that contains a remote heteroatom for stabilisation show that despite theoretical and experimental evidence stressing the requirement of strong p(π) donor atoms in the α-position,[16] this criterion is not always necessary.

Computational studies performed at the RI-BPS6/SVP level of theory on hypothetical *n*N^2HC^5, *n*N^1HC^6 and *r*N^1HC^6 free carbenes[17,18] indicated a few significant differences:

[12] J. Schwarz, V. P. W. Böhm, M. G. Gardiner, M. Grosche, W. A. Herrmann, W. Hieringer and G. Raudaschl-Sieber, *Chem. Eur. J.,* 2000, **6**, 1773.
[13] D. Bourissou, O. Guerret, F. P. Gabbaï and G. Bertrand, *Chem. Rev.,* 2000, **100**, 39.
[14] N. Hadei, E. A. B. Kantchev, C. J. O'Brien and M. G. Organ, *Org. Lett.,* 2005, **7**, 3805.
[15] W. H. Meyer, M. Deetlefs, M. Pohlmann, R. Scholz, M. W. Esterhuysen, G. R. Julius and H. G. Raubenheimer, *Dalton Trans.,* 2004, 413.
[16] N. Fröhlich, U. Pidun, M. Stahl and G. Frenking, *Organometallics,* 1997, **16**, 442.

i. the σ-donor HOMO of the rN^{1}HC^6 is higher in energy than the simple nN^{2}HC^5 making the *remote* carbene a far better σ-donor;

ii. the possibility for back-bonding to the nN^{2}HC^5 ligand from a metal moiety is restrained due to higher π-electron density located on its carbon atom compared to the situation in the rN^{1}HC^6;

iii. both the σ- and π-contributions are larger for the rN^{1}HC^6 complex than for the nN^{1}HC^6 and nN^{2}HC^5 complexes according to EDA analysis, while the σ-contribution is far more important than the π-component (*ca.* 6% to the bonding). The σ-bond strength in relation to the number and position of heteroatoms is in accord with Bent's rule:[19] the closer an electronegative donor atom (*eg.* N) to the carbene carbon, the more s-character is transferred to the σ-donor orbital and provided that the electron attraction and not orbital overlap[20] by C is the dominant factor in the covalent bond formation, the metal carbene bond weakens. The same trend was found for a systematic theoretical study performed on simple classical Fischer-type carbene complexes: Although π-donor groups α to the carbene carbon stabilise the complex against nucleophilic attack, they weaken the metal carbene bond.

iv. the metal (Ni) carbene bond is 7-24 kJmol^{-1} stronger in the nN^{1}HC^6 complexes than in the standard nN^{2}HC^5 complexes while the metal carbene bond is 13-17 kJmol^{-1} stronger in the rN^{1}HC^6 when compared to its strength in the nN^{1}HC^6 complexes;

v. the addition of more conjugated rings to the 'parent' pyridine unit (quinoline and acridine-derived model systems) as well as +I-influences (experimentally observable effect of the transmission of charge through a chain of atoms in a molecule by electrostatic induction, in this instance, electron releasing) result in stronger metal-carbon bonding.[21]

Another compound with possible application in carbene formation with remote stabilisation is 4,4-dimethyl-2-(2-thienyl)oxazoline. The synthetic versatility of the oxazolino moiety has been recognised at an early stage.[22] Research performed in the 1980s showed that the change of solvent and metallating agent controlled the regioselectivity of metallation in the lithiation of 4,4-dimethyl-2-(2-thienyl)oxazoline.[23,24] Not only the conditions for high yielding and regioselective synthesis of

---

[17] S. K. Schneider, G. R. Julius, C. Loschen, H. G. Raubenheimer, G. Frenking and W. A. Herrmann, *Dalton Trans.,* 2006, 1226.
[18] S. K. Schneider, P. Roembke, G. R. Julius, C. Loschen, H. G. Raubenheimer, G. Frenking and W. A. Herrmann, *Eur. J. Inorg. Chem.,* 2005, 2973.
[19] H. A. Bent, *Chem. Rev.,* 1961, **61**, 275.
[20] B. E. Douglas, D. H. McDaniel and J. J. Alexander, *Concepts and Models in Inorganic Chemistry,* John Wiley, New York, 3rd ed., 1994, p. 313.
[21] A. D. McNaught and A. Wilkinson, *IUPAC Compendium of Chemical Terminology*, *2nd Ed*., Royal Society of Chemistry, Cambridge, UK, 1997, p. 1124.
[22] Review: A. I. Meyers and E. D. Mihelich, *Angew. Chem. Int. Ed. Engl.,* 1976, **15**, 270.
[23] P. Ribéreau and G. Queguiner, *Tetrahedron,* 1984, **40**, 2107.
[24] A. J. Carpenter and D. J. Chadwick, *J. Chem. Soc., Perkin Trans. I,* 1985, 173.

the 3- and 5-lithio intermediates of 4,4-dimethyl-2-(2-thienyl)oxazoline, but also their subsequent reaction with a wide range of electrophiles have been established. A short summary of the result for different reaction conditions are: β-lithiation (3-lithio intermediate) predominates when *n*-BuLi is used as a base in ether or hexane and δ-lithiation (5-lithio intermediate) when LDA is used in THF. The 3-lithio-intermediate is inherently less reactive than the 5-intermediate as a result of the proximate oxazoline group. 4,4-Dimethyl-2-(2-thienyl)oxazoline can be dimetallated and reacted with electrophiles to yield 2,3,5-trisubstituted heterocycles.[25]

Interestingly, if 5-(2'-pyridyl)-2-thienyllithium (oxazoline group replaced by a pyridine) is reacted with $[Fe(Cp)(CO)_2Cl]$ and subsequently alkylated or protonated, the resulting product is carbene complex with more pyridinium than true carbene character.[26]

This type of remote stabilisation is also observed in nitrogen-stabilized alkenylidene complexes (**XVII**) which can be obtained from the complexes discussed in Chapter 2, *i.e.* either from alkenyl(ethoxy) carbene complexes (**XVI**)[27] or from alkynyl carbene complexes[28] (**XVIII**) as seen in Scheme 3.1.

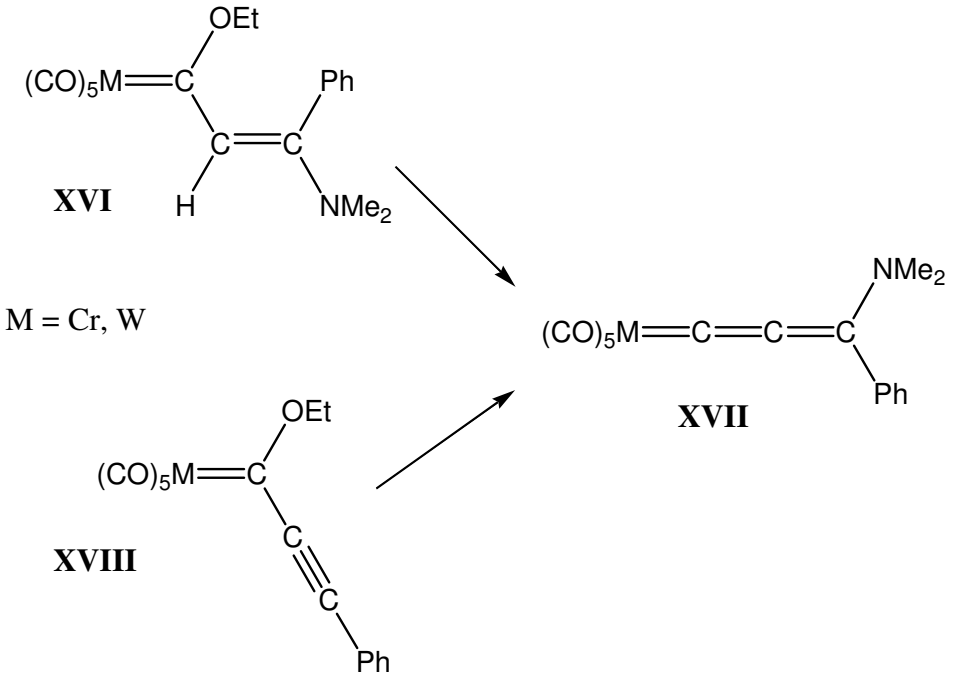

Scheme 3.1

[25] A. J. Carpenter and D. J. Chadwick, *Tetrahedron Lett.,* 1985, **26**, 5335.
[26] H. G. Raubenheimer, M. Desmet, P. Olivier and G. J. Kruger, *J. Chem. Soc., Dalton Trans.,* 1996, 4431.
[27] E. O. Fischer, H. J. Kalder, A. Frank, F. H. Köhler and G. Huttner, *Angew. Chem. Int. Ed. Engl.,* 1976, **15**, 623.
[28] M. Duetsch, F. Stein, R. Lackmann, E. Pohl, R. Herbst-Irmer and A. de Meijere, *Chem. Ber.,* 1992, **125**, 2051.

Complexes of this type incorporating a pyridine-derived ring at the remote γ-carbon (**XIX**), have also been reported starting with $(CO)_5M(THF)$ and Li[C≡C-Py].[29]

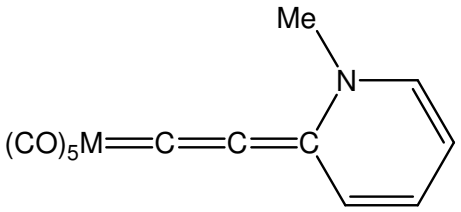

XIX

Normal pyridylidene Fischer-type carbene complexes (**XX**) have been previously prepared by the straightforward cyclization of 1-metalla-1,3,5-trienes (formed by addition of 4-(NH)amino-pent-3-en-2-ones to ethoxy-alkynylcarbene complexes) in dichloromethane in the presence of Et_3N.[30]

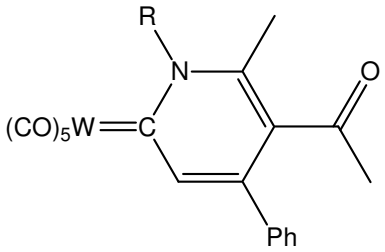

XX

The fact that group 6 metal Fischer carbene complexes may act as stable carbene sources was recognized in the 1970s in the cyclopropanation of olefins.[31] Nevertheless, the use of group 6 metal carbene complexes as stable reagents for carbene transfer has not yet claimed a place in modern organic synthesis. Examples of the transfer of carbene ligands include the formation of Fe complexes from the reaction of arylalkoxy, aryldialkylamino and dialkylaminoalkoxy carbene complexes of Cr, Mo and W with photochemically generated $Fe(CO)_5$.[32,33] The stoichiometric transmetalation of group 6 mononuclear alkoxypentacarbonylmetal carbene complexes to group 10 metal centers was first reported by Stone.[34] Group 6 metal carbonyl carbene complexes have been used as effective carbene transfer reagents for the formation of Pt, Pd, Au, Ru, Ag and Cu complexes.[35,36] Several Au(I)- and Au(III)-carbene complexes have been prepared from the reaction

[29] H. Fischer, N. Szesni, G. Roth, N. Burzlaff and B. Weibert, *J. Organomet. Chem.,* 2003, **683**, 301.
[30] R. Aumann, M. Kößmeier, K. Roths and R. Fröhlich, *Synlett,* 1994, 1041.
[31] E. O. Fischer and K. H. Dötz, *Chem. Ber.,* 1970, **103**, 1273.
[32] E. O. Fischer and H.-J. Beck, *Angew. Chem. Int. Ed. Engl.,* 1970, **9**, 72.
[33] E. O. Fischer, H.-J. Beck, C. G. Kreiter, J. Lynch, J. Müller and E. Winkler, *Chem. Ber.,* 1972, **105**, 162.
[34] T. V. Ashworth, M. Berry, J. A. K. Howard, M. Laguna and F. G. A. Stone, *J. Chem. Soc., Dalton Trans.,* 1980, 1615.
[35] S.-T. Liu, T.-Y. Hsieh, G.-H. Lee and S.-M. Peng, *Organometallics,* 1998, **17**, 993.

of $(CO)_5MC(Y)Ph$ (M = Cr, Mo, W; Y = OMe, NMe_2) with auric acid.[37,38] In many reactions carbene transfer from group 6 metal carbene complexes are Pd-catalysed to yield conjugated polyenes as well as enediyne derivatives or mono- and bicyclic derivatives if intramolecular carbene transfer occurs.[39] Catalytic transmetallations of alkoxychromium carbenes to late transition metals (*e.g.* Pd,[40] Rh,[41,42] Ni,[43] Cu[44]) to promote self-dimerization and cyclopropanation of the carbene ligand is a field of growing interest due to the great potential and tremendous versatility of these reactions in organic synthesis.[45,46,47] Many of the reaction products cannot be obtained by conventional routes. The use of transition-metal-based catalysts for the transfer of carbene units from diazo compounds constitutes a powerful tool in organic synthesis.[48] Nearly all 12 elements of Groups 8-11 (Fe, Ru, Os, Co, Rh, Pd, Pt and Cu,[44] Ir,[49] Ag[50] and Au[51]) have been found to decompose diazo compounds and transfer a carbene unit to saturated or unsaturated organic substrates.

Rather recently, the employment of NHC adducts as "protected forms" of the free carbene attracted much attention since the manipulation of the free carbenes was often difficult due to their highly reactive nature. Grubbs and co-workers reported the utilisation of NHC-alcohol or NHC–chloroform adducts for saturated NHCs,[52] and Lin *et al.* described the carbene transmetallation of silver complexes for unsaturated NHCs,[53] which is also a reliable method for the preparation of saturated NHC complexes.[54] The use of silver carbenes as transfer agents provided a convenient

---

[36] R.-Z. Ku, J. C. Huang, J.-Y. Cho, F.-M. Kiang, K. R. Reddy, Y.-C. Chen, K.-J. Lee, J.-H. Lee, S.-M. Peng and S.-T. Liu, *Organometallics,* 1999, **18**, 2145.
[37] R. Aumann and E. O. Fischer, *Chem. Ber.,* 1981, **114**, 1853; E. O. Fischer, M. Böck and R. Aumann, *Chem. Ber.,* 1983, **116**, 3618.
[38] R.-Z. Ku, J.-Ch. Huang, J.-Y. Cho, F.-M. Kiang, K. R. Reddy, Y.-Ch. Chen, K.-J. Lee, J.-H. Lee, G.-H. Lee, S.-M. Peng and S.-T. Liu, *Organometallics,* 1999, **18**, 2145.
[39] M. A. Sierra, J. C. del Amo, M. J. Mancheño and M. Gómez-Gallego, *J. Am. Chem. Soc.,* 2001, **123**, 851.
[40] H. Sakurai, K. Tanabe and K. Narasaka, *Chem. Lett.,* 1999, 75.
[41] R. Aumann, I. Göttker-Schnetmann, R. Fröhlich and O. Meyer, *Eur. J. Org. Chem.,* 1999, **64**, 2545.
[42] I. Göttker-Schnetmann and R. Aumann, *Organometallics,* 2001, **20**, 346.
[43] J. Barluenga, P. Barrio, L. A. López, M. Tómas, S. García-Granda and C. Álvarez-Rúa, *Angew. Chem. Int. Ed. Engl.,* 2003, **42**, 3008.
[44] J. Barluenga, L. A. López, O. Löber, M. Tómas, S. García-Granda, C. Álvarez-Rúa and J. Borge, *Angew. Chem. Int. Ed. Engl.,* 2001, **40**, 3392.
[45] J. C. del Amo, M. J. Mancheño, M. Gómez-Gallego and M. A. Sierra, *Organometallics,* 2004, **23**, 5021.
[46] M. Gómez-Gallego, M. J. Mancheño and M. A. Sierra, *Acc. Chem. Res.,* 2005, **38**, 44.
[47] M. Nakamura, T. Inoue and E. Nakamura, *J. Organomet. Chem.,* 2001, **624**, 300.
[48] M. P. Doyle, M. A. McKervey and T. Ye, *Modern Catalytic Methods for Organic Synthesis with Diazo Compounds,* Wiley, New York, 1998.
[49] T. Kubo, S. Sakagushi and Y. Ishii, *Chem. Commun.,* 2000, 625.
[50] J. Urbano, T. R. Belderraín, M. C. Nicasio, S. Trofimenko, M. M. Díaz-Requejo and P. J. Pérez, *Organometallics,* 2005, **24**, 1528.
[51] M. R. Fructos, T. R. Belderrain, P. de Frémont, N. M. Scott, S. P. Nolan, M. M. Díaz-Requejo and P. J. Pérez, *Angew. Chem. Int. Ed. Engl.,* 2005, **44**, 5284.
[52] M. Scholl, S. Ding, C. W. Lee and R. H. Grubbs, *Org. Lett.,* 1999, **1**, 953.
[53] H. M. J. Wang and I. J. B. Lin, *Organometallics,* 1998, **17**, 972.
[54] A. R. Chianese, X. Li, M. C. Janzen, J. W. Faller and R. H. Crabtree, *Organometallics,* 2003, **22**, 1663.

method for the formation of carbene complexes and assisted in overcoming the difficulties arising from the use of strong bases to generate free functionalised-carbene ligands which contain acidic protons associated with the functional group.[55] Silver(I) N-heterocyclic carbene complexes, obtained by the reaction of silver oxide with a imidazolium salt, were widely studied for their application as transmetallation or carbene transfer reagents to easily access various catalytically active transition-metal NHC complexes.[56] Coordination polymers of Ag(I) with bis(NHC) ligands were also used as carbene transfer reagents for the formation of chelating Pd NHC complexes in excellent yield.[57] Silver NHC compounds, unlike free NHC ligands, are air-stable and hence, considerably easier to handle.

The reaction of imidazolium salts with $LiBEt_3H$ affords triethylborane adducts of imidazol-2-ylidenes, which can act as a carbene precursors or carbene transfer reagents for the synthesis of main group element and transition metal complexes, probably due to their weak Lewis acidity. These adducts also show great stability towards air and moisture.[58]

3.1.2 Aims

As a result of previous studies in our laboratory, it became clear that the bonding and reactivity of *normal*, *abnormal* and *remote* pyridine derived carbene complexes required further investigation. In this part of the study we aimed to:

1. transform, *via* cyclisation, the α,β-unsaturated Fischer-type carbene complex, **2a** (discussed in Chapter 2) into a complex that contains a pyridine derived carbene ligand with a remote heteroatom and endeavour to transfer this carbene ligand to a Rh metal fragment;
2. prepare complexes to compare the influence that variations in the structure of the NHC ligand with regards to substituents, as well as the position of the N-atom with respect to the coordinating carbon atom, will have on the spectroscopic and bonding characteristics of the complexes; the study should include the preparation of 2-, 3- and 4-chloropyridinium ligand precursors and coordinating them to Ni and Pd for comparison;
3. using the compound 2,4-dichloro-*N*-methyl-pyridinium triflate that will create a competitive situation for oxidative substitution either at the *remote* site (C4) or at the *normal* site (C2), to determine which site is preferentially metallated; another competitive situation will be set up to

[55] D. S. McGuinness and K. J. Cavell, *Organometallics,* 2000, **19**, 741.
[56] J. C. Garrison and W. J. Youngs, *Chem. Rev.,* 2005, **105**, 3978.
[57] P. L. Chiu, C. Y. Chen, J. Y. Zeng, C. Y. Lu and H. M. Lee, *J. Organomet. Chem.,* 2005, **690**, 1682.
[58] Y. Yamaguchi, T. Kashiwabara, K. Ogata, Y. Miura, Y. Nakamura, K. Kobayashi and T. Ito, *Chem. Commun.,* 2004, 2160; K. Ogata, Y. Yamaguchi, T. Kashiwabara, and T. Ito, *J. Organomet. Chem.,* 2005, **690**, 5701.

determine whether oxidative substitution would occur at C7 (on an annealed ring, without a heteroatom) or C4 (on ring containing the N-atom) using the ligands 4,7-dichloro-*N*-methyl-quinolinium triflate and 4,7-dichloro-*N*H-quinolinium triflate;

4. expound, in collaboration with the laboratory of Frenking at the Philips University, Marburg, by quantum mechanical calculations, the differences in the metal carbene bonding for *n*NHC, *a*NHC and *r*NHC ligands;

5. explore, in general, the boundary situation between relative carbene character and pyridinium character in chosen complexes;

6. extend the class of Ni and Pd complexes with *remote* heteroatoms to include ligands with two N-atoms and 4,4-dimethyl-2-thiophen-2-yl-4,5-dihydro-oxazole containing three possible heteroatoms;

7. target the use of 4,4-dimethyl-2-thiophen-2-yl-4,5-dihydro-oxazole as ligand precursor for a carbene complex that contains Cr(0) uniquely bonded at C5 of the thiophene ring and thus affording a special type of remote carbene complex.

It was clear that crystal structure determinations of key complexes would form an indispensable part of the investigation and would also underpin the quantum mechanical calculations.

3.2 Results and discussion

3.2.1 Remote Fischer-type carbene ligands

The reaction of [(Z)-*β*-(monoalkylamino)vinyl]carbene complexes with alkynes $R^2C{\equiv}CH$ (R^2 = *n*Bu, Ph, CH_2OMe) results in the highly stereoselective formation of 4-(1*H*)-pyridylidene complexes $L_nM{=}\overline{C(CR^2{=}CH)\text{-}CH{=}CR\text{-}N}R^1$ (R = Ph, *n*Bu; R^1 = Me, *i*Pr, Ph, CH_2Ph; R^2 = *n*Bu, Ph CH_2OMe). Condensation of (β-aminovinyl)carbene complexes with alkynes leads to 4-(1*H*)-pyridylidene complexes.[59] Employing the same idea, we synthesised complex **8** by heating the Fischer-type α,β-unsaturated carbene complex described in Chapter 2, with 1-hexyne and purifying the product by column chromatography (Scheme 3.2). Since this type of *r*NHC complexes have been synthesised before, our aim was to transfer the carbene ligand to a chosen soft metal fragment for which *r*NHC compounds have not yet been described.

[59] R. Aumann and P. Hinterding, *Chem. Ber.,* 1992, **125**, 2765.

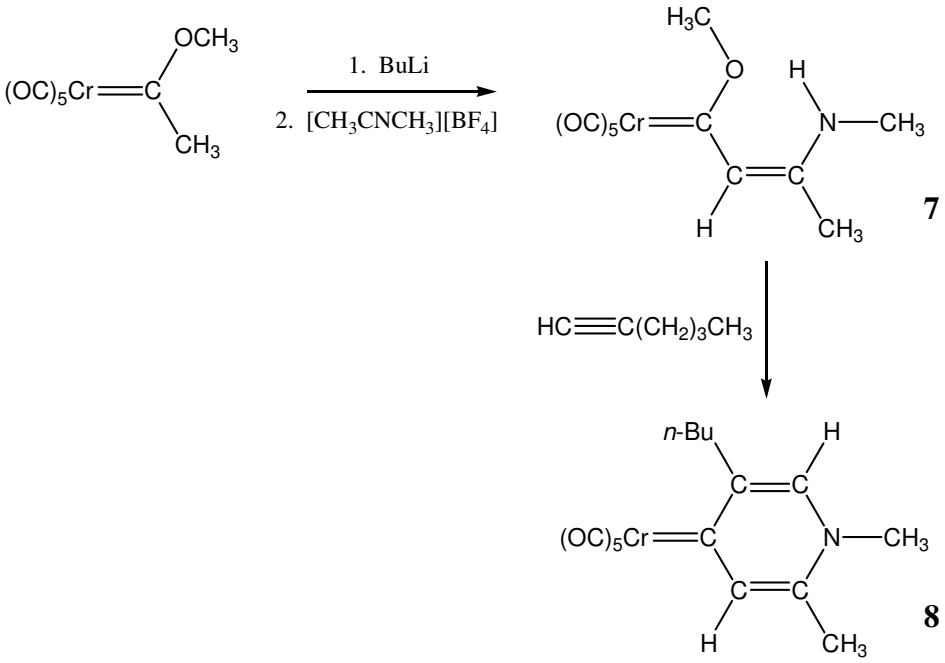

Scheme 3.2

3.2.1.1 Characterisation of $(CO)_5Cr=C[CH=C(CH_3)]N(CH_3)CH=C(nBu)$, 8

NMR spectroscopy

Although complex **7** has been characterised[60] the chemical shifts are given again for comparative reasons. No 4-(1*H*)-pyridylidene complexes of this type have been prepared with a CH_3 group on the carbon next to the nitrogen, though one with a Ph-group in that position is known.[59]

The ^1H chemical shifts for CCH (6.14 vs 8.41 ppm), NCH_3 (2.96 vs 3.80 ppm) and CCH_3 (1.98 vs 2.46 ppm) appear at a lower field for **8** than for **7** due to the aromatic nature of the latter compound compared to the situation in **7**. Comparing **8** with the similar Ph-substituted complex[30] ^1H NMR resonances appear generally more downfield for the latter due to the anisotropic shielding effect of the phenyl ring. The ^{13}C resonances are less influenced by the Ph substituent and therefore appear at similar chemical shifts. This is due to the fact that there are two components that contribute to the total chemical shift (σ) namely a paramagnetic component (σ_p) and a diamagnetic contribution (σ_d). The paramagnetic component can be ignored in ^1H NMR where the shifts reflect shielding and deshielding.[61] The diamagnetic component plays a more significant role in ^{13}C NMR and cannot be ignored.

[60] E. Stander, S. Cronje and H. G. Raubenheimer, *Dalton Trans.,* 2007, 5684.
[61] R. F. Fenske in *Organometallic Compounds, Synthesis, Structure and Theory,* Texas A & M University Press, Texas, 1983, p. 305.

Table 3.1 ^{1}H and ^{13}C-{^{1}H} NMR data of compounds **7** and **8** in CD_2Cl_2

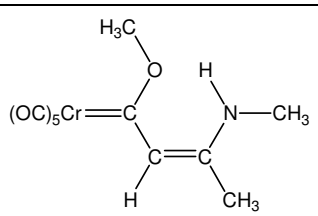

7

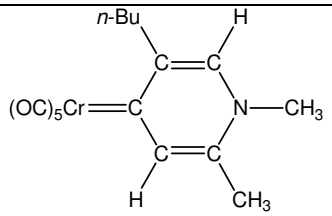

8

Assignment	δ / ppm*	
	7	**8**
^{1}H NMR		
NH	9.06 (1H, bs)	n.a.
CCH	6.14 (1H, s)	8.41 (1H, s)
NCH	n.a.	7.17 (1H, s)
OCH_3	4.36 (3H, s)	n.a.
NCH_3	2.96 (3H, d, $^{3}J_{H\text{-}H}$ = 5.4 Hz)	3.80 (3H, s)
CCH_3	1.98 (3H, s)	2.46 (3H, s)
$CH_2CH_2CH_2CH_3$	n.a.	3.08 (2H, m)
$CH_2CH_2CH_2CH_3$, $CH_2CH_2CH_2CH_3$	n.a.	1.56 (4H, m)
$CH_2CH_2CH_2CH_3$	n.a.	0.98 (3H, t, ^{3}J = 7.2 Hz)
^{13}C NMR		
$C^{carbene}$	285.0 (s)	232.5 (s)
CO^{trans}	224.6 (s)	226.1 (s)
CO^{cis}	219.7 (s)	221.0 (s)
CCH_3	157.6 (s)	135.5 (s)
CCH	119.1 (s)	146.9 (s)
C(n-Bu)	n.a.	153.7 (s)
OCH_3	64.3 (s)	n.a.
NCH_3	31.1 (s)	43.3 (s)
NCH	n.a.	131.4 (s)
CCH_3	19.7 (s)	38.9 (s)
$CH_2CH_2CH_2CH_3$	n.a.	34.1 (s)
$CH_2CH_2CH_2CH_3$	n.a.	22.9 (s)
$CH_2CH_2CH_2CH_3$	n.a.	18.8 (s)
$CH_2CH_2CH_2CH_3$	n.a.	14.1 (s)

Although the chemical shifts for the CO ligands in **7** and **8** are in the same region (δ 219 – 226 ppm), the $C_{carbene}$ signal for **7** is shifted downfield by 52.5 ppm compared to **8**. This huge difference can be ascribed to the "loss" of the electron withdrawing oxygen atom adjacent to the carbene carbon atom in **8**.

Mass spectrometry

The FAB MS data for complex **8** are summarised in Table 3.2. The typical fragmentation of carbonyl carbene complexes originating from consecutive CO ligand loss, is observed, as well as the molecular ion peak at *m/z* 355.0.

Table 3.2 FAB MS data of complexes **8**

m/z	Relative intensity	Fragment ion
355.0	5	$[M]^+$ (^{52}Cr)
327.3	6	$[M\text{-}CO]^+$
289.1	15	$[M\text{-}2CO]^+$
272.1	5	$[M\text{-}3CO]^+$
243.1	11	$[M\text{-}4CO]^+$
215.1	7	$[M\text{-}5CO]^+$

IR spectroscopy

Again, the data of the previously characterised complex, **7**, are listed together with the carbonyl frequencies observed for complex **8**. The number of bands observed is in accordance with complexes with a distorted C_{4v} symmetry. The IR-inactive, but Raman-active B_1 band is observed for complex **7**, but not for complex **8**. This indicates a lowering in local symmetry and probably a decrease in free rotation around the carbene bond. The fact that the A_1 band for **8** appears at a much lower frequency, indicates that the carbene ligand in **8** executes a higher π-back donation to the metal than the ligand in **7**. This observation confirms the fact that free rotation is restricted in complex **8**. These bands appear at similar frequencies observed for the previously prepared 4-(1*H*)-pyridylidene complexes.[59]

Tabel 3.3 IR data of complexes **7** and **8** in CH_2Cl_2

ν(CO)/cm^{-1}		
7	**8**	**Symmetry assignment**
2052.4 (m)	2040.4 (m)	$A_1^{(1)}$
1974.2 (w)	-	B_1
1926.4 (s)	1911.2 (s)	E
1899.4 (sh)	1881.6 (m)	$A_1^{(2)}$

3.2.2 The stoichiometric transfer of carbene ligands

An article summarising carbene transfer reactions between metal ions and illustrate the interesting features of this type of conversion in possible further applications, has already materialised in the late 1990s.[62] The extent of this type of transformation is however still very limited.

3.2.2.1 Synthesis and characterisation of a Rh(I) complex with a *r*NHC ligand

Since a compound containing a *r*NHC ligand bonded to the metal, rhodium, has not previously been reported, the complex described earlier, **8**, was dissolved with $[RhCl(CO)_2]_2$ in CH_2Cl_2 and the mixture stirred for 5 hours until carbon monoxide stopped evolving from the reaction mixture. During the process a dark coloured material, due to the decomposition of the $Cr(CO)_5$ complex, precipitated. A mixture of the *cis* and *trans* isomers (in ratio 1:0.8) of complex **9** was obtained as assessed by NMR spectroscopy. A single crystal X-ray analysis of suitable crystals obtained from the reaction mixture of **9** unequivocally confirmed the connectivities and electronic distribution within the *cis* isomer.

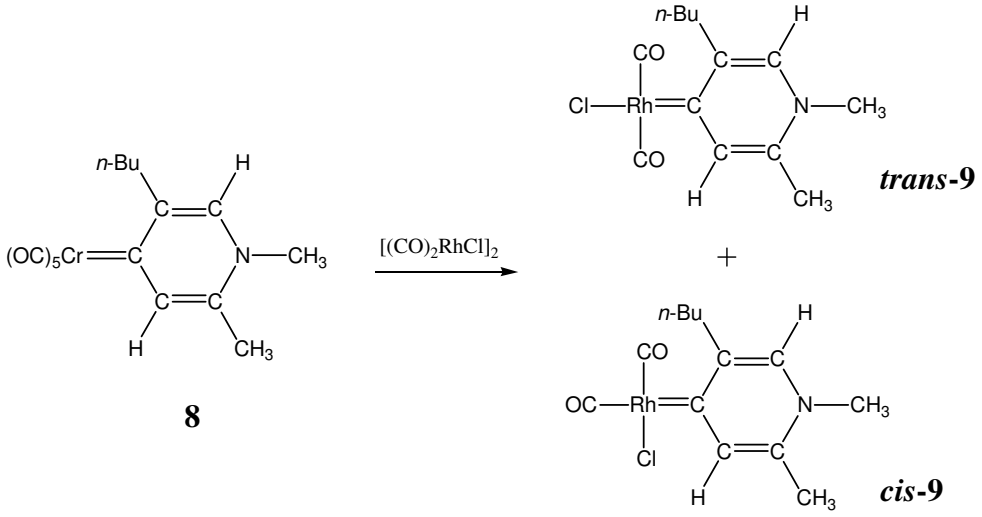

Scheme 3.3

3.2.2.2 Characterisation of *trans*-chloro(dicarbonyl)(*N*-methylpyrid-4-ylidene)rhodium(I), *trans*-9, and *cis*-chloro(dicarbonyl)(*N*-methylpyrid-4-ylidene)rhodium(I), *cis*-9

NMR spectroscopy

The assignment of the signals in the ^1H and ^{13}C NMR spectra of ***cis*-9** and ***trans*-9** are summarised in Table 3.4. Since separation of the geometric isomers could not be achieved by difference in

[62] S.-T. Liu and K. R. Reddy, *Chem. Soc. Rev.,* 1999, **28**, 315.

solubility or by column chromatography, NMR analysis was performed on the mixture of the two compounds. A complete set of signals for each of the two isomers was observed in both the ^{1}H and ^{13}C NMR spectra.

Table 3.4 ^{1}H and ^{13}C-{^{1}H} NMR data of compounds ***cis*-9** and ***trans*-9** in CD_2Cl_2

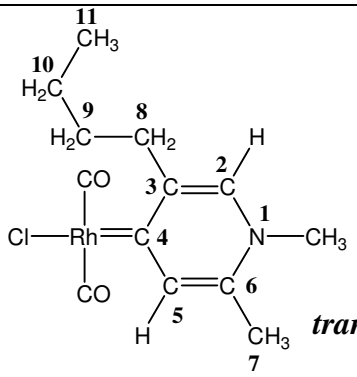

***trans*-9**

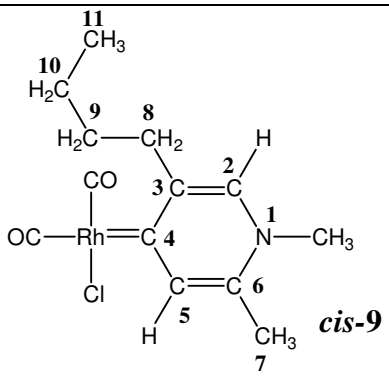

***cis*-9**

Assignment	δ / ppm*	
	***trans*-9**	***cis*-9**
^{1}H NMR		
NMe	3.94 (3H, s)	3.90 (3H, s)
H^2	7.60 (1H, s)	7.51 (1H, s)
H^5	8.11 (1H, s)	7.89 (1H, s)
H^7	2.54 (3H, s)	2.50 (3H, s)
H^8	3.04 (2H, m)	3.04 (2H, m)
H^9	1.80 (2H, m)	1.71 (2H, m)
H^{10}	1.48 (2H, m)	1.48 (2H, m)
H^{11}	1.02 (3H, m)	1.02 (3H, m)
^{13}C NMR		
NMe	44.1 (s)	44.4 (s)
C^2	135.3 (s)	135.3 (s)
C^3	150.3 (s)	149.7 (s)
C^4	211.0 (d, $^{2}J_{Rh-C}$ = 31.9 Hz)	209.2 (d, $^{2}J_{Rh-C}$ = 29.9 Hz)
C^5	141.8 (s)	141.8 (s)
C^6	138.8 (s)	139.6 (s)
C^7	37.8 (s)	38.5 (s)
C^8	33.1 (s)	33.1 (s)
C^9	23.0 (s)	22.8 (s)
C^{10}	19.5 (s)	19.5 (s)
C^{11}	14.1 (s)	14.1 (s)
CO (*trans*-**9**)	188.3 (d, $^{2}J_{Rh-C}$ = 50.9 Hz)	n.a.
CO_{cis} (*cis*-**9**)	n.a.	186.1 (d, $^{2}J_{Rh-C}$ = 79.7 Hz)
CO_{trans} (*cis*-**9**)	n.a.	192.2 (d, $^{2}J_{Rh-C}$ = 54.9 Hz)

The signals for NMe, H^2 and H^7 of ***cis*-9** and ***trans*-9** appear slightly downfield and H^5 slightly upfield in the ^{1}H NMR spectra when compared to the chemical shifts of these signals in complex **8**.

Four typical signals appear in the ^{1}H NMR spectra of ***cis*-9** and ***trans*-9** for the butyl substituents and only three in **8**, as a result of signal overlap. When comparing the two isomers, all the signals for ***trans*-9** appear at a somewhat lower field.

The carbonyl carbon *cis* to the carbene ligand in ***cis*-9** resonates as a doublet at δ 186.1 and the one *trans* to the carbene ligand at δ 192.2. This assignment is based on the difference in *trans* influence of the chloride ligand and the carbene ligand. The carbene ligand exhibits a larger *trans* influence than the chloride ligand and the ^{103}Rh-^{13}C coupling constant for the doublet assigned for the *trans*-carbonyl carbon (J = 54.9 Hz) should be smaller than that for the doublet assigned to the *cis*-carbonyl carbon (J = 79.7), as is indeed the case. The signal for the carbene carbon atom (C^4) of ***cis*-9** appears as a doublet at δ 209.2 (J = 29.9 Hz). This signal for C^4 has a smaller coupling constant because the CO ligand has a greater *trans* influence than the carbene ligand and an even greater *trans* influence than the chloride ligand. These assignments are consistent with the Rh(I) complexes with N^2HC^5 ligands reported by the group of Crabtree.[63]

The signal for the carbene carbon of ***trans*-9** appears ~2 ppm downfield compared to the chemical shift of the carbene carbon in ***cis*-9** (211.0 vs 209.2 ppm). A chemical shift of δ 172.4 is observed for the carbon donor in *trans*-carbonyl-(2,3,5,6-tetrafluoropyrid-4-yl)bis(triethylphosphine)-rhodium(I), one of the pyrid-4-yl-Rh(I) complexes reported before.[64] The coupling constant for the carbene carbon of ***trans*-9** is 2 Hz larger because the carbene ligand is located *trans* to the chloride (in ***cis*-9** the carbene ligand is located *trans* to a CO ligand) and halides have a much smaller *trans* influence than the CO-ligand.

Only one signal (δ 188.3) is observed for the CO ligands in ***trans*-9** since they are now in the same chemical environment and because of their greater *trans* influence they have a smaller rhodium-carbon coupling constant (50.9 Hz). The resonances of the other signals in the ^{13}C NMR spectrum of ***trans*-9** compare well with those in ***cis*-9**.

Mass spectrometry

The *cis*/*trans* complex mixture of compounds **9** was analysed by FAB MS and the results are listed in Table 3.5. No molecular ion peak is observed. Fragments with weak intensities are seen due to

[63] J. A. Mata, A. R. Chianese, J. R. Miecznikowski, M. Poyatos, E. Peris, J. W. Faller and R. H. Crabtree, *Organometallics,* 2004, **23**, 1253.
[64] D. Noveski, T. Braun, B. Neumann, A. Stammler and H.-G. Stammler, *Dalton Trans.,* 2004, 4106.

the loss of the chloride and the loss of two carbonyl ligands. A fragment with medium intensity due to the loss of both the halide and the CO ligands is observed.

Table 3.5 FAB MS data of compound ***cis/trans*-9**

m/z	Relative intensity	Fragment ion
322.2	7	$[M\text{-}Cl]^+$ (^{103}Rh)
301.6	5	$[M\text{-}2CO]^+$
264.0	45	$[M\text{-}2CO\text{-}Cl]^+$

Infrared spectroscopy

Carbonyl frequencies are sensitive to the electron density on the metal coordinated to it. Hence, the comparison of the CO stretching frequencies of complex **9** with those of analogous classical Rh-NHC complexes allows us to evaluate the donor strength of the pyridinyl-4-ylidene compared to ethyl methyl imidazol-2-ylidene ligand.[65] This method was utilised by Herrmann *et al.* and Bertrand *et al.* for a variety of carbenes.[66] In general a higher CO frequency indicates a lower electron density on the metal as affected by the σ-donation and π-acceptor ability of the ligand. A very σ-basic carbene ligand is characterised by strong σ-donation and little π-backdonation from the metal to such a ligand. It is believed that pyridylidene ligands are stronger σ-donors than imidazolylidene ligands as indicated by the DFT calculations performed by Frenking *et al.*,[17] and would therefore effect lower ν(CO) values.

Tabel 3.6 IR data of complexes ***cis*-9** and ***trans*-9** in CH_2Cl_2

ν(CO)/cm^{-1}	
***cis*-9**	***trans*-9**
2046.2 (s)	1915.1 (s)
1982.6 (s)	

Two bands are observed for ***cis*-9** as expected for the two CO ligands because they are chemically dissimilar. Comparing ***cis*-9** to *cis*-bromo(dicarbonyl)(1-ethyl-3-methyl-2,3-dihydro-*1*H-imidazol-2-ylidene)rhodium(I) (2079 and 2000 cm^{-1}; no solvent specified) and *cis*-chloro(dicarbonyl)[(*tert*-butyl)bis(diisopropylamino)ylidene]rhodium(I)[67] (2057 and 1984 cm^{-1}; considered to contain a very

[65] G. R. Julius, *PhD Dissertation*, University of Stellenbosch, December 2005, p 171.
[66] W. A. Herrmann, K. Öfele, D. von Preysing and E. Herdtweck, *J. Organomet. Chem.,* 2003, **684**, 235.
[67] V. Lavallo, J. Mafhouz, Y. Canac, B. Donnadieu, W. W. Schoeller and G. Bertrand, *J. Am. Chem. Soc.,* 2004, **126**, 8670.

basic ligand; no solvent specified), it is clear that pyrid-4-ylidene is significantly more π-basic than the two mentioned ligands.

Only one band is observed for the CO ligands in ***trans*-9**. These very strong π-acceptor ligands are mutually removing electron density from the metal into their π^*-orbitals, lowering the C-O bond orders and subsequently the CO-stretching frequencies.

3.2.2.3 Molecular and crystal structure of *cis*-9

A CH_2Cl_2 solution of the *cis*/*trans* mixture was layered with pentane (-20 °C) and yielded orange-yellow crystals of ***cis*-9**. The full molecular geometry of complex *cis*-**9** was elucidated by single-crystal X-ray diffraction. The POV-Ray diagram is shown in Figure 3.1 and selected bond distances and angles appear in Table 3.7.

An unknown electron density was identified as a solvent molecule that possible came from wet organic solvent used for crystallisation by using the SQUEEZE function in the Platon Software Package.[68] The water molecule was fixed as follows: O-H, 0.80 Å, H-H, 1.5 Å. All the water hydrogens have 1.5 times the U_{iso} of the oxygen atoms.

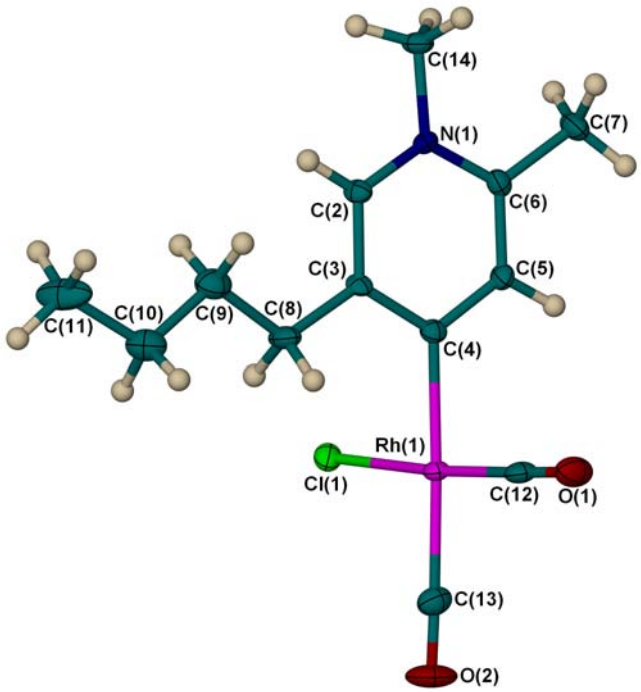

Figure 3.1 Molecular structure of ***cis*-9**, showing the numbering scheme, generated in POV-Ray; water solvent molecule omitted

[68] A. L. Apek, *J. Appl. Crystallogr.,* 2003, **36**, 7.

Table 3.7 Selected bond lengths (Å) and angles of complex ***cis*-9**

Bond lengths(Å)			
Rh(1)-C(12)	1.813(7)	N(1)-C(6	1.353(7)
Rh(1)-C(13)	1.930(6)	C(2)-C(3)	1.375(7)
Rh(1)-C(4)	2.067(5)	C(3)-C(4)	1.413(7)
Rh(1)-Cl(1)	2.383(2)	C(3)-C(8)	1.508(8)
O(1)-C(12)	1.151(7)	C(4)-C(5)	1.391(7)
O(2)-C(13)	1.121(7)	C(5)-C(6)	1.384(7)
N(1)-C(2)	1.351(7)		
Bond angles (º)			
C(12)-Rh(1)-C(13)	94.4(2)	N(1)-C(2)-C(3)	122.1(5)
C(12)-Rh(1)-C(4)	87.8(2)	C(2)-C(3)-C(4)	118.9(5)
C(13)-Rh(1)-C(4)	177.6(2)	C(5)-C(4)-C(3)	116.5(5)
C(12)-Rh(1)-Cl(1)	175.9(2)	C(5)-C(4)-Rh(1)	121.5(4)
C(13)-Rh(1)-Cl(1)	89.6(2)	C(3)-C(4)-Rh(1)	121.9(4)
C(4)-Rh(1)-Cl(1)	88.2(2)	C(6)-C(5)-C(4)	123.4(5)
C(2)-N(1)-C(6)	121.4(4)	N(1)-C(6)-C(5)	117.6(5)
C(2)-N(1)-C(14)	118.5(4)	O(1)-C(12)-Rh(1)	178.7(5)
C(6)-N(1)-C(14)	120.0(4)	O(2)-C(13)-Rh(1)	178.3(6)

The central metal in complex ***cis*-9** exhibits a distorted square-planar geometry in which the two CO ligands have a *cis* arrangement. The least square plane through the carbene ligand [N(1), C(2), C(3), C(4), C(5) and C(6)] has an angle of 75.43(15) ° with the least square plane through the metal and its other ligands [Rh(1), C(12), C(13) and Cl(1)].

A search on the CCSD gave no results for previously prepared pyrid-4-ylidene-Rh(I) complexes. A few examples, however, of pyrid-4-yl-Rh(I) complexes are known.[64] The Rh-C bond distances of these complexes range between 2.062(1) and 2.092(2) Å, similar to observations for the metal carbene bond in complex ***cis*-9** [2.067(5) Å]. It is interesting that the CO-ligand in *trans*-carbonyl(2,3,5,6-tetrafluoropyrid-4-yl)bis(triethylphosphine) rhodium(I)[64] exerts a stronger *trans* influence on the pyridyl ligand than the CO-ligand *trans* to the carbene ligand in ***cis*-9** on the carbene. The metal-carbon bond *trans* to the carbonyl group in *trans*-carbonyl-(2,3,5,6-tetrafluoropyrid-4-yl)bis(triethylphosphine)rhodium(I) of 1.849(2) Å does not differ significantly when compared to the Rh(1)-C(13) separation found in ***cis*-9**.

When comparing the pyridine ligands, the N-CH bond distances in ***cis*-9** are significantly longer than in *trans*-carbonyl(2,3,5,6-tetrafluoropyrid-4-yl)bis(triethylphosphine)rhodium(I) [1.351(7) compared to 1.324(2) Å]. Investigation of the remainder of the bond distances in the pyridine-derived ligands, reveals that they are similar in the two complexes. The bond angles are also similar, except the C-C(donor)-C angle in *trans*-carbonyl(2,3,5,6-tetrafluoropyrid-4-

yl)bis(triethylphosphine)-rhodium(I), which is 111.7(1) ° compared to 116.5(5) ° in the neutral carbene complex. This again indicates that the hybridisation of the two carbon donors differs, since steric reasons can not be the origin of the difference observed in the C-C(donor)-C angle. When the chemical shift of the carbon donors are compared in the ^{13}C NMR [δ 209.2 for ***cis*-9a** and δ 172.4 for *trans*-carbonyl(2,3,5,6-tetrafluoropyrid-4-yl)bis(triethylphosphine)rhodium(I)] the decrease of this angle is congruent with the high field shift of the complex. This phenomenon has been previously reported for N^2HC^5 ligands by Kunz and co-workers.[69]

Figure 3.2 shows the packing of the molecules of ***cis*-9** in the unit cell viewed along the b-axis. The molecules assemble in a diagonal fashion on top of one another with each alternating layer directed in the opposite direction. This leads to rows of ligand interchanged by rows of the Rh-center with the water molecules packed in the spaces in between.

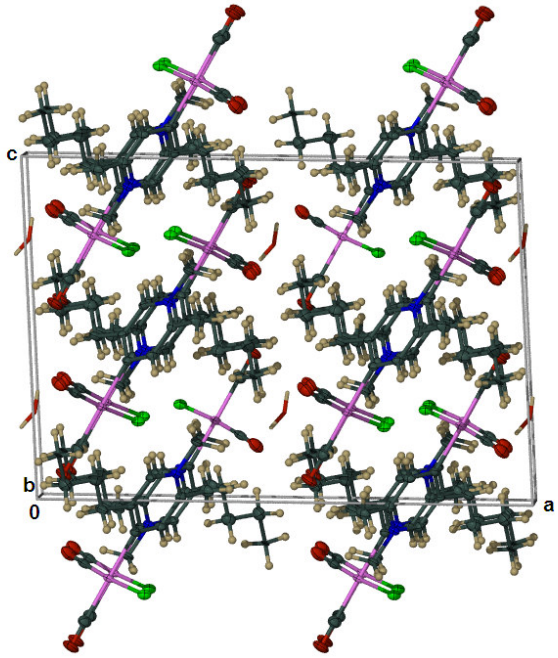

Figure 3.2 Packing diagram of the molecules of ***cis*-9** along the b-axis

3.2.3 Other attempts at stoichiometric carbene transfer

The Ag-carbene complex (**XXI**) undergoes a facile reaction with $(PhCN)_2PdCl_2$ to yield the carbene complex (C^N)$PdCl_2$ (**XXII**). The structural diversity of silver(I) N-heterocyclic carbenes have been widely studied as mentioned earlier, and their application as transmetalation reagents have

[69] M. Nonnenmacher, D. Kunz, F. Rominger and T. Oeser, *Chem. Commun.,* 2006, 1378.

widened their use as they provide easy access to various catalytic transition-metal NHC complexes.[70]

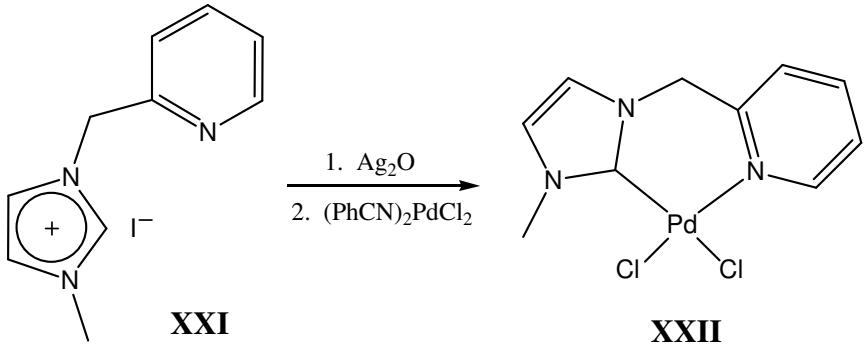

XXI **XXII**

The transfer of the nN^{1}HC^6 ligand from Ni to Pd was attempted by reacting *trans*-chloro(N-methyl-1,4-dihydro-pyrid-4-ylidene)bis(triphenylphosphine)Ni(II) tetrafluoroborate with $(PhCN)_2PdCl_2$ in CH_2Cl_2. The product formed single crystals that formed in the reaction mixture and were determined to be the halide bridged complex, **10** (Figure 3.3). The same complex was obtained as a byproduct when [PdCl(*C,N*4-$CH_2C_8H_5N_2$-5)(PPh_3)] was reacted with $(PhCN)_2PdCl_2$.[71] There was no indication of the expected product in the NMR spectrum of the reaction mixture, and signals for the unreacted Ni-complex could also be assigned. Halide-bridged complexes of palladium(II) and platinum(II) are extremely useful as starting materials in the syntheses of organometallic and coordination compounds.[72] By cleavage of the halide bridges with other ligands, many new complexes are accessible, some of which are most valuable as homogeneous catalysts. Since this Cl-bridged complex has been prepared and used as starting material in conjunction with diorganomercurials to form halide-bridged alkyl- and arylpalladium(II) dimers previously[73] and since the crystal structures of **10**[74] and its benzene solvate[75] have been reported, the CH_2Cl_2 solvate is briefly discussed for the sake of completeness.

Yellow crystals of complex **10** were obtained by layering the reaction mixture in CH_2Cl_2 with pentane at -20 °C. Complex **10** crystallises in the unusual space group $P4_12_12$ and Figure 3.3 shows a POV-Ray plot of the molecular structure. Selected bond lengths and angles are summarized in Table 3.8. The asymmetric unit consists of half of the molecule and the other half is generated through an inversion center indicated by the prime symbol.

---

[70] J. C. Garrison and W.J. Youngs, *Chem. Rev.,* 2005, **105**, 3978.
[71] J. Vicente, M.C. Lagunas, E. Bleuel and M. Ramírez de Arellano, *J. Organomet. Chem.,* 2002, **648**, 62.
[72] F. R. Hartley, *Organomet. Chem. Rev., Sect. A,* 1970, **6**, 119.
[73] G. K. Anderson, *Organometallics,* 1983, **2**, 665.
[74] X-ray crystallographic data (excluding structure factors) for *trans*-[PdCl(μ-Cl)(PPh_3)]$_2$ have been deposited with the Cambridge Crystallographic Data Centre as a Private Communication, J. Vicente, M.C. Lagunas, E. Bleuel and M. Ramírez de Arellano, CCDC-100877, 1997.
[75] C. Sui-Seng, F. Belanger-Ganepy and D. Zarganan, *Acta Cryst. E,* 2003, **59**, m618.

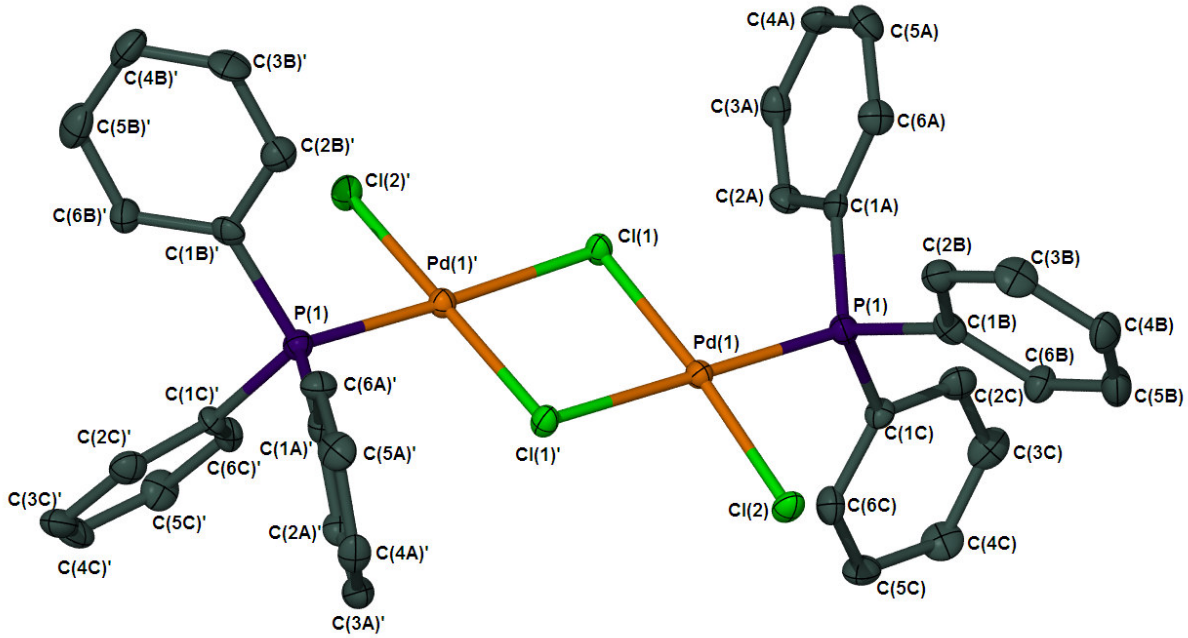

Figure 3.3 Molecular structure of **10**, CH_2Cl_2 molecule and H-atoms omitted for clarity

Binuclear complexes of Pd(II) and Pt(II) with a double halide or pseudohalide bridge are well known. Most of them exhibit a *trans* structure like **10** with the *cis* geometry being very rare.[76]

Table 3.8 Selected bond distances (Å) and bond angles (°) of compound **10**

Bond lengths(Å)			
Pd(1)-P(1)	2.222(2)	Pd(1)-Cl(1)'	2.317(2)
Pd(1)-Cl(2)	2.277(2)	Pd(1)-Cl(1)	2.423(2)
Bond angles (º)			
P(1)-Pd(1)-Cl(2)	87.02(6)	Cl(2)-Pd(1)-Cl(1)'	91.96(5)
P(1)-Pd(1)-Cl(1)	95.81(6)	Cl(1)-Pd(1)-Cl(1)'	85.38(5)
Cl(2)-Pd(1)-Cl(1)	175.25(6)	Pd(1)-Cl(1)-Pd(1)'	94.52(5)
P(1)-Pd(1)-Cl(1)'	177.30(6)		

The $Pd(PPh_3)Cl_3$ coordination is approximately square planar. As a result of the *trans* influence of the phosphine ligand the bond distance of Pd-Cl(1) [2.423(2) Å] is longer than the bond distance of Pd-Cl(1)' [2.317(2) Å] and Pd-Cl(2) [2.277(2) Å]. A search on the Cambridge crystallograhic and structural database lead to a selection of 29 compounds with the same backbone, $[ClP(PR_3)PdCl]_2$, as complex **10**. The bond lengths of these reported structures do not differ significantly from those

[76] R. J. Phuddephatt and P. J. Thompson, *J. Chem. Soc., Dalton Trans.,* 1977, 1219; G. K. Anderson, R. J. Cross and D. S. Rycroft, *J. Chem. Res. (s),* 1977, 120.

of the CH_2Cl_2 solvate. The small discrepancies observed in the respective bond angles are most probably only due to crystal packing forces.

The molecular packing of complex **10** as viewed along the c-axis is shown in Figure 3.4. The Pd-Cl moieties are arranged in pairs diagonally, two vertical alternated by two horisontal. The CH_2Cl_2 solvent molecules are located in voids between the pairs. Viewing the benzene solvate along the same axis a row of complex molecules is interchanged with a row of benzene solvent molecules.

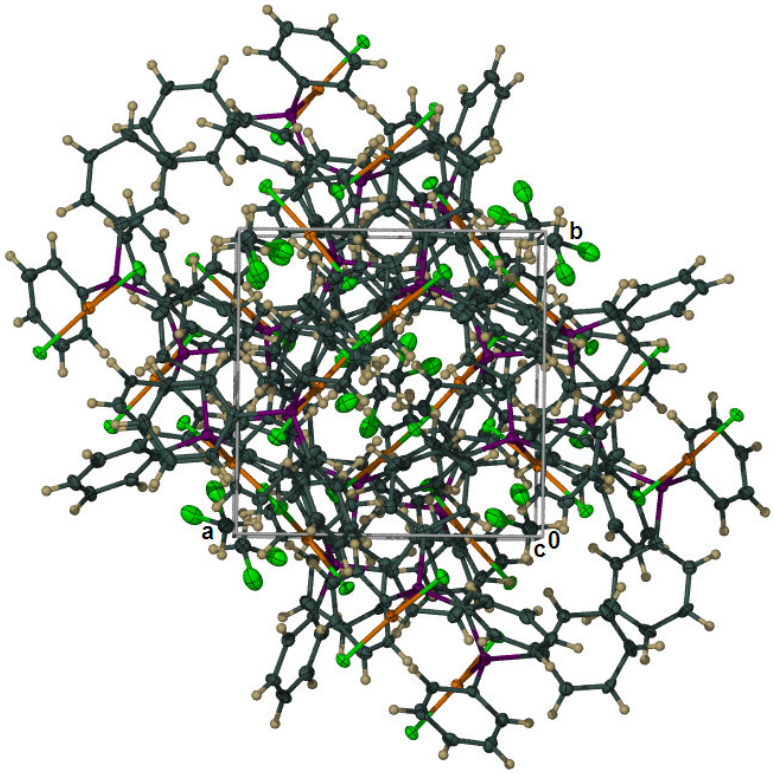

Figure 3.4 Molecular packing of complex **10** viewed along the c-axis

3.2.4 A comparison of the different positions of metal-carbon bonding in pyridinium-derived ligands

As mentioned in Section 3.1.1, a marked difference in activity and physical properties was observed for pyridylidene ligands (2- and 4-) bonded to Ni(II) and Pd(II),[17,18] thus we felt it necessary to also synthesise the 3-pyridinium salt precursor and its metal complexes (Ni and Pd) and compare these complexes both experimentally and computationally, and later catalytically (Chapter 5). Relevant to the present study, Schwarz and co-workers[77] generated both the *normal* and *abnormal* free carbene

[77] D. Lavorato, J. K. Terlouw, T. K. Dargel, W. Koch, G. A. McGibbon and H Schwarz, *J. Am. Chem. Soc.,* 1996, **118**, 11898.

isomers of pyridine in gas phase. The *normal* isomer is less stable than pyridine by nearly 50 kcal.mol^{-1} and *remote* free carbenes are even less stable. For the sake of completeness, the ligand precursors, pyrid-2-ylidene and pyrid-4-ylidene and their respective Ni(II) and Pd(II) complexes, previously prepared with tetrafluoroborate as anion, were resynthesised, now with $CF_3SO_3^-$ as counterion.

3.2.4.1 Synthesis of pyridinium-type ligands, 2-chloro-*N*-methylpyridnium triflate, 11, 3-chloro-*N*-methylpyridinium triflate, 12, and 4-chloro-*N*-methylpyridinium triflate, 13

Ligand precursors **11-13** were prepared by *N*-methylation of the corresponding starting materials with $CF_3SO_3CH_3$ in CH_2Cl_2 (Scheme 3.4). Washing the resulting precipitates with ether and/or THF, yielded compounds **11**-**13** as white powders in a moderate to high yield (55 - 98 %). In the method employed previously by Stone and co-workers,[78] the alkylation is performed in a mixture of CH_2Cl_2 and CH_3CN (3:1) as reaction solvent. Since the alkylating agent is capable of alkylating the acetonitrile as seen in Section 2.2.1, the reaction in our hands was preformed in neat CH_2Cl_2. Compounds **11**-**13** are soluble in dichloromethane, but not in pentane, diethyl ether or THF.

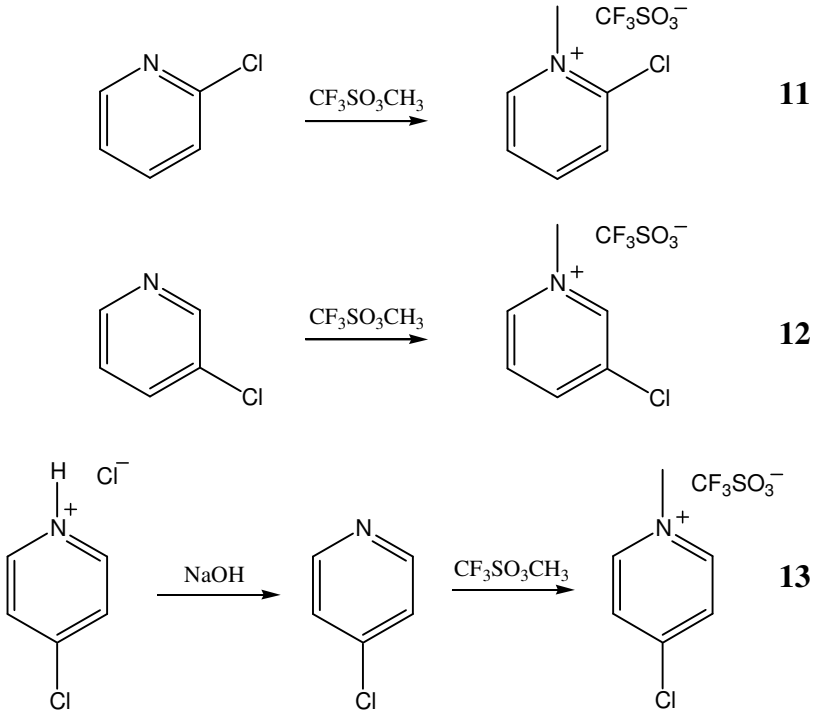

Scheme 3.4

[78] P. J. Fraser, W. R. Roper and F. G. A. Stone, *J. Chem. Soc., Dalton Trans.,* 1974, 760.

3.2.4.2 Spectroscopic characterisation of 2-chloro-*N*-methylpyridnium triflate , 11, 3-chloro-*N*-methylpyridinium triflate, 12, and 4-chloro-*N*-methylpyridinium triflate, 13

NMR spectroscopy

The NMR data of **11**, **12** and **13** are reported in Table 3.9. Although the NMR data of **11** in CD_3CN[79] and the tetrafluoroborate salts of **11**[80] and **13**[81] in CD_2Cl_2 has previously been discussed, the newly prepared $CF_3SO_3^-$ analogues is briefly discussed and compared to the 3-pyridinium salt (all collected in CD_2Cl_2).

The positions of the chemical shifts in the ^1H NMR spectra of compounds **11**-**13** can be explained by the positive charge on the nitrogen atom that can be localised at different carbon atoms as depicted in Scheme 3.5

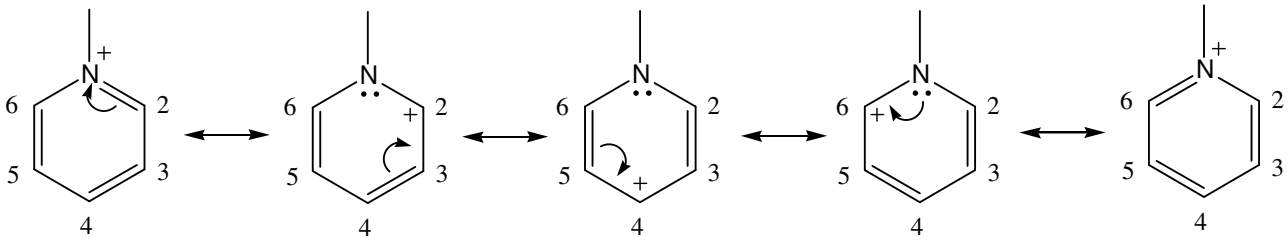

Scheme 3.5

The positive charge on the nitrogen can be localised at C^2, C^4 and C^6 and has a deshielding effect on the hydrogen atoms attached to it.[82] The electronegative nitrogen atom tries to retain its neutrality by draining electron density from the ring and thus increasing the nucleophilicity of the 4-position in the pyridnium salts.

H^6 appears at the lowest field for compounds **11** and **13**, H^2 and H^6 (symmetrical molecule) for compound **13** (δ 9.18 and 8.82 repectively) and H^2 for compound **12** (δ 9.38). These positions are elucidated by the fact that these hydrogen atoms are situated the closest to the positively charged N-atom. This positive charge on the N-atom can be localised at C^2, C^4 and C^6 and has a deshielding effect on the protons attached to the corresponding carbon atoms.[83] Deshielding due to the adjacent N-atom, combined with the further deshielding result of the resonance effect, verify the chemical

[79] J. J. Folmer, C. Acero, D. L. Thai and H. Rapoport, *J. Org. Chem.,* 1998, **63**, 8170.
[80] G. R. Julius, *PhD Dissertation*, University of Stellenbosch, December 2005, p 36.
[81] G. R. Julius, *PhD Dissertation*, University of Stellenbosch, December 2005, p 53.
[82] D. L. Pavia, G. M. Lampman, G. S. Kriz, *Intoduction to Spectroscopy,* 3rd Edition, Harcourt College Publishers, Fort Worth, 2001, p. 257.
[83] D. L. Pavia, G. M. Lampman and G. S. Kriz, *Introduction to Spectroscopy,* 3rd Ed., Harcourt College Publishers, Fort Worth, 2001, p. 111.

shift of H^6 even more. The even further deshielding effect of the electronegative chlorine atom for compound **12**, explains this position. The hydrogens at positions 3, 4 and 5 (if not substituted with a chlorine) appear more upfield because they are located further away from the positively charged N-atom. Typical fine structure is observed for all the protons owing to the respective coupling with other hydrogen atoms. Due to the aromatic nature of pyridinium ligands, even long range couplings over four bonds are observed *eg*. the signal for H^6 in complex **12** appears as a doublet of multiplets.

Table 3.9 NMR data of compounds **11**, **12** and **13** in CD_2Cl_2

11 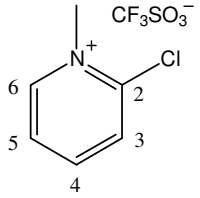

12 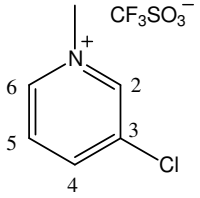

13 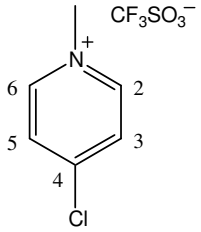

	δ / ppm*		
Assignment	**11**	**12**	**13**
^{1}H NMR			
NMe	4.49 (3H, s)	4.63 (3H, s)	4.45 (3H, s)
H^2	n.a.	9.38 (1H, d, ^4J = 0.5 Hz)	n.a.
H^3	8.06 (1H, dd, ^3J = 8.3 Hz, ^4J = 1.3 Hz)	n.a.	n.a.
H^4	8.45 (1H, td, ^3J = 8.3 Hz, ^3J = 1.7 Hz	9.15 (1H, d, ^3J = 6.3 Hz)	n.a.
H^5	8.02 (1H, m)	8.29 (1H, dd, ^3J = 8.3 Hz, ^3J = 6.3 Hz)	n.a.
H^6	9.18 (1H, dd, ^3J = 6.2 Hz, ^3J = 1.7 Hz	8.81 (1H, dm, ^3J = 8.3 Hz)	n.a.
H^2, H^6	n.a.	n.a.	8.82 (2H, d, ^3J = 6.8 Hz)
H^3, H^5	n.a.	n.a.	8.01 (2H, d, ^3J = 6.8 Hz)
^{13}C NMR			
NMe	48.5 (s)	49.7 (s)	49.0 (s)
C^2	n.a.	146.7 (s)	n.a.
C^3	130.0 (s)	136.1 (s)	n.a.
C^4	147.3 (s)	146.4 (s)	155.3 (s)
C^5	127.1 (s)	130.1 (s)	n.a.
C^6	n.a.	146.1 (s)	n.a.
C^2, C^6	149.4 (bs)	n.a.	147.0 (bs)
C^3, C^5	n.a.	n.a.	129.5 (s)

The signals for C^3 and C^5 appear at somewhat higher field strength than C^2, C^4 and C^6 in all three compounds because of the resonance effect discussed earlier (Scheme 3.5). The negative inductive effect of the chlorine atom does not result in significant deshielding for compound **11**, but it does in compounds **12** and **13** with the chemical shifts for C^3 and C^4, respectively, being more downfield than the comparative positions in the other compounds (**11** - **13**). C^3 and C^5 also appear at higher

field strength in all the compounds compared to the other positions since they do not experience the deshielding effect due to the resonance effect.

Mass spectrometry

Analysis of compound **12** by FAB-MS produced a spectrum with peaks matching the isotopic distribution expected in the theoretical isotope distribution for the chloro and nitrogen containing compound (Table 3.10). Since the BF_4^- salts of compound **11** and **13** have previously been analysed, the data are not reported here as they are similar to those for the triflate salts.

Table 3.10 FAB-MS data of compound **12**

Complex	*m/z*	Relative intensity	Fragment ion
12	130.1	35	$[M\text{-}CF_3SO_3]^+$ (^{37}Cl)
	128.1	100	$[M\text{-}CF_3SO_3]^+$ (^{35}Cl)

3.2.4.3 Synthesis of the carbene complexes *trans*-chloro(*N*-methyl-1,2-dihydro-pyrid-2-ylidene)bis(triphenylphosphine)palladium(II) triflate, 14a, *trans*-chloro(*N*-methyl-1,2-dihydro-pyrid-2-ylidene)bis(triphenylphosphine)nickel(II) triflate, 14b, *trans*-chloro(*N*-methyl-1,3-dihydro-pyrid-3-ylidene)bis(triphenylphosphine)palladium(II) triflate, 15a, *trans*-chloro(*N*-methyl-1,3-dihydro-pyrid-3-ylidene)bis(triphenylphosphine)nickel(II) triflate, 15b, *trans*-chloro(*N*-methyl-1,4-dihydro-pyrid-4-ylidene)bis(triphenylphosphine)palladium(II) triflate, 16a, and *trans*-chloro(*N*-methyl-1,4-dihydro-pyrid-4-ylidene)bis(triphenylphosphine)-nickel(II) triflate, 16b

Procedures documented in literature were slightly modified[17,84] to obtain the cationic complexes of Pd(II) and Ni(II) by oxidative substitution. The ligand precursors **11**-**13** were reacted overnight with $M(PPh_3)_4$ at either 60 °C in toluene (Pd) or room temperature in THF (Ni) according to Scheme 3.6. Since oxidative substitution of imidazolium salts to Ni is much more favourable than to Pd due to a much smaller activation barrier,[85] the reactions for Ni were executed at room temperature. These complexes were all obtained in very good yields as microcrystalline powders, some of which had a metallic lustre. These products are soluble in dichloromethane and acetone, less soluble in diethyl ether and very sparingly in paraffins.

[84] S. K. Schneider, P. Roembke, G. R. Julius, H. G. Raubenheimer and W. A. Herrmann, *Adv. Synth. Catal.,* 2006, **348**, 1862

[85] D. S. McGuinness, K. J. Cavell, B. F. Yates, B. W. Skelton and A. H. White, *J. Am. Chem. Soc.,* 2001, **123**, 8317.

Complexes **14** and **16** are written in the pyridylidene form and complex **15** in the pyridinium form owing to the *abnormal* coordination in the latter that disallows the other canonical structure.

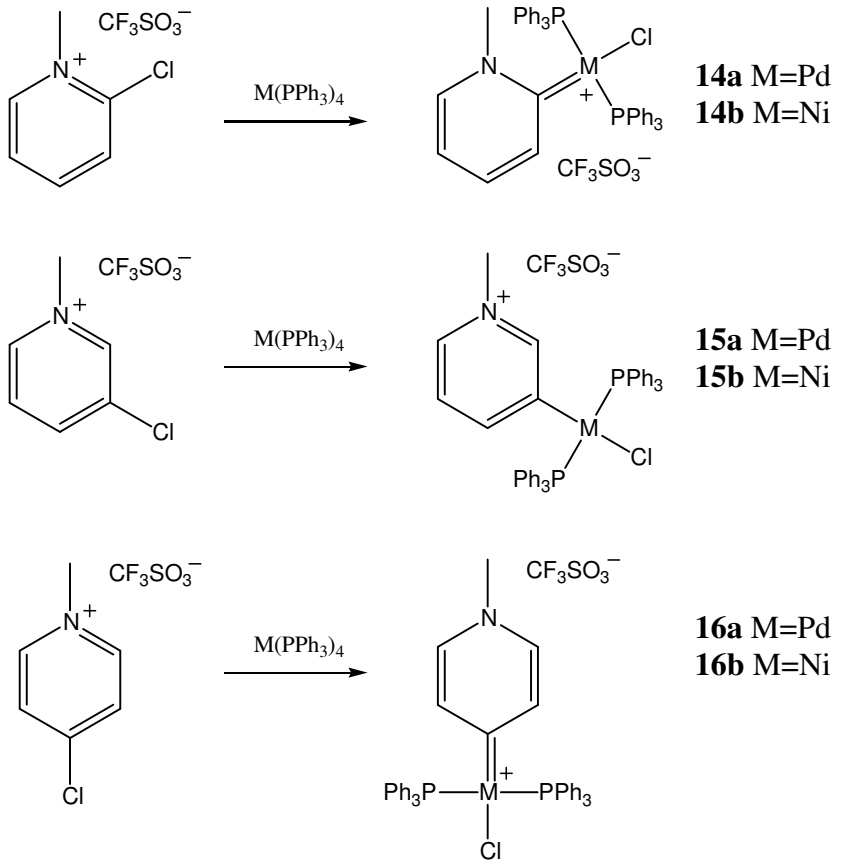

Scheme 3.6

NMR spectroscopy

The unambiguous assignments of the peaks in the NMR spectra of complexes **14** - **16** were performed with the help of ghsqc and ghmqc two-dimensional NMR techniques. The upfield positions of the complex signals compared to the carbene ligand precursors are attributed to the fact that palladium containing $MCl(PR_3)_2$ groups have been described as strong electron donors to aromatic rings in both resonance and inductive modes.[86] The NMR data of complexes **14a**, **15a** and **16a** are listed in Table 3.11 and those of complexes **14b**, **15b** and **16b** in Table 3.12.

[86] G.W. Parshall, *J. Am. Chem. Soc.,* 1966, **88**, 704; G. W. Parshall, *J. Am. Chem. Soc.,* 1974, **96**, 2360.

Table 3.11 NMR data of complexes **14a**, **15a** and **16a** in CD_2Cl_2

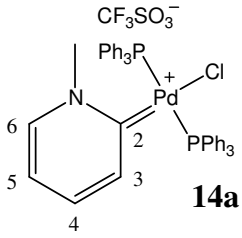

14a

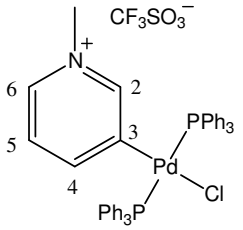

15a

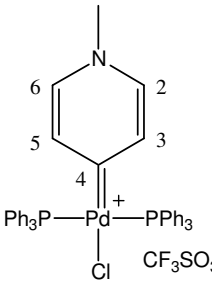

16a

Assignment	δ / ppm*		
	14a	**15a**	**16a**
^{1}H NMR			
NMe	3.96 (3H,s)	3.54 (3H, s)	3.80 (3H, s)
H^2	n.a.	7.26 (1H, bs)	n.a.
H^3	7.89 (1H, d, ^3J = 6.0 Hz)	n.a.	n.a.
H^4	n.a.	7.78 (1H, d, ^3J = 7.7 Hz)	n.a.
H^5	n.a.	6.73 (1H, dd, ^3J = 7.7 Hz, ^3J = 6.0 Hz)	n.a.
H^4, H^5	7.00 (2H, m)	n.a.	n.a.
H^6	n.a.	7.82 (1H, d, ^3J = 6.0 Hz)	n.a.
H^2, H^6	n.a.	n.a.	7.16 (2H, d, ^3J = 6.4 Hz)
Ph, H^3, H^5	n.a.	n.a.	7.39 (14H, m)
Ph, H^6	7.52, 7.40 (31H, 2 x m)	n.a.	n.a.
Ph	n.a.	7.58, 7.49, 7.40 (30H, 3 x m)	7.62, 7.50 (18H, m)
^{13}C NMR			
NMe	52.8 (s)	47.9 (s)	46.5 (s)
C^2	189.3 (t, $^2J_{C\text{-}P}$ = 6.5 Hz)	148.0 (t, $^3J_{C\text{-}P}$ = 4.9 Hz)	n.a.
C^3	138.1 (t, $^3J_{C\text{-}P}$ = 3.9 Hz))	165.0 (t, $^2J_{C\text{-}P}$ = 6.9 Hz)	n.a.
C^4	137.3 (s)	151.7 (t, $^3J_{C\text{-}P}$ = 3.5 Hz)	197.7 (t, ^2J = 6.5 Hz)
C^5	122.3 (s)	124.8 (s)	n.a.
C^6	145.4 (s)	137.9 (s)	n.a.
C^2, C^6	n.a.	n.a.	137.4 (s)
C^3, C^5	n.a.	n.a.	136.8 (bs)
Ph^{ipso}	128.9 (m)	129.0 (m)	130.0 (m)
Ph^{ortho}	134.3 (m)	134.8 (m)	135.2 (m)
Ph^{meta}	129.3 (m)	129.4 (m)	129.2 (m)
Ph^{para}	131.8 (s)	131.4 (s)	131.7 (s)
^{31}P NMR			
PPh_3	22.7 (s)	24.9 (s)	23.6 (s)

The ^{1}H NMR data of complex **14a** are similar to those reported for *trans*-chloro-(*N*-methyl-1,2-dihydro-pyrid-2-ylidene)bis(triethylphosphine)palladium(II) perchlorate[87] and *trans*-chloro-(*N*-methyl-1,2-dihydro-pyrid-2-ylidene)bis(triphenylphosphine)palladium(II) tetrafluoroborate and the

[87] B. Cociani, F. Di Bianca, A. Giovenco and A. Scrivanti, *J. Organomet. Chem.,* 1983, **251**, 393.

data of **16a** is similar to *trans*-chloro-(*N*-methyl-1,4-dihydro-pyrid-4-ylidene)bis(triethylphosphine) palladium(II) tetrafluroborate.[84]

Replacement of the Cl atom in compounds **11** - **13** by Pd-units causes a marked change to higher field of the heterocyclic ring protons. The greatest upfield change in chemical shift in the ^{1}H NMR spectra are observed for H^2 and H^6 because these protons are more deshielded as a result of the resonance effect earlier described, but due to the positive charge being located primarily on the metal the deshielding is minimised. The same trend is observed for the oxidative substitution complex *trans*-[PdCl{C_5H_3N(6-Cl)-C^2}(PPh_3)$_2$].[88] ^{13}C NMR spectra of metallated pyridines have previously been shown to involve large up-field changes in chemical shift for the pyridine carbons compared to those in the uncoordinated pyridine rings, suggesting an increase in electron density in the pyridine ring upon coordination.[89]

The *para* carbon atoms resonate as singlets and the *ortho, meta* and *ipso* carbon atoms of the phenyl rings resonate as pseudo-triplets due to magnetic inequivalence, in other words, coupling between the phosphorous atom and phenyl carbons results in a second order spectrum. These spectra can be analysed by calculations performed by simulation and iteration methods.[90]

The signals for carbene carbons of nN^{2}HC^5 Pd complexes appear in the range 161 – 182 ppm.[91] The most significant feature of the complexes is the resonance of the carbon donor atom. Complexes **14a** and **16a** exhibit a resonance at δ 189.3 and δ 197.7 respectively, compared to the same signal in **15a** which is *ca.* 30 ppm shifted upfield. In the latter instance, the pyridine ring therefore coordinates to the Pd center as a deprotonated pyridinium ligand. In contrast to this, the resonances at lower field for the Pd-C bonded carbons in **14a** and **16a** indicate carbenic character, that is, the C_5N ring may also be partially represented as a pyridylidene ligand. Such a remarkable difference was also observed for bis(pyridine)ruthenium(II) complexes induced by cyclometalation of *N*'-methylated bipyridinium analogues.[92] The compound bound through C^3 (**A**) exhibits typical pyridinium character (40 ppm upfield change in chemical shift compared to the same signal in the free ligand) whereas the compound bound through C^4 (**B**) displays pyridylidene.

[88] A. Mantovani, *J. Organomet. Chem.,* 1983, **255**, 385.
[89] R. R. Schrock and J. A. Osborn, *Chem. Commun.,* 1970, 567.
[90] H. Freibolin, in *Basic One- and Two-Dimensional NMR Spectroscopy,* Wiley-VCH, Weinheim, 4th ed., 2005, p. 124-125.
[91] X. Wang, S. Liu, L.-H. Weng and G.-X. Jin, *Organometallics,* 2006, **25**, 3565.
[92] T. Koizumi, T. Tomon and K. Tanaka, *J. Organomet. Chem.,* 2005, **690**, 1258.

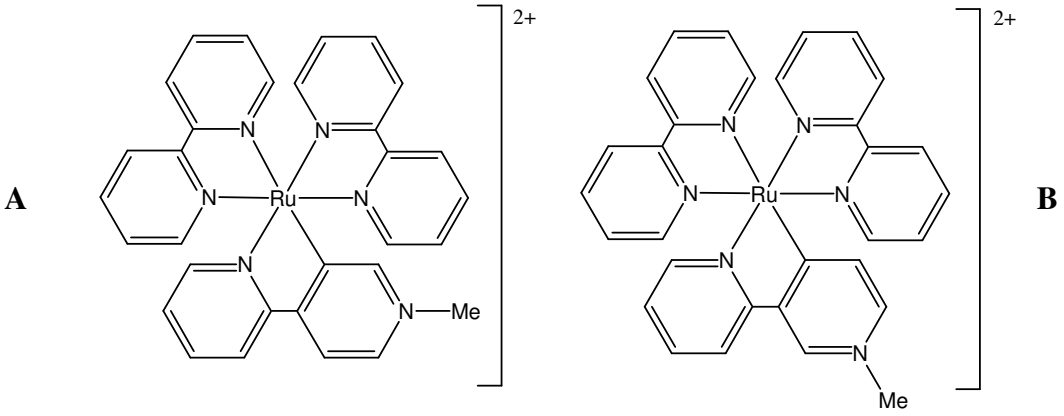

The same trend was also observed when terpyridine (N,N,C)-tridentate ligands were cyclometalated with Ru(II).[93] The same authors also reported the coordination of the related bidentate 1,8-naphthyridine and terpyridine tridentate ligands to Ru(II) showing either pyridinium or pyridylidene character.[94] However, this crude approach takes mainly accounts for the metal's pulling effect, whereas carbene bonding type is responsible for the pushing (*i.e*. backbonding) component. Examination of the shielding in the backbone of the ligand in **15a** upon metallation yields upfield shifts from about 5 to 10 ppm. The *normal* and *remote* ligands are more closely related to each other than to the abnormal one, but absolute carbene carbon ^{13}C NMR shifts should not be taken as a measure of carbene character. The chemical shifts of the metal bonded carbons in *normal* M-pyridylidene complexes are in the range 211-260 ppm (M = Cr),[95] 212-219 ppm (M = W),[96] 241 – 242 ppm (M = Mn)[97] and 252 ppm (M = Rh).[98] This change in chemical shift is of the same order of magnitude as those reported for Pd compounds upon metal-carbon bond formation.[99] The metal-C carbon signals appear as triplets with coupling constants of about 5 – 7 Hz, indicating the *trans* arrangement of the two phosphine ligands in solution.

The synthesis of a *remote* NHC complex (**XXIII**) was reported by Albrecht and co-worker.[100] The claim was made on the basis of a chemical shift of 176.2 ppm for the carbon directly bonded to the palladium. This chemical shift is however low compared to pyridine-derived carbene complexes

[93] T. Koizumi, T. Tomon and K. Tanaka, *Organometallics,* 2003, **22**, 970.
[94] T. Koizumi, T. Tomon and K. Tanaka, *J. Organomet. Chem.,* 2005, **690**, 4272.
[95] F. Stein, M. Duetsch, M. Noltemeyer and A. de Meijere, *Synlett,* 1993, 486; R. Aumann and P. Hinterding, *Chem. Ber.,* 1992, **125**, 2765.
[96] R. Aumann, M. Kössmeier, K. Roths and R. Fröhlich, *Synlett,* 1994, 1041; R. Aumann, K. Roths and M. Grehl, *Synlett,* 1993, 669.
[97] U. Kirchgässner, H. Piana and U. Schubert, *J. Am. Chem. Soc.,* 1991, **113**, 2228; C. Gimenes, N. Lugan, R. Marthien and G. L. Geoffroy, *J. Organomet. Chem.,* 1996, **517**, 133.
[98] U. Schubert and S. Seebald, *J. Organomet. Chem.,* 1994, **472**, C15.
[99] B. E. Mann and B. F. Taylor, in ^{13}C NMR Data for Organometallic Compounds, ed. P. M. Maitlis, F. G. A. Stone and R. West, Academic Press, London, 1981.
[100] M. Albrecht and H. Stoeckli-Evans, *Chem. Commun.,* 2005, 4705.

previously described by our group. No molecular structure determination was reported for **XXIII**. The assignment above is also doubted by Rourke *et al.*[101] who synthesised a platinum carbene complex from the reaction of a 2,6-disubstituted pyridine with potassium tetrachloroplatinate. Three other complexes with different co-ligands were also synthesised but described as pyridinium salts (zwitterionic structure) due to their high field ^{13}C chemical shifts (165.6 – 177.0 ppm) for the metal bonded carbon.

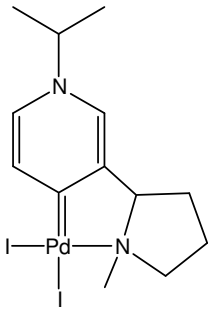

XXIII

All PPh_3 ligands display similar resonances in the ^{13}C NMR spectra; the C_{ipso} (128.9 – 130.0 ppm), C_{ortho} (134.2 – 134.8 ppm), C_{meta} (129.2 – 129.4 ppm) and C_{para} (131.4 – 131.8 ppm) chemical shifts are akin to those previously reported for PPh_3.[102] The second-order splitting patterns observed for the phenyl carbon atoms are due to the fact that the carbon atoms are not magnetically equivalent. The carbon nuclei therefore do not couple to the other nuclei (P-atoms) in the same spin system, but result in an AXX' spin system.[103,104] The PPh_3 protons resonate as broad multiplets between 7.39 and 7.62 due to $J_{H\text{-}P}$ coupling. These phenomena were observed in all the NHC carbene complexes discussed in this dissertation and those previously reported.[17,84] The signals of H^3 and H^5 for complex **16a** and H^6 for complex **14a** are obscured by these multiplets.

The single resonance observed for the complexes in their ^{31}P NMR spectra in a narrow range between 22.7 and 24.9 ppm, clearly shows the equivalence of the two phosphorous ligands in each compound, and thus a *trans* positioning of these ligands in solution. Complex connectivity and bond properties derived from single crystal X-ray diffraction studies (see Section 3.2.4.4) for complex **15a** confirmed this observation.

[101] C. P. Newman, G. J. Clarkson, N. W. Alcock and J. P. Rourke, *Dalton Trans.,* 2006, 3321.
[102] A. Fürstner, G. Seidel, D. Kremzow and C. W. Lehmann, *Organometallics,* 2003, **22**, 907.
[103] R. M. Siverstein and F. X. Webster, in *Spectroscopic Identification of Organic Compounds,* John Wiley and Sons, New York, 6th ed., 1998, p. 200.
[104] H. Günther, *Angew. Chem. Int. Ed. Engl.,* 1972, **11**, 861.

Table 3.12 NMR data of complexes **14b**, **15b** and **16b** in CD_2Cl_2

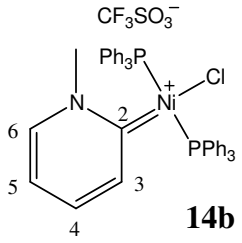

14b

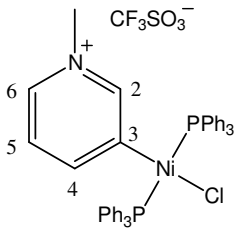

15b

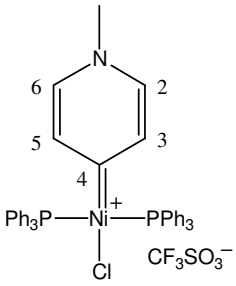

16b

Assignment	δ / ppm*		
	14b	**15b**	**16b**
^{1}H NMR			
NMe	4.22 (3H, s)	3.36 (3H, s)	3.70 (3H, s)
H^2	n.a.	8.09 (1H, d, ^{4}J = 4.4 Hz)	n.a.
H^3	7.85 (1H, m)	n.a.	n.a.
H^4	6.91 (1H, td, ^{3}J = 7.7 Hz, ^{4}J = 1.4 Hz	7.11 (1H, bs)	n.a.
H^5	6.81 (1H, m)	6.69 (1H, m)	n.a.
H^2, H^6	n.a.	n.a.	6.91 (2H, d, ^{3}J = 5.9 Hz)
Ph, H^3, H^5	n.a.	n.a.	7.68, 7.49, 7.40 (32H, 3 x m)
Ph, H^6	7.57, 7.42 (31H, 2 x m)	7.66, 7.48, 7.40 (31H, 3 x m)	n.a.
^{13}C NMR			
NMe	52.4 (s)	47.7 (s)	46.1 (s)
C^2	193.6 (t, $^{2}J_{C\text{-}P}$ = 33.0 Hz)	150.7 (bs)	n.a.
C^3	138.2 (bs)	174.1 (bs)	n.a.
C^4	134.7 (s)	148.2 (s)	205.0 (t, ^{3}J = 31.2 Hz)
C^5	121.5 (s)	123.0 (s)	n.a.
C^6	146.0 (s)	136.5 (s)	n.a.
C^2, C^6	n.a.	n.a.	134.0 (s)
C^3, C^5	n.a.	n.a.	136.0 (bs)
Ph^{ipso}	128.9 (m)	129.7 (m)	129.7 (m)
Ph^{ortho}	134.5 (m)	134.7 (m)	134.7 (m)
Ph^{meta}	129.4 (m)	128.9 (m)	128.8 (m)
Ph^{para}	131.8 (s)	131.2 (s)	131.2 (s)
^{31}P NMR			
PPh_3	21.2 (s)	23.0 (s)	22.4 (s)

All the signals for the protons of the carbene ligands in complexes **14b**, **15b** and **16b** appear at a higher field when compared to the signals of compounds **11**, **12** and **13** respectively due to metal coordination. The ^{1}H NMR data of complexes **14b** and **16b** are similar to those reported for *trans*-chloro-(*N*-methyl-1,2-dihydro-pyrid-2-ylidene)bis(triphenylphosphine)nickel(II) tetrafluoroborate and the complex *trans*-chloro-(*N*-methyl-1,4-dihydro-pyrid-4-ylidene)bis(triethylphosphine)-nickel(II) tetrafluroborate.[17]

For all the complexes, the chemical shifts arising from PPh_3 are unexceptional, some of them overlapping the pyridine signals in the ^{1}H NMR (H^3/H^5 in complexes **16b**; H^6 in complexes **14b** and **15b**). Again only one signal is observed in the ^{31}P NMR spectra indicative of the *trans* arrangement around the metal centre. Although both series of pyridine-derived complexes (**14 – 16**) show the same trend, the differences are marginal and insufficient for drawing conclusions about the ligand's donor properties.

It can be concluded upon comparison of the ^{1}H NMR data of these complexes with their palladium analogues (Table 3.11) that the signals appear more upfield in the Ni-complexes than in the Pd-complexes, except for **15b**, where the resonance for H^2 is observed more downfield than in **15a**.

Comparison of the ^{13}C NMR spectra show that the signals of the analogous complexes are similar, except for the carbon donors, which appear at a lower field strength ($\Delta\delta$ 4.3 for **14**; $\Delta\delta$ 9.1 for **15** and $\Delta\delta$ 7.3) for the nickel complexes due to higher deshielding effect of the more electronegative metal. Again the carbenic character (pyridylidene ligands) can be seen in complex **14b** and **16b** upon comparison of the same signals in ligands **11** and **13** respectively ($\Delta\delta$ 44.2 for **14b** $\Delta\delta$ 49.7 for **16b**). The signal for the carbon donor in the *a*NHC ligand (**15b**) has a downfield change in chemical shift of only $\Delta\delta$ 38.0, indicative of a possibly larger pyridinium ligand character.

The carbene carbons in **14b** and **16b** appear as triplets at δ 193.6 and δ 205.0 respectively with coupling constants of 33.0 Hz and 31.2 Hz due to phosphorous-carbon coupling. This fine structure could not be observed for the signal of the carbon donor in **15b** at δ 174.1 which appeared as a broad singlet.

Mass spectrometry

Only the FAB-MS spectrum of complexes **15a** and **15b** (Table 3.13) were determined since the spectra of **14** and **16** are known for their BF_4^- analogues. Multiple peaks due to the several isotopes of Pd and Cl for **15a** and Ni and Cl for **15b** are observed. The cation of the molecular ion of complex **15b** is observed as a weak intensity signal at *m/z* 711.8 and for **15a** as a relatively strong intensity signal at *m/z* 759.6. The complexes show similar fragmentation patterns consisting of the sequential loss of PPh_3 and chloride. These fragmentations are akin to those observed for the BF_4^- analogues.[17,84]

Table 3.13 Mass spectrometry data of compound **15a**

Complex	*m/z*	Relative intensity	Fragment ion
15a	759.6	52	$[M\text{-}CF_3SO_3]^+$ (^{35}Cl, ^{106}Pd)
	498.0	66	$[M\text{-}PPh_3\text{-}CF_3SO_3]^+$
	460.1	21	$[M\text{-}PPh_3\text{-}Cl\text{-}CF_3SO_3]^+$
	384.7	10	$[M\text{-}2PPh_3\text{-}Cl\text{-}CF_3SO_3]^+$
15b	711.8	8	$[M\text{-}CF_3SO_3]^+$ (^{37}Cl, ^{58}Ni)
	449.6	70	$[M\text{-}PPh_3\text{-}CF_3SO_3]^+$
	413.0	24	$[M\text{-}PPh_3\text{-}Cl\text{-}CF_3SO_3]^+$

3.2.4.4 Crystal and molecular structure of *trans*-chloro(*N*-methyl-1,3-dihydro-pyrid-3-ylidene)bis(triphenylphosphine)palladium(II) triflate, 15a, *trans*-chloro(*N*-methyl-1,3-dihydro-pyrid-3-ylidene)bis(triphenylphosphine)nickel(II) triflate, 15b

Single crystals suitable for X-ray crystallography of complexes **15a** and **15b** were grown from a dichloromethane solution into which diethyl ether vapour was allowed to diffuse slowly at -15 °C. The molecular structure of complex **15a**, generated in POV-Ray, is shown in Figure 3.5. Since complex **15b** is isostructural to complex **15a**, only the molecular structure of **15a** is depicted here. The bond distances and angles are summarised in Table 3.14 and 3.15 respectively.

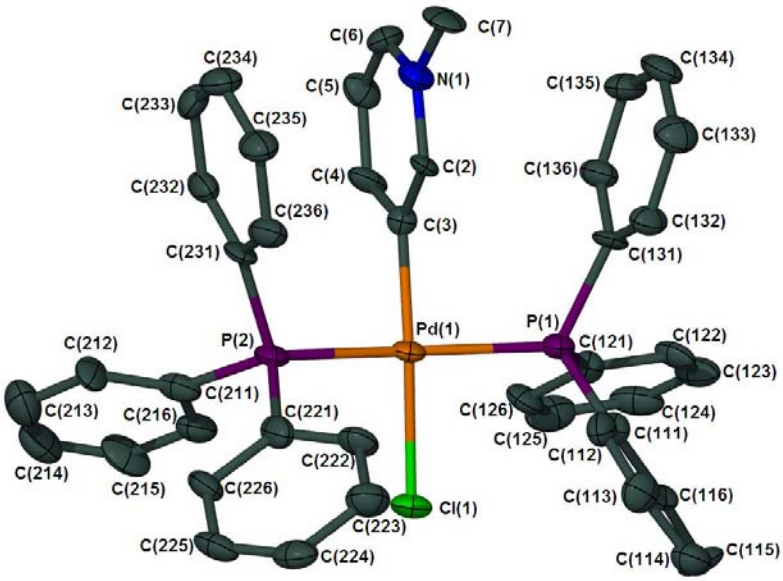

Figure 3.5 Molecular structure of *trans*-chloro(*N*-methyl-1,3-dihydro-pyridin-3-ylidene)bis-(triphenylphosphine)palladium(II) triflate, **15a**; H-atoms, the counterion and two CH_2Cl_2 molecules are omitted for clarity

Table 3.14 Selected bond lengths (Å) and angles (°) of complex **15a**

*Bond lengths (*Å)			
Pd(1)-C(3)	1.99(1)	N(1)-C(7)	1.48(2)
Pd(1)-P(1)	2.317(3)	C(2)-C(3)	1.39(2)
Pd(1)-P(2)	2.321(3)	C(3)-C(4)	1.41(2)
Pd(1)-Cl(1)	2.371(3)	C(4)-C(5)	1.37(2)
N(1)-C(6)	1.34(2)	C(5)-C(6)	1.35(2)
N(1)-C(2)	1.38(1)		
Bond angles (º)			
C(3)-Pd(1)-P(1)	90.4(3)	C(2)-N(1)-C(7)	118.0(11)
C(3)-Pd(1)-P(2)	90.5(3)	N(1)-C(2)-C(3)	120.3(11)
P(1)-Pd(1)-P(2)	165.6(1)	C(2)-C(3)-C(4)	116.9(11)
C(3)-Pd(1)-Cl(1)	170.4(3)	C(2)-C(3)-Pd(1)	122.9(8)
P(1)-Pd(1)-Cl(1)	89.6(1)	C(4)-C(3)-Pd(1)	120.1(9)
P(2)-Pd(1)-Cl(1)	91.8(1)	C(5)-C(4)-C(3)	120.2(12)
C(6)-N(1)-C(2)	121.4(11)	C(6)-C(5)-C(4)	121.2(12)
C(6)-N(1)-C(7)	120.6(10)	N(1)-C(6)-C(5)	119.9(11)

Table 3.15 Selected bond lengths (Å) and angles (°) of complex **15b**

*Bond lengths (*Å)			
Ni(1)-C(3)	1.879(6)	N(1)-C(7)	1.472(8)
Ni(1)-Cl(1)	2.205(2)	C(2)-C(3)	1.397(8)
Ni(1)-P(2)	2.216(2)	C(3)-C(4)	1.373(9)
Ni(1)-P(1)	2.220(2)	C(4)-C(5)	1.399(9)
N(1)-C(6)	1.344(8)	C(5)-C(6)	1.374(9)
N(1)-C(2)	1.359(7)		
Bond angles (º)			
C(3)-Ni(1)-Cl(1)	167.1(2)	C(2)-N(1)-C(7)	118.9(5)
C(3)-Ni(1)-P(2)	91.0(2)	N(1)-C(2)-C(3)	120.7(5)
Cl(1)-Ni(1)-P(2)	90.10(6)	C(4)-C(3)-C(2)	117.2(5)
C(3)-Ni(1)-P(1)	90.1(2)	C(4)-C(3)-Ni(1)	119.8(4)
Cl(1)-Ni(1)-P(1)	92.06(6)	C(2)-C(3)-Ni(1)	123.0(4)
P(2)-Ni(1)-P(1)	165.04(7)	C(3)-C(4)-C(5)	121.5(6)
C(6)-N(1)-C(2)	121.8(5)	C(6)-C(5)-C(4)	118.9(6)
C(6)-N(1)-C(7)	119.3(5)	N(1)-C(6)-C(5)	119.8(6)

The asymmetric unit of complex **15a** consists of the positively charged carbene complex, the counter-anion and two CH_2Cl_2 solvent molecules. One of the CH_2Cl_2 molecules is disordered to such an extent that one chlorine atom occupies two positions (80:20), which were modelled but are not shown in Figure 3.5. The same circumstance occurs in the molecular structure of complex **15b** where one CH_2Cl_2 molecule has a chlorine modelled anisotropically in two sites (50:50). In both instances the C-Cl bonds were fixed with SADI to be of equal length.

The cations of both the complexes contain the metal atom in a square planar environment with the carbene ligand perpendicular to this plane, and the two PPh_3 ligands *trans* to each other.

Although no hydrogen bond could be located between O(3) of the triflate anion and C(2) of the carbene ligand in both complexes (just outside the allowed SHELX range for hydrogen bonding), there probably should be some interaction, resulting in the particular alignment of the triflate (Figure 3.6).

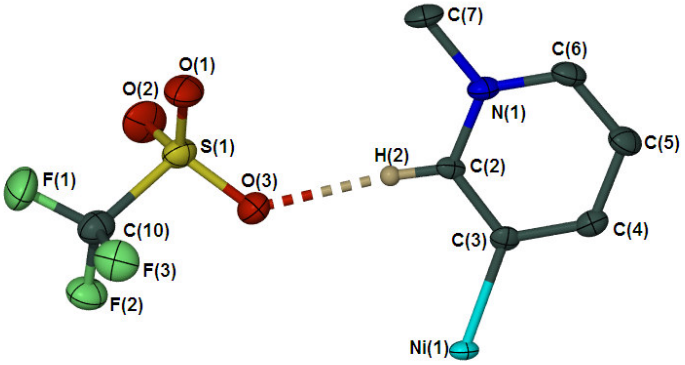

Figure 3.6 A section of the molecular structure of complex **15b** to illustrate the interaction between the anion and cation.

The metal-C(3) bond lengths for the two new *abnormal*, one-N, six-membered NHCs, are respectively 1.99(1) Å (**15a**) and 1.879(6) Å (**15b**), which are in the range typically observed for similar C(2) (*n*NHC) and C(4) (*r*NHC) bound analogs,[17,84] which indicate that no satisfactory distinction can be made on this basis between the bonding in pyridine-derived ligands that have different percentages of pyridinium character. The metal-halide bond of **15b** is similar to that in the classical N^2HC^5 carbene complex, *trans*-chloro(1,3-dimethyl-2,3-dihydro-1*H*-imidazol-2-ylidene)bis(triphenylphosphine)nickel(II) tetrafluoroborate[17] (2.205(12) vs 2.187(1) Å) which points to comparable *trans* influences. The latter exerts a similar *trans* influence to the C(2)-bound pyridylidene ligand in *trans*-chloro(*N*-methyl-1,2-dihydro-pyrid-2-ylidene)bis(triphenyl-phosphine)nickel(II) tetrafluoroborate[17] [Ni-Cl, 2.203(1) Å]. Upon comparison of the Pd-Cl bond length of 2.371(3) Å to that of a previously reported $n N^1HC^6$ complex, *trans*-chloro(*N*-methyl-1,2-dihydro-pyrid-2-ylidene)bis(triphenylphosphine)palladium(II) tetrafluoroborate [2.3632(9) Å] and $r N^1HC^6$, *trans*-chloro(*N*-methyl-1,4-dihydro-pyrid-4-ylidene)bis(triphenylphosphine) palladium(II) tetrafluoroborate [2.3938(17) Å], it is obvious that the *trans* influence of complex **15a** is similar to the $n N^1HC^6$ complex and less than the $r N^1HC^6$ complex.

Although the ^{13}C NMR spectra clearly indicated the large pyridinium character of **15a** and **15b**, the solid state structure when compared to C2 (*normal*) and C4 (*remote*) carbene complexes are not that different. The same was also observed for the Ru(II) complexes mentioned earlier.[92,93] A search on the Cambridge Crystallographic and Structural Database (CCSD) produced no examples of C3 bonded pyridylidene complexes of palladium.

Since the packing of the two complexes are the same, only the packing of complex **15b** (Figure 3.7) is discussed here. The cations of complex **15b** are arranged on top of each other along the a-axis and in layers parallel to the b-axis. In the layers along the b-axis the cations are aggregated with the carbene ligand alternating up or down. The $CF_3SO_3^-$ anions are situated between the carbene ligands of two cations packed on top of each other along the a-axis. CH_2Cl_2 molecules are located in spaces created by the PPh_3 ligands.

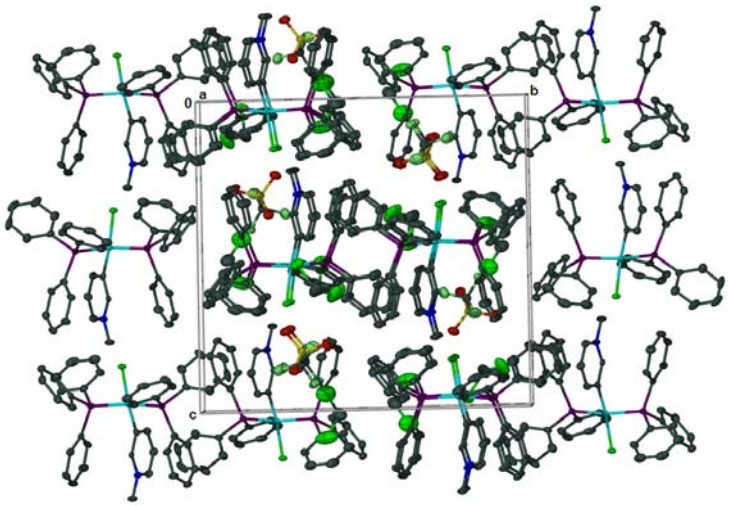

Figure 3.7 Molecular packing on complex **15b** viewed along the a-axis

3.2.5 Oxidative substitution occurring in competitive situations

The results obtained from computational calculations mentioned in Section 3.1.1 are worth proving experimentally. For this we decided to choose a ligand (2,4-dichloro-*N*-methyl-pyridinium triflate) that will create a competitive situation for oxidative substitution either at the 'remote' site or at the 'normal' site. In pyridinium salts nucleophilic addition readily takes place at the C-2(6) position, since the inductive effect of the positively nitrogen atom is the greatest here.[105]

Recently, the first *r*NHC complexes with no heteroatom in the carbene carbon containing ring were synthesised. Existing literature procedures were followed or slightly modified to prepare the

[105] M. Sainsbury, *Heterocyclic chemistry,* RSC, Cambridge, 2001, p. 34.

cationic complexes *trans*-bromo(2-methyl-2,6-dihydro-isoquinol-6-ylidene)bis(triphenyl-phosphine)-palladium(II) triflate (**XXIV**) and *trans*-chloro(1,2-dimethyl-1,7-dihydro-quinol-7-ylidene)bis(triphenylphosphine)palladium(II) (**XXV**).[106]

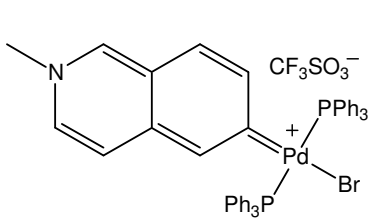

XXIV

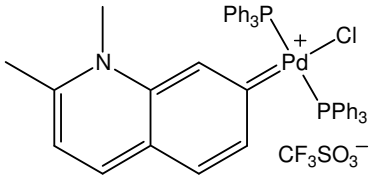

XXV

Compound **XXIV** pushes the boundaries of rN[1]HC ligands, with the carbene carbon (confirmed by ^{13}C NMR) situated five bonds away from the heteroatom. Another competitive situation to be investigated is therefore whether oxidative substitution would occur at C7 or C4 when the ligand 4,7-dichloro-*N*-methyl-quinolinium triflate is employed.

3.2.5.1 Synthesis of 2,4-dichloro-*N*-methylpyridinium triflate, 17, and 4,7-dichloro-*N*-methyl-quinolinium triflate, 18 and their respective Pd(II) (19a, 20a) and Ni(II)-complexes (19b, 20b)

The compounds **17** and **18** were synthesised in excellent yields (99 %) in a manner similar to that employed for compound **11**. Compounds **17** and **18** are soluble in polar solvents like CH_2Cl_2, but less soluble in diethyl ether, THF and other non-polar solvents such as pentane.

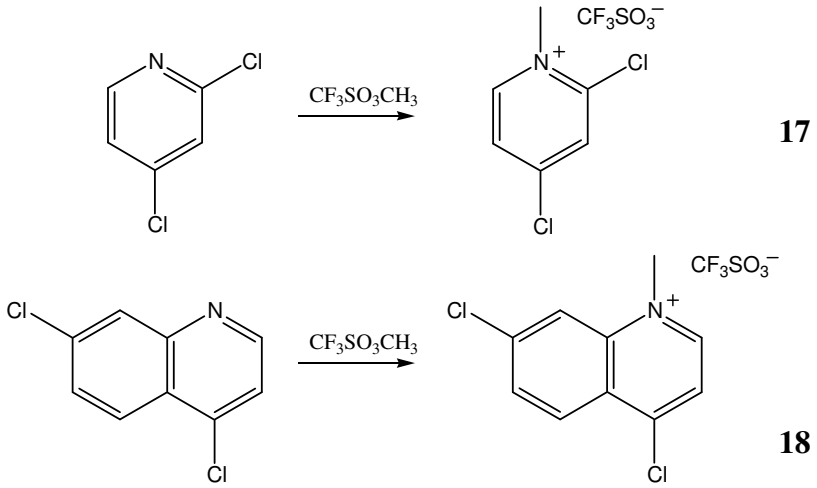

Scheme 3.7

Reacting ligand precursor **17** with $M(PPh_3)_4$ (M = Pd, Ni) led in both instances to the complexes (**19a** and **19b**) with the carbene donor solely at the site remote from the heteroatom in reasonably good yields (74 and 63 %). Similarly complexes **20b** and **20b** (62 and 80 % yield) formed

[106] O. B. Schuster and H. G. Raubenheimer, *Inorg. Chem.,* 2006, **45**, 7997.

exclusively when compound **18** was reacted with $M(PPh_3)_4$ (M = Pd, Ni) according to the reactions shown in Scheme 3.8. According to the more upfield shift for C4 (*vide infra*) in the pyridinium salt, obviously the unexpected product is formed *via* an attack of the presumably less nucleophilic site. The same synthetic procedures were followed as discussed for complexes **14a** and **14b** respectively. The microcrystalline materials obtained are soluble in CH_2Cl_2 and acetone and insoluble in pentane and diethyl ether.

These compounds which are potentially bifunctional in the oxidative substitution reaction, reacted only with an equimolar amount of $[M(PPh_3)_4]$ (M = Pd, Ni) when mixed with two molar amounts of the metal compound. One of the causative factors might be the higher electron density on the metallated aromatic ring, which could inhibit the second oxidative substitution, as was observed for the non-alkylated ligand 2,6-dichloropyridine.[105]

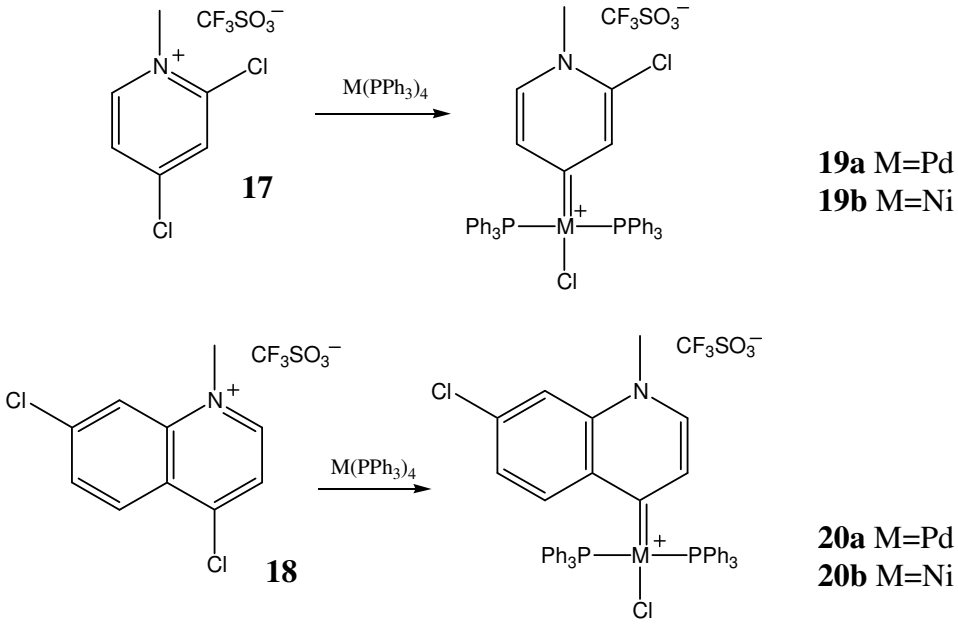

Scheme 3.8

3.2.5.2 Spectroscopic characterisation of 2,4-dichloro-*N*-methylpyridinium triflate, 17, *trans*-chloro(2-chloro-*N*-methyl-1,2,4-trihydro-pyrid-4-ylidene)bis(triphenylphosphine)-palladium(II) triflate, 19a and *trans*-chloro(2-chloro-*N*-methyl-1,2,4-trihydro-pyrid-4-ylidene)bis(triphenylphosphine)nickel(II) triflate, 19b

NMR spectroscopy

Table 3.16 contains the chemical shifts of the resonances and their assignments, as observed for compounds **17**, **19a** and **19b** in their respective ^{1}H, ^{13}C and ^{31}P NMR spectra. The regiochemistry of the oxidative substitution products was determined by two dimensional NMR (ghsqc and ghmqc).

The ^{1}H NMR spectrum of complex **19a** was collected at different temperatures to see if the formed product (oxidative substitution at C4) would transform to the product where oxidative substitution occurs at C^{2}. No changes were observed in the spectra collected.

Table 3.16 NMR data of complexes **17**, **19a** and **19b** in CD_2Cl_2

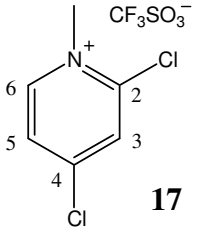

17

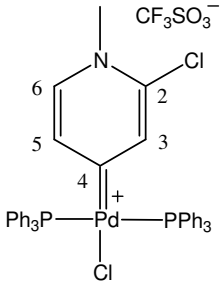

19a

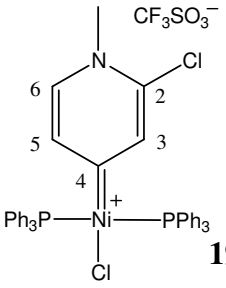

19b

	δ / ppm*		
Assignment	**17**	**19a**	**19b**
^{1}H NMR			
NMe	4.42 (3H, s)	3.82 (3H, s)	3.71 (3H, s)
H^3	8.05 (1H, d, ^{4}J = 2.3 Hz)	7.16 (1H, bs)	7.16 (1H, bs)
H^5	7.99 (1H, dd, ^{3}J = 6.8 Hz, ^{4}J = 2.3 Hz)	n.a.	7.76 (1H, d, ^{3}J = 6.4 Hz)
H^6	9.14 (1H, dd, ^{3}J = 6.8 Hz, ^{5}J = 0.4 Hz)	7.69 (1H, d, ^{3}J = 6.4 Hz)	n.a.
Ph^{para}, H^5	n.a.	7.49 (7H, m)	n.a.
Ph^{para}, H^6	n.a.	n.a.	7.48 (7H, m)
Ph^{ortho}	n.a.	7.63 (12H, m)	7.69 (12H, m)
Ph^{meta}	n.a.	7.41 (12H, m)	7.41 (12H, m)
^{13}C NMR			
NMe	48.1 (s)	45.4 (s)	45.0 (s)
C^2	156.0 (s)	139.2 (s)	136.9 (s)
C^3	130.1 (s)	136.7 (t, $^{4}J_{P\text{-}C}$ = 3.7 Hz)	136.6 (s)
C^4	148.9 (s)	202.3 (t, $^{2}J_{P\text{-}C}$ = 6.1 Hz)	210.8 (s)
C^5	127.7 (s)	134.6 (t, $^{3}J_{P\text{-}C}$ = 3.7 Hz)	133.8 (bs)
C^6	150.0 (s)	140.0 (s)	136.8 (s)
Ph^{ipso}	n.a.	129.3 (m)	129.4 (m)
Ph^{ortho}	n.a.	134.8 (m)	134.7 (m)
Ph^{meta}	n.a.	128.9 (m)	128.9 (m)
Ph^{para}	n.a.	131.5 (s)	131.5 (s)
^{31}P NMR			
PPh_3	n.a.	23.6 (s)	22.5 (s)

The fact that only one set of signals is observed in the various NMR spectra is indicative of only one product. The position of oxidative substitution is confirmed by the fine structure that originates from coupling and the number of chemically equivalent proton signals.

Comparison of the ligand **17** precursor to 2-chloro-N-methyl-pyridinium triflate, **11** (Section 3.2.4) and 4-chloro-N-methyl-pyridinium triflate, **13**, shows that the signals in the ^{1}H NMR are within 0.04 ppm of one another except for H^6 which is more than 20 ppm more upfield in compound **13** than in **11** and **17** due to the remoteness of a chlorine atom. The ^{13}C NMR resonances are similar except for C^2 which is significantly more downfield in **17** (δ 156.0) than in compound **11** (δ 149.4) and **13** (δ 147.0). Although C^4 of compound **17** has an electronegative chlorine attached to it, it resonates 6.4 ppm lower than C^4 in compound **13** (δ 155.3) that also has a chlorine attached to it.

All the signals of the protons in complex **19a** and **19b** move upfield in small amounts (Δδ 0.23 to 1.66) when compared to the same signals observed for compound **17**. The signals of H^5 for complex **19a** and H^6 for complex **19b** are obscured by the signal of some of the phenyl protons of the phosphine ligands. A downfield change in chemical shift (Δδ 6.1 – 6.5) when compared to the signals in **17** is observed for C^3 and C^5 in **19a** and **19b** due to the influence of the coordinated metal. This influence is most distinctly demonstrated in the signals of the carbene donor atom – a downfield shift of 53.4 ppm for complex **19a** and 61.9 ppm for complex **19b** - rather typical, but large for these type of ligands upon coordination. The carbene carbon of complex **19a** resonates at 202.3 ppm compared to 189.3 ppm in **14a** (nN^{1}HC^6) and at 197.7 ppm in complex **14a** (rN^{1}HC^6). In the Ni-complexes, the carbene carbon **14b** resonates at exceptionally lowfield 210.8 ppm when compared to 193.6 ppm in **14b** and 205.0 ppm in **14b**. Clearly the extra electron withdrawing group, chlorine, affords a larger downfield shift for C^4 upon coordination. The coupling of C^4 with the P-atoms could only be observed in complex **19a**. The sample containing complex **19b** was probably too low in concentration to yield proper resolution of the signals.

The singlets at respectively 23.6 ppm (**19a**) and 22.5 (**19b**) for the P-atoms in the ^{31}P NMR spectra compare well with similar complexes described in this chapter and in literature,[17,84] confirming the *trans* arrangement around the metal atom.

Mass spectrometry

The FAB mass spectrometric data for compounds **17**, **19a** and **19b** are summarised in Table 3.17. A peak representing the cationic complex ion is observed in the spectra of all three compounds and the two main isotopes of chlorine are seen in compound **17** with *m/z* 163.0 and 161.9. The isotopic cluster of the ions at *m/z* 794.0 and 746.3 reveals a composition of the compounds related to $C_{42}H_{36}NP_2Cl_2Pd$ and $C_{42}H_{36}NP_2Cl_2Ni$ for complex **19a** and **19b** respectively. The peaks representing the cations of the molecular ion for the two complexes are followed by the fragment

ions representing the loss of one Cl, followed by the loss of PPh_3 ligand. The fragment obtained after the loss of both Cl and PPh_3 is only observed for complex **19a**.

Table 3.17 Mass spectrometry data of complexes **17**, **19a** and **19b**

Complex	*m/z*	Relative intensity	Fragment ion
17	163.0	77	$[M\text{-}CF_3SO_3]^+$ (^{37}Cl)
	161.9	100	$[M\text{-}CF_3SO_3]^+$ (^{35}Cl)
19a	794.0	41	$[M\text{-}CF_3SO_3]^+$ (^{106}Pd, ^{35}Cl]
	758.6	4	$[M\text{-}Cl\text{-}CF_3SO_3]^+$
	531.9	46	$[M\text{-}PPh_3\text{-}CF_3SO_3]^+$
	496.2	8	$[M\text{-}Cl\text{-}PPh_3\text{-}CF_3SO_3]^+$
19b			
	746.3	40	$[M\text{-}CF_3SO_3]^+$ (^{58}Ni, ^{35}Cl]
	710.8	9	$[M\text{-}Cl\text{-}CF_3SO_3]^+$
	484.0	12	$[M\text{-}PPh_3\text{-}CF_3SO_3]^+$

3.2.5.3 Molecular structures of complexes *trans*-chloro(2-chloro-*N*-methyl-1,2,4-trihydro-pyrid-4-ylidene)bis(triphenylphosphine)palladium(II) triflate, 19a, and *trans*-chloro(2-chloro-*N*-methyl-1,2,4-trihydro-pyrid-4-ylidene)bis(triphenylphosphine)nickel(II) triflate, 19b

X-ray crystal determinations unambiguously confirmed the coordination sites deduced by NMR. The molecular structures of the cationic complexes in compound **19a** (Figure 3.8) and **19b** (Figure 3.9) are depicted below. Crystal data and experimental details are given in the Experimental section, and selected bond distances and bond angles in Table 3.18 and Table 3.19 respectively.

Complex **19a** crystallises as colourless prisms in the space group $P2_1/c$ and complex **19b** as yellow cubes in the space group $P2_1/n$. These crystals suitable for X-ray analysis were obtained by slow diffusion of pentane into a concentrated CH_2Cl_2 solution of the respective complexes.

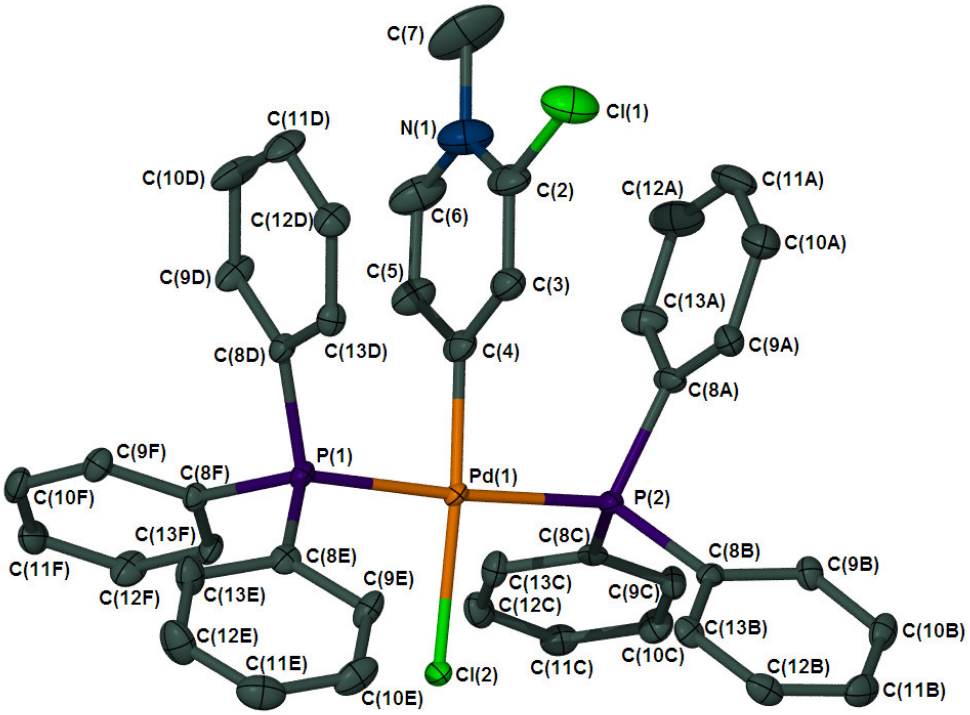

Figure 3.8 Molecular structure of **19a**; two dichloromethane solvent molecules, a triflate ion and H-atoms are omitted for clarity

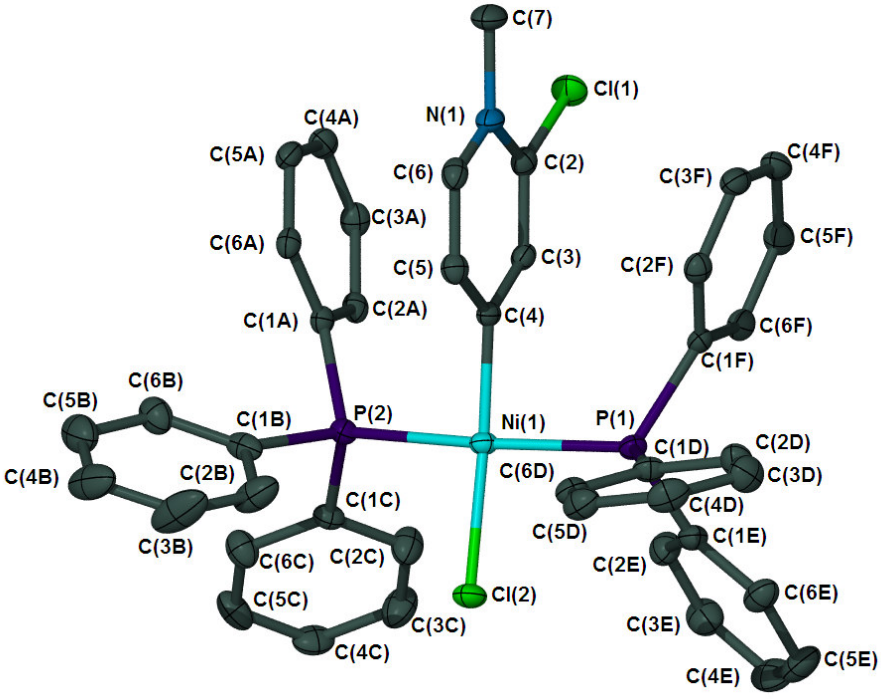

Figure 3.9 Molecular structure of **19b**; a CH_2Cl_2 solvent molecule, a triflate ion and H-atoms are omitted for clarity

Table 3.18 Selected bond lengths (Å) and angles (°) of complex **19a**

*Bond lengths (*Å)			
Pd(1)-C(4)	1.972(5)	N(1)-C(6)	1.349(7)
Pd(1)-P(1)	2.338(1)	N(1)-C(7)	1.407(8)
Pd(1)-P(2)	2.348(1)	C(2)-C(3)	1.389(7)
Pd(1)-Cl(2)	2.379(1)	C(3)-C(4)	1.385(7)
Cl(1)-C(2)	1.713(6)	C(4)-C(5)	1.411(7)
N(1)-C(2)	1.321(7)	C(5)-C(6)	1.358(7)
Bond angles (º)			
C(4)-Pd(1)-P(1)	87.4(1)	N(1)-C(2)-C(3)	121.6(5)
C(4)-Pd(1)-P(2)	89.0(1)	N(1)-C(2)-Cl(1)	118.5(4)
P(1)-Pd(1)-P(2)	176.30(4)	C(3)-C(2)-Cl(1)	119.9(4)
C(4)-Pd(1)-Cl(2)	172.9(1)	C(4)-C(3)-C(2)	120.6(5)
P(1)-Pd(1)-Cl(2)	92.00(4)	C(3)-C(4)-C(5)	115.8(4)
P(2)-Pd(1)-Cl(2)	91.69(4)	C(3)-C(4)-Pd(1)	123.1(4)
C(2)-N(1)-C(6)	119.6(5)	C(5)-C(4)-Pd(1)	121.1(4)
C(2)-N(1)-C(7)	124.0(5)	C(6)-C(5)-C(4)	121.1(5)
C(6)-N(1)-C(7)	116.4(5)	N(1)-C(6)-C(5)	121.3(5)

Table 3.19 Selected bond lengths (Å) and angles (°) of complex **19b**

*Bond lengths (*Å)			
Ni(1)-C(4)	1.853(2)	N(1)-C(6)	1.356(3)
Ni(1)-Cl(2)	2.2120(6)	N(1)-C(7)	1.479(3)
Ni(1)-P(1)	2.2285(6)	C(2)-C(3)	1.371(3)
Ni(1)-P(2)	2.2309(6)	C(3)-C(4)	1.402(3)
Cl(1)-C(2)	1.713(2)	C(4)-C(5)	1.409(3)
N(1)-C(2)	1.355(3)	C(5)-C(6)	1.359(3)
Bond angles (º)			
C(4)-Ni(1)-Cl(2)	170.22(7)	N(1)-C(2)-C(3)	122.3(2)
C(4)-Ni(1)-P(1)	88.73(7)	N(1)-C(2)-Cl(1)	116.9(2)
Cl(2)-Ni(1)-P(1)	91.56(2)	C(3)-C(2)-Cl(1)	120.8 (2)
C(4)-Ni(1)-P(2)	88.54(7)	C(2)-C(3)-C(4)	119.8(2)
Cl(2)-Ni(1)-P(2)	92.70(2)	C(3)-C(4)-C(5)	116.5(2)
P(1)-Ni(1)-P(2)	170.34(3)	C(3)-C(4)-Ni(1)	125.2(2)
C(2)-N(1)-C(6)	118.9(2)	C(5)-C(4)-Ni(1)	118.3(2)
C(2)-N(1)-C(7)	122.0(2)	C(6)-C(5)-C(4)	121.3(2)
C(6)-N(1)-C(7)	119.0(2)	N(1)-C(6)-C(5)	121.1(2)

The X-ray structure of complexes **19a** and **19b** reveals the formation of $r\mathrm{N}^1\mathrm{HC}^6$ complexes in which the metal is bound in a square planar environment while the two PPh_3 ligands occupy *trans* positions. The planes of the carbene ligand makes an angle of 87.42(9) ° (**19a**) and 85.20(4) ° (**19b**)

with the square planar environment implying a quasi-perpendicular disposition of the ligand with respect to the coordination plane.

The Pd-C(carbene) distance of complex **19a** [1.972(5) Å] falls within the previously obtained range [1.979(7) – 2.029(9) Å] for Pd(II) N^1HC^6 complexes.[84] The same is true for the Ni-C(carbene) distance of **19b** [1.853(2) Å] which is at the shorter end of the range in bond distances reported for Ni(II) N^1HC^6 complexes previously [1.861(5) – 1.874(6) Å].[17,107] The seemingly shorter but not significantly shorter metal carbene bonds observed, result from the extra electron withdrawing Cl-atom on the ligand which lowers the σ-contribution. The Pd-C(carbene) distance is similar to the same distance in **15a**, [1.990(11) Å], described earlier, whereas the Ni-C(carbene) distance is slightly shorter than the corresponding Ni complex, **15b** [1.879(6) Å]. As mentioned before, pyridine-derived carbenes act as strong σ-donors (even more than classical NHCs) and consistent with this view, the M-$C_{carbene}$ bond lengths lie in the range of normal M-C(sp^3/sp^2) single bonds.[108] It is important to remember though that the π-contributions are larger for the *r*N^1HC^6 complex than for the *n*N^1HC^6 and *n*N^2HC^5 complexes according to EDA analysis.[17,18]

No *cis* orientation of the phosphine ligands was found in the solid state as previously seen for chloro-(*N*-methyl-4-methylquinol-2-ylidene)bis(triphenylphosphine)palladium(II) tetrafluoroborate.[84] Only the *trans*-isomer is present in solution (as shown by ^{31}P NMR). The occurrence of a *cis*-isomer in the solid state was previously ascribed to the possible energy advantage during crystal aggregation.

The Pd-Cl bond distance [2.3788(10) Å] is similar to that of complex **15a**, *trans*-chloro-(*N*-methyl-1,3-dihydro-pyrid-3-ylidene)bis(triphenylphosphine)palladium(II) triflate, [2.371(3) Å] and significantly shorter than previously prepared *r*N^1HC complexes such as *trans*-chloro(1,2-dimethyl-1,7-dihydroquinol-7-ylidene)bis(triphenylphosphine)palladium(II) triflate [2.4005(12) Å],[106] and *trans*-chloro-(*N*-methyl-1,4-dihydro-pyrid-4-ylidene)bis(triphenylphosphine) palladium(II) tetrafluoroborate [2.3938(17) Å][84] indicating a weaker *trans* influence. Although the *trans* influence is weaker than in other *r*N^1HC complexes, it still is stronger than in the *n*N^1HC complex *trans*-chloro-(*N*-methyl-1,2-dihydro-quinol-2-ylidene)bis(triphenylphosphine) palladium(II) tetrafluoroborate [Pd-Cl, 2.3465(11) Å].[84] This can be correlated to the increased π-contribution of the carbon donor due to the influence of the Cl-atom mentioned earlier.

---

[107] S. K. Schneider, C. F. Rentzsch, A. Krüger, H. G. Raubenheimer and W. A. Hermann, *J. Mol. Cat. A: Chem.,* 2007, **265**, 50.
[108] W. A. Hermann, M. Elison, J. Fischer, C. Köcher and G. R. J. Artus, *Angew. Chem. Int. Ed. Engl.,* 1995, **34**, 2371.

Interestingly, the Ni-Cl distance of 2.2120(6) Å in complex **19b** does not differ significantly from the complex *trans*-chloro-(*N*-methyl-1,3-dihydro-pyrid-3-ylidene)bis (triphenylphosphine)nickel(II) triflate, **15b** [2.2053(15) Å] or the rN^{1}HC^6 complex *trans*-chloro-(*N*-methyl-1,4-dihydro-pyrid-4-ylidene)bis(triphenylphosphine)nickel(II) tetrafluoroborate [2.217(1) Å][107] or the nN^{1}HC^6 complex, *trans*-chloro-(*N*-methyl-1,2-dihydro-quinol-2-ylidene)bis(triphenylphosphine)nickel(II) tetrafluoroborate [2.216(2) Å][17] as observed for the palladium complexes. This suggests comparable *trans* influences for the carbene ligands when bonded to Ni(II).

The cations of complex **19a** are arranged in columns on top of one another along the b-axis (Figure 3.10) with the carbene ligand pointing diagonally upwards in one row and then alternating by pointing diagonally downwards in the next. The triflate anions are positioned in the spaces between the carbene ligands. The layers of cations are separated by CH_2Cl_2 molecules.

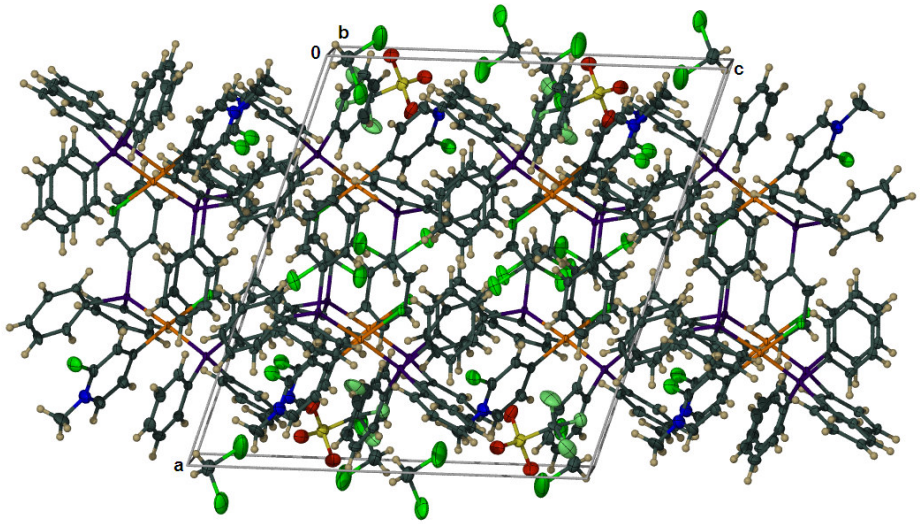

Figure 3.10 Molecular packing of complex **19a** viewed along the b-axis

The packing diagram in the unit cell of complex **19b** is shown in Figure 3.11. The cations are arranged on top of each other along the a-axis and in layers parallel to the c-axis, with the carbene ligands alternating up and down along the c-axis. The $CF_3SO_3^-$ anions are situated between the carbene ligands and CH_2Cl_2 molecules fill spaces between the phenyl rings of the PPh_3 ligands.

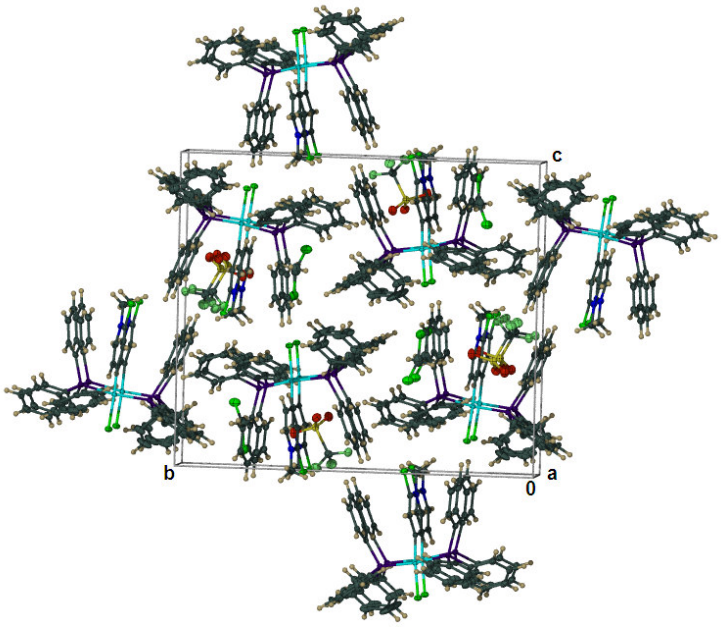

Figure 3.11 Molecular aggregation of complex **19b** viewed along the a-axis

3.2.5.4 Spectroscopic characterisation of 4,7-dichloro-*N*-methylquinolinium triflate, 18, *trans*-chloro(7-chloro-*N*-methyl-1,4,7-trihydro-quinol-4-ylidene)bis(triphenylphosphine) palladium(II) triflate, 20a and *trans*-chloro(7-chloro-*N*-methyl-1,4,7-trihydro-quinol-4-ylidene)bis(triphenylphosphine)nickel(II) triflate, 20b

The ^{1}H, ^{13}C and ^{31}P NMR data of compound **18** and complexes **20a** and **20b** are summarised in Table 3.20. The assignments were made with the aid of two dimensional NMR techniques (ghsqc and ghmqc).

In general the signals of the respective C and H atoms appear upfield with respect to the corresponding values of the ligand precursor, **18**. However, in the case of C^{3}, C^{5} and C^{10} the signals appear downfield due to deshielding caused by the positive charge that may mainly be situated on the closely situated metal atoms rather than on the N-atom as in the ligand precursor. The chemical shifts and coupling constants observed are in accordance with the results reported for halogenoquinolines reported previously.[109]

[109] A. G. Osborne, J. M. Buley, H. Clarke, R. C. H. Dakin and P. I. Price, *J. Chem. Soc., Perkin Trans. 1,* 1993, 2747.

Table 3.20 ^{1}H and ^{13}C-{^{1}H} and NMR data of compound **18** and complexes **20a** and **20b** in CD_2Cl_2

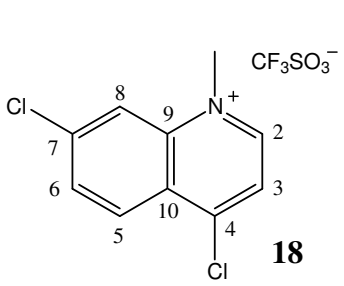

18

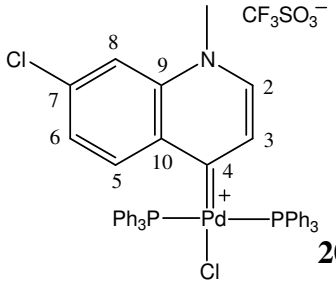

20a

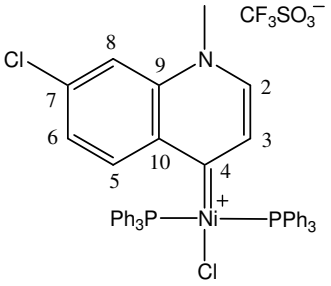

20b

Assignment	δ / ppm*		
	18	**20a**	**20b**
^{1}H NMR			
NMe	4.65 (3H, s)	4.03 (3H, s)	3.90 (3H, s)
H^2	9.44 (1H, d, ^{3}J = 6.5 Hz)	8.74 (1H, d, ^{3}J = 8.8 Hz)	9.44 (1H, d, ^{3}J = 8.8 Hz)
H^3	8.12 (1H, d, ^{3}J = 6.5 Hz)	7.64 (1H, d, ^{3}J = 6.4 Hz)	7.66 (1H, d, ^{3}J = 6.3 Hz)
H^5	8.56 (1H, d, ^{3}J = 9.0 Hz)	7.95 (1H, d, ^{3}J = 6.4 Hz)	7.89 (1H, d, ^{3}J = 6.3 Hz)
H^6	8.03 (1H, dd, ^{3}J = 9.0 Hz, ^{4}J = 1.8 Hz)	n.a.	n.a.
H^8	8.36 (1H, d, ^{4}J = 1.8 Hz)	n.a.	n.a.
Ph^{ortho}	n.a.	n.a.	n.a.
Ph^{ortho}, H^6, H^8	n.a.	7.54 (14H, m)	n.a.
Ph^{ortho}, H^6	n.a.	n.a.	7.59 (13H, m)
Ph^{para}, H^8	n.a.	n.a.	7.42 (7H, m)
Ph^{meta}	n.a.	7.28 (12H, m)	7.29 (12H, m)
Ph^{para}	n.a.	7.40 (6H, m)	n.a.
^{13}C NMR			
NMe	46.4 (s)	43.5 (s)	43.0 (s)
C^2	151.2 (s)	141.8 (s)	137.9 (s)
C^3	123.2 (s)	130.6 (t, $^{3}J_{C\text{-}P}$ = 3.6 Hz)	130.6 (bs)
C^4	154.6 (s)	206.6 (t, $^{2}J_{C\text{-}P}$ = 5.5 Hz)	216.7 (t, $^{2}J_{C\text{-}P}$ = 30.5 Hz)
C^5	128.7 (s)	137.0 (s)	136.6 (s)
C^6	132.7 (s)	n.o.	128.8 (s)
C^7	144.4 (s)	141.2 (s)	140.9 (s)
C^8	119.1 (s)	117.2 (s)	117.2 (s)
C^9	139.9 (s)	135.1 (s)	133.3 (s)
C^{10}	126.8 (s)	134.5 (bs)	135.3 (s)
Ph^{ipso}	n.a.	n.a	129.3 (m)
Ph^{ipso}, C^6		129.3 (m)	n.a.
Ph^{ortho}	n.a.	134.6 (m)	134.6 (m)
Ph^{meta}	n.a.	128.7 (m)	128.6 (m)
Ph^{para}	n.a.	131.4 (s)	131.2 (s)
^{31}P NMR			
PPh_3	n.a.	23.2 (s)	21.9 (s)

In compound **18**, H^2 couples with H^3 with a coupling constant of 6.5 Hz and H^5 couples with H^6 with a coupling constant of 9.0 Hz. The resonance of H^6 is a doublet of doublets with coupling constants of 9.0 Hz and 1.8 Hz (coupling respectively with H^5 and H^8). Similar coupling patterns are also observed for the metal complexes, although some of the fine structure is masked by overlapping signals with the phenyl protons.

The carbene carbon (C^4) of complex **20a** has a chemical shift of 206.6 ppm, 52 ppm downfield from the corresponding carbon signal in compound **18** and almost identical to the carbene signal in *trans*-chloro(*N*-methyl-1,4-dihydro-quinol-4-ylidene)bis(triphenylphosphine)palladium(II) tetrafluoroborate.[84] In the Ni-analogue (**20b**), the carbon donor resonates at δ 216.7; 62.1 ppm downfield from the same carbon in the ligand precursor and very similar to the carbene signal in *trans*-chloro(*N*-methyl-1,4-dihydro-quinol-4-ylidene)bis(triphenylphosphine)nickel(II) tetrafluoroborate.[107]

Similar to the other complexes already discussed in this chapter, the P-atoms resonate as singlets at δ 23.2 (**20a**) and δ 21.9 (**20b**) indicating the equivalence of the atoms and a *trans* arrangement of the PPh_3 ligands with respect to each other. Support for this arrangement is further provided by the carbene signals which appear as triplets with coupling constants of 5.5 Hz (**20a**) and 30.5 Hz (**20b**).

Mass spectrometry

The fragmentation patterns for **18**, **20a** and **20b** are summarised in Table 3.21. Multiple peaks due to many isotopes of the metal atoms, are observed in the spectra of complexes **20a** and **20b**, whereas the two main isotopes of Cl are observed in the spectrum of **18** at respectively *m/z* 214.0 and 212.0.

Table 3.21 FAB MS data of compound **18** and complexes **20a** and **20b**

Complex	*m/z*	Relative intensity	Fragment ion
18	214.0	69	$[M\text{-}CF_3SO_3]^+$ (^{37}Cl)
	212.0	100	$[M\text{-}CF_3SO_3]^+$ (^{35}Cl)
20a	844.0	74	$[M\text{-}CF_3SO_3]^+$ (^{35}Cl,^{106}Pd)
	581.9	100	$[M\text{-}PPh_3\text{-}CF_3SO_3]^+$
	546.0	13	$[M\text{-}Cl\text{-}PPh_3\text{-}CF_3SO_3]^+$
	404.1	54	$[M\text{-}L\text{-}PPh_3\text{-}CF_3SO_3]^+$
20b	796.2	19	$[M\text{-}CF_3SO_3]^+$ (^{35}Cl, ^{58}Ni)
	533.9	68	$[M\text{-}PPh_3\text{-}CF_3SO_3]^+$

Peaks representing the cation in the salt or complex are observed for compound **18** as well as for the two complexes. Calculated isotopic distributions of the fragments are in good agreement with the observed spectra for all 3 compounds. The base peaks in the spectra of complex **20a** and **20b** are due to an $[M\text{-}PPh_3\text{-}CF_3SO_3]^+$ fragment. For complex **20a** the fragments due to further loss of either a Cl atom (*m/z* 546.0) or the ligand (*m/z* 404.1) are also detected.

3.2.5.5 Molecular and crystal structure of *trans*-chloro(7-chloro-*N*-methyl-1,4,7-trihydro-quinol-4-ylidene)bis(triphenylphosphine)palladium(II) triflate, 20a

Several attempts were made to grow crystals of complex **20b** suitable for X-ray crystallography but all crystals obtained diffracted very poorly. Single crystals of **20a** suitable for X-ray structure determination were grown by vapour diffusion of pentane into a dichloromethane solution of the microcrystalline material to give colourless needles. The complex crystallises in the spacegroup *P*-1. The asymmetric unit in the unit cell consists of two identical molecules of complex **20a** with some minor differences in bond angles and distances and four CH_2Cl_2 solvent molecules. The orientation of the molecules are illustrated in Figure 3.12. The molecular structure of one of the cations of the asymmetric unit is presented in Figure 3.13. The atoms of the molecules are numbered in the same fashion, but for the second molecule the numbers are primed Selected bond angles and distances are given in Table 3.22.

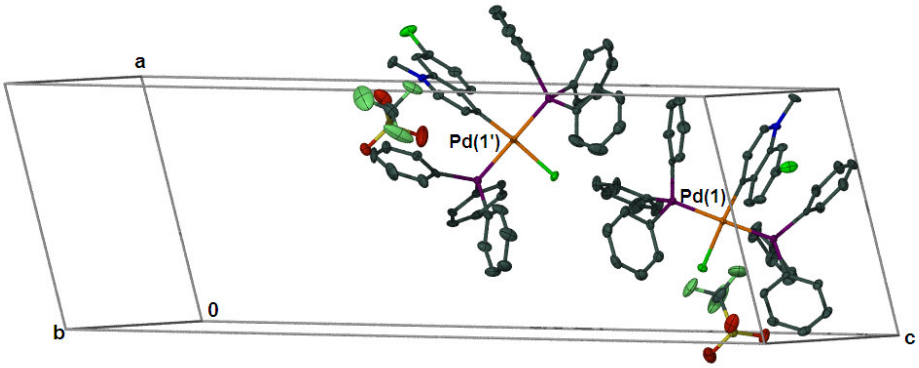

Figure 3.12 Projection of the cations in the asymmetric unit of complex **20a**. Thermal ellipsoids with 50% probability are shown for the non-hydrogen atoms, the H-atoms as well as solvent molecules (four CH_2Cl_2) are omitted for clarity.

The X-ray study confirms a *trans* arrangement of the phosphine ligands and a nearly perfect square planar coordination geometry (Figure 3.13). The angle between the square plane and the plane of the carbene ligand is 89.73(6) ° and 89.83(9) °. The carbene ligand skeleton is obligate planar and coplanar with Pd(1) and Cl(1).

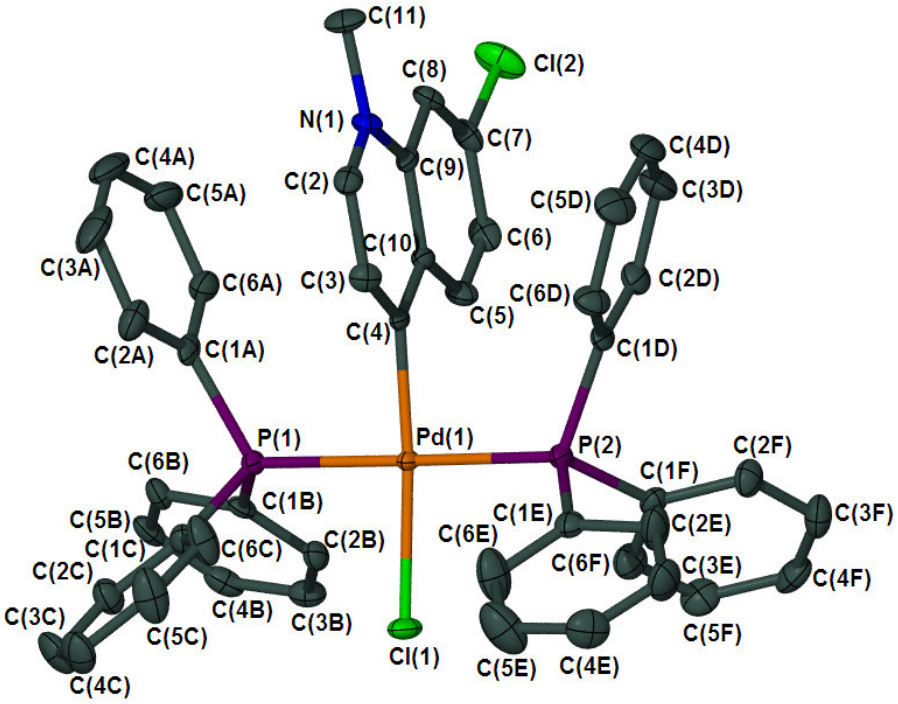

Figure 3.13 Molecular structure of complex **20a**, generated in POV-Ray; H-atoms, two CH_2Cl_2 molecules and the triflate anion are omitted for clarity

No significant difference in the bond lengths or bond distances of the two cations in the asymmetric unit can be observed. The Pd-C(carbene) bond lengths of 1.991(5) Å and 1.980(5) Å are very similar to those of the previously reported palladium(II) carbene complexes carrying either a 2-methoxy-*N*-methylquinol-4-ylidene ligand [1.986(3) Å],[15] a 2-methyl-*N*-methylquinol-4-ylidene ligand [1.986(2) Å][84] or a *N*-methylquinol-4-ylidene ligand [1.999(4) Å].[110]

Comparison of the *trans* influence of the carbene ligand in complex **20a** with the other complexes mentioned above by evaluating the Pd-Cl distances shows that the carbene ligands can be arranged in order of increasing *trans* influence: 7-chloro-*N*-methylquinol-4-ylidene [2.3631(13) and 2.3563(13) Å] < 2-methoxy-*N*-methylquinol-4-ylidene [2.380(1) Å] ≈ *N*-methylquinol-4-ylidene [2.377(1) Å] < 2-methyl-*N*-methylquinol-4-ylidene [2.3916(6) Å].

[110] A. Krüger, *MSc Thesis,* University of Stellenbosch, 2007, p. 44.

Table 3.22 Selected bond lengths (Å) and angles (°) of complex **20a**

*Bond lengths (*Å)			
Pd(1)-C(4)	1.991(5)	Pd(1')-C(4')	1.980(5)
Pd(1)-P(1)	2.329(1)	Pd(1')-P(1')	2.335(1)
Pd(1)-P(2)	2.335(1)	Pd(1')-P(2')	2.342(1)
Pd(1)-Cl(1)	2.363(1)	Pd(1')-Cl(1')	2.356(1)
Cl(2)-C(7)	1.740(6)	Cl(2')-C(7')	1.730(5)
N(1)-C(2)	1.331(7)	N(1')-C(2')	1.327(7)
N(1)-C(9)	1.391(6)	N(1')-C(9')	1.387(6)
N(1)-C(11)	1.474(7)	N(1')-C(11')	1.473(6)
C(2)-C(3)	1.387(7)	C(2')-C(3')	1.374(7)
C(3)-C(4)	1.387(7)	C(3')-C(4')	1.374(7)
C(4)-C(10)	1.410(7)	C(4')-C(10')	1.424(7)
C(5)-C(6)	1.369(8)	C(5')-C(6')	1.356(8)
C(5)-C(10)	1.417(7)	C(5')-C(10')	1.424(7)
C(6)-C(7)	1.411(8)	C(6')-C(7')	1.412(8)
C(7)-C(8)	1.362(8)	C(7')-C(8')	1.358(8)
C(8)-C(9)	1.408(7)	C(8')-C(9')	1.407(7)
C(9)-C(10)	1.416(7)	C(9')-C(10')	1.414(7)
Bond-angles (º)			
C(4)-Pd(1)-P(1)	88.8(1)	C(4')-Pd(1')-P(1')	89.1(1)
C(4)-Pd(1)-P(2)	90.5(1)	C(4')-Pd(1')-P(2')	90.1(2)
P(1)-Pd(1)-P(2)	177.63(5)	P(1')-Pd(1')-P(2')	177.67(5)
C(4)-Pd(1)-Cl(1)	175.4(2)	C(4')-Pd(1')-Cl(1')	175.3(2)
P(1)-Pd(1)-Cl(1)	87.44(5)	P(1')-Pd(1')-Cl(1')	87.29(5)
P(2)-Pd(1)-Cl(1)	93.22(5)	P(2')-Pd(1')-Cl(1')	93.38(5)
C(2)-N(1)-C(9)	120.3(4)	C(2')-N(1')-C(9')	120.8(4)
C(2)-N(1)-C(11)	119.7(4)	C(2')-N(1')-C(11')	119.3(4)
C(9)-N(1)-C(11)	120.0(4)	C(9')-N(1')-C(11')	119.9(4)
N(1)-C(2)-C(3)	122.0(5)	N(1')-C(2')-C(3')	121.6(5)
C(2)-C(3)-C(4)	120.9(5)	C(2')-C(3')-C(4')	121.9(5)
C(3)-C(4)-C(10)	117.1(5)	C(3')-C(4')-C(10')	116.7(4)
C(3)-C(4)-Pd(1)	119.4(4)	C(3')-C(4')-Pd(1')	120.5(4)
C(10)-C(4)-Pd(1)	123.4(4)	C(10')-C(4')-Pd(1')	122.7(4)
C(6)-C(5)-C(10)	121.7(5)	C(6')-C(5')-C(10')	121.9(5)
C(5)-C(6)-C(7)	118.7(5)	C(5')-C(6')-C(7')	119.0(5)
C(8)-C(7)-C(6)	122.5(5)	C(8')-C(7')-C(6')	121.9(5)
C(8)-C(7)-Cl2	118.9(4)	C(8')-C(7')-Cl(2')	119.5(4)
C(6)-C(7)-Cl2	118.6(4)	C(6')-C(7')-Cl(2')	118.5(4)
C(7)-C(8)-C(9)	118.4(5)	C(7')-C(8')-C(9')	119.0(5)
N(1)-C(9)-C(8)	119.9(5)	N(1')-C(9')-C(8')	120.5(4)
N(1)-C(9)-C(10)	118.8(5)	N(1')-C(9')-C(10')	118.4(4)
C(8)-C(9)-C(10)	121.3(5)	C(8')-C(9')-C(10')	121.1(5)
C(4)-C(10)-C(9)	120.7(4)	C(4')-C(10')-C(9')	120.4(5)
C(4)-C(10)-C(5)	121.9(5)	C(4')-C(10')-C(5')	122.5(4)
C(9)-C(10)-C(5)	117.4(5)	C(9')-C(10')-C(5')	117.1(5)

The molecular assembly of complex **20a** is shown in Figure 3.14. The asymmetric units (shown in magenta) are stacked on top of one another as viewed along the a-axis to form alternate layers of the

cation and anion that are orientated diagonally to the c- and b-axis. CH_2Cl_2 molecules fill the spaces between the anions.

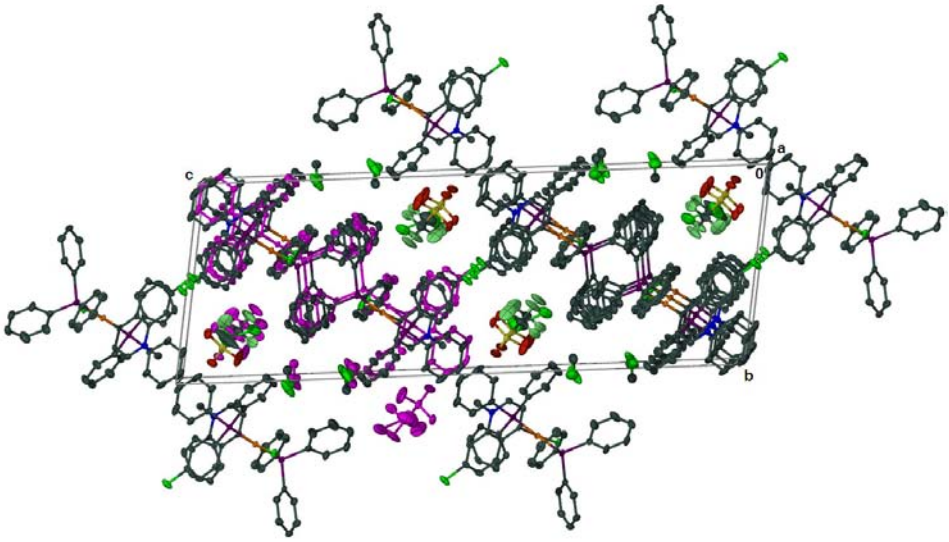

Figure 3.14 Molecular assembly of complex **20a** as seen along the a-axis; asymmetric unit highlighted in magenta

3.2.6 The function of steric influence when setting up a competitive situation for oxidative substitution

Although carbene complexes with the $M(PPh_3)_2Cl$ group attached to the carbon atom next to the heteroatom form readily when $M(PPh_3)_4$ is reacted with methylated pyridinium derived ligands, the fact that the 4-ylidene product selectively forms when $M(PPh_3)_4$ is reacted with 2,4-dichloro-*N*-methyl-pyridinium triflate (**17**), might be the result of two effects: either the thermodynamically more stable product forms as a result of the steric bulk of the methylated nitrogen and/or the higher M=C bond strength for the *r*NHC product compared to the *n*NHC product (better σ-donor as discussed earlier) is responsible. Since the protonated ligand may be regarded as having very little steric requirement and thus providing the possibility for the formation of the 2-substituted product (or the 7-ylidene product for 4,7-dichloroquinolin), the reactions discussed in Sections 3.2.5 were repeated utilising the protonated ligand precursors.

3.2.6.1 Synthesis of pyridinium-type ligands, 2,4-dichloro-pyridinium triflate, 21, and 4,7-dichloro-quinolinium triflate, 22

The protonated ligands **21** and **22** are available by straightforward protonation. The reactions were executed at room temperature overnight in dichloromethane using methyltrifluorosulphonic acid

(CH_3SO_3H). After diethyl ether was added to precipitate the product, the solvent was removed *via* a cannula and the resulting white precipitate was washed several times with diethyl ether to yield 85.7 % of compound **21** and 98.0 % of compound **22** respectively (Scheme 3.9).

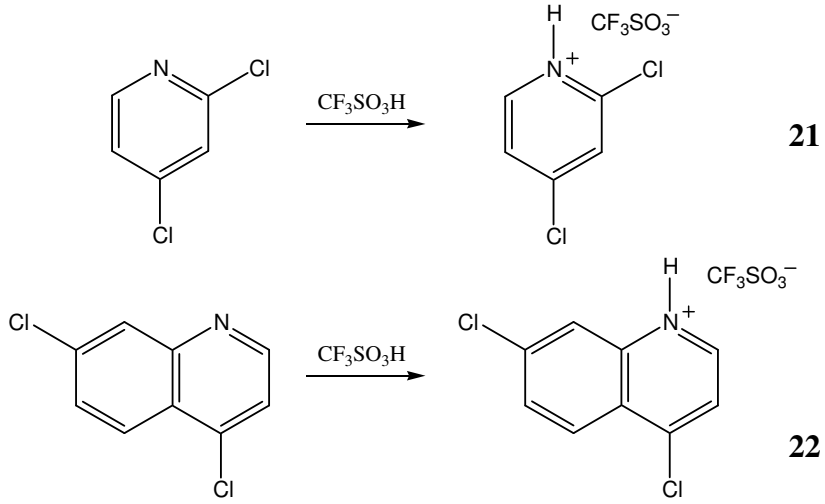

Scheme 3.9

3.2.6.2 Reaction of $M(PPh_3)_4$ (M = Pd or Ni) with 2,4-dichloro-pyridinium triflate, 21, or 4,7-dichloro-quinolinium triflate, 22

Reaction of $Pd(PPh_3)_4$ with compound **21** at 60°C in toluene for 16 hours, again yielded the C4 bonded *remote* carbene complex (Scheme 3.10), but two other unidentifiable products were also present which could not be separated from the target complex. The attack at the 4-position has to be electronically favoured, because steric blocking of the 2-position by the proton can be ruled out. On the other hand, reaction of $Ni(PPh_3)_4$ with compound **21** at room temperature in THF, produced a light yellow microcrystalline product which formed a red brown oily residue when dissolved in CH_2Cl_2. ^{31}P NMR indicated the presence of five products, making the ^{1}H and ^{13}C NMR spectra impossible to interpret.

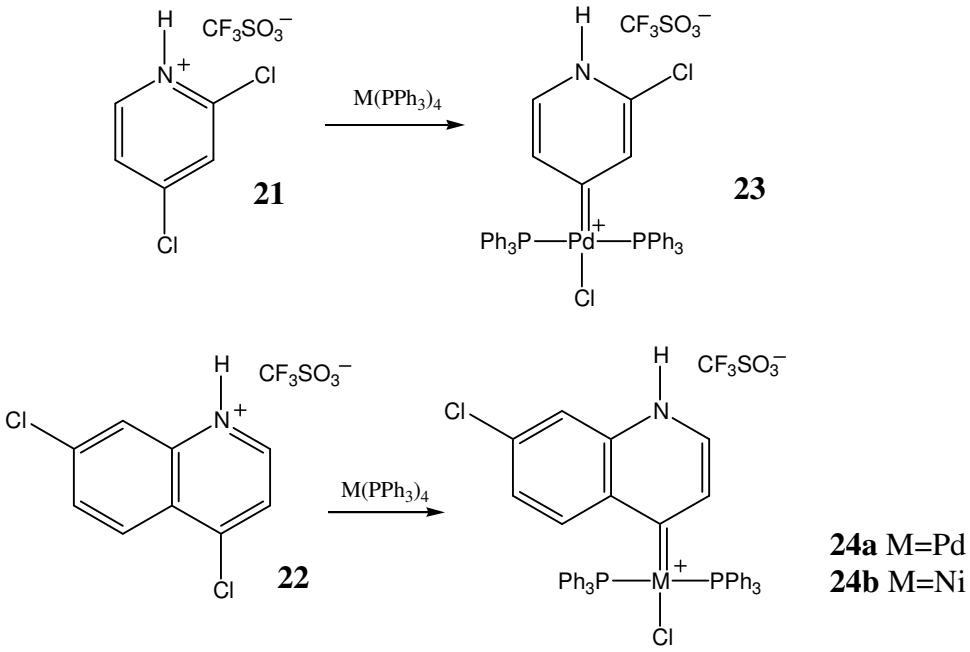

Scheme 3.10

Following the same procedure as employed for complexes **20a** and **20b** respectively, complexes **24a** and **24b** (Scheme 3.10) were obtained when $M(PPh_3)_4$ (M = Pd, Ni) was reacted with 4,7-dichloro-quinolinium triflate, **22**. This result again shows that oxidative substitution preferably occurs on the ring that contains the heteroatom.

3.2.6.2 Spectroscopic characterisation of 2,4-dichloro-pyridinium triflate, 21, and *trans*-chloro(2-chloro-2,4-dihydro-pyrid-4-ylidene)bis(triphenylphosphine)palladium(II) triflate, 23

NMR spectroscopy

The NMR (^{1}H, ^{13}C and ^{31}P) spectroscopic data for compound **21** and the carbene complex **23** are summarised in Table 3.23. As previously mentioned, even with the assistance of 2D-NMR techniques (ghsqc and ghmqc), assignment of the signals for the Pd-complex, **23**, was very laborious due to the presence of three species. The protons give rise to broad misshapen multiplets or doublets making integration of the peaks non-representative. The integration values that were ambiguously obtained are therefore indicated in italics in Table 3.23. A good agreement with the shifts in **19a** and especially the C-P coupling for two adjacent carbon atoms in addition to the carbene carbon atom resonance, are indicative for the formation of the 4-pyridylidene isomer. The ratio of the three species present according to ^{31}P NMR measurements is 26:2:1 of which the carbene complex **23** is the most abundant. The predominant formation of the 4-ylidene rather the 2-ylidene is indicated clearly by the fine structure observed in the proton couplings. Since the resonances of both H^3 and H^5 appear as triplets (coupling with the P-atoms with a coupling constant

of 3.7 Hz) and not just H^3 (observed when the metal is bonded in the C2 position), the *trans*-chloro(2-chloro-2,4-dihydro-pyrid-4-ylidene)bis(triphenylphosphine)palladium(II) triflate has certainly formed. The NH resonance could not even be observed with the NOESY 2D NMR technique.

Table 3.23 NMR data of complexes **21** and **23** in CD_2Cl_2

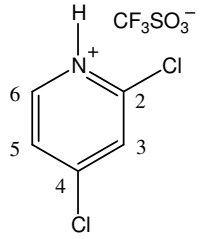

21

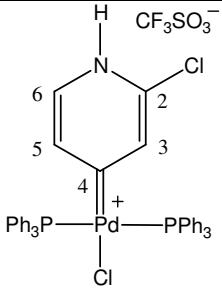

23

Assignment	δ / ppm*	
	21	**23**
^{1}H NMR		
NH	n.a.	n.a.
H^3	n.a.	7.15 (1H, bs)
H^5	n.a.	7.37 (*1H*, m)*
H^6	8.79 (1H, m)	7.18 (*1H*, m)*
H^3, H^5	7.94 (2H, m)	n.a.
Ph	n.a.	7.63, 7.50, 7.41 (*30H*, 3 x m)*
^{13}C NMR		
C^2	157.0 (s)	137.4 (s)
C^3	128.7 (s)	135.3 (t, $^3J_{P\text{-}C}$ = 4.3 Hz)
C^4	146.6 (s)	204.6 (t, $^2J_{P\text{-}C}$ = 6.1 Hz)
C^5	126.8 (s)	133.2 (t, $^3J_{P\text{-}C}$ = 3.6 Hz)
C^6	144.7 (s)	134.6 (s)
Ph^{ipso}	n.a.	129.2 (m)
Ph^{ortho}	n.a.	134.7 (m)
Ph^{meta}	n.a.	128.9 (m)
Ph^{para}	n.a.	131.7 (s)
^{31}P NMR		
PPh_3	n.a.	24.0 (s)

* obscured by by-product signals

The proton and carbon signals resonate upfield for both **21** and **23** compared to their methylated analogues except the resonance for C2 in **21** which shows no significant difference. The general upfield shift results from the smaller inductive effect of the proton compared to a methyl group.

The C^4 resonance of complex **23** appears as a triplet at δ 204.6, representing a downfield shift, Δδ of *ca.* 2 from the corresponding signal in compound **19a** (δ 202.3). It resonates well within the chemical shift range (189.5 – 216.8 ppm) observed for previously documented Pd(II)-N^1HC^6 complexes.[84]

The P-atoms resonate as a singlet at 24.0 ppm, again signifying the equivalence of the PPh_3-ligands and their *trans* arrangement to one another around the metal centre.

Mass spectrometry

The FAB mass spectrometry data of compound **21** and complex **23** (obtained from the crude mixture) are given in Table 3.24. The compounds exhibit a fragmentation pattern in which the cation is observed as the fragment with the highest molecular mass. For complex **23** the loss of Cl is followed by the loss of one PPh_3 ligand and subsequently another Cl-atom.

Table 3.24 FAB-MS data of **21** and **23**

Complex	*m/z*	Relative intensity	Fragment ion
21	147.9	100	$[M\text{-}CF_3SO_3]^+$ (^{35}Cl)
23	780.3	6	$[M\text{-}CF_3SO_3]^+$ (^{35}Cl, ^{106}Pd)
	744.5	3	$[M\text{-}Cl\text{-}CF_3SO_3]^+$
	482.2	15	$[M\text{-}Cl\text{-}PPh_3\text{-}CF_3SO_3]^+$
	446.2	3	$[M\text{-}2Cl\text{-}PPh_3\text{-}CF_3SO_3]^+$

3.2.6.3 Spectroscopic characterisation of compounds 4,7-dichloroquinolinium triflate, 22, *trans*-chloro(7-chloro-4,7-dihydro-quinol-4-ylidene)bis(triphenylphosphine)palladium(II) triflate, 24a and *trans*-chloro(7-chloro-4,7-dihydro-quinol-4-ylidene)bis(triphenyl-phosphine)nickel(II) triflate, 24b

The signals in the NMR spectra of **22**, **24a** and **24b** (Table 3.25) have been assigned using the same principles as applied for **18**, **20a** and **20b** respectively. As discussed for the ligand precursors, **11** - **13**, the shielding of the carbon atoms in aromatic heterocyclic compounds are determined by the heteroatom.[111] The resonance structures of a quinolinium salt can be represented as shown in Scheme 3.11. The carbon atoms in the α- and γ-positions, as well as the hydrogens bonded to it will experience a deshielding effect owing to the distribution of the positive charge.

[111] H. Freibolin, in *Basic One- and Two-Dimensional NMR Spectroscopy,* Wiley-VCH, Weinheim, 4th ed., 2005, p. 65.

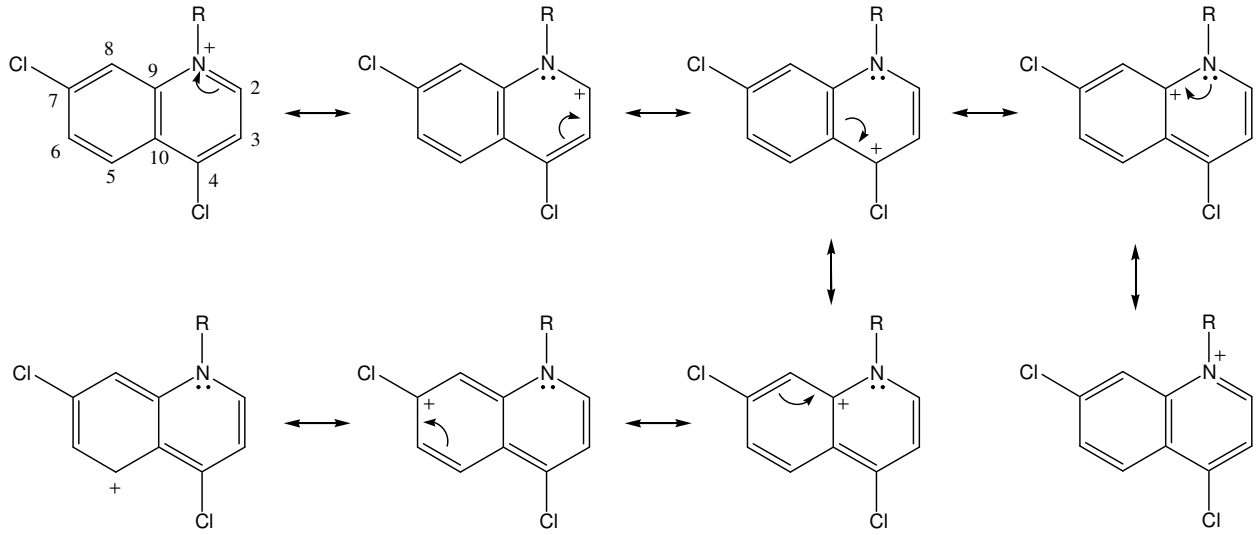

Scheme 3.11

This deshielding resonance effect can be clearly seen in the chemical shifts of H^2, H^5, C^2, C^4, C^5, C^7 and C^9 of compound **22**, appearing more downfield than H^3, H^6, H^8 and C^3. Comparison of compound **22** to the methylated analogue, **18**, shows that the small but definite larger inductive effect of the methyl group when compared to the hydrogen is seen in the more upfield signals of the methylated product. The exceptions to this is the chemical shifts of C^2, C^6 and C^8 of compound **22** which appear more downfield.

When the carbene ligand is bonded to the metal, the resonances are shifted upfield compared to that of the methylated product (**20a** and **20b**). As mentioned previously, the positive charge may be situated on the metal to the highest degree rather than the N-atom after complexation, and even more so now, with the less inductive hydrogen group on the nitrogen.

The signal of the carbene carbon of complex **24a** [δ 207.2] appears 62.1 ppm downfield to that of the ligand precursor (**22**) and at a similar chemical shift to that of the same signal for complex **20a**, while the chemical shift of C^4 of **24b** (δ 216.6) is nearly the same as for the methylated compound (**20b**, δ 216.7), situated 71.5 ppm downfield from the same signal in **22**. This illustrates the higher electronegativity of the Pd(II) center compared to that of Ni(II).

Table 3.25 ^{1}H and ^{13}C-{^{1}H} and NMR data of complexes **22**, **24a** and **24b** in CD_2Cl_2

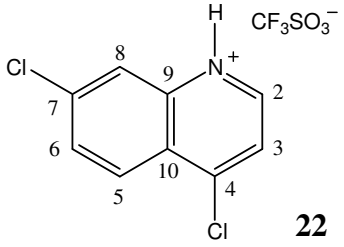

22

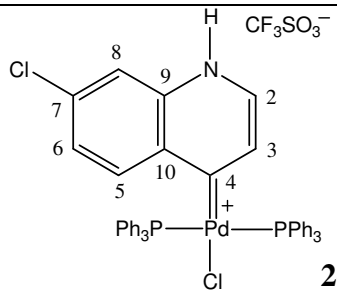

24a

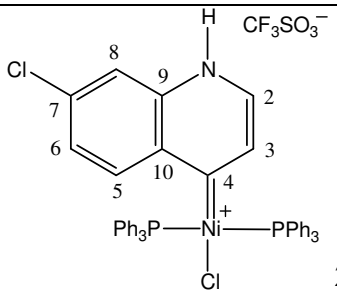

24b

Assignment	δ / ppm*		
	22	**24a**	**24b**
^{1}H NMR			
NH	n.o.	n.o.	n.o.
H^2	9.10 (1H, d, ^{3}J = 6.0 Hz)	7.49 (1H, d, ^{3}J = 5.8 Hz)	7.77 (1H, d, ^{3}J = 5.8 Hz)
H^3	8.08 (1H, d, ^{3}J = 6.0 Hz)	n.o.	n.o.
H^5	n.o.	8.55 (1H, d, ^{3}J = 8.8 Hz)	9.19 (1H, d, ^{3}J = 8.8 Hz)
H^6	8.00 (1H, dd, ^{3}J = 9.0 Hz, ^{4}J = 2.0 Hz)	7.43 (1H, dd, ^{3}J = 8.8 Hz, ^{4}J = 2.0 Hz)	7.48 (1H, dd, ^{3}J = 8.8 Hz, ^{4}J = 1.9 Hz)
H^8	n.o.	7.69 (1H, d, ^{4}J = 2.0 Hz)	n.o.
H^5, H^8	8.47 (2H, m)	n.a.	n.a.
Ph	n.a.	7.41, 7.27 (18H, 2 x m)	7.40 (6H, m)
Ph, H^3	n.a.	7.52, (13H, m)	7.28 (13H, m)
Ph, H^8	n.a.	n.a.	7.55 (13H, m)
^{13}C NMR			
C^2	155.1 (s)	135.6 (s)	132.0 (s)
C^3	122.8 (s)	129.6 (t, $^{3}J_{C\text{-}P}$ = 4.3 Hz)	129.6 (t, $^{3}J_{C\text{-}P}$ = 3.7 Hz)
C^4	145.1 (s)	207.2 (t, $^{2}J_{C\text{-}P}$ = 5.5 Hz)	216.6 (t, $^{2}J_{C\text{-}P}$ = 30.0 Hz)
C^5	133.2 (s)	135.2 (s)	134.9 (s)
C^6	127.3 (s)	129.3 (s)	128.7 (s)
C^7	143.9 (s)	140.2 (s)	140.0 (s)
C^8	121.3 (s)	120.2 (s)	120.3 (s)
C^9	139.1 (s)	129.4 (s)	132.0 (s)
C^{10}	126.4 (s)	133.8 (t, $^{3}J_{C\text{-}P}$ = 2.5 Hz)	134.7 (bs)
Ph^{ipso}	n.a.	129.2 (m)	129.3 (m)
Ph^{ortho}	n.a.	134.5 (m)	134.4 (m)
Ph^{meta}	n.a.	128.7 (m)	128.6 (m)
Ph^{para}	n.a.	131.5 (s)	131.3 (s)
^{31}P NMR			
PPh_3	n.a.	23.8 (s)	22.6 (s)

As seen for all the complexes thus far discussed, the H-atoms of PPh_3 appear as multiplets at $\delta > 7.0$ and the fine structure of the phenyl C-atoms conform to an AXX' spin system. Again, the *trans* arrangement of the PPh_3 ligands is confirmed by the singlet observed in the ^{31}P NMR spectrum and

the triplet observed for the carbene carbons, originating from a $^{2}J_{C\text{-}P}$ coupling system with two equivalent P-atoms.

Mass spectrometry

The fragmentation patterns of compound **22** and complexes **24a** and **24b** are shown in Table 3.26. Peaks representing the cation in each compound are observed. Peaks representing the sequential loss of a Cl and a PPh_3 ligand and, for **24a**, both a Cl and PPh_3 ligand are observed. The $[M\text{-}PPh_3\text{-}CF_3SO_3]^+$ fragment is not observed for complex **24b**.

Table 3.26 FAB MS data of compound **22** and complexes **24a** and **24b**

Complex	*m/z*	Relative intensity	Fragment ion
22	198.0	100	$[M\text{-}H\text{-}CF_3SO_3]^+$ (^{35}Cl)
24a	830.4	5	$[M\text{-}CF_3SO_3]^+$ (^{35}Cl, ^{106}Pd)
	794.5	1	$[M\text{-}Cl\text{-}CF_3SO_3]^+$
	568.3	5	$[M\text{-}PPh_3\text{-}CF_3SO_3]^+$
	532.3	1	$[M\text{-}Cl\text{-}PPh_3\text{-}CF_3SO_3]^+$
24b	782.1	3	$[M\text{-}CF_3SO_3]^+$ (^{35}Cl, ^{58}Ni)
	746.9	1	$[M\text{-}Cl\text{-}CF_3SO_3]^+$
	520.0	10	$[M\text{-}Cl\text{-}PPh_3\text{-}\ CF_3SO_3]^+$

3.2.7 Quantum mechanical calculations

As previously stated, computational studies on the nature of the bonding in nN^{2}HC^5 carbene complexes have shown that the electrostatic contribution to the bond has a highly important role in the interaction[112] and that the covalent portion of the bond is mostly σ, with minimal π-contribution.[113] π-Backdonation is diminished because the two N-atoms adjacent to the carbene carbon donate some π-electron density into the formally empty *p*-orbital on the carbene carbon, limiting the ability of the ligand to accept electron density from the metal.

In our work on *r*NHCs and their complexes we have demonstrated that, as with other carbenes, most of the attraction between that ligand and the metal centre is electrostatic[18] and that the covalent contribution mostly constitutes σ-interaction. Crystallographic data support our theoretical results suggesting that the *trans* influence of the carbene ligand increases when the heteroatom N is farther

[112] C. Boehme and G. Frenking, *Organometallics,* 1998, **17**, 5801.
[113] J. C. Green, R. G. Scurr, P. L. Arnold and F. G.N. Cloke, *J. Chem. Soc., Chem. Commun.,* 1997, 1963.

away from the carbene carbon.[17] This implies that the *r*NHCs might be better σ-donors and/or π-acceptors than the *n*NHCs.

In order to understand from a chemical viewpoint the reasons behind the formation of the products obtained in Section 3.2.4, to compare the bond differences in complexes **14** - **16** and to compare the synthesised products to other model compounds the metal carbene bonds were analyzed theoretically.[114]

To carry out the calculations within reasonable limits, model compounds (**M**) with phenyl and methyl substituents mainly replaced by hydrogen atoms were chosen (Figure 3.15).

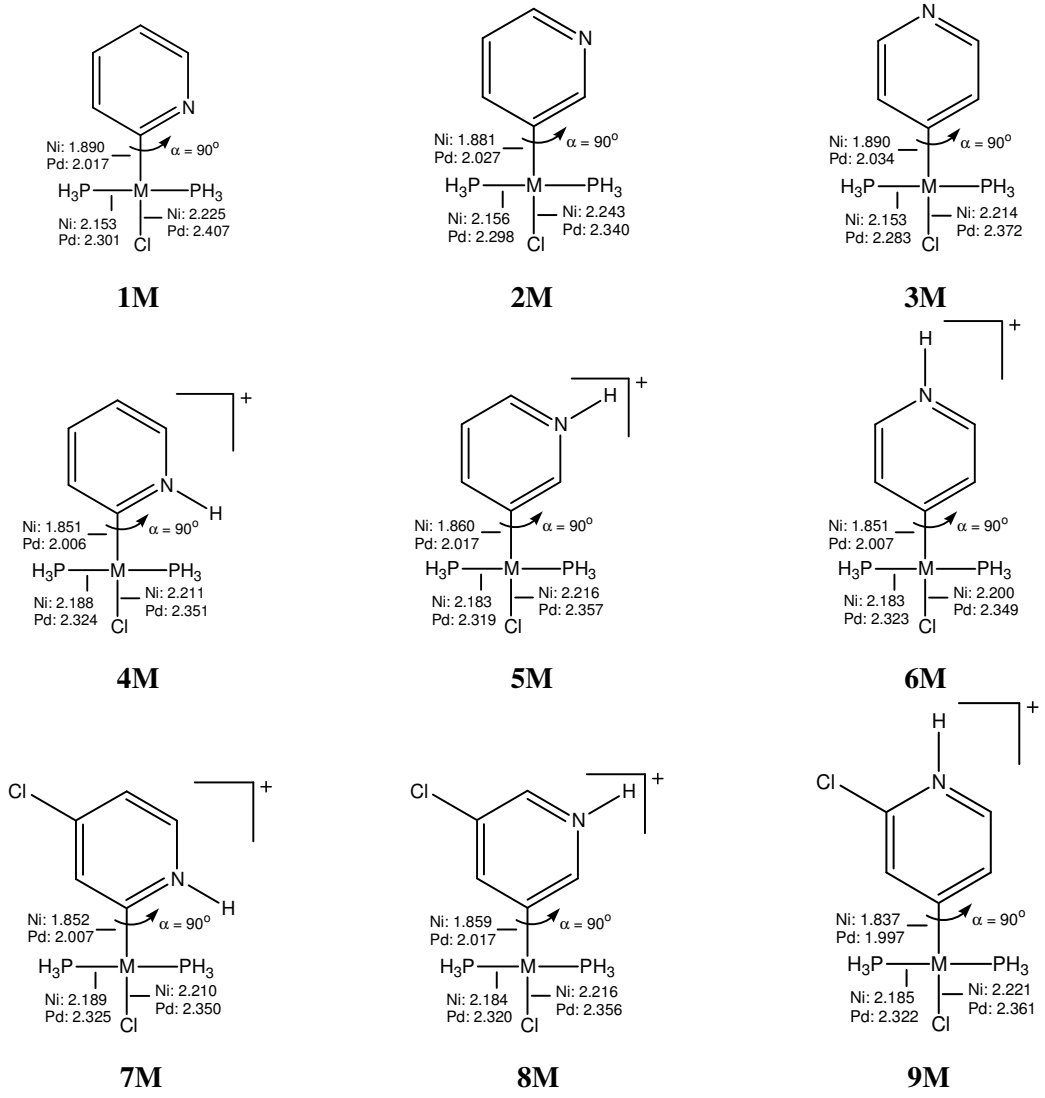

Figure 3.15 The calculated model complexes of Ni and Pd. The optimised bond lengths for the M-C, M-PH_3 and M-Cl bonds are given in Å. The angle (α) is the dihedral angle of the plane consisting of the $M(PH_3)_2Cl$ fragment with the heterocyclic ring.

[114] G. Heydenrych, E. Stander, O. B Schuster, H. G. Raubenheimer and G. Frenking, *to be submitted for publication.*

Their geometries were optimized at the RI-BP86/SV level. The interatomic interactions were analyzed by means of an energy decomposition scheme developed independently by Morokuma[115] and by Ziegler and Rauk[116] calculating the bond dissociation energy. All the calculations were carried out by a previous member of our group, Greta Heydenrych, and for the sake of completeness, the most important results are reported here.

All complexes were optimised with C_s symmetry, and contain the ring(s) in the mirror plane. Three sets of complexes were optimised. In the first set (pyridyl complexes, **1M**-**3M**) the N-atom is *orto*, *meta* or *para* to the metal coordinated carbon and unprotonated. The N-atom is protonated in the second set (pyridylidene complexes, **4M**-**6M**) whereas the third set (pyridylidene complexes, **7M**-**9M**) has the N-atom protonated as well as a Cl-substituent *meta* to the carbene carbon.

Considering the geometries obtained for the complexes (Figure 3.15), the position of the heteroatom does not give rise to any significant trend in the M-C bond lengths (as was also found in the X-ray analysis). Protonation tends to shorten the M-C bonds somewhat, as expected upon carbene formation, except for **4M** where the effect might have steric grounds.

The relative energies for complexes **1M** – **9M** are shown in Table 3.27. Among the neutral pyridyl complexes, **3M**, has the lowest energy. The lowest-energy complex in the group of carbene complexes is **4M**, and for the chlorinated complexes, **7M**. Generally, the Ni-complexes span a larger energy range than the Pd-complexes, but otherwise the two metals display very similar trends. An interesting observation concerns the effects of the position of the heteroatom. For the neutral pyridyl complexes and the Cl-substituted protonated (pyridylidene) complexes, having the heteroatom *meta* relative to the carbene carbon atom tends to be unfavourable. However, for the protonated complexes and without further substitution (chlorine-free), the relative energies increase in the order *ortho* < *meta* < *para*. The energy results presented thus far are contradictory to what is observed experimentally, since the *para*-product is formed preferentially when in competition with the formation of the *ortho*-product (see Sections 3.2.5 and 3.2.6). This is possibly the result of not taking the energy *differences* between[17] the newly formed M-C and M-Cl bonds and the enery from breaking the carbon-chloride bonds in the precursors as well as the two metal-phosphine bonds in $M(PPh_3)_4$ into account – the latter is constant.

[115] K. Morokuma, *J. Phys. Chem.,* 1971, **55**, 1236.
[116] T. Ziegler and A. Rauk, *Inorg. Chem.,* 1979, **18**, 1755.

Table 3.27 Relative energies (kcal/mol) of the calculated pyridyl and pyridylidene model complexes at the RI-MP2/TZ2P level.

	Ni	Pd
Neutral complexes[a]		
1M	0.93	2.61
2M	1.09	2.85
3M	0.00	0.00
Protonated complexes[b]		
4M	0.00	0.00
5M	3.29	3.63
6M	5.43	5.40
Chlorinated and protonated complexes[c]		
7M	0.00	0.00
8M	5.92	6.24
9M	4.97	5.18

[a] Relative to **3M**. [b] Relative to **4M**. [c] Relative to **7M**.

Bond dissociation energies (BDEs) calculations for the metal carbon bond (Table 3.28), indicated that the Ni-complexes have slightly stronger bonds than the Pd-complexes. It was also shown that the BDEs of the charged pyridylidene (carbene) complexes (**4M**-**6M**) increase as the N-heteroatom is moved progressively farther away from the M-$C_{carbene}$ bond, whereas the opposite is generally true for the neutral pyridyl (non carbene) complexes (**1M**-**3M**). This is consistent with previous observations made by Frenking *et al*. for similar complexes.[17] For a given metal, the metallic fragment $M(PH_3)_2Cl^+$ is the same for all the complexes. Therefore, any changes in BDEs and the various components of ΔE_{int} and ΔE_{orb} are due to the differences between the heterocyclic ligands.

Table 3.28 BDEs of model complexes, in kcal/mol (RI-BP86/TZ2P).

1M_Pd	-212.3	**5M_Ni**	-105.1
1M_Ni	-216.1	**6M_Pd**	-99.8
2M_Pd	-202.0	**6M_Ni**	-110.0
2M_Ni	-206.2	**7M_Pd**	-83.8
3M_Pd	-202.2	**7M_Ni**	-93.2
3M_Ni	-213.2	**8M_Pd**	-95.1
4M_Pd	-86.5	**8M_Ni**	-100.1
4M_Ni	-96.9	**9M_Pd**	-96.4
5M_Pd	-100.2	**9M_Ni**	-105.6

A look at the HOMOs of the pyridyl complexes – in all cases the σ-donating orbital of the metal bonded carbon atom – shows that the energies of these orbitals decrease as the heteroatom is moved away from the metal bonded carbon (Table 3.29).

Table 3.29 Orbital energies for the σ-donating orbitals (HOMO) of the free heterocyclic ligands in eV.

Heterocyclic ligand	*Complex*	*Energy (eV)*
2-pyridyl	**1M**	0.067
3-pyridyl	**2M**	0.048
4-pyridyl	**3M**	0.046
2-pyridylidene	**4M**	-0.158
3-pyridylidene	**5M**	-0.148
4-pyridylidene	**6M**	-0.130
5-chloro-2-pyridylidene	**7M**	-0.170
5-chloro-3-pyridylidene	**8M**	-0.162
5-chloro-4-pyridylidene	**9M**	-0.145

For the neutral free carbenes (found in **4M** – **9M**), the energy of the HOMO increases as the heteroatom is moved away from the carbene carbon atom. It is well-known that the energy of the σ-donating orbital of the free carbene is an indicator of its σ-donating ability, with a higher orbital energy within a group of tautomers corresponding to a higher σ-basicity. Therefore, the σ-basicity of the free heterocyclic ligand depends on the position of the N-heteroatom as well as the carbene character. This dual dependency is subsequently seen in the bond strengths of the resulting carbene complexes.

It was also observed that the amount of π-bonding in the pyridyl and pyridylidene complexes is always slightly lower when the heteroatom is *meta* to the metal bonded carbon (that is in the *a*NHCs), indicating that the relative positioning of the heteroatom does not only affect BDE, but can also be used to fine-tune the π-bonding ability of the heterocyclic ligand. Protonation (thus carbene formation) tends to increase the relative amount of π-bonding, but this is due to a decrease in σ-overlap upon protonation. In earlier work[117] it was shown that, regardless of the metal centre, the BDEs of the various ligands decrease in the order $\boldsymbol{a}\mathbf{N^2HC^5} > \boldsymbol{n}\mathbf{N^2HC^5}$, reflecting their σ-donating strengths. In all cases, the Pd complexes have the largest relative amount of electrostatic

[117] R. Tonner, G. Heydenrych, G. Frenking, *Chem. Asian J.* 2008, in print.

interaction, followed by Ni. The relative σ-component of the ΔE_{orb} term decreases slightly in the order Pd > Ni for both the ligands – something also observed for the *r*NHCs.

Futhermore, it was found that the electrostatic contribution for the neutral pyridiyl is higher than for the charged complexes. Some variation is observed for the extent of π-bonding, with the ***r*NHC**s and ***n*NHCs** having very similar relative contributions. The relative π-bonding contributions for the neutral pyridyl complexes are somewhat lower.

It would therefore appear that the complex with the metal at position 2 (complex **14**), would be thermodynamically more stable, but the complex with the metal at the 4-position (complex **16**) features the stronger bond (methylated and protonated). As mentioned before, one should preferably compare the total process of oxidative substitution *i.e.* energy from newly formed M-C and M-Cl bonds and the enery from breaking the carbon-chloride bonds in the precursors as well as the two metal-phosphine bonds in $M(PPh_3)_4$.

3.2.8 An NHC ligand with two remote nitrogens

Only one other example of a complex with an *r*NHC ligand which contains more than one heteroatom is known. With ligand precursor, 4-chloro-2-methoxy-*N*-methylquinolinium tetrafluoroborate (**XV**), carbene complex preparation is accomplished with alkylation of the oxygen atom, with both a distant oxygen and nitrogen atom which can aid in carbene stabilization.[15]

Since the classical N^2HC^5 ligands contain two nitrogen atoms, a comprehensive comparative study of N^2HC^5 and NHC^6 would require the preparation of a *r*NHC ligand with two nitrogens in order to determine the influence of the presence of the second heteroatom on the physical properties of the resulting carbene complex compared to that of an *r*NHC ligand with only one nitrogen.

3.2.8.1 Preparation of the ligand precursors (4-chloro-*N*-methylpyrid-2-ylidene)methyl amine, 25, and (4-chloro-*N*-methylpyrid-2-ylidene)dimethylmethylammonium triflate, 26

The compound, (4-chloro-*N*-methyl-pyrid-2-ylidene)methyl amine, was prepared according to a method described by Ahlbrecht[118] for the preparation of analogous compounds which can provide reactive intermediates for the synthesis of various quinolines. Reaction of 2,4-dichloropyridinium

[118] H. Ahlbrecht and C. Vonderheid, *Chem. Ber.,* 1975, **108**, 2300

triflate (**17**) with a primary amine leads to aminolysis and substitution at position 2. Work-up afforded the isolation of a very hygroscopic compound, **25**, in 51 % yield. Treatment of **25** with $CF_3SO_3CH_3$ yielded the quaternized compound **26** in 83 % yield (Scheme 3.12).

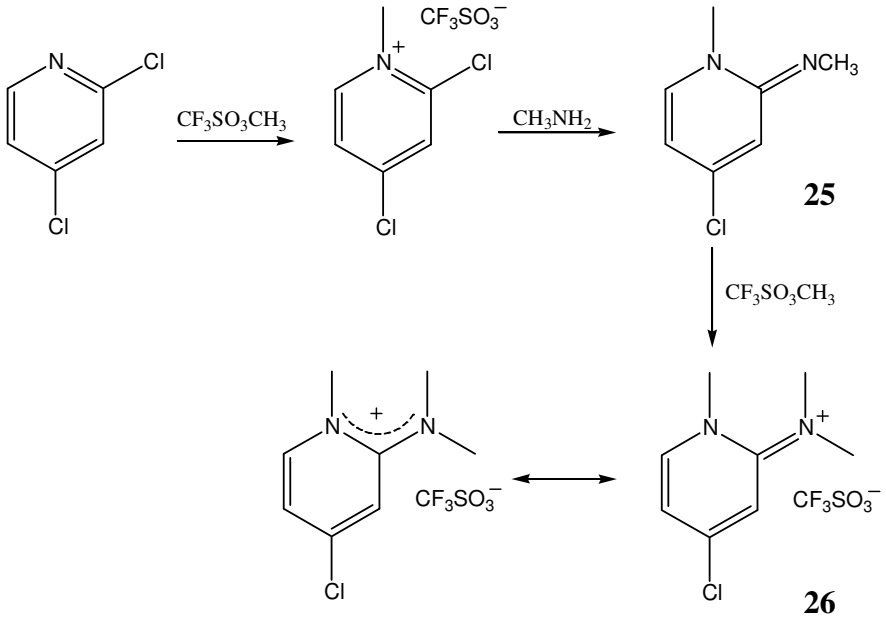

Scheme 3.12

3.2.8.2 Spectroscopic characterisation of (4-chloro-*N*-methylpyrid-2-ylidene)methylamine, 25, and (4-chloro-*N*-methylpyrid-2-ylidene)dimethylmethyl ammonium triflate, 26

NMR spectroscopy

The ^{1}H and ^{13}C NMR spectroscopic data of the ligand precursors **25** and **26** are tabulated below. The signals for the protons of the NMe peaks are more downfield for the alkylated ligand due to the deshielding effect of the positive charge. Similarly H^3, H^5 and H^6 of **26** also appear more downfield than the corresponding protons in **25**, with H^6 being the most downfield due to the resonance effect (Scheme 3.12) and inductive effect of the closely situated electronegative N-atom. H^3 and H^6 appear in both compounds as doublets effected by coupling with H^5. The signal of H^5 appears as a doublet of doublets, coupling with both H^3 (2.4 Hz in **25** and 2.3 Hz in **26**) and H^5 (7.3 Hz in **25** and 7.2 Hz in **26**).

The carbon signals in compound **26** also appear downfield compared to the same signals in **25**, again due to the positive charge, except C^4 which remains essentially unchanged. Akin to all the compounds discussed so far, the signals of C^2, C^4 and C^6 appear downfield compared to the signals

of C^3 and C^5, owing to resonance originating from the lone pair of electrons (in **26**) and the inductive effect (both **25** and **26**) of the electronegative N-atom.

Table 3.30 ^1H and ^{13}C-{^1H} and NMR data of compounds **25** and **26** in CD_2Cl_2

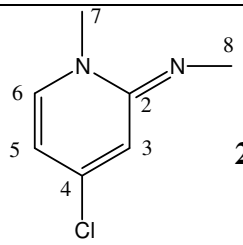

25

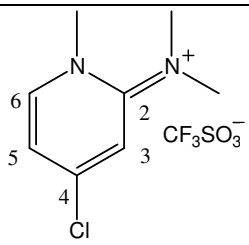

26

Assignment	δ / ppm*	
	25	**26**
^1H NMR		
NMe	3.27 (3H, s)	4.05 (3H, s)
=NMe	2.88 (3H, s)	n.a.
NMe_2	n.a.	3.15 (6H, s)
H^3	6.38 (1H, d, ^4J = 2.4 Hz)	7.31 (1H, d, ^4J = 2.3 Hz)
H^5	5.65 (1H, dd, ^3J = 7.3 Hz, ^4J = 2.4 Hz)	7.22 (1H, dd, ^3J = 7.2 Hz, ^4J = 2.3 Hz)
H^6	6.99 (1H, d, ^3J = 7.3 Hz)	8.22 (1H, d, ^3J = 7.2 Hz)
^{13}C NMR		
NMe	35.2 (s)	45.4 (s)
=NMe	39.1 (s)	n.a.
NMe_2	n.a.	43.1 (s)
C^2	142.9 (s)	160.1 (s)
C^3	110.1 (s)	119.0 (s)
C^4	153.6 (s)	152.7 (s)
C^5	102.1 (s)	118.0 (s)
C^6	140.1 (s)	145.6 (s)

3.2.8.3 Synthesis of *trans*-chloro(1-methyl-1,2,4-trihydro-pyrid-2-methylimine-bis(triphenylphosphine)palladium(II), 27, *trans*-chloro(*N*-methyl-1,2,4-trihydro-2-dimethyl-aminepyrid-4-ylidene)bis(triphenylphosphine)palladium(II) triflate, 28a, and *trans*-chloro(*N*-methyl-1,2,4-trihydro-2-dimethylaminepyrid-4-ylidene)bis(triphenylphosphine)nickel(II) triflate, 28b

Heating a THF solution of the imine ligand precursor **25** with an slight excess of $Pd(PPh_3)_4$ at 70°C for 16 hours, followed by filtration of the reaction mixture through Celite afforded a white precipitate that was washed with THF and dissolved with CH_2Cl_2 to yield after solvent evaporation the complex **27**. Similarly, complex **28b** was obtained by stirring compound **26** with $Ni(PPh_3)_4$ at

room temperature for 4 hours. Complex **28a** was made by employing the same procedure as used for the synthesis of complex **14a** (Scheme 3.13).

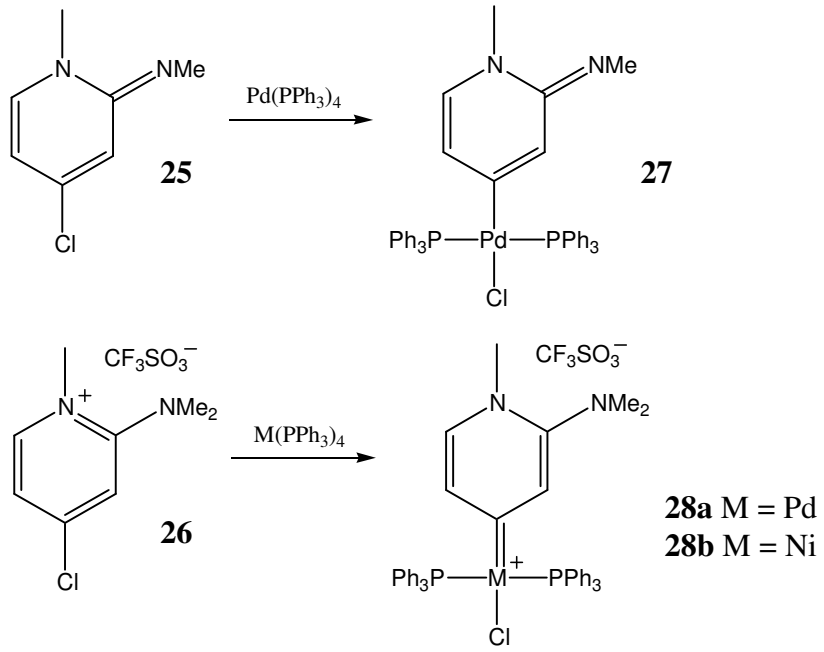

Scheme 3.13

3.2.8.4 Spectroscopic characterisation of *trans*-chloro(1-methyl-1,2,4-trihydro-pyrid-2-methyliminebis(triphenylphosphine)palladium(II), 27, *trans*-chloro(*N*-methyl-1,2,4-trihydro-2-dimethylaminepyrid-4-ylidene)bis(triphenylphosphine)palladium(II) triflate, 28a, and *trans*-chloro(*N*-methyl-1,2,4-trihydro-2-dimethylaminepyrid-4-ylidene)bis(triphenylphosphine)-nickel(II) triflate, 28b

NMR spectroscopy

The ^{1}H, ^{13}C-{^{1}H} and ^{31}P NMR data are collated in Table 3.31. All the ^{1}H and ^{13}C signals of **27, 28a** and **28b** appear upfield with respect to the corresponding values of their ligand precursors **25** and **26**, except H^5 of **27** and **28b** that appears more downfield in the ^{1}H NMR spectra and C^5 and C^6 of **28a** and **28b** in the ^{13}C NMR spectra.

The C^4 resonance of complex **27** appears at δ 148.5, also representing an upfield change in chemical shift, Δδ, of 5.1 ppm from the corresponding signal in compound **25**, whereas the C^4 resonances of both **28a** (δ 194.0) and **28b** (δ 203.5) appear downfield (41.3 and 50.8 ppm respectively) to the same signal in **26**. These latter downfield changes in chemical shift are of the same order of magnitude as those reported previously for heterocyclic group 10 compounds upon metal-carbon bond formation (Section 3.2.5). The carbene character of the alkylated complex, **28a**, compared to the Pd complex (**27**), can be seen in the Δδ 45.5 downfield shift of the signal for C^4 observed for

former complex. For the ligand, 4-chloro-2-methoxy-*N*-methylquinolinium tetrafluoroborate, the difference between the alkylated ligand and the non-alkylated Pd-complex is 32.1 ppm (δ 208.1 vs. δ 176.0).[15]

Table 3.31 ^{1}H, ^{13}C-{^{1}H} and ^{31}P NMR data of complexes **27, 28a** and **28b** in CD_2Cl_2

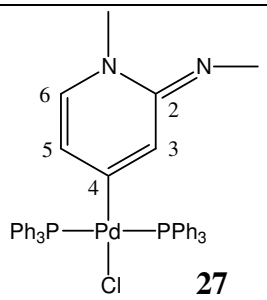

27

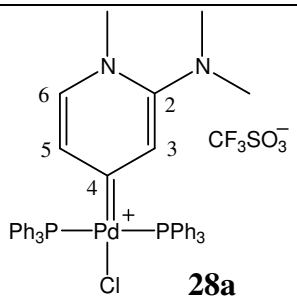

28a

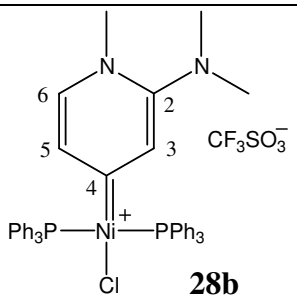

28b

Assignment	δ / ppm*		
	27	**28a**	**28b**
^{1}H NMR			
NMe	3.52 (3H, s)	3.52 (3H, s)	3.43 (3H, s)
=NMe	2.48 (3H, s)	n.a.	n.a.
NMe_2	n.a.	2.48 (6H, s)	2.39 (6H, s)
H^3	6.00 (1H, d, ^{4}J = 2.3 Hz)	6.45 (1H, d, ^{4}J = 1.0 Hz)	6.43 (1H, d, ^{4}J = 1.0 Hz)
H^5	6.35 (1H, dd, ^{3}J = 6.8 Hz, ^{4}J = 1.3 Hz)	n.o.	n.o.
H^6	6.17 (1H, d, ^{3}J = 6.8 Hz)	n.o.	6.82 (1H, d, ^{3}J = 6.5 Hz)
H^5, H^6	n.a.	6.99 (2H, m)	n.a.
Ph^{meta}, H^5	n.a.	n.a.	7.38 (13H, m)
Ph^{ortho}	7.64 (12H, m)	7.64 (12H, m)	7.69 (12H, m)
Ph^{meta}	7.38 (12H, m)	7.40 (12H, m)	n.o.
Ph^{para}	7.48 (6H, m)	7.50 (6H, m)	7.50 (6H, m)
^{13}C NMR			
NMe	42.6 (s)	43.0 (s)	42.7 (s)
=NMe	29.2 (s)	n.a.	n.a.
NMe_2	-	42.4 (s)	42.4 (s)
C^2	133.3 (s)	153.7 (s)	151.8 (s)
C^3	117.5 (bs)	125.0 (t, $^{3}J_{P\text{-}C}$ = 4.3 Hz)	127.4 (bs)
C^4	148.5 (s)	194.0 (t, $^{2}J_{P\text{-}C}$ = 5.5 Hz)	203.5 (s)
C^5	121.3 (bs)	127.5 (bs)	132.5 (bs)
C^6	125.2 (s)	136.8 (s)	134.4 (bs)
Ph^{ipso}	130.0 (m)	129.9 (m)	130.5 (m)
Ph^{ortho}	134.9 (m)	134.9 (m)	135.2 (m)
Ph^{meta}	128.6 (m)	128.8 (m)	129.1 (m)
Ph^{para}	131.2 (s)	131.3 (s)	131.4 (s)
^{31}P NMR			
PPh_3	24.0 (s)	23.7 (s)	22.8 (s)

The carbene carbon signal of the remote complex **28a** appears the most upfield of all the new Pd-carbene complexes (197.7 - 207.2 ppm) discussed so far in this chapter. The same can be said for the Ni-complex **28b** (203.5 ppm compared to 205.0 – 216.7). It would therefore appear that the two nitrogen atoms decrease the σ-donor capability of the ligand compared to the one N-systems (in line with theoretical calculations).[17,18] The fact that the carbene signal of the complex with 4-chloro-2-methoxy-*N*-methylquinolinium tetrafluoroborate as ligand (also two heteroatoms) falls within this range (208.1), accentuates the fact that carbene stabilization occurs mainly from the nitrogen and not the oxygen as reported previously.[15] For complex **28a** and **28b** stabilisation originates from both the nitrogens, creating a similar situation to N^2HC^5 ligands, which diminishes the ability to receive electron density from the metal through π-backdonation.

Single peaks in the ^{31}P NMR spectra indicate single phosphorous environments (as would be expected with two triphenylphosphine groups mutually *trans* as seen from X-ray analysis of the complexes). The carbene carbons are triplets as a result of coupling to two identical phosphorous atoms.

Mass spectrometry

FAB mass spectral data (Table 3.32) of **25** and **27** exhibit the molecular ions, whereas the cationic ions of the ion pairs of **26**, **28a** and **28b** are visible as peaks of weak intensity.

Table 3.32 FAB MS data of compounds **25** and **26** and complexes **27**, **28a** and **28b**

Complex	*m/z*	Relative intensity	Fragment ion
25	159.1	7	$[M]^+$ (^{37}Cl)
	157.1	18	$[M]^+$ (^{35}Cl)
	90.0	8	$[M\text{-}2Me\text{-}Cl]^+$
26	173.1	35	$[M\text{-}CF_3SO_3]^+$ (^{37}Cl)
	171.1	95	$[M\text{-}CF_3SO_3]^+$ (^{35}Cl)
	157.1	37	$[M\text{-}Me\text{-}CF_3SO_3]^+$
27	787.0	6	$[M]^+$ (^{35}Cl, ^{106}Pd)
	525.0	8	$[M\text{-}PPh_3]^+$
	489.9	1	$[M\text{-}Cl\text{-}PPh_3]^+$
28a	801.4	8	$[M\text{-}CF_3SO_3]^+$ (^{35}Cl, ^{106}Pd)
	541.2	5	$[M\text{-}PPh_3\text{-}CF_3SO_3]^+$
	136.1	82	$[M\text{-}Cl\text{-}2PPh_3\text{-}Pd\text{-}CF_3SO_3]^+$
28b	754.9	2	$[M\text{-}CF_3SO_3]^+$ (^{35}Cl, ^{58}Ni)
	491.2	4	$[M\text{-}PPh_3\text{-}CF_3SO_3]^+$
	136.1	77	$[M\text{-}Cl\text{-}2PPh_3\text{-}Ni\text{-}CF_3SO_3]^+$

The fragmentation patterns of the three complexes are remarkably similar and consist of the sequential loss of a PPh_3, followed by a chloride for complex **27** and a Cl, two PPh_3 ligands and the metal centre for complexes **28a** and **28b**.

3.2.8.5 Crystal and molecular structures *trans*-chloro(*N*-methyl-1,2,4-trihydro-2-dimethyl-aminepyrid-4-ylidene)bis(triphenylphosphine)palladium(II) triflate, 28a and *trans*-chloro(*N*-methyl-1,2,4-trihydro-2-dimethylaminepyrid-4-ylidene)bis(triphenylphosphine)nickel(II) triflate, 28b

Selected bond lengths and angles are listed in Table 3.33 (**28a**) and Table 3.34 (**28b**) and the molecular structures appear in Figure 3.16. Complex **28a** crystallised as colourless blocks in the space group $P2_1/c$ and **28b** as yellow needles in $P2_1$.

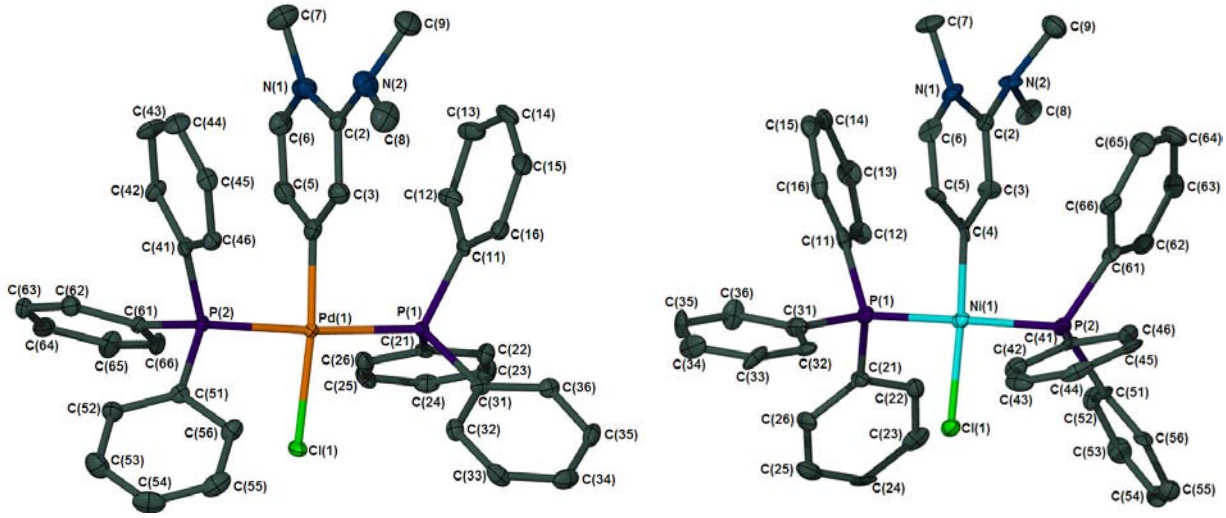

Figure 3.16 Molecular structures of complex **28a** (H-atoms, the triflate counterion, and two CH_2Cl_2 solvent molecules omitted for clarity) on the left and molecular structure of complex **28b** on the right (H-atoms and triflate counterion omitted for clarity) showing the numbering scheme and generated in POV-Ray

The carbene ligand in **28a** is essentially flat with C(9) deviating the most from the least square plane defined by N(1), C(2), C(3), C(4), C(5), C(6) and N(2) by 0.9686(66) Å. This plane is not perpendicular to the slightly distorted square plane calculated through C(4), Pd(1), Cl(1), P(1) and P(2), but turned at an angle of 82.82(9) °. The plane, defined by the same atoms in **28a** (also with C(9) deviating the most – 1.0673(12) Å), has an angle of 84.01(18) ° with the slightly distorted square plane calculated through C(4), Ni(1), Cl(1), P(1) and P(2) in complex **28b**. The angles around the Pd-center deviate from the ideal 90 °, with C(4)-Pd(1)-Cl(1) being really bent

[169.92(13) °]. The distortion is less pronounced in complex **28b**, with the angle P(2)-Ni(1)-P(1) [172.06(11) °] being the furthest from ideal.

Table 3.33 Bond lengths (Å) and angles of complex **28a**

Bond lengths (Å)			
Pd(1)-C(4)	1.990(4)	C(6)-C(5)	1.359(6)
Pd(1)-P(2)	2.332(1)	C(6)-N(1)	1.372(5)
Pd(1)-P(1)	2.336(1)	N(1)-C(2)	1.368(5)
Pd(1)-Cl(1)	2.3821(9)	N(1)-C(7)	1.462(6)
N(2)-C(2)	1.360(5)	C(2)-C(3)	1.412(5)
N(2)-C(8)	1.433(6)	C(4)-C(3)	1.359(6)
N(2)-C(9)	1.484(6)	C(4)-C(5)	1.417(6)
Bond angles (º)			
C(4)-Pd(1)-P(2)	86.9(1)	C(2)-N(1)-C(7)	121.9(4)
C(4)-Pd(1)-P(1)	89.3(1)	C(6)-N(1)-C(7)	117.3(4)
P(2)-Pd(1)-P(1)	175.91(4)	N(2)-C(2)-N(1)	118.6(4)
C(4)-Pd(1)-Cl(1)	169.9(1)	N(2)-C(2)-C(3)	123.6(4)
P(2)-Pd(1)-Cl(1)	91.21(4)	N(1)-C(2)-C(3)	117.7(4)
P(1)-Pd(1)-Cl(1)	92.77(3)	C(3)-C(4)-C(5)	117.3(4)
C(2)-N(2)-C(8)	119.5(4)	C(3)-C(4)-Pd(1)	124.1(3)
C(2)-N(2)-C(9)	120.9(4)	C(5)-C(4)-Pd(1)	118.6(3)
C(8)-N(2)-C(9)	112.7(4)	C(6)-C(5)-C(4)	119.9(4)
C(5)-C(6)-N(1)	121.8(4)	C(4)-C(3)-C(2)	122.8(4)
C(2)-N(1)-C(6)	120.1(4)		

Table 3.34 Bond lengths (Å) and angles of complex **28b**

Bond lengths (Å)			
Ni(1)-C(4)	1.850(9)	N(2)-C(2)	1.388(8)
Ni(1)-P(2)	2.207(3)	N(2)-C(8)	1.48(1)
Ni(1)-P(1)	2.208(3)	N(2)-C(9)	1.50(1)
Ni(1)-Cl(1)	2.219(3)	C(4)-C(5)	1.42(1)
N(1)-C(2)	1.357(9)	C(4)-C(3)	1.46(1)
N(1)-C(6)	1.37(1)	C(5)-C(6)	1.33(1)
N(1)-C(7)	1.49(1)	C(3)-C(2)	1.388(5)
Bond angles (º)			
C(4)-Ni(1)-P(2)	90.9(3)	C(8)-N(2)-C(9)	113.1(7)
C(4)-Ni(1)-P(1)	90.0(3)	C(5)-C(4)-C(3)	115.8(7)
P(2)-Ni(1)-P(1)	172.1(1)	C(5)-C(4)-Ni(1)	120.7(6)
C(4)-Ni(1)-Cl(1)	173.1(3)	C(3)-C(4)-Ni(1)	123.3(6)
P(2)-Ni(1)-Cl(1)	90.3(1)	C(6)-C(5)-C(4)	121.6(8)
P(1)-Ni(1)-Cl(1)	89.7(1)	C(5)-C(6)-N(1)	122.6(9)
C(2)-N(1)-C(6)	118.6(7)	C(2)-C(3)-C(4)	118.5(4)
C(2)-N(1)-C(7)	122.2(7)	N(1)-C(2)-N(2)	116.5(6)
C(6)-N(1)-C(7)	118.3(8)	N(1)-C(2)-C(3)	122.4(4)
C(2)-N(2)-C(8)	117.7(6)	N(2)-C(2)-C(3)	121.0(4)
C(2)-N(2)-C(9)	119.7(6)		

In order to minimize steric repulsion, the "imine plane" is tilted away form the plane of the pyridine backbone resulting in a torsion angle of -47.4(6) ° for C(9)-N(2)-C(2)-N(1) and 163.7(4) ° for C(8)-N(2)-C(2)-N(1) in complex **28a** and 53.6(10) ° for C(9)-N(2)-C(2)-N(1) and -162.4(7) ° for C(8)-N(2)-C(2)-N(1) in complex **28b**.

The Pd-C(carbene) bond length [1.990(4) Å] is slightly shorter than the predicted value (2.05 Å)[119] where pure Pd-C σ-bonding is considered, but falls in the range documented previously for *r*N^{1}HC Pd(II) carbene complexes. The same holds true for the Ni-C(carbene) bond length, although at the shorter end of the range.

The bond distances of N(1)-C(2) and C(2)-N(2) are at 1.368(5) and 1.360(5) respectively, both longer than an N(sp^2)=C(sp^2) double bond (1.27 Å[120]), but still having some double bond character. This is also seen in the distorted planar configuration observed around N(2), probably implying that stabilisation of the carbon donor originates from both nitrogens. In complex **28b** the bond lengths are 1.357(9) and 1.388(8) respectively, also illustrating the same scenario.

The assembly of the molecules in the asymmetric unit of **28a** and **28b** in the unit cell along the b-axis are shown in Figure 3.17 and 3.18 respectively. The cations of complex **28a** are arranged on top of each other along the b-axis and in a layer along the c-axis. In the layers along the c-axis, the cations are packed with the carbene ligand alternating diagonally up and diagonally down, with the triflate counterions situated between the carbene ligands. CH_2Cl_2 molecules, in a regular manner, fill some of the spaces created by the PPh_3-ligands as well as in between the layers along the c-axis.

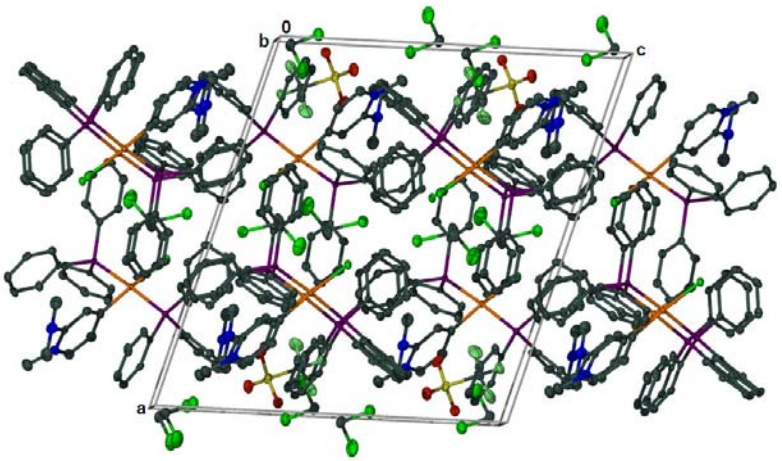

Figure 3.17 Molecular assembly of complex **28a** viewed along the b-axis; H-atoms omitted for clarity

[119] F. H. Allen, O. Kennard and D. G. Watson, *J. Chem. Soc., Perkin Trans. II,* 1989, S15.
[120] F. H. Allen, O. Kennard and D. G. Watson, *J. Chem. Soc., Perkin Trans. II,* 1987, S11.

The cations in complex **28b** are ordered on top of one another in columns along the b-axis, with each alternating column being related by inversion. The anions are situated in voids between the carbene ligand and spaces created by the bulky PPh_3 ligands.

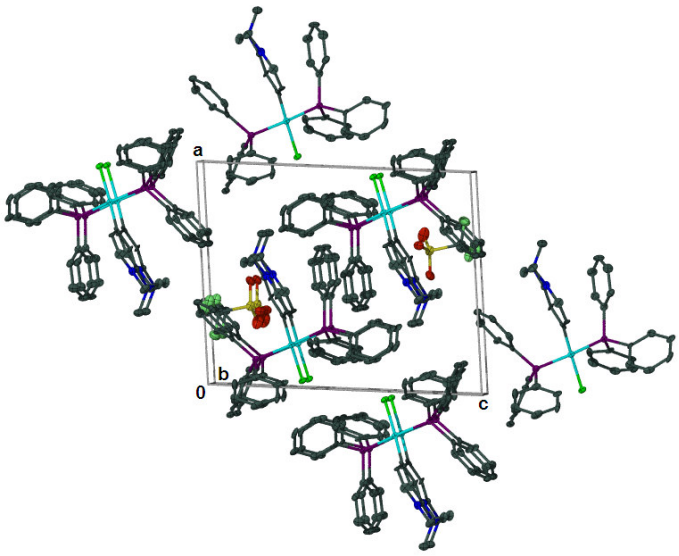

Figure 3.18 Molecular packing of complex **28a** viewed along the b-axis; H-atoms omitted for clarity

3.2.9 The synthesis of a complex that contains two nitrogens with an aromatic R group on one of the nitrogens

In an extension to the synthetic study to prepare a *r*NHC ligand precursor with two nitrogens in order to determine the influence of the presence of the second heteroatom on the physical properties of the resulting carbene complex compared, a similar procedure as for compound **25** was followed using analine instead of methyl amine. Interestingly enough, aminolysis occurred selectively at C4, then followed by protonation (Scheme 3.14) to form compound **29** as an orange coloured microcrystalline product in 63 % yield. When Ahlbrecht *et al.*[118] have used benzylamine, substitution occurrs at position 2. The reason for the different result may largely be attributed to steric reasons, since the extra methylene group in benzylamine reduces the steric strain that is caused by the methyl group on the ring nitrogen. Furthermore, imine-N protonation (with water being the proton source during work-up) did not occur during the synthesis of compound **25**. The protonation result can be influenced by various overlap, basicity and solvent effects and is not readily rationalised.

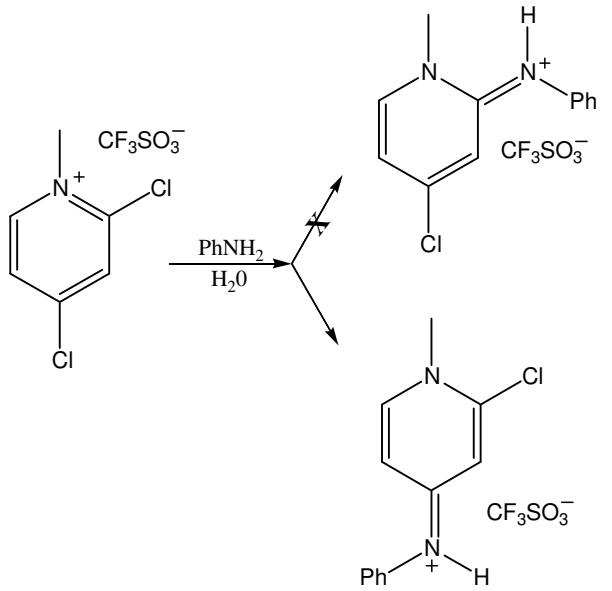

Scheme 3.14

Although the targeted product (**XXVI**) was not obtained, the resulting precursor (**29**) was used in the synthesis of carbene complexes **30a** and **30b** both containing a remote and adjacent heteroatom for carbene stabilisation, the first of its kind (Scheme 3.15). The complexes were prepared *via* the same methods as employed for the *trans*-chloro(*N*-methyl-1,3-dihydro-pyridin-3-ylidene)-bis(triphenylphosphine) metal complexes (Section 3.2.3) taking the different experimental conditions for palladium and nickel into consideration.

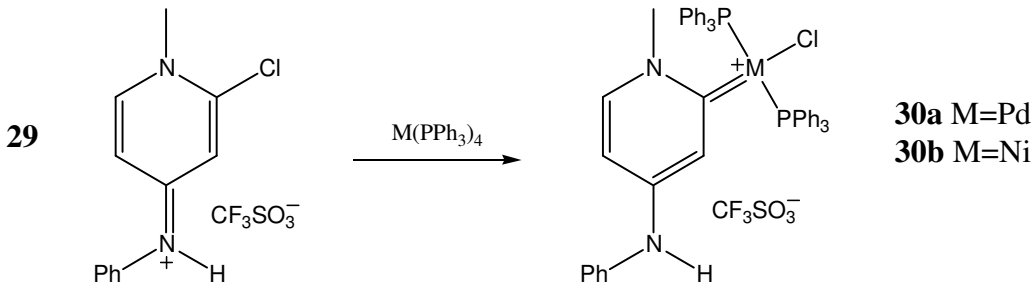

Scheme 3.15

3.2.9.1 Characterisation of (2-chloro-*N*-methylpyrid-4-ylidene)phenylamineammonium triflate, 29, *trans*-chloro(*N*-methyl-1,2,4-trihydro-4-phenylaminepyrid-2-ylidene)bis(triphenylphosphine)palladium(II) triflate, 30a and *trans*-chloro(*N*-methyl-1,2,4-trihydro-4-phenylaminepyrid-2-ylidene)bis(triphenylphosphine)nickel(II) triflate, 30b

NMR spectroscopy

The NMR assignments for the ligand precursor, **29**, and both complexes, **30a** and **30b**, are based on two dimensional experiments (ghsqc and ghmqc) and are listed in Table 3.35.

Table 3.35 ^{1}H and ^{13}C-{^{1}H} NMR data of compound **29** and ^{1}H, ^{13}C-{^{1}H} and ^{31}P NMR data of complexes **30a** and **30b** in CD_2Cl_2

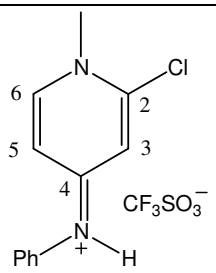

29

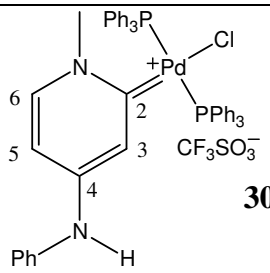

30a

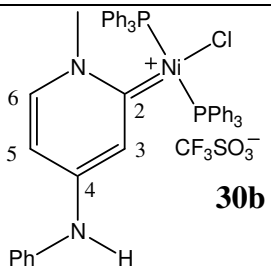

30b

Assignment	δ / ppm*		
	29	**30a**	**30b**
^{1}H NMR			
NH	9.67 (bs)	8.63 (bs)	8.56 (bs)
NMe	4.11 (3H, s)	3.41 (3H, bs)	3.62 (3H, bs)
H^3	7.01 (1H, d, ^{4}J = 2.3 Hz)	n.o.	n.o.
H^5	6.94 (1H, dd, ^{3}J = 7.2 Hz, ^{4}J = 2.3 Hz)	6.78 (1H, m)	n.o.
H^6	n.o.	6.80 (1H, d, ^{3}J = 7.3 Hz)	6.63 (1H, d, ^{3}J = 7.3 Hz)
H^3, H^5	n.a.	n.a.	6.75 (2H, pseudo-d)
Ph, H^6	7.41 (7H, m)	n.a.	n.a.
Ph, H^3	n.a.	7.56, 7.50, 7.40 (36H, 3 x m)	n.a.
Ph	n.a.	n.a.	7.60, 7.50, 7.40 (35H, 3 x m)
^{13}C NMR			
NMe	43.4 (s)	49.4 (s)	49.0 (s)
C^2	129.5 (s)	182.0 (s)	194.1 (s)
C^3	154.1 (s)	n.o.	n.o.
C^4	145.2 (s)	150.2 (s)	148.0 (s)
C^5	151.9 (s)	n.o.	n.o.
C^6	135.9 (s)	142.3 (s)	142.6 (s)
C^3, C^5	-	123.4 (s)	123.7 (s)
Ph^{ipso}	129.5 (s)	129.4 (s)$	129.2 (m)
Ph^{ortho}	130.9 (s)	134.4 (m)	134.4 (bs)
Ph^{meta}	126.3 (s)	129.1 (m)	129.0 (m)
Ph^{para}	129.0 (s)	131.6 (s)	131.4 (s)
^{31}P NMR			
PPh_3	-	22.8 (s)	21.0 (s)

$ obscured by the Ph^{meta} signal

As for all the previously discussed examples, the signals observed in the ^{1}H NMR spectra of complexes **30a** and **30b** are all upfield compared to the same signals in the ligand precursor and can be attributed to the positive charge which is now possible located on both the metal and the nitrogen outside the main ring system and thus decreases the deshielding effect of the aromatic ring current on the protons. The chemical shifts for C^2, C^4 and C^6 in the ^{13}C NMR spectra appear downfield in

30a and **30b** compared to the same signals in **29** which are an effect of coordination of the metal groups. The signals for C^3 and C^5 in **30a** and **30** appear upfield when compared to the same signals in **29** and reflects the shielding of the protons.

The NH units for all three compounds are indicated by broad signals above δ 8.5 ppm in the ^1H NMR spectra, as expected, with the NH resonance of **29** having the most downfield shift (δ 9.67), since none or very little of the positive charge on the N-atom is shared with a metal centre and therefore the attached hydrogen experiences more deshielding.

In the ^{13}C NMR spectra a downfield change in chemical shift of Δ 52.5 ppm (**30a**) and Δ 64.6 ppm (**30b**) for C^2 is observed upon oxidative substitution on the metal, exemplifying the formation of a carbene complex. The expected coupling with the P-atoms is not observed, probably due to the low concentration of the NMR sample. The chemical shifts of these carbene carbons appear at the highest field strength of all the complexes discussed so far in the dissertation.

Again, one signal is observed for the PPh_3 ligands in complexes **30a** and **30b**, illustrating the *trans* arrangement around the metal centre.

Mass spectrometry

The FAB-MS information of compound **29** and complexes **30a** and **30b** are listed in the table below. The peak representing the cation in the complex compound **29** is observed as two peaks (*m/z* 221.1 and 219.1) due to the presence of chlorine isotopes.

Table 3.36 FAB-MS data of compound **29** and complexes **30a** and **30b**

Complex	*m/z*	Relative intensity	Fragment ion
29	221.1	35	$[M\text{-}CF_3SO_3]^+$ (^{37}Cl)
	219.1	77	$[M\text{-}CF_3SO_3]^+$ (^{35}Cl)
30a	849.3	12	$[M\text{-}CF_3SO_3]^+$ (^{106}Pd)
	587.2	14	$[M\text{-}PPh_3\text{-}CF_3SO_3]^+$
	551.8	5	$[M\text{-}Cl\text{-}PPh_3\text{-}CF_3SO_3]^+$
30b	803.0	9	$[M\text{-}CF_3SO_3]^+$
	539.2	32	$[M\text{-}PPh_3\text{-}CF_3SO_3]^+$

Like many of the previously discussed complexes, the fragments of complex **30b** comprise of the cation of the molecular ion (*m/z* 849.3), followed by fragments showing the consecutive loss of a PPh_3 ligand and a Cl-atom. The latter fragment is not observed for complex **30b**.

3.2.9.2 Crystal and molecular structures of (2-chloro-*N*-methylpyrid-4-ylidene)phenylamine ammonium triflate, 29, and *trans*-chloro(*N*-methyl-1,2,4-trihydro-4-phenylaminepyrid-2-ylidene)bis(triphenylphosphine)palladium(II) triflate, 30a

The crystals for both the precursor compound and the carbene complex were suitable for X-ray crystallographic investigations making it possible to compare the two structures. This could ascertain whether any significant change in the bond lengths could be observed upon carbene ligand formation. POV-Ray drawings of **29** and **30a** are depicted in Figures 3.19 and 3.20 respectively and selected bond distances and angles are summarised in Tables 3.37 and 3.38. Compound **29** was obtained as orange needles (spacegroup $P2_1/c$) by vapour diffusion of pentane into a CH_2Cl_2 solution of the product and complex **30a** was obtained as yellow prisms (spacegroup $P2_1/c$) using the same method of crystallisation.

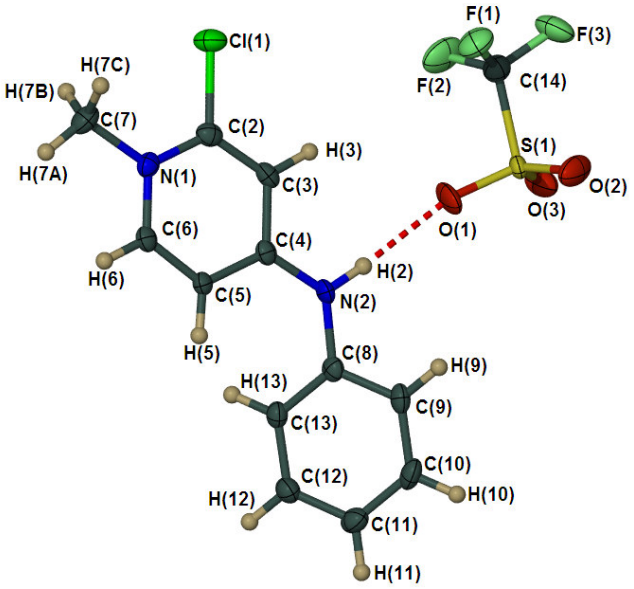

Figure 3.19 Molecular structure of **29**, indicating the atom numbering scheme, generated in POV Ray; some hydrogens are omitted for clarity.

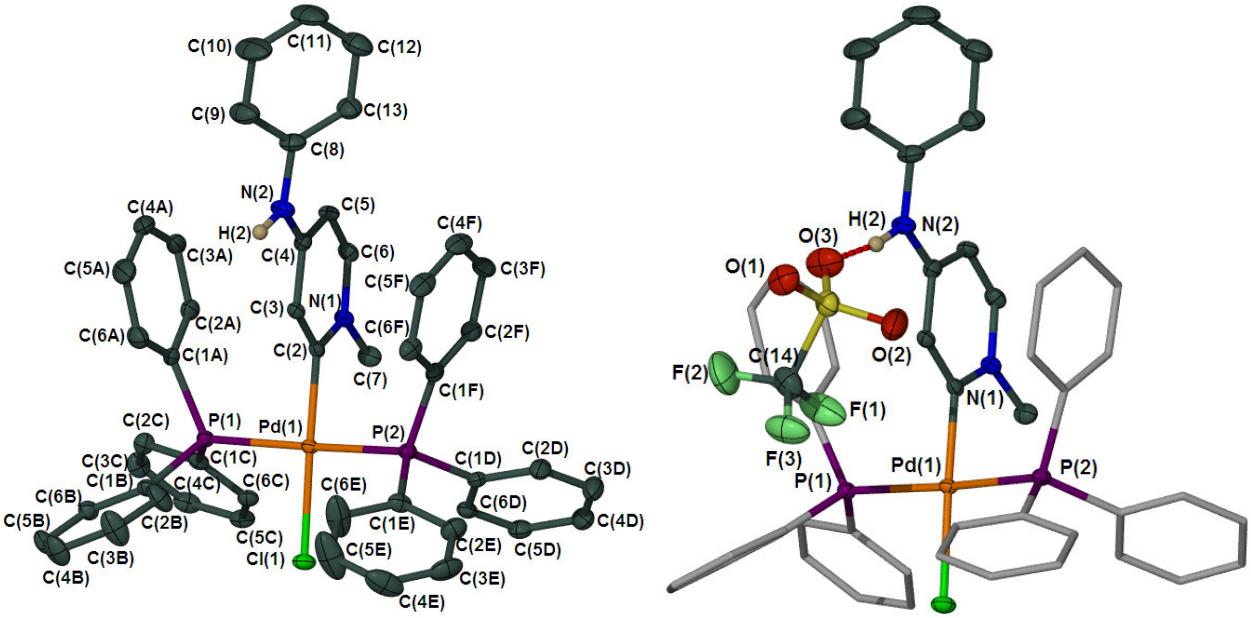

Figure 3.20 Molecular structure of **30a**, indicating atom numbering scheme, generated in POV Ray; some hydrogens, two CH_2Cl_2 molecules and the triflate counterion are omitted for clarity on the left while the counterion on the right shows a unique H-bond

Table 3.37 Bond lengths (Å) and angles of complex **29**

Bond lengths (Å)			
Cl(1)-C(2)	1.718(2)	C(4)-C(5)	1.414(3)
N(1)-C(6)	1.355(3)	C(5)-C(6)	1.363(3)
N(1)-C(2)	1.361(3)	C(8)-C(9)	1.390(3)
N(1)-C(7)	1.476(3)	C(8)-C(13)	1.392(3)
N(2)-C(4)	1.350(3)	C(9)-C(10)	1.385(3)
N(2)-C(8)	1.417(3)	C(10)-C(11)	1.385(3)
N(2)···O(1)	2.815(2)	C(11)-C(12)	1.393(3)
C(2)-C(3)	1.352(3)	C(12)-C(13)	1.383(3)
C(3)-C(4)	1.412(3)		
Bond angles (º)			
C(6)-N(1)-C(2)	117.9(2)	C(6)-C(5)-C(4)	119.8(2)
C(6)-N(1)-C(7)	119.9(2)	N(1)-C(6)-C(5)	122.6(2)
C(2)-N(1)-C(7)	122.2(2)	C(9)-C(8)-C(13)	120.4(2)
C(4)-N(2)-C(8)	127.2(2)	C(9)-C(8)-N(2)	117.9(2)
C(3)-C(2)-N(1)	123.0(2)	C(13)-C(8)-N(2)	121.6(2)
C(3)-C(2)-Cl(1)	119.9(2)	C(10)-C(9)-C(8)	119.7(2)
N(1)-C(2)-Cl(1)	117.1(2)	C(9)-C(10)-C(11)	120.4(2)
C(2)-C(3)-C(4)	119.8(2)	C(10)-C(11)-C(12)	119.5(2)
N(2)-C(4)-C(3)	118.7(2)	C(13)-C(12)-C(11)	120.7(2)
N(2)-C(4)-C(5)	124.4(2)	C(12)-C(13)-C(8)	119.3(2)
C(3)-C(4)-C(5)	117.0(2)	N(2)-H(2)···O(1)	151.5*

*The standard deviation cannot be determined since H(2) is calculated

Table 3.38 Bond lengths (Å) and angles of complex **30a**

Bond lengths (Å)			
Pd(1)-C(2)	1.998(3)	N(2)-C(8)	1.418(4)
Pd(1)-P(2)	2.3306(7)	C(2)-C(3)	1.369(4)
Pd(1)-P(1)	2.3346(7)	C(3)-C(4)	1.408(4)
Pd(1)-Cl(1)	2.3613(7)	C(4)-C(5)	1.413(4)
N(1)-C(6)	1.361(3)	C(5)-C(6)	1.354(4)
N(1)-C(2)	1.375(3)	C(8)-C(13)	1.386(4)
N(1)-C(7)	1.469(3)	C(8)-C(9)	1.389(4)
N(2)-C(4)	1.351(4)	C(9)-C(10)	1.391(5)
N(2)···O(3)	2.829(3)		
Bond angles (º)			
C(2)-Pd(1)-P(2)	89.04(8)	N(2)-C(4)-C(3)	118.6(3)
C(2)-Pd(1)-P(1)	89.71(8)	N(2)-C(4)-C(5)	125.0(3)
P(2)-Pd(1)-P(1)	172.64(3)	C(3)-C(4)-C(5)	116.4(3)
C(2)-Pd(1)-Cl(1)	177.68(8)	C(6)-C(5)-C(4)	119.3(3)
P(2)-Pd(1)-Cl(1)	90.77(3)	C(5)-C(6)-N(1)	122.6(3)
P(1)-Pd(1)-Cl(1)	90.78(2)	C(13)-C(8)-C(9)	119.9(3)
C(6)-N(1)-C(2)	120.7(2)	C(13)-C(8)-N(2)	123.1(3)
C(6)-N(1)-C(7)	118.5(2)	C(9)-C(8)-N(2)	116.8(3)
C(2)-N(1)-C(7)	120.8(2)	C(8)-C(9)-C(10)	119.7(3)
C(4)-N(2)-C(8)	129.7(2)	C(11)-C(10)-C(9)	120.5(3)
C(3)-C(2)-N(1)	117.6(2)	C(10)-C(11)-C(12)	119.9(3)
C(3)-C(2)-Pd(1)	122.9(2)	C(11)-C(12)-C(13)	120.4(3)
N(1)-C(2)-Pd(1)	119.5(2)	C(8)-C(13)-C(12)	119.6(3)
C(2)-C(3)-C(4)	123.3(3)	N(2)-H(2)···O(3)	162.2*

*The standard deviation can not be determined since H(2) is calculated

The least square plane defined by N(2), C(8), C(9), C(10), C(11), C(12) and C(13) makes an angle of 45.61(5) º with the one through the pyridine part, defined by N(1), C(2), C(3), C(4), C(5) and C(6) in compound **29**. The corresponding angle in complex **30b** is 40.01(13) º. The square planar coordination sphere defined by the least square plane through C(2), P(1), Pd(1), P(2) and Cl(1) occurs at an angle of 86.97(6) º with the plane of the carbene ligand [N(1), C(2), C(3), C(4), C(5) and C(6)], showing the perpendicular arrangement typical for these type of complexes.[121]

In both compound **29** and complex **30a** a hydrogen bond exists between the hydrogen on the "external" nitrogen and one of the oxygens of the triflate anion. The distances between the nitrogen and oxygen are approximately similar, 2.829(3) Å in **30a** and 2.815(2) Å in **29**.

[121] H. G. Raubenheimer and S. Cronje, *Dalton Trans.,* 2008, 1265.

The Pd(1)-C(2) distance of 1.998(3) Å is similar to that observed for *trans*-chloro(*N*-methyl-1,2,4-trihydro-2-dimethylaminepyrid-4-ylidene)bis(triphenylphosphine)palladium(II) triflate, **28a** [1.990(4) Å], but the Pd(1)-Cl(1) length of **28a** is significantly longer than in **30a** [2.3821(9) Å *vs.* 2.3613(7) Å] implying that the carbene ligand in **28a**, the one-N complex, has a larger *trans* influence than in complex **30a**.

From a comparison of the bond distances of N(1)-C(6), N(1)-C(2), C(2)-C(3), C(3)-C(4), C(4)-C(5), C(5)-C(6), N(2)-C(4) and N(2)-C(8) in **29** and **30b** it is evident that **XXVII** is the most important contributing structure for both the compounds with C(2)-C(3), C(5)-C(6) and N(2)-C(4) having double bond character (range between 1.351(4) and 1.375(3) Å) and C(3)-C(4), C(4)-C(5) and N(2)-C(8) showing single bond character (range between 1.412(3) and 1.418(4) Å). With these bond lengths being very similar in both compounds, it seems that the same amount of positive charge is located on N(2) in both instances (**XXVII** in Scheme 3.16). The NMR spectra however indicate otherwise with the NH chemical shift being much more upfield in the complex than in the precursor compound (**XXIX** in Scheme 3.16), which can also be attributed to H-bonding or concentration effects.

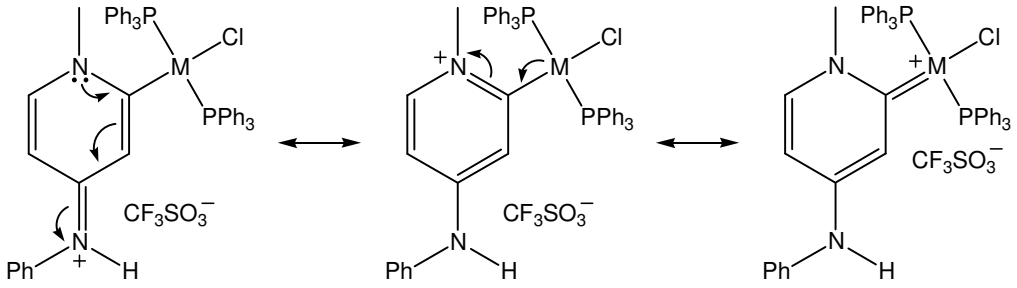

XXVII **XXVIII** **XXIX**

Scheme 3.16

The bond angles of the two compounds are very similar and those that differ, differ by not more than 3 º. All these results would lead one to postulate an iminium structure, rather than a typical carbene one, but could be characterised as either.

Figure 3.21 shows the molecular assembly of compound **29** as viewed along the b-axis. The cations are stacked on top of one another along the b-axis with N(2) aligned and alternating molecules related by inversion, with the counterions in the spaces in-between the columns. The columns form rows along the c-axis.

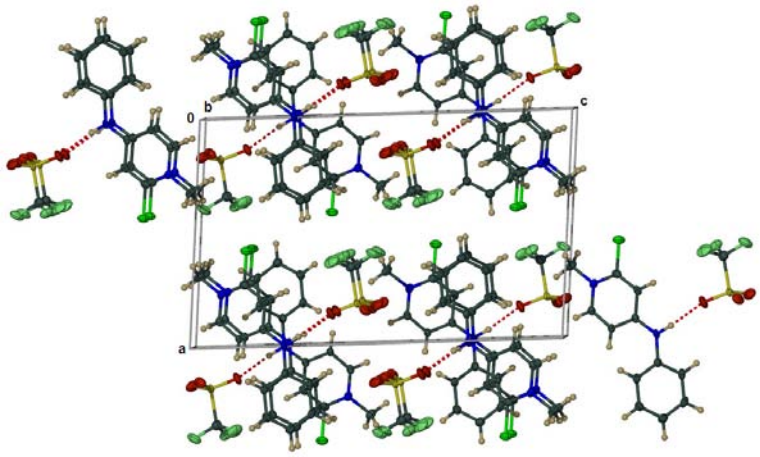

Figure 3.21 Molecular assembly of complex **29** viewed along the b-axis

The arrangement of the molecules of complex **30a** as viewed along the b-axis is illustrated in Figure 3.22. The cations are ordered in pairs on top of one another in columns along the b-axis which are related by inversion (indicated by magenta). CH_2Cl_2 molecules are arranged in pairs on top of one another in the spaces in between the columns of cations.

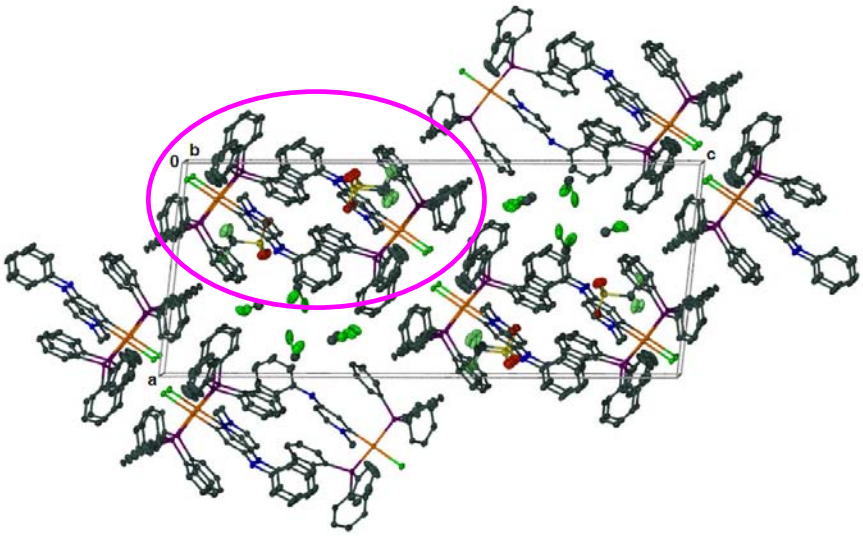

Figure 3.22 Molecular asembly of complex **30a** viewed along the b-axis

3.2.10 The boundaries pushed too far

As mentioned before, *r*NHC carbene complexes have been prepared where the heteroatom responsible for stabilisation is situated five bonds away (and in an annealed ring) from the carbon donor and still have remarkable carbene character as illustrated by the ^{13}C NMR data.[106] A most intriguing question is when this boundary between still having some carbene character *versus* only

pyridinium (or iminium) character is crossed. One precursor that can be used to really test the limit, is a stilbazolium salt.

Stilbazolium salts have the possibility of application in various optical devices due to their large optical non-linearities.[122,123] These salts can be engineered by simply varying the counterion to give a variety of crystalline materials with very large macroscopic optical nonlinearities.[124]

4-[2-(4-Bromophenyl)ethenyl]-*N*-methylpyridine was alkylated with $CF_3SO_3CH_3$ and reacted with $Pd(PPh_3)_4$ overnight at 60° (Scheme 3.17). Notably, the reaction of 4-[*trans*-2-(4-bromophenyl)ethenyl]pyridine with $Pt(PEt_3)_4$ at room temperature leads to η^2-coordination of the metal center to the C=C double bond. When the same reaction is carried out at 65°C, the oxidative substitution product is obtained.[125] A metal complex "walking" over electron-rich π-conjugated systems is believed to be a key process in many chemical transformations involving arene functionalization and activation of strong C-C, C-H and C-X (X = halides) bonds.[126]

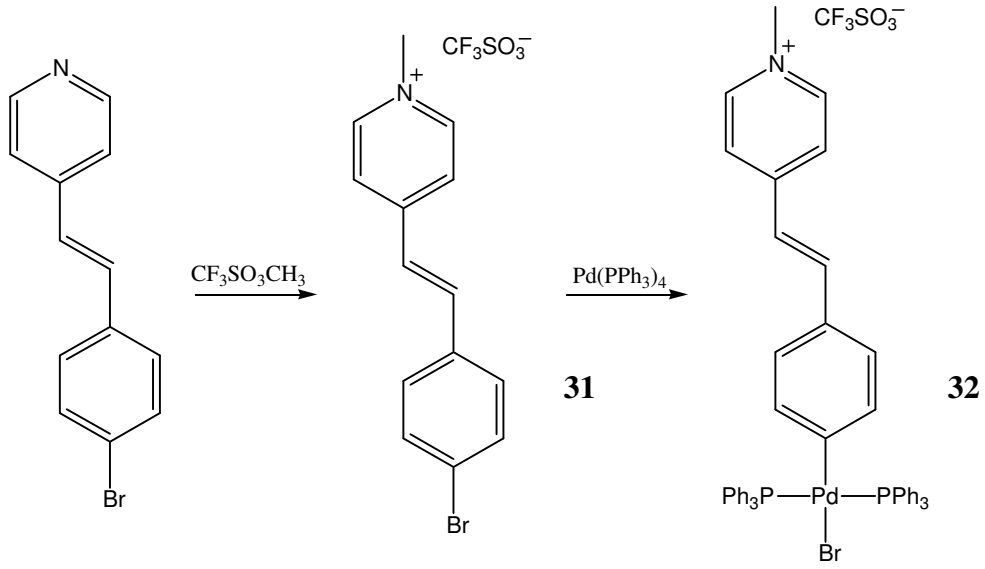

Scheme 3.17

Similar products[127] (with PMe_3, PEt_3 and P^iPr_3 and a different alkylating agent) have been prepared but the ^{13}C NMR data has not been reported. Since the degree of carbene-like character can often be

[122] P. C. Ray, *Chem. Phys. Lett.,* 2004, **394**, 354.
[123] S. R. Marder, J. W. Perry and C. P. Yakymyshyn, *Chem. Mater.* 1994, **6**, 1137.
[124] S. R. Marder, J. W. Perry and W. P. Schaefer, *Science,* 1989, **245**, 626.
[125] D. Strawser, A. Karton, O. V. Zenkina, M. A. Iron, L. J. W. Shimon, J. M. L. Martin and M. E. van der Boom, *J. Am. Chem. Soc.,* 2005, **127**, 9322.
[126] W. D. Harmann, *Coord. Chem. Rev.,* 2004, **248**, 853; J. P. Collman, L. S. Hegedus, J. R. Norton and R. G. Finke, *Principles and Applications of Organotransition Metal Chemistry,* University Science Books, Mill Valley, CA, 1987.
[127] J. Burdeniuk and D. Milstein, *J. Organomet.Chem.,* 1993, **451**, 213.

estimated from the carbon chemical shift of the carbon-metal donor, we decided to synthesise such a compound.

Isolation of single crystals suitable for X-ray diffraction studies was unsuccessful and regardless of solvent system, **32** crystallised with too much interstitial solvent to survive even gentle handling.

3.2.10.1 Physical characterisation of 4-[2-(4-bromophenyl)ethenyl]-N-methylpyridinium triflate, 31, and 4-*trans*-chloro-{[2-(4-bromophenyl)vinyl]-1-methylpyridinium}-(istriphenylphosphine)pallalium (II) triflate, 32

NMR Spectroscopy

The NMR data that was collected, was assigned with the aid of two-dimensional NMR techniques, and is presented in Table 3.39.

A comparison of the chemical shifts of the resonances in the ^{1}H NMR spectrum of **31** with previously prepared 4-[2-(4-chlorophenyl)ethenyl]-*N*-methylpyridinium tetraphenylborate,[128] shows that the pyridinium hydrogens appear at a somewhat higher field for **31** due to the different counterion and the Ph hydrogens at a somewhat lower field.

The chemical shifts of complex **32** also appear more upfield than those of 4-*trans*-chloro-{[2-(4-bromophenyl)vinyl]pyridin}bistriphenylphosphine platinum(II).[125] It seems that the positively charged nitrogen atom has a lesser influence than the metal present.

Again, only one peak is observed in the ^{31}P NMR spectrum of complex **32** illustrating the *trans* arrangement of the PPh_3 ligands.

[128] D. Jin, F. Zhang, Y. Zhang and D.-C. Zhang, *Acta Cryst. E,* 2005, **E61**, o3618.

Table 3.39 ^{1}H and ^{13}C-{^{1}H} NMR data compound **31** and ^{1}H, ^{13}C-{^{1}H} and ^{31}P- NMR data of complex **32** in CD_3CN

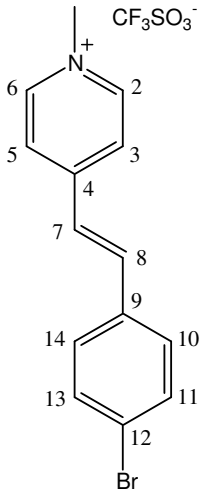

31

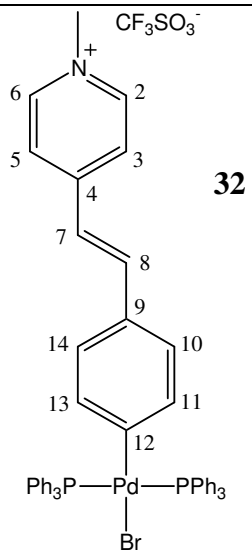

32

Assignment	δ / ppm*	
	31	**32**
^{1}H NMR		
NMe	4.21 (3H, s)	4.14 (3H, s)
H^2, H^6	8.48 (2H, d, ^{3}J = 6.9 Hz)	8.34 (2H, d, ^{3}J = 6.9 Hz)
H^3, H^5	8.01 (2H, d, ^{3}J = 6.9 Hz)	7.83 (2H, d, ^{3}J = 6.9 Hz)
H^7	7.36 (1H, d, ^{3}J = 16.6 Hz)	6.90 (1H, d, ^{3}J = 16.2 Hz)
H^8	7.75 (1H, d, ^{3}J = 16.6 Hz)	n.o.
H^{10}, H^{14}, H^{11}, H^{13}	7.63 (4H, m)	n.a.
H^{10}, H^{14}	n.a.	6.54 (2H, d, ^{3}J = 8.0 Hz)
H^{11}, H^{13}	n.a.	6.84 (2H, d, ^{3}J = 8.0 Hz)
PPh, H^8	n.a.	7.43 (32H, m)
^{13}C NMR		
NMe	48.2 (s)	47.9 (s)
C^2, C^6	146.8 (s)	145.3 (s)
C^3, C^5	125.0 (s)	124.0 (s)
C^4	154.2 (s)	155.0 (s)
C^7	124.5 (s)	120.5 (s)
C^8	140.7 (s)	143.9 (s)
C^9	135.2 (s)	129.9 (s)
C^{10}, C^{14}	130.7 (s)	127.9 (s)
C^{11}, C^{13}	133.2 (s)	137.6 (s)
C^{12}	125.1 (s)	188. 7 (s)
PPh^{ipso}	n.a.	obscured by the Ph signal
PPh^{ortho}	n.a.	135.6 (bs)
PPh^{meta}	n.a.	129.0 (bs)
PPh^{para}	n.a.	131. 1 (s)
^{31}P NMR		
PPh_3	n.a.	24.6 (s)

As for all the complexes discussed so far, the signals in the ^{1}H NMR spectrum of complex **32** appear more downfield than those of the compound, **31**, the exceptions are the signals for $C^{2/6}$, $C^{3/5}$, C^{7}, C^{9} and $C^{10/14}$. Coordination of the metal moiety results in a downfield shift of 63.6 ppm for the chemical shift for C^{12} in the ^{13}C NMR spectrum, much in the same range as that observed upon carbene formation for the complexes discussed earlier. However, the three-bond coupling constant between the protons on the carbon-carbon double bond (C^{7} and C^{8}) is *ca.* 16 Hz for both compounds, indicative of a *trans* configuration about a double bond, showing that the main contributing structure is again that of **XXX** (Scheme 3.18).

XXX

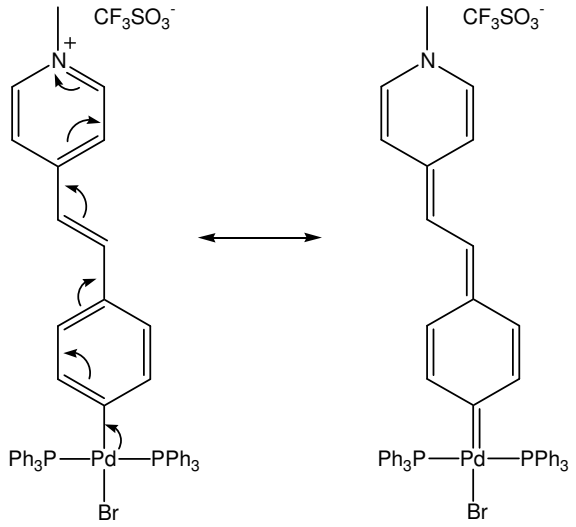

Scheme 3.18

Mass spectrometry

The data of the FAB mass spectra of compound **31** and complex **32** are collected in Table 3.40. The peaks representing the cation in the compounds **31** and **32**, are observed. The peak for compound **31** had a relative intensity of 100 % and is therefore also the base peak. The $[M\text{-}CF_3SO_3]^+$ fragment of complex **32** has a very low intensity. The only other peak observed for **31** is due to the fragment, $[M\text{-}Br\text{-}CF_3SO_3]^+$ at *m/z* 196.1. Complex **32** had two other identifiable fragments, $[M\text{-}PPh_3\text{-}CF_3SO_3]^+$ and $[M\text{-}2PPh_3\text{-}Pd\text{-}Br\text{-}CF_3SO_3]^+$ at *m/z* 644.0 and 196.2 respectively.

Table 3.40 FAB MS data of compound **31** and complex **32**

Complex	*m/z*	Relative intensity	Fragment ion
31	276.0	100	$[M\text{-}CF_3SO_3]^+$ (^{79}Br)
	196.1	30	$[M\text{-}Br\text{-}CF_3SO_3]^+$
32	908.1	6	$[M\text{-}CF_3SO_3]^+$ (^{79}Br, Pd)
	644.0	20	$[M\text{-}PPh_3\text{-}CF_3SO_3]^+$
	196.2	55	$[M\text{-}2PPh_3\text{-}Pd\text{-}Br\text{-}CF_3SO_3]^+$

3.2.11 Utilising 4,4-dimethyl-2-(2-thienyl)oxazole as a heterocyclic carbene ligand

When 4,4-dimethyl-2-(2-thienyl)oxazole is lithiated at position 5 and reacted with $[Fe(Cp)(CO)_2Cl]$ (Cp = η-cyclopentadienyl), an organo(thio)carbene complex is afforded, whereas lithiation in the 3-position of the thienyl ring, yields an chelate aminoacyl product (the nucleophilic nitrogen atom intramolecularly attacked one of the carbonyl ligands on the $Fe(Cp)(CO)_2$ unit, coordinated to position 3, to form a chelate complex) which after alkylation or protonation afforded a metallacyclic carbene complex.[26]

Despite various attempts,[129] a Cr(0) or W(0) complex with the metal group bonded at position 3 could not be isolated. One of these attempts involves blocking position 5 with a methyl group.[130] Unfortunately this ligand with the methyl group at position 5 could not be separated from the unreacted ligand and therefore the mixture was used without further purification.

Since the separation of the methyl derivative of 4,4-dimethyl-2-(2-thienyl)oxazoline and the underivatised compound was problematic, it was decided to attach a bulkier ligand ($SiPPh_3$) to 4,4-dimethyl-2-(2-thienyl)oxazoline so that the product could possibly be separated more readily from the underivatised compound by means of column chromatography (Scheme 3.19).

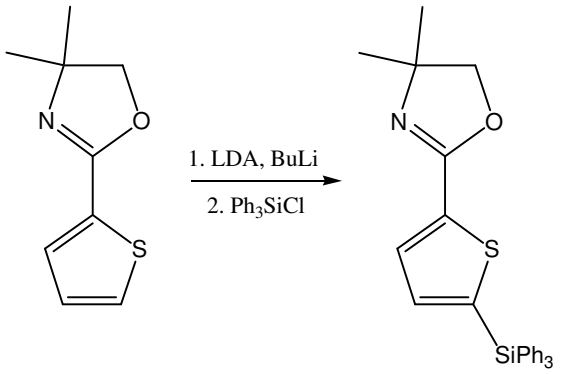

33

Scheme 3.19

Initial reactions of of 4,4-dimethyl-2-(2-thienyl)oxazole with BuLi in ether at -78 ºC were unsuccessful. It has been noted that 3-metallation of 5-silylated intermediates can be accelerated by the addition of LiCl.[25] It was decided to use Schlosser's base[131] and although the reaction of 4,4-dimethyl-2-(2-thienyl)oxazole with 1 equivalent of Schlosser's base and subsequent reaction with $[Cr(CO)_5Br][Net_4]$ at -78 ºC gave a product isolated by flash chromatography, the expected 3-

[129] Y. Stander, *MSc Thesis*, Rand Afrikaans University, 1996, p.110.
[130] G. R. Julius, *PhD Thesis,* University of Stellenbosch, 2005, p. 60.
[131] M. Schlosser, *J. Organomet. Chem.*, 1967, **8**, 9.

organo(thio)carbene complex, **35** (Scheme 3.20) was not obtained when the latter product was reacted with $CF_3SO_3CH_3$.

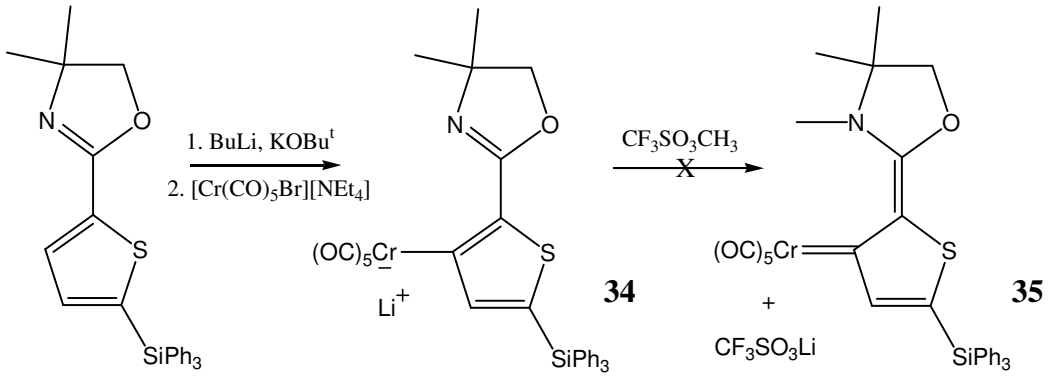

Scheme 3.20

One of the carbonyl ligands may have formed a chelate complex by intramolecular reaction (Scheme 3.21) as was observed when 4,4-dimethyl-2-(2-thienyl)oxazole lithiated at position 3 is reacted with $[Fe(Cp)(CO)_2Cl]$[26] preventing the formation of the expected product. Unfortunately the product (whether **34** or the chelate complex) could not be isolated as single crystals suitable for X-ray diffraction studies.

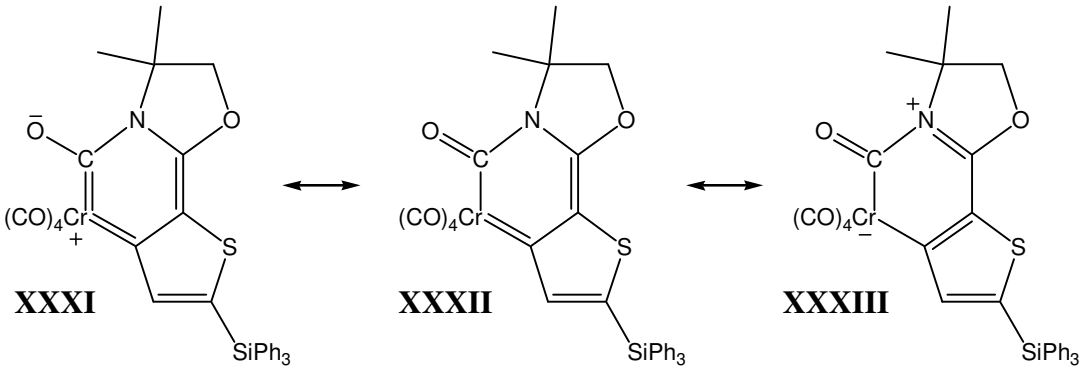

Scheme 3.21

3.2.11.1 Physical characterisation of compound 33 and complex 34

NMR spectroscopy

The NMR data of compound **33** and complex **34** are tabulated below (Table 3.41). In the NMR of **35** there is clearly evidence of decomposition of the complex to **33** and $Cr(CO)_6$. After 17 hours in solution the compound decomposed to 57% of the original amount of **34**. There is no sign of a carbenic carbon (expected above 200 ppm) and the 4:1 ratio in the peak height of the CO ligand signals indicates a $Cr(CO)_5$ compound, so it is therefore suspected that either the lithium salt is the isolated product or **XXXIII** in Scheme 3.21.

Table 3.41 ^{1}H and ^{13}C-{^{1}H} and NMR data of complexes **33** and **34** in CD_2Cl_2

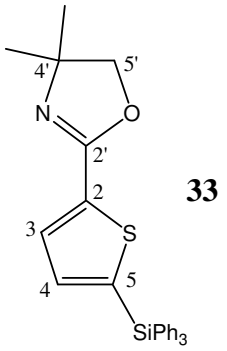

33

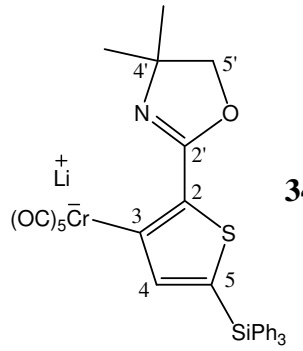

34

Assignment	δ / ppm*	
	33	**34**
^{1}H NMR		
Me	1.32 (6H, s)	1.49 (6H, s)
$H^{5'}$	4.08 (2H, s)	4.13 (2H, s)
H^{3}	7.64 (1H, d, ^{3}J = 3.8 Hz)	7.79 (1H, ^{3}J = 3.5 Hz)
H^{4}	7.30 (1H, d, ^{3}J = 3.8 Hz)	n.o.
Ph	7.59, 7.48, 7.41 (15H, 3 x m)	7.60, 7.48 (9H, 2 x m)
Ph, H^{4}	n.a.	7.42 (7H, m)
^{13}C NMR		
Me	28.3 (s)	27.4 (s)
$C^{2'}$	157.6 (s)	141.4 (s)
$C^{4'}$	68.3 (s)	72.3 (s)
$C^{5'}$	79.7 (s)	79.2 (s)
C^{2}	139.8 (s)	138.6 (s)
C^{3}	131.1 (s)	165.0 (s)
C^{4}	138.7 (s)	134.2 (s)
C^{5}	138.0 (s)	133.2 (s)
Ph^{ipso}	128.2 (s)	128.6 (s)
Ph^{ortho}	136.3 (s)	136.3 (s)
Ph^{meta}	128.3 (s)	128.4 (s)
Ph^{para}	130.4 (s)	130.6 (s)
CO^{trans}	n.a.	221.3 (s)
CO^{cis}	n.a.	214.9 (s)

No resonance for H^{3} is observed in **34** whereas it appears as a doublet in **33** due to coupling with H^{4}. The fact that only two CO signals, rather than four as expected for the chelate complex are observed, confirms that the product obtained is **34**, although this is in conflict with the successful separation of the product with column chromatography.

The resonance for $C^{2'}$ appears 16.2 ppm more upfield in the metal complex (δ 141.4) than in the ligand precursor (δ 157.6). The fact that the Cr-metal is coordinated on position 3, can be deduced from the downfield change in chemical shift of C^3 in **34** (δ 165.0) of 33.9 ppm compared to the same carbon in **33**.

There is little change in the chemical shifts of the remaining carbons in the precursor ligand and lithiated/chelate compound.

Mass spectrometry

It is suspected that complex **34** decomposed upon addition to the matrix therefore **34** is probably too unstable to obtain a spectrum with any valuable information. The base peak of compound **33** is also the molecular ion peak of the compound at *m/z* 440.3. Fragments due to the loss of a methyl and phenyl group are also observed, as well as the fragment, $[Ph_3Si]^+$, at *m/z* 259.2.

Table 3.42 FAB MS data of compounds **33**

m/z	Relative intensity	Fragment ion
440.3	100	$[M]^+$
424.2	12	$[M\text{-}Me]^+$
362.2	20	$[M\text{-}Ph]^+$
259.2	25	$[Ph_3Si]^+$

3.2.12 Oxidative substitution complexes with 4,4-dimethyl-2-(2-thienyl)oxazoline as carbene ligand – a completely different type of *remote* carbene ligand

The unsuccessful reactions with group VI metals initiated the synthesis of a 4,4-dimethyl-2-(2-thienyl)oxazoline compound which could oxidatively add to a group 10 metal, distant or removed from the heteroatoms. The ligand precursor, 3'-chloro-4,4-dimethyl-2-(2-thienyl)oxazoline, **36**, was prepared using a similar procedure as described for the reaction of electrophiles with 3-lithiated 4,4-dimethyl-2-(2-thienyl)oxazoline[24,132] using $Cl_2C{=}CCl_2$ as Cl-source. Compound **36** was alkylated as previously described for the pyridine-derived ligands, to give 61 % of *N*-methyl[3'-chloro-4,4-dimethyl-2-(2-thienyl)]oxazoline as a white crystalline material (Scheme 3.22).

[132] L. Brandsma and H. D. Verkruijsse, *Preparative Polar Organometallic Chemistry, Vol.1,* Springer-Verlag, Berlin pp. 168-169

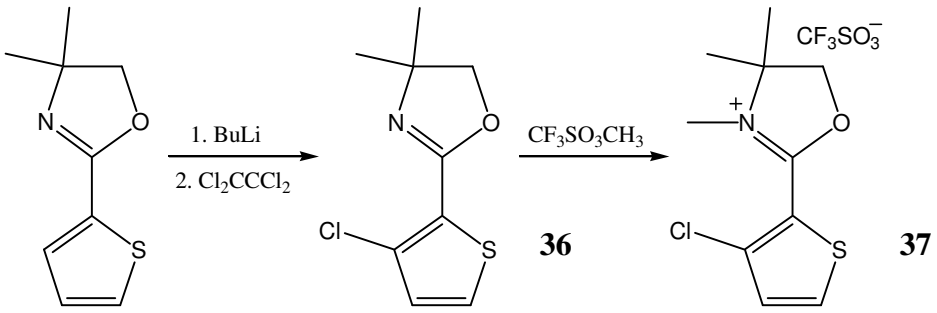

Scheme 3.22

Complex **38a**, *trans*-chloro(*N*-methyl[3'-chloro-4,4-dimethyl-2-(2-thienyl)]oxazolin-3'-idene)bis-(triphenylphosphine)palladium(II) was prepared (Scheme 3.23) using the same procedure as followed to synthesise complex **14a** (Section 3.2.4.3) but rather using THF instead of toluene as solvent to obtain **38a** in 89 % yield as a white microcrystalline product. The Ni-analogue, **38b**, was obtained as a yellow powder in 79% yield, employing the same procedure as used for the synthesis of complex **14b** described in Section 3.2.4.3. Complexes **38a** and **38b** are soluble in CH_2Cl_2 and THF and insoluble in diethyl ether, hexane and pentane.

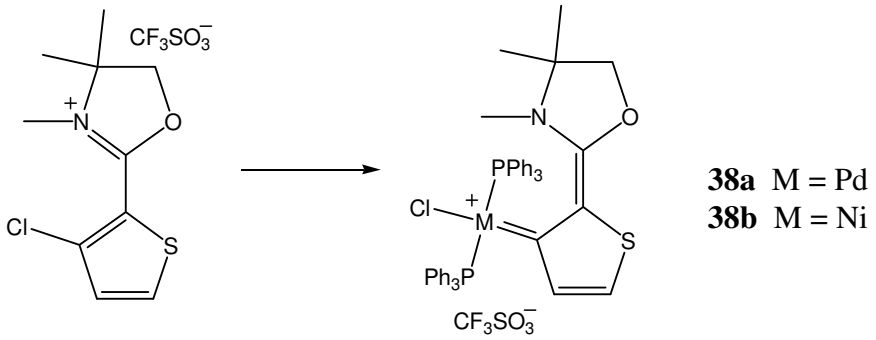

Scheme 3.23

3.2.12.1 Physical characterisation of 3-chloro-4',4'-dimethyl-2'-thiophen-2-yl-4,5-dihydro-oxazole 36, *N*-methyl-4',4'-dimethyl-2'-thiophen-3-chloro-2-yl-4,5-dihydro-oxazole, 37, *trans*-chloro(*N*-methyl-4',4'-dimethyl-2'-thiophen-3-chloro-2-yl-4,5-dihydro-oxazolin-3'-ylidene)bis(triphenylphosphine)palladium(II) triflate, 38a and *trans*-chloro(*N*-methyl-4',4'-dimethyl-2'-thiophen-3-chloro-2-yl-4,5-dihydro-oxazolin-3'-ylidene)bis(triphenylphosphine) palladium(II) triflate 38b

NMR spectroscopy

Two dimensional NMR techniques (ghsqc and ghmqc) were employed to assign (Table 3.43) the resonances observed in the ^{1}H and ^{13}C NMR spectra of compounds **36**, **37**, **38a** and **38b**.

Table 3.43 ^{1}H and ^{13}C-{^{1}H} and NMR data of complexes **36**, **37**, **38a** and **38b** in CD_2Cl_2

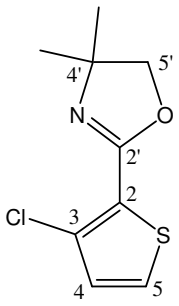

36

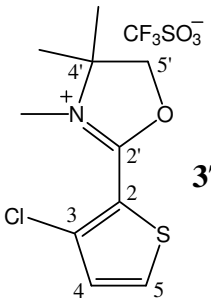

37

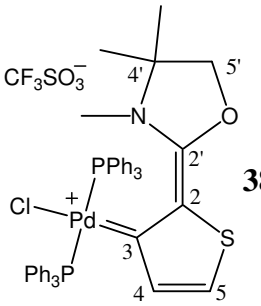

38a

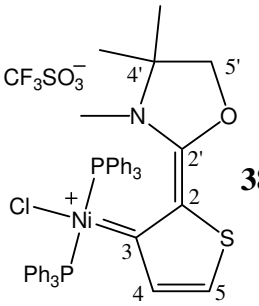

38b

Assignment	δ / ppm*			
	36	**37**	**38a**	**38b**
^{1}H NMR				
Me	1.34 (6H, s)	1.68 (6H, s)	1.36 (6H, s)	1.38 (6H, s)
NMe	n.a.	3.45 (3H, s)	2.92 (3H, s)	2.81 (3H, s)
H^4	6.98 (1H, d, ^{3}J = 5.3 Hz)	7.23 (1H, d, ^{3}J = 5.3 Hz)	n.o.	n.o.
H^5	7.40 (1H, d, ^{3}J = 5.3 Hz)	8.05 (1H, d, ^{3}J = 5.3 Hz)	7.10 (1H, d, ^{3}J = 4.9 Hz)	n.o.
$H^{5'}$	4.08 (2H, s)	4.92 (2H, s)	4.56 (2H, s)	4.87 (2H, s)
Ph, H^4	n.a.	n.a.	7.49, 7,38 (31H, 2 x m)	n.a.
Ph, H^4, H^5	n.a.	n.a.	n.a.	7.55, 7.47, 7.38 (32H, 3 x m)
^{13}C NMR				
Me	28.3 (s)	23.9 (s)	24.1 (s)	24.1 (s)
NMe	n.a.	31.8 (s)	30.2 (s)	29.8 (s)
C^2	124.3 (s)	115.2 (s)	116.6 (s)	117.3 (s)
C^3	127.3 (s)	134.9 (s)	182.6 (t, $^{2}J_{C\text{-}P}$ = 7.4 Hz)	187.4 (t, $^{2}J_{C\text{-}P}$ = 34.2 Hz)
C^4	130.0 (s)	137.7 (s)	137.6 (s)	136.6 (s)
C^5	128.4 (s)	130.2 (s)	136.1 (s)	135.8 (s)
$C^{2'}$	156.3 (s)	166.1 (s)	163.8 (s)	163.2 (s)
$C^{4'}$	68.3 (s)	68.9 (s)	67.9 (s)	67.9 (s)
$C^{5'}$	79.5 (s)	82.4 (s)	80.8 (s)	81.1 (s)
Ph^{ipso}	n.a.	n.a.	130.2 (m)	130.4 (m)
Ph^{ortho}	n.a.	n.a.	134.4 (m)	134.3 (m)
Ph^{meta}	n.a.	n.a.	128.8 (m)	128.7 (m)
Ph^{para}	n.a.	n.a.	131.1 (s)	130.4 (s)
^{31}P NMR				
PPh_3	n.a.	n.a.	23.2 (s)	20.82 (s)

As seen in the ^{1}H NMR spectra, all the protons in **37** are deshielded ($\Delta\delta$ 0.25 – 0.84) upon alkylation. The coupling between H^4 and H^5 could not be observed for complexes **38a** and **38b** since the resonances are obscured by the signals of the phenyl ligands. The carbons of the methyl groups on $C^{4'}$ and C^2 of **36** resonate at a higher field in the ^{13}C NMR spectrum, while the rest of the carbons appear at a lower field when compared to those in **37**.

Upon complex formation the ^{13}C signals shift downfield compared to those in the precursor, **37**, except for the carbon signals of NMe, $C^{4'}$, $C^{2'}$, C^{4} and $C^{5'}$ that remain essentially similar.

The ^{13}C-{^{1}H} NMR data for complex **38a** shows that the carbene carbon (C^{3}) resonates at δ 182.6 and that it is shifted downfield with respect to the carbon of the precursor, **37**, which resonates at δ 134.9 (Δδ = 47.7). In complex **38b** the carbene carbon (δ 187.4) also resonates at a much lower field than that of the precursor **37**. This constitutes a downfield shift of 52.5 ppm.

Mass spectrometry

The positive-ion FAB mass spectra of **37**, **38a** and **38b** exhibited fragments at *m/z* 230.0, 861.7 and 814.0 respectively, ascribable to the molecular ion of **37** and the cation of the metal complex compounds. The molecular ion peak plus H was observed for compound **36**. Both complexes **38a** and **38b** display fragments due to the sequential loss of a PPh_3 ligand and Cl ([M-PPh_3-CF_3SO_3]; [M-Cl-PPh_3-CF_3SO_3]).

Table 3.44 FAB MS data of compounds **36** and **37** and complexes **38a** and **38b**

Complex	*m/z*	Relative intensity	Fragment ion
36	218.1	36	$[M+H]^+$ (^{37}Cl)
	216.1	100	$[M+H]^+$ (^{35}Cl)
	200.0	13	$[M-Me]^+$
37	232.0	43	$[M-CF_3SO_3]^+$ (^{37}Cl)
	230.0	100	$[M-CF_3SO_3]^+$ (^{35}Cl)
38a	861.7	5	$[M-CF_3SO_3]^+$ (^{35}Cl, ^{106}Pd)
	600.0	31	$[M-PPh_3-CF_3SO_3]^+$
	486.0	6	$[M-Cl-PPh_3-CF_3SO_3]^+$
38b	814.0	6	$[M-CF_3SO_3]^+$ (^{35}Cl. ^{58}Ni)
	551.9	70	$[M-PPh_3-CF_3SO_3]^+$
	516.3	11	$[M-Cl-PPh_3-CF_3SO_3]^+$

3.2.12.2 The crystal and molecular structure of *trans*-chloro(*N*-methyl[3'-chloro-4,4-dimethyl-2-(2-thienyl)]oxazolin-3'-ylidene)bis(triphenylphosphine)palladium(II), 38a

Colourless crystals of complex **38a** that were suitable for single crystal X-ray analysis were obtained by slow vapour diffusion of pentane into a concentrated dichloromethane solution of the

complex. The molecular structure is shown in Figure 3.23 and selected bond angles and lengths are given in Table 3.45.

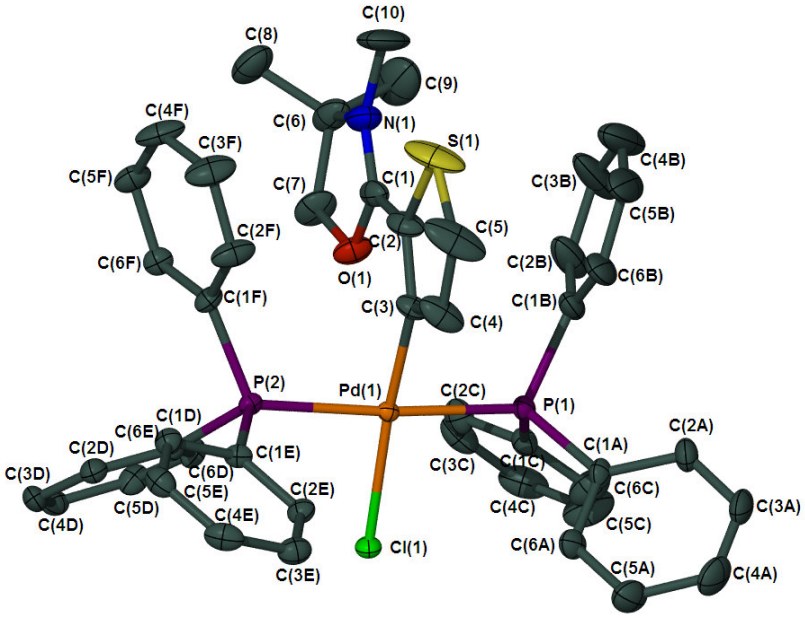

Figure 3.23 Molecular structure of **38a**, indicating atom numbering scheme, generated in POV Ray; hydrogens, two CH_2Cl_2 molecules and the counter ion are omitted for clarity.

Table 3.45 Bond lengths (Å) and angles of complex **38a**

Bond lengths (Å)			
Pd(1)-C(3)	1.989(4)	N(1)-C(6)	1.502(8)
Pd(1)-P(1)	2.327(1)	C(1)-C(2)	1.432(7)
Pd(1)-P(2)	2.328(1)	C(2)-C(3)	1.383(7)
Pd(1)-Cl(1)	2.365(1)	C(3)-C(4)	1.414(7)
O(1)-C(1)	1.316(6)	C(4)-C(5)	1.347(8)
O(1)-C(7)	1.475(6)	C(6)-C(8)	1.504(8)
N(1)-C(1)	1.286(6)	C(6)-C(7)	1.526(8)
N(1)-C(10)	1.474(8)	C(6)-C(9)	1.549(8)
C(5)-S(1)	1.701(7)	C(2)-S(1)	1.745(5)
Bond angles (°)			
C(3)-Pd(1)-P(1)	89.3(1)	C(3)-C(2)-S(1)	111.7(4)
C(3)-Pd(1)-P(2)	88.4(1)	C(1)-C(2)-S(1)	121.8(4)
P(1)-Pd(1)-P(2)	175.26(4)	C(2)-C(3)-C(4)	110.9(4)
C(3)-Pd(1)-Cl(1)	170.3(1)	C(2)-C(3)-Pd(1)	130.7(4)
P(1)-Pd(1)-Cl(1)	90.65(4)	C(4)-C(3)-Pd(1)	118.4(4)
P(2)-Pd(1)-Cl(1)	92.34(4)	C(5)-C(4)-C(3)	113.6(5)
C(1)-O(1)-C(7)	108.8(4)	C(4)-C(5)-S(1)	113.1(4)
C(1)-N(1)-C(10)	127.5(5)	N(1)-C(6)-C(8)	111.0(5)
C(1)-N(1)-C(6)	112.3(5)	N(1)-C(6)-C(7)	99.6(4)
C(10)-N(1)-C(6)	120.1(5)	C(8)-C(6)-C(7)	112.5(5)
N(1)-C(1)-O(1)	113.3(5)	N(1)-C(6)-C(9)	110.8(6)
N(1)-C(1)-C(2)	130.4(5)	C(8)-C(6)-C(9)	111.1(5)
O(1)-C(1)-C(2)	116.3(4)	C(7)-C(6)-C(9)	111.3(5)
C(3)-C(2)-C(1)	126.4(4)	O(1)-C(7)-C(6)	105.2(5)

The molecular structure reveals that the geometry at the metal atom is essentially square planar, with angles of ~90 ° between the four substituents [C(3)-Pd(1)-P(1), 89.27(14) °; C(3)-Pd(1)-P(2), 88.40(14) °; P(1)-Pd(1)-Cl(1), 90.65(4) °; P(2)-Pd(1)-Cl(1), 92.34(4) °].

The bond lengths of the carbene ligand of **38a** compare well with the oxazoline ligands in the dimeric complex [Au{C=C(C=NMe$_2$CH$_2$O)SCH=CH}]$_2$[133] and *N*-methyl[3'-chloro-4,4-dimethyl-2-(2-thienyl)]oxazolin-5'-ylidene)pentacarbonylchromium(0).[134] The bond lengths C(4)-C(5) and C(3)-C(4) fall in the range for aromatic conjugated systems.[15] N(1)-C(1) [1.286(6) Å] has significant double bond character, while the N(1)-C(6) distance [1.502(8) Å] is typical of a single bond when comparing it to the C(sp^2)=N(sp^2) double bond distance of 1.271(5) Å reported for the complex {[(p-methoxyphenyl)imino](2-pyridyl)methyl}palladium(II) by Crociani and co-workers.[135] Most importantly, the relatively long C(1)-C(2) bond length of 1.432(7) Å, show that the iminium form is the most important contributing structure. The chemical shift of C3 in the ^{13}C NMR spectrum of **38a** suggests that one may call the product a carbene complex.

A search in CCSD yielded only 5 complexes with a metal bonded at position 3 of the 4,4-dimethyl-2-(2-thienyl)oxazoline ligand. One of these is the Fe(I) chelate mentioned earlier,[26] the dimeric Au complex, [Au{C=C(C=NMe$_2$CH$_2$O)SCH=CH}]$_2$ cited above and three tin complexes. Two of them are also chelate aminoacyl products and the other an organo(thio) complex.[136] All of these complexes exhibit similar bond lengths in the ligand, and the various small differences in bond angles are due to ring strain from the chelate formation and bulky ligands on the metal centre.

The essentially normal Pd-C distance of 1.989(4) Å is consistent with values seen in the already mentioned Pd-carbene complexes.

The molecules of complex **38a** are assembled (viewed along the a-axis, Figure 3.24) in columns on top of one another to form layers (parallel to the c-axis) of PPh_3 ligands alternating with the carbene ligands, CH_2Cl_2 molecules and triflate anions.

[133] M. Desmet, H. G. Raubenheimer and G. J. Kruger, *Organometallics,* 1997, **16**, 3324.
[134] G. R. Julius, *PhD Thesis,* University of Stellenbosch, 2005, p. 107.
[135] B. Crociani, M. Sala, A. Polo and G. Bombieri, *Organometallics,* 1986, **5**, 1369.
[136] K. Mun Lo, S. Selvaratnam, S. Weng, C. Wei and V. G. K. Das, *J. Organomet. Chem.,* 1992, **430**, 149.

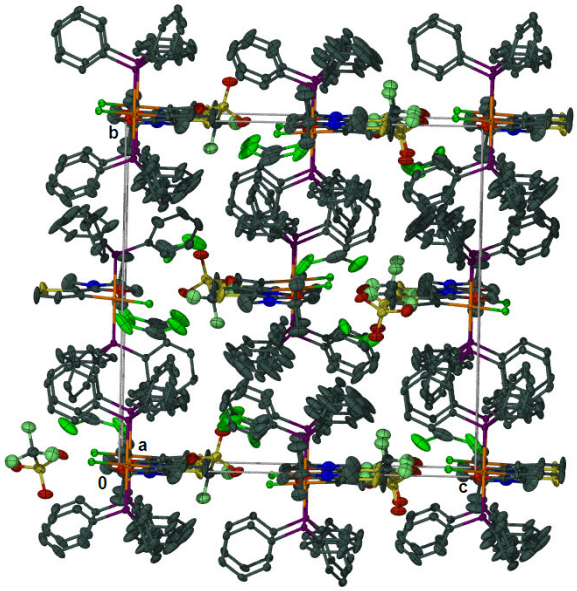

Figure 3.24 Molecular assembly of complex **38a** as viewed along the a-axis

3.3 Conclusions

An α,β-unsaturated Fischer-type carbene complex **2a** was successfully employed to prepare a *r*NHC complex of chromium pentacarbonyl, $(CO)_5\overline{Cr=C(CH=C(CH_3)N(CH_3)CH=C}(n\text{Bu})$, **8**. This *r*NHC ligand was successfully transferred to a softer Rh metal fragment, forming both *trans*-chloro(dicarbonyl)(*N*-methylpyrid-4-ylidene)rhodium(I), ***trans*-9**, and *cis*-chloro(dicarbonyl)(*N*-methylpyrid-4-ylidene)rhodium(I), ***cis*-9**, the first examples of this type, containing a group 9 metal. These complexes were fully characterised and the molecular structure of ***cis*-9a** was determined by X-ray diffraction.

Palladium and nickel carbene complexes with pyridine and quinoline derived carbene ligands were successfully prepared by oxidative substitution and fully characterised, most of them also by crystal structure determinations. All the metal centra in these complexes have a square planar geometry with the carbene ligand orientated almost perpendicular to the coordination plane around the metal.

Using the chemical shift of the metal bonded carbon in the ^{13}C NMR spectra as an indicator, the pyridine derived ligands of complexes **14** - **16** could be arranged in increased order of carbene (pyridylidene) character : *a*NHC (**15**) < *n*NHC (**14**) < *r*NHC (**16**). The carbene ligands in these nickel and palladium complexes (**14** – **16**), using the M-Cl bond distance as a probe, could be arranged in a series of increasing *trans* influence: $n\text{N}^2\text{HC}^5$ ~ $a\text{N}^1\text{HC}^6$ (**15**) ~ $n\text{N}^1\text{HC}^6$ (**14**) < $r\text{N}^1\text{HC}^6$ (**16**). The effect of the bonding site in the ligands on the respective metal carbene bond distances in

the palladium as well as the nickel complexes were minimal or even negligible, which indicates bond distance cannot be used to determine the relative carbene or pyridinium character in such products.

Upon creation of a competitive situation for oxidative substitution either at the *remote* site (C4) or at the *normal* site (C2), *r*NHC complexes of both Ni (**19b**) and Pd (**19a**) were obtained. Oxidative substitution occurs on the ring that contains the heteroatom when the ligand 4,7-dichloro-*N*-methyl-quinolinium triflate was reacted with $M(PPh_3)_4$ (M = Pd or Ni). Replacement of the methyl group on the nitrogen of the ligand precursors with a hydrogen also yielded the same results, implying that electronic, rather than steric factors determine the selectivity during product formation.

From the calculations performed at the RI-BP86/SV level of theory, we could see that the chosen carbene ligand has a much larger influence than the metal, both on the overall bond strength and the composition of the bond. Generally, the farther away the N-atom is from the carbene carbon, the stronger the bond, but the effect becomes weaker when the number of bonds separating the heteroatom and the carbene carbon becomes larger than three. The π-bonding is decreased when the N-heteroatom is *meta* to the carbene carbon atom in pyridylidene complexes.

The obtained result that the substitution site influences the strength of the metal carbene bond implies that *r*NHCs can be fine-tuned for σ-donating strength to a remarkable degree. This has definite implications for rational catalyst design, given the already proven activity of NHC-containing transition metal complexes in catalysis.

Experiments with 4-[2-(4-bromophenyl)ethenyl]-N-methylpyridinium triflate emphasised the fact that the chemical shift of the metal bonded carbon in the ^{13}C NMR spectrum can not be used as absolute measure of carbene character, but only in a related family of compounds.

The library of carbene complexes containing *r*NHC ligands were extended particularly by the successful preparation of *trans*-chloro(*N*-methyl-1,2,4-trihydro-2-dimethylaminepyrid-4-ylidene)bis(triphenylphosphine)palladium(II) triflate (**28a**) and *trans*-chloro(*N*-methyl-1,2,4-trihydro-2-dimethylaminepyrid-4-ylidene)bis(triphenylphosphine)nickel(II) triflate (**28b**), both having a ligand with two remote nitrogens, one of which is situated outside the main ring system. In the attempt to replace the methyl on the external nitrogen of the ligand precursor with a phenyl group, the compound 2-chloro-1-methyl-1*H*-pyrid-4-ylidenephenylammonium triflate, **29**, was obtained. This ligand was employed in the synthesis of complexes **30a** and **30b**, which contain a

carbene ligand with both a remote as well as an additional nitrogen in the α postion to the carbon donor.

N-methyl-4',4'-dimethyl-2'-thiophen-3-chloro-2-yl-4,5-dihydro-oxazole served as a *r*NHC type precursor ligand to prepare carbene complexes that contained three different heteroatoms in their ligand.

The attempted preparation of the carbene complex with the $Cr(CO)_5$ fragment bonded in the 3-position of the ligand, 4,4-dimethyl-2-thiophen-2-yl-4,5-dihydro-oxazole, that was blocked in the 5-position using a $SiPPh_3$ group was unsuccessful. Theoretical studies could provide a better understanding of this bonding and may reveal what effect the steric requirements of the $Cr(CO)_5$ unit would have on this bonding.

3.4 Possible future work

Reacting $M(PPh_3)_4$ (M = Pd, Ni) with 4,7-dichloro-*N*-methyl-quinolinium triflate resulted in the complex where the carbon donor is situated in the ring containing the heteroatom and complexes have been prepared where the carbon donor is situated in the annealed ring. It would be interesting to investigate where oxidative substitution will occur when $M(PPh_3)_4$ is reacted with 7-bromo-4-chloroquinolinium triflate (**XXXIV**) since oxidative substitution of Pd into a C-Br bond is more favourable than a C-Cl bond.

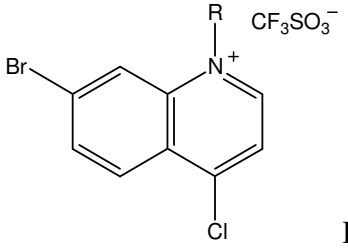

XXXIV

R = H, CH_3

Chelating ligand systems based on 1,3-disubstituted benzene have been extensively studied, with donor atoms nitrogen,[137] phosphorous[138] and sulfur the most plentiful. Reactions with suitable metal precursors lead to the isolation of orthometallated complexes (**XXXV**).[139] These ligands have the possibility of fine tuning their electronic nature by the introduction of substituents or incorporation

[137] Review: G. van Koten, *Pure Appl. Chem.,* 1989, **61**, 1681.
[138] C. L. Moulton and B. L. Shaw, *J. Chem. Soc., Dalton Trans.,* 1976, 1020; S.-Y. Liou, M. Gozin and D. Milstein, *J. Am. Chem. Soc.,* 1995, **117**, 9774.
[139] A. L. Seligson and W. C. Trogler, *Organometallics,* 1993, **12**, 744.

of a heteroatom in the ring.[140] The use of chelating donor groups attached to the carbene ligand, may produce a more stable catalyst. These type of ligands with sulphur donor atoms have very recently been quaternized[141] and are described as pyridinium complexes, although the authors recognize the contribution of a resonance structure of the carbene derivative. The complexes should rather be seen as carbene complexes (pyridylidene) since the carbon donors resonate between 206 – 212 ppm. The scope for this type of ligands (**XXXVI)** is still wide and unexplored.

XXXV

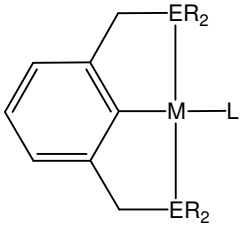

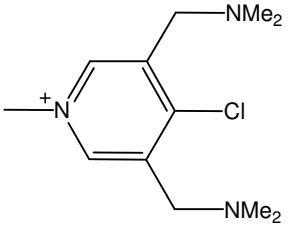

XXXVI

Given that oxidative substitution of $M(PR_3)_4$ to halo-pyridine-derived ligands give high yields, the scope of utilising pyridine type ligands with substituents that have modifying possibilities (Scheme 3.24) is wide open.

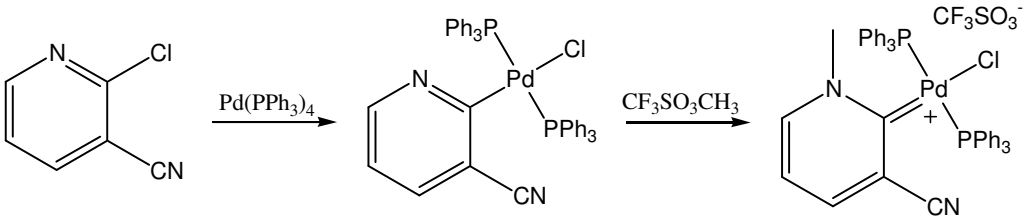

Scheme 3.24

Second generation Grubbs catalysts make use of N^2HC^5 as ligands and prove to be much more stable and active in some cases. Would it be possible to transfer the pyridine-derived carbene ligands with remote heteroatoms by using the Fischer-type carbene route described in Section 3.2.2 and what would the catalytic activity of the formed complexes be?

[140] A. Weisman, M. Gozin, H.-B. Kraatz and D. Milstein, *Inorg. Chem.,* 1996, **35**, 1792.
[141] H. Meguro, T. Koizumi, T. Yamamoto and T. Kanbara, *J. Organomet. Chem.,* 2008, **693**, 1109.

3.5 Experimental

3.5.1 General

The general techniques described in Section 2.4.1, Chapter 2, were also applied to the work in this chapter. For the synthesis of 4,4-dimethyl-2-(2-thienyl)oxazoline,[24] $[Cr(CO)_5Br][NEt_4]$,[142] $[RhCl(CO)_2]_2$,[143] 4'-bromo-4-stilbazole,[127] $(PhCN)_2PdCl_2$[144] and $Pd(PPh_3)_4$[145] previously published protocols were followed. The chemicals used as starting materials were purchased and used without further purification.

3.5.2 Synthetic procedures and physical data

3.5.2.1 The synthesis of $(CO)_5Cr=C[CH=C(CH_3)]N(CH_3)CH=C(nBu)$, 8

The method described by Aumann *et al.*[59] was utilised for the synthesis of complex **8** from 0.207 g (0.678 mmol) of **7** (synthesis described in Section 2.4.2) and 0.139 g (0.19 ml, 1.70 mmol) of 1-hexyne to afford 0.152 g (0.428 mmol) of **8**.

Table 3.46 Physical data of compound **8**

Yield		63.1 %
Colour		Yellow
Melting point		114 °C with decomposition
Elemental analysis	% calculated	C 54.09, H 4.82, N 3.94
$C_{16}H_{17}CrNO_5$	% found	C 54.49, H 4.95, N 4.14

3.5.2.2 Transfer of the carbene ligand on complex 8 to Rh(I), the synthesis of complex 9

A Schlenk tube was charged with 0.081 g (0.228 mmol) of complex **8** and 0.022 g (0.057 mmol) of $[(CO)_2RhCl]_2$ and 20 ml of CH_2Cl_2 and connected to a bubbler. The solution was stirred for 5 hours at room temperature until no CO formation was observed anymore as indicated by the bubbler. The solution turned form yellow to black. The solution was filtered through celite and the resulting filtrate was layered with ether and stored at -20°C overnight. The precipitate was separated by filtration and the resulting filtrate was dried *in vacuo* to afford 0.050 g of *cis*- and *trans*- **37**. No

[142] G. Brauer, *Handbuch der Präparativen Anorganischen Chemie, Vol.* 3, Verlag, Stuttgart, 1981 p 1946
[143] G. Brauer, *Handbuch der Präparativen Anorganischen Chemie, Vol.* 3, Verlag, Stuttgart, 1981 p 1961
[144] G. A. Anderson and M. Lin, *Inorg. Synth.,* 1990, **28**, 61.
[145] F. Ozawa, in: *Synthesis of Organometallic Compounds,* Ed. S. Komiya, John Wiley & Sons, Chichester, 1997, p. 286.

separation of the isomers was performed, since TLC showed no indication of the possibility with the various solvent systems tried. Crystallization of the mixture by dissolving a small amount in CH_2Cl_2 and layering it with pentane afforded a few single crystals of *cis*-**9**.

Table 3.47 Physical data of compound **9**

Compound	***cis*-9**	***trans*-9**
Yield (according to NMR)	56 % (0.078 mmol)	44 % (0.062 mmol)
Colour	yellow	yellow

3.5.2.3 Attempt to transfer a pyridine-derived carbene ligand from Ni(II) to Pd(II) yielding a Cl bridged Pd complex, 10

$(PhCN)_2PdCl_2$ (0.030 g, 0.0782 mmol) and 0.056 g (0.0703 mmol) of *trans*-chloro-(*N*-methyl-1,2-dihydropyrid-2-ylidene)bis(triphenylphosphine)nickel(II) tetrafluoroborate were stirred at room temperature for 24 hours after which the mixture was filtered through celite. The resulting filtrate was concentrated and layered with pentane and stored at -20 °C to afford a few crystals of complex **10** suitable for an X-ray crystal structure determination.

3.5.2.4 The synthesis of 2-chloro-*N*-methylpyridinium triflate, 11

Methyl trifluoromethanesulfonate (4.33g , 3.00 ml, 26.4 mmol) was added dropwise to a solution of 2-chloropyridine (2.73 g, 24.0 mmol) in 20 ml of CH_2Cl_2. The solution was stirred for 18 hours at room temperature where after the solvent was removed by cannula. The resulting precipitate was washed with ether (3 x 10 ml) and dried under high vacuum for a few hours to yield 6.51 g (23.4 mmol) of compound **11**.

Table 3.48 Physical data of compound **11**

Yield		88.8 %
Colour		White
Melting point		163.3 – 165.0 °C
Elemental analysis	% calculated	C 30.28, H 2.54, N 5.04
$C_7H_7NO_3SClF_3$	% found	C 30.01, H 2.41, N 4.93

3.5.2.5 The synthesis of 3-chloro-*N*-methylpyridinium triflate, 12

The ligand precursor, 3-chloropyridine (1.00 g, 8.81 mmol), was dissolved in 20 ml of CH_2Cl_2. $CF_3SO_3CH_3$ (1.10 ml, 1.59 g, 9.69 mmol) was added dropwise with a syringe at room temperature

and the solution was stirred overnight. The solvent was removed under vacuum and the residue was washed with 15 ml of diethyl ether, yielding 2.41 g (8.68 mmol) of compound **12**.

Table 3.49 Physical data of compound **12**

Yield		98.5 %
Colour		White
Melting point		60.8 – 62.3 °C
Elemental analysis	% calculated	C 30.28, H 2.54, N 5.04
$C_7H_7NO_3SClF_3$	% found	C 30.80, H 2.30, N 5.09

3.5.2.6 The synthesis of 4-chloro-*N*-methylpyridinium triflate, 13

4-Chloropyridine·HCl (5.00 g, 33.3 mmol) was dissolved in 50 ml of distilled water and 40 ml 1 M NaOH was added. The aqueous solution was extracted with ether (3 x 40 ml). The organic phase was washed with brine, dried with $MgSO_4$ and concentrated in a brown Schlenk tube. The oil (2.18 g, 19.2 mmol) was dissolved in CH_2Cl_2, cooled to -78 °C and methyl trifluoromethanesulfonate (3.46 g, 2.40 ml, 21.1 mmol) was added drop wise. The mixture was stirred overnight while it was allowed to warm up to room temperature. The solvent was removed *in vacuo* and the resulting product was washed 1 x 10 ml of THF and 2 x 10 ml of diethyl ether to give 5.13 g (18.5 mmol) of compound **13**.

Table 3.50 Physical data of compound **13**

Yield		55.5 %
Colour		White
Melting point		135.1 – 136.6 °C
Elemental analysis	% calculated	C 30.28, H 2.54, N 5.04
$C_7H_7NO_3SClF_3$	% found	C 30.01, H 2.61, N 5.11

3.5.2.7 The synthesis of *trans*-chloro(*N*-methyl-1,2-dihydro-pyrid-2-ylidene)bis(triphenyl-phosphine)palladium(II) triflate, 14a

Compound **11** (0.257 g, 0.917 mmol) and $Pd(PPh_3)_4$ (1.07g, 0.926 mmol) were suspended in 30 ml of toluene and stirred for 17 hours at 60 °C. The white suspension in a light yellow solution was allowed to cool to room temperature and filtered through celite. The solid on the filter was washed with 4 x 5ml toluene and the product was dissolved in CH_2Cl_2 and filtered, to yield after solvent evaporation *in vacuo* 0.802 g (0.883 mmol) of complex **14a**.

Table 3.51 Physical data of compound **14a**

Yield		96.3 %
Colour		White
Melting point		248 °C decomposed
Elemental analysis	% calculated	C 56.84, H 4.10, N 1.54
$C_{43}H_{37}NO_3P_2SClF_3Pd$	% found	C 57.03, H 4.19, N 1.60

3.5.2.8 The synthesis of *trans*-chloro(*N*-methyl-1,2-dihydro-pyrid-2-ylidene)bis(triphenyl-phosphine)nickel(II) triflate, 14b

$Ni(PPh_3)_4$ (0.330 g, 0.298 mmol) and the triflate salt **11** (0.082 g, 0.295 mmol) were suspended in THF (20 ml) and the mixture was stirred at room temperature for 17 hours. The resulting yellow precipitate in a brown solution was filtered through celite was washed with 3 x 5 ml toluene. The product was dissolved in CH_2Cl_2, filtered and dried under high vacuum to yield 0.151 g (0.175 mmol) of **14b**.

Table 3.52 Physical data of compound **14b**

Yield		58.9 %
Colour		Yellow
Melting point		187 °C decomposed
Elemental analysis	% calculated for	C 59.99, H 4.33, N 1.63
$C_{43}H_{37}NO_3P_2SClF_3Ni$	% found	C 60.32, H 4.24, N 1.49

3.5.2.9 The synthesis of *trans*-chloro(*N*-methyl-1,3-dihydropyrid-3-ylidene)bis(triphenyl-phosphine)palladium(II) triflate, 15a

A suspension of 0.173 g (0.616 mmol) of compound **12** and 0.719 g (0.622 mmol) of $Pd(PPh_3)_4$ in toluene was stirred for 64 hours at 60 °C. The resulting white suspension in a light yellow solution was filtered over celite and washed with 2 x 10 ml toluene. The crude product containing some of the unreacted ligand was washed through with 3 x 10 ml CH_2Cl_2 and dried *in vacuo*. The product was obtained as an analyticallypure sample by dissolving the crude mixture in CH_2Cl_2 and allowing pentane to diffuse slowly into the mixture to yield 0.508 g (0.559 mmol) of **15a**.

Table 3.53 Physical data of compound **15a**

Yield		90.8 %
Colour		White metallic
Melting point		195 °C decomposed
Elemental analysis	% calculated	C 56.84, H 4.10, N 1.54
$C_{43}H_{37}NO_3P_2SClF_3Pd$	% found	C 56.99, H 4.01, N 1.60

3.5.2.10 The synthesis of *trans*-chloro(*N*-methyl-1,3-dihydropyrid-3-ylidene)bis(triphenylphosphine)nickel(II) triflate, 15b

The same procedure as described for complex **14b** was utilised with 0.183 g (0.660 mmol) **12** and 0.739 g (0.667 mmol) $Ni(PPh_3)_4$ to yield 0.282 g (0.328 mmol) of complex **15b**.

Table 3.54 Physical data of compound **15b**

Yield		49.6 %
Colour		Light yellow
Melting point		135-138 °C
Elemental analysis	% calculated	C 59.99, H 4.33, N 1.63
$C_{43}H_{37}NO_3P_2SClF_3Ni$	% found	C 60.24, H 4.21, N 1.72

3.5.2.11 The synthesis of *trans*-chloro(*N*-methyl-1,4-dihydropyrid-4-ylidene)bis(triphenylphosphine)palladium(II) triflate, 16a

The same method as described for complex **14a** was used and 0.331 g (1.19 mmol) of **3** and 1.39 g and (1.21 mmol) of $Pd(PPh_3)_4$ produced 1.07 g (1.18 mmol) of complex **16a**.

Table 3.55 Physical data of compound **16a**

Yield		99.0 %
Colour		White
Melting point		189 °C decomposed
Elemental analysis	% calculated	C 56.84, H 4.10, N 1.54
$C_{43}H_{37}NO_3P_2SClF_3Pd$	% found	C 56.61, H 3.98, N 1.59

3.5.2.12 The synthesis of *trans*-chloro(*N*-methyl-1,4-dihydropyrid-4-ylidene)bis(triphenyl-phosphine)nickel(II) triflate, 16b

The same method as described for complex **14b** was used, with 0.114 g (0.412 mmol) of **3** and 0.461 g (0.416 mmol) of $Ni(PPh_3)_4$ to obtain 0.162 g (0.188 mmol) of complex **16b**.

Table 3.56 Physical data of compound **16b**

Yield		45.7 %
Colour		Yellow
Melting point		153 °C decomposed
Elemental analysis	% calculated	C 59.99, H 4.33, N 1.63
$C_{43}H_{37}NO_3P_2SClF_3Ni$	% found	C 60.21, H 4.23, N 1.54

3.5.2.13 The synthesis of 2,4-dichloro-*N*-methylpyridinium triflate, 17

Following the same procedure as for the preparation of **12**, compound **17** was prepared from 2,4-dichloropyridine (0.70 g, 4.75 mmol) and $CF_3SO_3CH_3$ (0.60 ml, 0.86 g, 5.23 mmol) to yield 1.48 g (4.74 mmol) of compound **17**.

Table 3.57 Physical data of compound **17**

Yield		99.8 %
Colour		White
Melting point		95.8 – 97.7 °C
Elemental analysis	% calculated	C 26.94, H 1.94, N 4.49
$C_7H_6NO_3SCl_2F_3$	% found	C 26.88, H 1.99, N 4.57

3.5.2.14 The synthesis of 4,7-dichloro-*N*-methylquinolinium triflate, 18

The same method was used as described for compound **17** to prepare compound **18** from 4,7-dichloroquinoline (1.39 g, 7.00 mmol) and $CF_3SO_3CH_3$ (0.95 ml, 1.38 g, 8.40 mmol) in CH_2Cl_2. The residue was washed twice with 30 ml of diethyl ether, yielding 2.51 g (6.93 mmol) of **18**.

Table 3.58 Physical data of compound **18**

Yield		99.0 %
Colour		White
Melting point		108 – 111 °C
Elemental analysis	% calculated	C 36.48, H 2.23, N 3.87
$C_{11}H_8NO_3SCl_2F_3$	% found	C 36.26, H 2.29, N 3.78

3.5.2.15 The synthesis of *trans*-chloro(2-chloro-*N*-methyl-1,2,4-trihydro-pyrid-4-ylidene)bis(triphenylphosphine)palladium(II) triflate, 19a

$Pd(PPh_3)_4$ (0.182 g, 0.157 mmol) and the triflate salt **17** (0.049 g, 0.157 mmol) were suspended in toluene (30 ml) and the mixture was stirred at 60°C for 17 hours. The toluene was removed by a cannula and the resulting precipitate was washed with 15 ml toluene. The product was dried under high vacuum to yield 0.110 g (0.117 mmol) of **19a**. Crystallisation of the microcrystalline powder from pentane diffusing into a solution of **19a** in CH_2Cl_2 (-20°C) yielded white crystals suitable for a single crystal X-ray structure determination.

Table 3.59 Physical data of compound **19a**

Yield		74.3 %
Colour		Metallic white
Melting point		200 °C decomposed
Elemental analysis	% calculated	C 54.76, H 3.85, N 1.49
$C_{43}H_{36}NO_3P_2SCl_2F_3Pd$	% found	C 54.55, H 3.78, N 1.55

3.5.2.16 The synthesis of *trans*-chloro(2-chloro-*N*-methyl-1,2,4-trihydro-pyrid-4-ylidene)-bis(triphenylphosphine)nickel(II) triflate, 19b

$Ni(PPh_3)_4$ (0.593 g, 0.535 mmol) and the triflate salt **17** (0.152 g, 0.487 mmol) were suspended in THF (30 ml) and the mixture was stirred for 17 hours at room temperature. The light brown solution with a yellow suspension was filtered through celite and washed with 3 x 10 ml THF to remove the unreacted $Ni(PPh_3)_4$. The product was washed through with 50 ml of CH_2Cl_2 and the solvent was removed by vacuum to yield 0.272 g (0.304 mmol) of **19b**. Crystallisation of **19b** in CH_2Cl_2 into which pentane diffuses slowly at -20°C gave the yellow crystals suitable for a single crystal X-ray structure determination.

Table 3.60 Physical data of compound **19b**

Yield		62.4 %
Colour		Yellow
Melting point		160 °C decomposed
Elemental analysis	% calculated	C 57.68, H 4.05, N 1.56
$C_{43}H_{36}NO_3P_2SCl_2F_3Ni$	% found	C 58.05, H 4.16, N 1.50

3.5.2.17 The synthesis of *trans*-chloro(7-chloro-*N*-methyl-1,4,7-trihydro-quinol-4-ylidene)-bis(triphenylphosphine)palladium(II) triflate, 20a

The same procedure as used for the preparation of complex **19a** was employed to prepare 0.110 g (0.111 mmol) of **20a**, as a microcrystalline material, from $Pd(PPh_3)_4$ (0.240 g, 0.208 mmol) and the triflate salt **18** (0.064 g, 0.176 mmol).

Table 3.61 Physical data of compound **20a**

Yield		62.9 %
Colour		Off-white
Melting point		204°C decomposed
Elemental analysis	% calculated	C 56.84, H 3.86, N 1.41
$C_{47}H_{38}NO_3P_2SCl_2F_3Pd$	% found	C 56.66, H 3.72, N 1.53

3.5.2.18 The synthesis of *trans*-chloro(7-chloro-*N*-methyl-1,4,7-trihydro-quinol-4-ylidene)-bis(triphenylphosphine)nickel(II) triflate, 20b

Complex **20b** was synthesised in a similar fashion as **19b** with 0.458 g (0.413 mmol) of $Ni(PPh_3)_4$ and 0.136 g (0.376 mmol) of the triflate salt **18** to yield 0.286 g (0.302 mmol) of **20b**.

Table 3.62 Physical data of compound **20b**

Yield		80.4 %
Colour		Yellow
Melting point		176 °C decomposed
Elemental analysis	% calculated	C 59.71, H 4.05, N 1.48
$C_{47}H_{38}NO_3P_2SCl_2F_3Ni$	% found	C 59.99, H 4.11, N 1.38

3.5.2.19 The synthesis of 2,4-dichloropyridinium triflate, 21

Compound **21** was prepared by reacting 2,4-dichloropyridine (1.19 g, 8.06 mmol) with CF_3SO_3H (0.78 ml, 1.33 g, 8.86 mmol) at room temperature for 18 hours. Diethyl ether was added and a white precipitate formed. The solvent was removed *via* a cannula and the resulting solid washed with 4 x 20 ml diethyl ether and dried *in vacuo* to yield 2.06 g (6.91 mmol) of compound **21**.

Table 3.63 Physical data of compound **21**

Yield		85.7%
Colour		White (hygroscopic)
Melting point		115.4 – 117 °C
Elemental analysis	% calculated	C 24.18, H 1.35, N 4.70
$C_6H_4NO_3SCl_2F_3$	% found	C 23.29, H 1.41, N 4.54

3.5.2.20 The synthesis of 4,7-dichloroquinolinium triflate, 22

Compound **22** was prepared in a similar fashion as compound **21** using 4,7-dichloroquinoline (0.303 g, 1.53 mmol) and CF_3SO_3H (0.15 ml, 0.253 g, 1.68 mmol) as starting materials to furnish 0.522 g (1.50 mmol) of **22**.

Table 3.64 Physical data of compound **22**

Yield		98.0 %
Colour		White
Melting point		146.4 – 147.2 °C
Elemental analysis	% calculated	C 34.50, H 1.74, N 4.02
$C_{10}H_6NO_3SCl_2F_3$	% found	C 34.28, H 1.81, 4.12

3.5.2.21 The synthesis of *trans*-chloro(2-chloro-2,4-dihydro-pyrid-4-ylidene)bis(triphenyl-phosphine)palladium(II) triflate, 23a

The procedure followed for complex **14a** was used to react $Pd(PPh_3)_4$ (1.91 g, 1.66 mmol) with the ligand precursor **21** (0.470 g, 1.58 mmol) to yield 1.01g of a white microcrystalline material that contained three products of which two are unidentifiable. A yield of 89 % for **23a** is calculated from the ^{31}P NMR spectrum of the crude mixture.

3.5.2.22 The attempted synthesis of *trans*-chloro(2-chloro-2,4-trihydropyrid-4-ylidene)-bis(triphenylphosphine)nickel(II) triflate, 23b

$Ni(PPh_3)_4$ (0.270 g, 0.244 mmol) and compound **21** (0.069 g, 0.232 mmol) were suspended in THF (30 ml) and the mixture was stirred for 17 hours at room temperature. Pentane was added to the yellow-brown solution with a tar-like residue on the side. The precipitate was filtered off through celite and washed with 5 ml of toluene to yield 0.070g of a light yellow microcrystalline product. When the resulting precipitate on the celite was washed with CH_2Cl_2 a red brown oily residue was formed.

3.5.2.23 The synthesis of *trans*-chloro(7-chloro-4,7-dihydroquinol-4-ylidene)bis(triphenyl-phosphine)palladium(II) triflate, 24a

Following the same procedure as for the preparation of complex **14a**, 0.239 g (0.244 mmol) of complex **24a** was prepared from $Pd(PPh_3)_4$ (0.347 g, 0.300 mmol) and compound **30** (0.100 g, 0.286 mmol).

Table 3.65 Physical data of compound **24a**

Yield		85.3 %
Colour		White
Melting point		207 °C decompose
Elemental analysis	% calculated	C 56.43, H 3.71, N 1.43
$C_{46}H_{36}NO_3P_2SCl_2F_3Pd$	% found	C 56.22, H 3.87, N 1.46

3.5.2.24 The synthesis of *trans*-chloro(7-chloro-4,7-dihydroquinolin-4-ylidene)bis(triphenyl-phosphine)nickel(II) triflate, 24b

Employing the same procedure as for complex **14b**, complex **24b** (0.170 g, 0.183 mmol) was synthesised from 0.312 g (0.282 mmol) of $Ni(PPh_3)_4$ and 0.093 g (0.268 mmol) of compound **22**.

Table 3.66 Physical data of compound **24b**

Yield		68.1 %
Colour		Yellow
Melting point		197 °C decompose
Elemental analysis	% calculated	C 59.32, H 3.90, N 1.50
$C_{46}H_{36}NO_3P_2SCl_2F_3Ni$	% found	C 59.11, H 4.02, N 1.63

3.5.2.25 The synthesis of 4-chloro-1-methyl-*1H*-pyrid-2-methylamine, 25

Compound **17** (0.22 g, 0.70 mmol) was dissolved in 4 ml water at 0ºC and CH_3NH_2 gas was bubbled through the solution until the solution became light yellow. The excess methyl amine was removed under vacuum. A light yellow precipitate formed which was filtered off. The resulting solid was dissolved in CH_2Cl_2, dried with $MgSO_4$, filtered and dried *in vacuo* to yield a hygroscopic light yellow solid (0.051g, 0.35 mmol).

Table 3.67 Physical data of compound **25**

Yield		50.7 %
Colour		Light yellow
Melting point		30-32 °C
Elemental analysis	% calculated	C 53.68, H 5.79, N 17.89
$C_7H_9N_2Cl$	% found	C 53.10, H 5.88, N 17.97

3.5.2.26 The synthesis of 4-chloro-1-methyl-*1H*-pyrid-2-dimethylammonium triflate, 26

Compound **25** (0.134 g, 0.927 mmol) was dissolved in 20 ml of dry CH_2Cl_2. $CF_3SO_3CH_3$ (0.182 g, 0.13 ml, 1.11 mmol) was added drop wise and the solution was stirred overnight at room temperature. The solvent was evaporated and the residue was washed with 15 ml dry ether and 15 ml dry pentane to yield the off-white product, **26** (0.239 g, 0.774 mmol).

Table 3.68 Physical data of compound **26**

Yield		83.5 %
Colour		White
Melting point		57.1 – 58.9 °C
Elemental analysis	% calculated	C 33.70, H 3.77, N 8.73
$C_9H_{12}N_2O_3SClF_3$	% found	C 34.22, H 3.60, N 8.80

3.5.2.27 The synthesis of *trans*-chloro(1-methyl-1,2,4-trihydro-pyrid-2-methylimine-bis(triphenylphosphine)palladium(II), 27

$Pd(PPh_3)_4$ (0.315 g, 0.273 mmol) and the imine ligand **25** (0.030 g, 0.192 mmol) were suspended in THF (20 ml) and the mixture was stirred at 70°C for 16 hours. The resulting precipitate was filtered through celite and washed with 3 x 5 ml THF. The product was dissolved in CH_2Cl_2, filtered and dried under high vacuum to yield 0.085 g (0.108 mmol) of **27**.

Table 3.69 Physical data of compound **27**

Yield		56.3 %
Colour		White
Melting point		182 °C decomposed
Elemental analysis	% calculated	C 65.57, H 4.99, N 3.56
$C_{43}H_{39}N_2P_2ClPd$	% found	C 65.21, H 5.08, N 3.45

3.5.2.28 The synthesis of *trans*-chloro(*N*-methyl-1,2,4-trihydro-2-dimethylaminepyrid-4-ylidene)bis(triphenylphosphine)palladium(II) triflate, 28a

Complex **28a** (0.480 g, 0.504 mmol) was prepared in an analogous way to complex **14a** from 0.169 g (0.547 mmol) of **26** and 0.664 g (0.575 mmol) of $Pd(PPh_3)_4$

Table 3.70 Physical data of compound **28a**

Yield		92.2 %
Colour		Metallic white
Melting point		195 °C decomposed
Elemental analysis	% calculated	C 56.79, H 4.45, N 2.94
$C_{45}H_{42}N_2O_3P_2SClF_3Pd$	% found	C 56.66, H 4.54, N 2.88

3.5.2.29 The synthesis of *trans*-chloro(*N*-methyl-1,2,4-trihydro-2-dimethylaminepyrid-4-ylidene)bis(triphenylphosphine)nickel(II) triflate, 28b

Compound **26** (0.017 g, 0.055 mmol) and $Ni(PPh_3)_4$ were dissolved in THF and stirred for 4 hours at room temperature. The solution was then filtered through celite, washed with 2 x 10 ml THF and the product was washed through with CH_2Cl_2 to furnish after solvent evaporation 0.045 g (0.0498 mmol) of complex **28b**.

Table 3.71 Physical data of compound **28b**

Yield		90.4 %
Colour		Light yellow
Melting point		162 °C decomposed
Elemental analysis	% calculated	C 59.79, H 4.68, N 3.10
$C_{45}H_{42}N_2O_3P_2SClF_3Ni$	% found	C 60.03, H 4.58, N 3.22

3.5.2.30 The synthesis of 2-chloro-1-methyl-1*H*-pyrid-4-ylidenephenylammonium triflate, 29

The compound was prepared by a similar method as described above for the preparation of **25**. Compound **17** (0.62 g, 2.0 mmol) was dissolved in 4 ml water at 0ºC and analine (0.18 ml, 0.19 g, 2.0 mmol) was added drop wise. The solution became yellow and then a light yellow precipitate formed. CH_2Cl_2 (20 ml) was added, the organic phase was separated, dried with $MgSO_4$, filtered and dried *in vacuo* to yield a light orange solid (0.461 g, 1.25 mmol).

Table 3.72 Physical data of compound **29**

Yield		62.5 %
Colour		peach
Melting point		98.5 – 102.1 °C
Elemental analysis	% calculated	C 42.34, H 3.28, N 7.60
$C_{13}H_{12}N_2O_3SClF_3$	% found	C 43.01, H 3.12, N 7.72

3.5.2.31 Synthesis of *trans*-chloro(*N*-methyl-1,2,4-trihydro-4-phenylaminepyrid-2-ylidene)bis-(triphenylphosphine)palladium(II) triflate, 30a

The same synthetic procedure used for the preparation of complex **14a** was employed for the synthesis of 0.377 g (0.377 mmol) of complex **30a** from 0.167 g (0.453 mmol) of **29** and 0.854 g (0.739 mmol) of $Pd(PPh_3)_4$.

Table 3.73 Physical data of compound **30a**

Yield		83.2 %
Colour		White
Melting point		239 °C decomposed
Elemental analysis	% calculated	C 58.87, H 4.23, N 2.80
$C_{49}H_{42}N_2O_3P_2SClF_3Pd$	% found	C 58.80, H 4.32, N 2.73

3.5.2.32 Synthesis of *trans*-chloro(*N*-methyl-1,2,4-trihydro-4-phenylaminepyrid-2-ylidene)bis-(triphenylphosphine)nickel(II) triflate, 30b

Complex **30b** (0.162 g, 0.170 mmol) was obtained in a similar fashion as complex **14b** from 0.095 g (0.257 mmol) of **29** and 0.299 g (0.270 mmol) of $Ni(PPh_3)_4$.

Table 3.74 Physical data of compound **30b**

Yield		66.1 %
Colour		Light yellow
Melting point		200 °C decomposed
Elemental analysis	% calculated	C 61.82, H 4.45, N 2.94
$C_{49}H_{42}N_2O_3P_2SClF_3Ni$	% found	C 60.98, H 4.52, N 2.63

3.5.2.33 The preparation of 4-[2-(4-bromophenyl)ethenyl]-N-methylpyridinium triflate, 31

$CF_3SO_3CH_3$ (0.417 g, 0.29 ml, 2.54mmol) was added to a solution of 4-[2-(4-chlorophenyl)ethenyl]-*N*-methylpyridin (0.551 g, 2.12 mmol) in CH_2Cl_2 and stirred for 16 hours at room temperature. The bright yellow suspension was filtered and the precipitate was washed with 1 x 5 ml THF to yield after a few hours under high vacuum, 0.699 g (1.65 mmol) of **31**.

Table 3.75 Physical data of compound **31**

Yield		77.8 %
Colour		Bright yellow
Melting point		229 °C decomposed
Elemental analysis	% calculated	C 42.47, H 3.09, N 3.30
$C_{15}H_{13}NO_3SBrF_3$	% found	C 41.22, H 3.22, N 3.03

3.5.2.34 The synthesis of 4-*trans*-chloro-{[2-(4-bromophenyl)vinyl]-1-methylpyridinium}-bistriphenylphosphinepallalium (II) triflate, 32

Compound **31** (0.061 g, 0.143 mmol) and $Pd(PPh_3)_4$ (0.198 g, 0.171 mmol) were stirred for 18 hours at 60 °C. The solution was allowed to reach room temperature and the solvent removed *in vacuo*. The resulting precipitate was extracted with toluene (3 x 10 ml) and dried under vacuum to furnish 0.051 g (0.0483 mmol) of **32.**

Table 3.76 Physical data of complex **32**

Yield		33.8 %
Colour		Mustard yellow
Melting point		130 °C decompose
Elemental analysis	% calculated	C 58.05, H 4.11, N 1.33
$C_{51}H_{43}NO_3P_2SBrF_3Pd$	% found	C 56.98, H 3.91, N 1.47

3.5.2.35 The synthesis of 5-triphenylsilyl-4',4'-dimethyl-2'-thiophen-2-yl-4,5-dihydro-oxazole, 33

The synthesis of this complex was based on literature procedures.[24] To a solution of 4',4'-dimethyl-2'-thiophen-2-yl-4,5-dihydro-oxazole (0.833g, 4.60 mmol) in THF at -78 °C was added slowly a solution of LDA (3.34 ml, 1.43 M, 4.78 mmol BuLi and 0.483 g, 0.67 ml, 4.78 mmol diisopropylamine). This mixture was stirred for 30 minutes at -78 °C, Ph_3SiCl (1.37 g, 4.66 mmol) was added and the mixture was stirred for an additional 30 minutes at -78 °C, where after it was allowed to slowly warm up to room temperature. The solvent was removed *in vacuo*. The product was adsorbed unto silica and column chromatographically purified at room temperature with CH_2Cl_2/ hexane (2:1) as eluant and TLC was used to monitor the product fractions to obtain 0.782 g (1.78 mmol) of compound **33**. Crystals suitable for a single crystal X-ray structure determination to confirm the position of the $SiPh_3$ group was obtained from a slow evaporation of a CH_2Cl_2 solution of **33**.

Table 3.77 Physical data of compound **33**

Yield		38.7 %
Colour		White
Melting point		127.8 – 128.6
Elemental analysis $C_{27}H_{25}NOSSi$	% calculated	C 73.76, H 5.73, N 3.19
	% found	C 73.57, H 5.68, N 3.24

3.5.2.36 The synthesis of 5-triphenylsilyl 4',4'-dimethyl-2'-thiophen-2-yl-4,5-dihydro-oxazole pentacarbonylchromium lithium, 34

A solution of 0.068 g (0.605 mmol) $KOBu^t$ in 10 ml THF was added dropwise over a period of 10 minutes to a solution of BuLi (0.41 ml, 0.605 mmol, 1.49 M) in hexane at -100 °C.[146] The ligand precursor, 5-triphenylsilyl-4',4'-dimethyl-2'-thiophen-2-yl-4,5-dihydro-oxazole (0.242 g, 0.550 mmol), in 10 ml diethyl ether at -100 °C, was transferred to the basic solution *via* a cannula, where after the reaction mixture was allowed to warm up to -70 °C. $[Cr(CO)_5Br][NEt_4]$ (0.221 g, 0.550 mmol) in 10 ml of diethyl ether at -70 °C was added *via* a cannula. The reaction mixture was allowed to warm up to room temperature over a period of 3 hours. The solvent was removed under vacuum and the resulting red-yellow tar-like product was purified with column chromatography (-15 °C) using CH_2Cl_2/hexane (2:1) to remove $Cr(CO)_6$ and CH_2Cl_2 to obtain 0.060 g (0.094 mmol) of **35**. The column stayed yellow, and washing it with THF only yielded unreacted ligand precursor

[146] L. Brandsma and H. D. Verkruijsse, *Preparative Polar Organometallic Chemistry, Vol.1,* Springer-Verlag, Berlin, p. 18.

or ligand from decomposed complex that should have been eluated before **34** when using CH_2Cl_2 as eluant.

Table 3.78 Physical data of compound **34**

Yield	17.1 %
Colour	Light yellow
Melting point	Not obtained, not pure compound

3.5.2.37 The attempted synthesis of *N*-methyl-5-triphenylsilyl 4',4'-dimethyl-2'-thiophen-2-yl-4,5-dihydro-oxazolepentacarbonylchromium, 35

Complex **35** was dissolved in 5 ml of CH_2Cl_2 and cooled to -50 °C. $CF_3SO_3CH_3$ (0.0044 g , 3.00 µl) was added. The solution was allowed to slowly reach room temperature. It was quickly filtered through a short path of silica in a pasteur pipet and evaporated to dryness to yield 0.016 g of product. NMR indicated that is it was contaminated with $Cr(CO)_6$ and very unstable.

3.5.2.38 The synthesis of 3-chloro-4',4'-dimethyl-2'-thiophen-2-yl-4,5-dihydro-oxazole, 36

A solution of 2 ml (2.96 mmol, 1.49 M) BuLi in 10 ml of diethyl ether was cooled to -50 °C and 0.487 g (2.69 mmol) 4',4'-dimethyl-2'-thiophen-2-yl-4,5-dihydro-oxazole in 10 ml of diethyl ether was added dropwise over a period of 1 minute. The cooling bath was replaced by another one at -10°C and the solution was stirred for 10 minutes. The mixture was then cooled to -80 °C and 0.636 g (2.69 mmol) of hexachloro etane dissolved in 15 ml diethyl ether was added over a period of 25 minutes, ensuring that the temperature never rose above -60 °C. After addition, the temperature was allowed to warm up to -20 °C and 50 ml of water was added while the solution was stirred vigorously. The mixture was extracted 3 x 20 ml with diethyl ether, the organic layer dried with $MgSO_4$ and filtered. The product mixture was column chromatographically separated at room temperature with CH_2Cl_2 as eluant to give 0.275 g (1.27 mmol) of **36** and 0.060 g (0.331 mmol) of unreacted oxazoline.

Table 3.79 Physical data of compound **36**

Yield		47.2 %
Colour		White
Melting point		49.2 – 50.9 °C
Elemental analysis	% calculated	C 50.11, H 4.67, N 6.49
$C_9H_{10}NOSCl$	% found	C 49.95, H 4.53, N 6.37

3.5.2.39 The synthesis of *N*-methyl-4',4'-dimethyl-2'-thiophen-3-chloro-2-yl-4,5-dihydro-oxazole, 37

Compound 19 (0.193 g, 0.508 mmol) was obtained by stirring 0.180 g (0.834 mmol) of **36** and 0.151 g (0.10 ml, 0.918 mmol) of $CF_3SO_3CH_3$ in 20 ml CH_2Cl_2 for 17 hours at room temperature. The solution was concentrated until a precipitate formed and the pinkish solvent was removed with a syringe. The resulting residue was washed 2 x 4 ml of diethyl ether and dried *in vacuo*.

Table 3.80 Physical data of compound **37**

Yield		60.9 %
Colour		White
Melting point		124.9 – 126.9 °C
Elemental analysis	% calculated	C 34.79, H 3.45, N 3.69
$C_{11}H_{13}NO_4S_2ClF_3$	% found	C 34.63, H 3.78, N 3.89

3.5.2.40 The synthesis of *trans*-chloro(*N*-methyl-4',4'-dimethyl-2'-thiophen-3-chloro-2-yl-4,5-dihydro-oxazolin-3'-ylidene)bis(triphenylphosphine)palladium(II) triflate, 38a

A similar procedure was followed as was used for complex **14a**, but THF instead of toluene was used as solvent. Complex **38a** (0.090 g, 0.089 mmol) was synthesized from 0.038 g (0.100 mmol) of **37** and 0.121 g (0.105 mmol) of $Pd(PPh_3)_4$.

Table 3.81 Physical data of compound **38a**

Yield		89.0 %
Colour		White
Melting point		213 °C decomposed
Elemental analysis	% calculated	C 55.85, H 4.29, N 1.39
$C_{47}H_{43}NO_4P_2S_2ClF_3Pd$	% found	C 55.97, H 4.33, N 1.30

3.5.2.41 The synthesis *trans*-chloro(*N*-methyl-4',4'-dimethyl-2'-thiophen-3-chloro-2-yl-4,5-dihydro-oxazolin-3'-ylidene)bis(triphenylphosphine)nickel(II) triflate, 38b

Complex **38b** (0.171 g, 0.178 mmol) was obtained from 0.085 g (0.224 mmol) of **37** and 0.261 g (0.236 mmol) of $Ni(PPh_3)_4$ utilizing the same procedure followed for the synthesis of complex **14b**.

Table 3.82 Physical data of compound **38b**

Yield		79.2 %
Colour		Yellow
Melting point		180 °C decomposed
Elemental analysis	% calculated	C 58.61, H 4.50, N 1.45
$C_{47}H_{43}NO_4P_2S_2ClF_3Ni$	% found	C 59.92, H 4.71, N 1.56

3.4.3 Computational methods

All geometries were fully optimised at the RI-BP86/SVP level of theory (BP86 denotes the generalized gradient approximation (GGA) to density functional theory (DFT) using the exchange functional of Becke[147] in conjunction with the correlation functional of Perdew.[148,149]) using the Gaussian03[150] optimizer (Berny algorithm[151]) together with TurboMole5[152] energies and gradients. Subsequently they were characterized as minima by calculating the Hessian matrix at the stationary points analytically. To do the NBO-analysis, all geometries were optimized under constraint of C_s-symmetry. Thus, we could separate σ- and π-bonding contributions during the NBO-analysis. To do this, the RI-BP86/SVP geometries were optimised with the ADF2006.01 program package[153,154] using the BP86 functional and employing uncontracted Slater-type orbitals (STOs) as basis functions for the SCF calculations.[155] The basis sets for all elements have triple-ζ quality augmented by two sets of polarization functions (ADF-basis set "TZ2P"). Core electrons (i.e., 1s for second- and [He]2s2p for third-period atoms including first row transition metals, [Ne]3s3p3d for second row and [Ar]4s4p4d for third row transition metals) were treated by the frozen-core approximation. An auxiliary set of s, p, d, f, and g STOs was used to fit the molecular densities and to represent the

[147] A. D. Becke, *Phys. Rev. A,* 1988, **38**, 3098.
[148] J. P. Perdew, *Phys. Rev. B,* 1986, **34**, 7406.
[149] J. P. Perdew, *Phys. Rev. B,* 1986, **33**, 8822.
[150] M. J. Frisch, G. W. Trucks, H. B. Schlegel, G. E. Scuseria, M. A. Robb, J. R. Cheeseman, J. J. A. Montgomery, T. Vreven, K. N. Kudin, J. C. Burant, J. M. Millam, S. S. Iyengar, J. Tomasi, V. Barone, B. Mennucci, M. Cossi, G. Scalmani, N. Rega, G. A. Petersson, H. Nakatsuji, M. Hada, M. Ehara, K. Toyota, R. Fukuda, J. Hasegawa, M. Ishida, T. Nakajima, Y. Honda, O. Kitao, H. Nakai, M. Klene, X. Li, J. E. Knox, H. P. Hratchian, J. B. Cross, V. Bakken, C. Adamo, J. Jaramillo, R. Gomperts, R. E. Stratmann, O. Yazyev, A. J. Austin, R. Cammi, C. Pomelli, J. W. Ochterski, P. Y. Ayala, K. Morokuma, G. A. Voth, P. Salvador, J. J. Dannenberg, V. G. Zakrzewski, S. Dapprich, A. D. Daniels, M. C. Strain, O. Farkas, M. D. Malick, A. D. Rabuck, K. Raghavachari, J. B. Foresman, J. V. Ortiz, Q. Cui, A. G. Baboul, S. Clifford, J. Cioslowski, B. B. Stefanov, G. Liu, A. Liashenko, P. Piskorz, I. Komaromi, R. L. Martin, D. J. Fox, T. Keith, M. A. Al-Laham, C. Y. Peng, A. Nanayakkara, M. Challacombe, P. M. W. Gill, B. Johnson, W. Chen, M. W. Wong, C. Gonzalez, J. A. Pople, *Gaussian 03, Revision D.01*, Wallingford CT, 2004.
[151] C. Peng, P. Ayala, H. B. Schlegel, M. J. Frisch, *J. Comp. Chem.* 1996, **17**, 49.
[152] R. Ahlrichs, M. Baer, M. Haeser, H. Horn, C. Koelmel, *Chem. Phys. Lett.* 1989, **162**, 165.
[153] F. M. Bickelhaupt, E. J. Baerends, in *Reviews In Computational Chemistry, Vol 15,* Wiley-Vch, Inc, New York, 2000, p. 1.
[154] G. Te Velde, F. M. Bickelhaupt, E. J. Baerends, C. Fonseca Guerra, S. J. A. Van Gisbergen, J. G. Snijders, T. Ziegler, *J. Comp. Chem.* 2001, **22**, 931.
[155] J. G. Snijders, E. J. Baerends, P. Vernoojs, *At. Data Nucl. Data Tables* 1982, **26**, 483.

Coulomb and exchange potentials accurately in each SCF cycle.[156] Scalar relativistic effects have been incorporated by applying the zeroth-order regular approximation (ZORA).[157,158,159]

3.4.4 X-ray structure determinations

The most important crystallographic data of complexes ***cis*-9**, **10**, **15a**, **15b**, **19a**, **19b**, **20a**, **28a**, **28b**, **29**, **30a**, **38a** are listed in Tables 3.83 – 3.86. Data sets were collected and processed as described in Section 2.4.9 The structures were solved by direct methods (***cis*-9**, **10**, **15b**, **19b**, **28b**, **29** and **38a**) or interpretation of Patterson synthesis (**15a**, **19a**, **20a**, **28a** and **30a**), which yielded the position of the metal atom, and conventional Fourier methods. The positions of the hydrogen atoms were calculated by assuming ideal geometry and their coordinates were refined together with those of the attached carbon atoms as "riding model" for all the complexes. After establishing the connectivity of ***cis*-9**, additional diffuse electron density which belongs to co-crystallised H_2O solvent was located on the difference map. The water molecule was fixed as follows: O-H, 0.80 Å, H-H, 1.5 Å. All the water hydrogens have 1.5 times the U_{iso} of the oxygen atoms. Additional information regarding these crystal structures is available from Prof H. G. Raubenheimer, Department of Chemistry and Polymer Science, University of Stellenbosch.

[156] J. Krijn, E. J. Baerends, *Fit Functions in the HFS-Method*, Internal Report (in Dutch), Vrije Universiteit Amsterdam, The Netherlands, 1984.
[157] E. van Lenthe, E. J. Baerends, J. G. Snijders, *J. Chem. Phys.,* 1993, **99**, 4597.
[158] E. van Lenthe, E. J. Baerends, J. G. Snijders, *J. Chem. Phys.,* 1994, **101**, 9783.
[159] E. van Lenthe, A. Ehlers, E. J. Baerends, *J. Chem. Phys.,* 1999, **110**, 8943.

Table 3.83 Crystal data and structure refinement parameters of complexes **9**, **10** and **15a**

Complex	***cis*-9·H_2O**	**10·CH_2Cl_2**	**15a·2CH_2Cl_2**
Empirical formula	$C_{13}H_{19}NO_3ClRh$	$C_{37}H_{32}P_2Cl_6Pd_2$	$C_{45}H_{41}NO_3P_2SF_3Cl_5Pd$
Formula weight / g.mol^{-1}	375.65	964.07	1078.44
Temperature/ K	100(2)	273(2)	100(2)
Crystal colour and habit	orange blocks	orange prisms	yellow blocks
Space group	C_2/c	$P4_12_12$	$P2_1/n$
a / Å	19.339(3)	9.5406(3)	14.672(5)
b / Å	11.734(2)	9.5406(3)	18.609(6)
c / Å	13.384(2)	39.962(3)	18.404(6)
α / °	90.0	90.0	90.0
β / °	93.381(3)	90.0	107.724(5)
γ / °	90.0	90.0	90.0
V (Å^3)	3032.0(7)	3637.4(3)	4786(3)
Z	4	4	4
$D_{calc.}$ / g.cm^{-3}	1.607	1.760	1.497
Adsorption coefficient / mm^{-1}	1.301	1.545	0.829
F(000)	1480	1912	2184
θ (min – max) / °	2.03 – 26.45	2.04 – 26.44	1.82 – 26.46
Reflections collected	8775	40720	26691
Independent reflections	2504	3390	4033
Data/restraints/parameters	3123/3/177	3719/0/213	9779/537/1
Final *R* indices [$I>2\sigma(I)$]	$R_1 = 0.0501$, $wR_2 = 0.1164$	$R_1 = 0.0496$, $wR_2 = 0.0912$	$R_1 = 0.0976$, $wR_2 = 0.2383$
R indices (all data)	$R_1 = 0.0659$, $wR_2 = 0.1251$	$R_1 = 0.0578$, $wR_2 = 0.0976$	$R_1 = 0.2315$, $wR_2 = 0.3371$
Goodness-of-fit on F^2	1.058	1.135	1.034
Largest peak / e Å^{-3}	2.370	1.332	2.119

Table 3.84 Crystal data and structure refinement parameters of complexes **15b**, **19a** and **19b**

Complex	**15b·2CH$_2$Cl$_2$**	**19a·2CH$_2$Cl$_2$**	**19b·CH$_2$Cl$_2$**
Empirical formula	$C_{45}H_{41}NO_3P_2SF_3Cl_5Ni$	$C_{45}H_{40}NO_3P_2SF_3Cl_6Pd$	$C_{44}H_{38}NO_3P_2SF_3Cl_4Ni$
Formula weight / g.mol^{-1}	1030.75	1112.88	980.26
Temperature/ K	100(2)	273(2)	273(2)
Crystal colour and habit	yellow blocks	colourless prisms	yellow blocks
Space group	$P2_1/n$	$P2_1/c$	$P2_1/n$
a / Å	14.678(2)	17.679(2)	10.5898(7)
b / Å	18.491(2)	16.937(2)	21.8258(14)
c / Å	18.317(2)	16.341(2)	19.7422(13)
α / °	90.0	90.0	90.0
β / °	109.068(2)	106.954(2)	104.713(1)
γ / °	90.0	90.0	90.0
V (Å^3)	4698.6(10)	4680.5(8)	4413.4(5)
Z	4	4	4
$D_{calc.}$ / g.cm^{-3}	1.457	1.579	1.475
Adsorption coefficient / mm^{-1}	0.862	0.905	0.855
F(000)	2112	2248	2008
θ (min – max) / °	1.61 – 26.32	1.70 – 26.44	2.00 – 26.40
Reflections collected	25371	26373	25153
Independent reflections	6576	8197	7907
Data/restraints/parameters	9329/1/561	9607/0/560	9018/0/533
Final *R* indices [$I>2\sigma(I)$]	$R_1 = 0.0753$, $wR_2 = 0.1156$	$R_1 = 0.0580$, $wR_2 = 0.1258$	$R_1 = 0.0404$, $wR_2 = 0.0995$
R indices (all data)	$R_1 = 0.1927$, $wR_2 = 0.2479$	$R_1 = 0.0698$, $wR_2 = 0.1314$	$R_1 = 0.0469$, $wR_2 = 0.1032$
Goodness-of-fit on F^2	1.086	1.098	1.032
Largest peak / e Å^{-3}	2.795	1.882	0.750

Table 3.85 Crystal data and structure refinement parameters of complexes **20a**, **28a** and **28b**

Complex	**20b·2CH$_2$Cl$_2$**	**28a·2CH$_2$Cl$_2$**	**28b**
Empirical formula	$C_{49}H_{42}NO_3P_2SF_3Cl_6Pd$	$C_{47}H_{46}N_2O_3P_2SF_3Cl_5Pd$	$C_{45}H_{42}N_2O_3P_2SF_3ClPd$
Formula weight / g.mol^{-1}	1162.94	1121.51	903.97
Temperature/ K	273(2)	273(2)	100(2)
Crystal colour and habit	colourless needles	colourless blocks	yellow needles
Space group	*P*-1	$P2_1/c$	$P2_1$
a / Å	11.472(2)	17.927(2)	12.601(6)
b / Å	13.832(3)	16.984(2)	10.875(5)
c / Å	34.952(7)	16.266(2)	15.497(7)
α / °	81.490(3)	90.0	90.0
β / °	89.833(4)	106.089(2)	95.23(1)
γ / °	65.550(4)	90.0	90.0
V (Å^3)	4982.7(17)	4758.7(9)	2114.8(17)
Z	4	4	2
$D_{calc.}$ / g.cm^{-3}	1.550	1.565	1.420
Adsorption coefficient / mm^{-1}	0.854	0.837	0.703
F(000)	2352	2280	936
θ (min – max) / °	1.64 – 26.52	1.68 – 26.43	1.62 – 26.41
Reflections collected	29453	27321	12249
Independent reflections	14273	7521	4895
Data/restraints/parameters	20053/0/1191	9740/0/580	8040/1/515
Final *R* indices [$I>2\sigma(I)$]	$R_1 = 0.0631$, $wR_2 = 0.1514$	$R_1 = 0.0479$, $wR_2 = 0.1116$	$R_1 = 0.0936$, $wR_2 = 0.1475$
R indices (all data)	$R_1 = 0.0942$, $wR_2 = 0.1677$	$R_1 = 0.0687$, $wR_2 = 0.1214$	$R_1 = 0.1557$, $wR_2 = 0.1725$
Goodness-of-fit on F^2	1.035	1.032	1.006
Largest peak / e Å^{-3}	2.251	2.950	0.965

Table 3.86 Crystal data and structure refinement parameters of complexes **29**, **30a** and **38a**

Complex	**29**	**30a·2CH$_2$Cl$_2$**	**30a·2CH$_2$Cl$_2$**
Empirical formula	$C_{13}H_{12}N_2O_3SF_3Cl$	$C_{51}H_{46}N_2O_3P_2SF_3Cl_5Pd$	$C_{49}H_{47}NO_4P_2S_2F_3Cl_5Pd$
Formula weight / g.mol^{-1}	368.76	1169.55	1180.59
Temperature/ K	100(2)	100(2)	173(2)
Crystal colour and habit	orange needles	yellow prisms	yellow needles
Space group	$P2_1/c$	$P2_1/c$	$P2_12_12_1$
a / Å	11.373(4)	14.1762(9)	15.0432(9)
b / Å	7.316(3)	10.6605(7)	18.174(1)
c / Å	18.520(7)	34.249(2)	18.405(1)
α / °	90.0	90.0	90.0
β / °	94.242(6)	96.183(1)	90.0
γ / °	90.0	90.0	90.0
V (Å^3)	1536.8(10)	5145.8(6)	5032.1(5)
Z	4	4	4
$D_{calc.}$ / g.cm^{-3}	1.594	1.510	1.558
Adsorption coefficient / mm^{-1}	0.432	0.778	0.837
F(000)	752	2376	2400
θ (min – max) / °	1.80 – 26.40	1.62 – 26.40	1.57 – 26.44
Reflections collected	8412	29643	28697
Independent reflections	2712	9476	9835
Data/restraints/parameters	3121/0/209	10483/0/614	10258/0/607
Final R indices [$I>2\sigma(I)$]	$R_1 = 0.0409$, $wR_2 = 0.1071$	$R_1 = 0.0418$, $wR_2 = 0.0938$	$R_1 = 0.0460$, $wR_2 = 0.1176$
R indices (all data)	$R_1 = 0.0475$, $wR_2 = 0.1124$	$R_1 = 0.0474$, $wR_2 = 0.0966$	$R_1 = 0.0482$, $wR_2 = 0.1194$
Goodness-of-fit on F^2	1.063	1.104	1.053
Largest peak / e Å^{-3}	0.600	0.852	1.386

4 COMPLICATIONS WITH S- AND O-ATOMS IN THE SYNTHESIS OF HETEROCYLCIC CARBENE COMPLEXES

4.1 Introduction and Aims

4.1.1 Background

All the *r*NHC carbene complexes discussed so far in the dissertation contain nitrogen as a heteroatom for stabilization. Two of the precursors used (*N*-methyl-2-methoxyquinolium and *N*-methyl-4,4-dimethyl-2-(2-thienyl)oxazolinium salts, Chapter 3), however contain other heteroatoms but they do not make a contribution to the eventual carbene stabilization. Various examples of Fischer-type carbene complexes are known from the early days where atoms, such as sulphur and oxygen (*eg*. $(CO)_5M{=}C(YR)R$, M = Cr, W; R = alkyl, aryl; Y = S, O)[1] play a crucial role in the stabilisation of the carbene donor. Fewer heterocyclic carbene complexes are known which are stabilised in this manner, some of which were prepared by reacting *trans*-$[PtX(CF_3)(PR_3)_2]$ (X = H, Cl) with alcohols or thiols to produce stable carbene complexes with two oxygen or sulphur atoms, α to the carbene donor.[2]

Thiolate complexes have been used profusely due to their relevance in the design of complexes able to mimic biological functions of active centers in different metalloenzymes *eg*. nitrogenase.[3] Organotransition metal thiolate complexes, apart from their diverse structural features,[4] are also believed to be key intermediates in metal-catalysed organic transformations such as desulfurisation of organosulphur compounds and the coupling reaction of organic halides with allyl aryl sulphides to give dialkyl sulfides.[5] Thiols can be tuned both sterically and electronically and they have been widely used as auxiliary ligands.[6]

---

[1] D. J. Cardin, B. Çetinkaya and M. F. Lappert, *Chem. Rev.,* 1971, **72**, 545.
[2] R. A. Michelin, G. Facchin and R. Ros, *J. Organomet. Chem.,* 1985, **279**, C25; R. A. Michelin, R. Ros, G. Guadalupi, G. Bombieri, F. Benetollo and G. Chapuis, *Inorg. Chem.,* 1989, **28**, 840.
[3] J. D. Niemoth-Anderson, K. A. Clark, T. A. George and C. R. Ross, *J. Am. Chem. Soc.,* 2000, **122**, 3977.
[4] P. J. Blower and J. R. Dilworth, *Coord. Chem. Rev.,* 1987, **76**, 121.
[5] K. Osakada, Y. Ozawa and A. Yamamoto, *J. Chem. Soc., Dalton Trans.,* 1991, 759.
[6] O. Crespo, F. Canales, M. C. Gimeno, P. G. Jones and A. Laguna, *Organometallics,* 1999, **18**, 3142; V. D. de Castro, G. M. de Lima, A. O. Porto, H. G. L. Siebald, J. D. de Souza Filho, J. D. Ardisson, J. D. Ayala and G. Bombieri, *Polyhedron,* 2004, **23**, 63.

4.1.2 Aims

We planned to extend the synthetic study and attempt to:

1. synthesise carbene complexes with *remote* heteroatoms other than nitrogen;
2. functionalise the Cl-ligand in chosen pyridylidene complexes by replacing it with a thiolate group;
3. synthesise complexes that contain two metal centra by double oxidative substitution, while having oxygen as a possible remote heteroatom.

4.2 Results and discussion

4.2.1 Reaction of $Pd(PPh_3)_4$ with 4-bromo-dithiobenzoic acid methyl ester

We intended to synthesise a complex where the heteroatom is sulphur and situated five bonds away from the carbon donor atom and with the intention to determine if the metal carbon bond still has carbene character as in the previously prepared compound, *trans*-bromo(2-methyl-2,6-dihydroisoquinol-6-ylidene)bis(triphenylphosphine)palladium(II) triflate with a remote nitrogen heteroatom.[7] The chosen ligand, 4-bromo-dithiobenzoic acid methyl ester, was reacted with $Pd(PPh_3)_4$ at 70 ºC. The complex, **39**, with the metal coordinated to the carbon-sulphur double bond (*vide infra*) was obtained, instead of the targeted oxidative substitution product (Scheme 4.1).

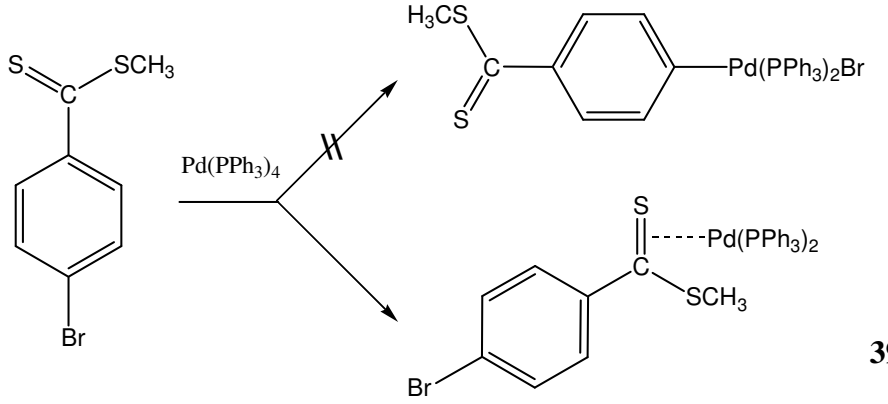

39

Scheme 4.1

In hindsight, this result is not too surprising, since various examples are known where palladium coordinates in a η^2 fashion to a C=S moiety.[8] Examples are also known where nickel[9] and

[7] O. Schuster, and H. G. Raubenheimer, *Inorg. Chem.,* 2006, **45**, 7997.
[8] K.-H. Yih, G.-H. Lee and Y. Wang, *Inorg. Chem.,* 2000, **39**, 2445.
[9] J. Campora, E. Carmona, E. Guberrez-Puebia, M. L. Poveda and C. Ruiz, *Organometallics,* 1988, **7**, 2577; C. Bianchini, C. A. Ghilardi, A. Meli, S. Midollini and A. Orlandini, *J. Chem. Soc., Chem. Commun.,* 1983, 753.

platinum[10] coordinate in a similar way. A literature search showed the tendency of Pd(0) to undergo oxidative substitution of Pd(0) in preference to η^2-coordination to the C=S functional group. However, reaction of $M(PPh_3)_4$ (M = Pt, Pd) with *N,N*-dimethylthiocarbamoyl chloride, $Me_2NC(=S)Cl$, at -20 ºC yielded the complexes $[Pt(PPh_3)_2(\eta^1\text{-}SCNMe_2)Cl]$[11]and $[Pd(PPh_3)_2(\eta^1\text{-}SCNMe_2)Cl]$, showing that the coordination product, rather than the oxidative addition product is formed. [12] The complex $[Pt(PPh_3)_2(\eta^2\text{-}SCNMe_2)][PF_6]$ [13] can be obtained by reaction of $[Pt(PPh_3)_2(\eta^1\text{-}SCNMe_2)Cl]$ with NH_4PF_6 in acetone at room temperature, whereas variable temperature NMR experiments[12] of $[Pd(PPh_3)_2(\eta^1\text{-}SCNMe_2)Cl$ (273 K) show dissociation of either the chloride or the triphenylphosphine to form the complex $[Pd(PPh_3)_2(\eta^2\text{-}SCNMe_2)][Cl]$ (best observed at 233K) or the dipalladium complex $[Pd(PPh_3)Cl]_2(\mu,\eta^2\text{-}SCNMe_2)_2$ (most predominant at 298 K).

4.2.1.1 Characterisation of η^2-$[CS(SCH_3)PhBr]Pd(PPh_3)_2$, 39

NMR spectroscopy

The chemical shifts and their assignments observed for complex **39** are listed in Table 4.1. The assignments of the chemical shifts were performed with the aid of two dimensional NMR techniques (ghsqc and ghmqc).

The signals of H^3 and H^5 are the most downfield and are masked by the phenyl protons. The chemical shifts of H^2 and H^6 appear a bit more upfield due to the thio-ester group that is less electron withdrawing than the bromine atom.

The ^1H NMR spectrum of **39** exhibits a resonance at δ 2.31 assignable to the methyl protons and the corresponding ^{13}C NMR signal appears at δ 19.6. These shifts are comparable to those observed for $(Ph_3P)Pd[\mu\text{-}\eta^1\text{-}\eta^2\text{-}(CS_2Me)PPh_2]_2$[13] at δ 2.18 and δ 19.7 respectively. The C=S resonance is however much more upfield in complex **39** (δ 148.9) compared to $(Ph_3P)Pd[\mu\text{-}\eta^1\text{-}\eta^2\text{-}(CS_2Me)PPh_2]_2$ (δ 198.1), most probably due to the anisotropic effect of the phenyl group attached to the thioketone carbon.

[10] W. Weigand, R. Wunsch, C. Robl, G. Mioston, H. Noth and M. Schmidt, *Z. Naturforsch., B Chem. Sci.,* 2000, **55**, 453; W.S. Carr, R. Colton and D. Dakternieks, *Inorg. Chem.,* 1984, **23**, 720.
[11] C. R. Green and R. J. Angelici, *Inorg. Chem.,* 1972, **11**, 2095.
[12] K.-H. Yih, G.-H. Lee and Y. Wang, *Inorg. Chem. Commun.,* 2003, **6**, 577.
[13] K.-H. Yih, G.-H. Lee and Y. Wang, *J. Chin. Chem. Soc.,* 2004, **51**, 31.

Table 4.1 ^{1}H, ^{13}C and ^{31}P NMR data of complex **39** in CD_2Cl_2

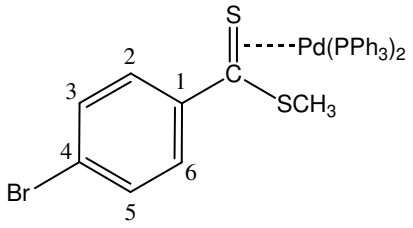

	δ / ppm*
^{1}H NMR	
SMe	2.31 (3H, s)
H^2, H^6	6.98 (2H, d, ^{3}J = 8.8 Hz)
Ph, H^3, H^5	7.23 (20H, m)
Ph	7.06 (12H, m)
^{13}C NMR	
SMe	19.6 (s)
C^2, C^6	129.8 (d, $^{4}J_{C\text{-}P}$ = 8.6 Hz)
Ph^{meta}, H^3, H^5	128.4 (m)
C^4	144.7 (s)
C=S	148.9 (s)
Ph^{ipso}	n.o.
Ph^{ortho}	134.4 (m)
Ph^{para}	132.2 (s)
^{31}P NMR	
PPh_3	26.0 (d, $^{2}J_{P\text{-}P}$ = 23.6 Hz); 25.1 (d, $^{2}J_{P\text{-}P}$ = 23.6 Hz)

The ^{31}P NMR spectrum of complex **39** contains two doublets at 26.0 and 25.1 ppm (with a P-P coupling constant of 23.6 Hz), showing the inequivalence of each phosphine ligand and are in favour of a *cis* geometry for the phosphines on the Pd-atom.

Mass spectrometry

The FAB-MS data for compound **39** are summarised in Table 4.2.

Table 4.2 FAB-MS data of complex **39**

m/z	Relative intensity	Fragment ion
830.6	24	$[M\text{-}SMe]^+$
629.7	35	$[Pd(PPh_3)_2]^+$
568.7	38	$[M\text{-}SMe\text{-}PPh_3]^+$
339.0	13	$[M\text{-}SMe\text{-}2PPh_3]^+$

The positive molecular ion is not observed, but the ion due to the loss of a SMe-group. This is followed by peaks originating from the consecutive loss of two PPh_3 ligands. The theoretical isotopic distribution of the sample compares very well to that observed experimentally.

4.2.1.2 Crystal and molecular structure of η^2-[CS(SCH$_3$)PhBr]Pd(PPh$_3$)$_2$, 39

Complex **39** was also characterised by an X-ray diffraction analysis. Its POV-Ray diagram with atom labelling is shown in Figure 4.1. Table 4.3 contains selected bond distances and angles.

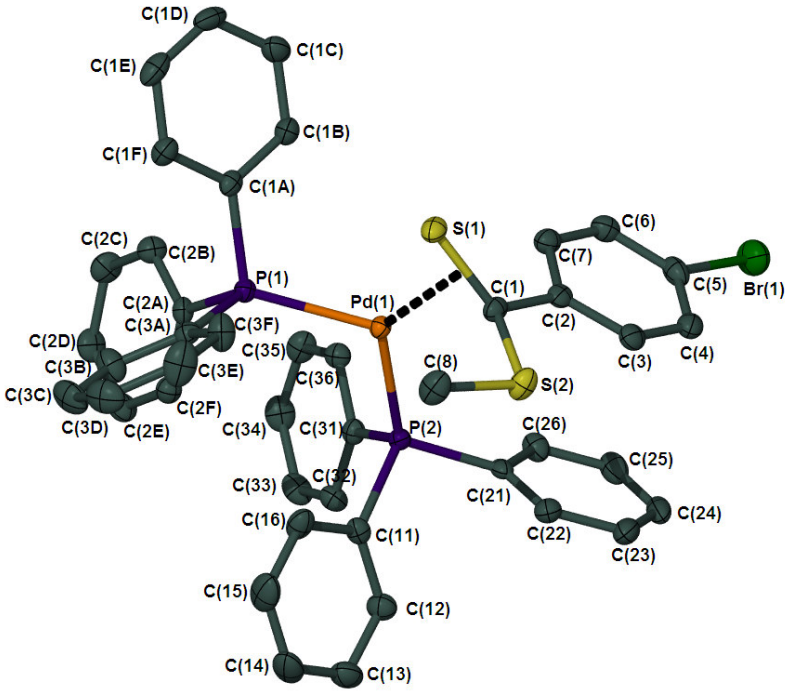

Figure 4.1 Molecular structure of **39**, showing the numbering scheme, generated in POV-Ray; H-atoms and CH_2Cl_2 solvent molecule omitted for clarity.

The most remarkable feature of the whole structure is the η^2-bonding of the C=S moiety in the 4-bromo-dithiobenzoic acid methyl ester ligand to the Pd-atom. The Pd atom and its neighbouring atoms, P(1), P(2), S(1) and C(1), lie in a distorted square plane, the distortion being mainly due to the short bite of the C=S linkage [C(1)-Pd(1)-S(1) = 46.15(9) °]. The S(1)-C(1) bond length of 1.746(3) Å is longer than the corresponding carbon-sulphur bond distances observed in η^2-CS_2 (sp^2) transition metal complexes [1.65(3) Å in [$(PPh_3)_2Pd(\eta^2$-$CS_2)$], [14] 1.674(6) Å in $(PPh_3)Pt(\mu^2$-$CS_2)_2Pt(PPh_3)$[15]]. The C-S distance is also longer than those in free CS_2 (1.554 Å), indicating coordination of the C=S in a η^2-fashion, which reduces the bond order of the C=S bond. The

[14] T. Kashiwagi, N. Yasuoka, T. Ueki, N. Kasai, M. Kakudo, S. Takahashi and N. Hagihara, *Bull. Chem,. Soc. Jpn.,* 1968, 296.
[15] D. H. Farrar, R. R. Gukathasan and S. A. Morris, *Inorg. Chem.,* 1984, **23**, 3258.

triatomic PdCS linkage exhibits a bonding situation [C(1)-S(1) 1.746(3) Å] which is comparable to that found in molybdemum[16] [1.769(2) Å] and vanadium[17] [1.762(4) Å] η^2-thioketone compounds.

Table 4.3 Bond lengths (Å) and angles (º) of complex **39**

Bond lengths (Å)			
Pd(1)-C(1)	2.134(3)	C(1)-C(2)	1.492(5)
Pd(1)-S(1)	2.3033(9)	C(2)-C(3)	1.388(5)
Pd(1)-P(2)	2.3063(8)	C(2)-C(7)	1.418(5)
Pd(1)-P(1)	2.3490(8)	C(3)-C(4)	1.385(5)
Br(1)-C(5)	1.902)(3)	C(4)-C(5)	1.379(5)
S(1)-C(1)	1.746(3)	C(5)-C(6)	1.384(5)
S(2)-C(8)	1.795(4)	C(6)-C(7)	1.381(5)
S(2)-C(1)	1.808(3)		
Bond angles (º)			
C(1)-Pd(1)-S(1)	46.15(9)	S(1)-C(1)-S(2)	119.1(2)
C(1)-Pd(1)-P(2)	148.70(3)	C(2)-C(1)-Pd(1)	113.5(2)
S(1)-Pd(1)-P(2)	148.45(9)	S(1)-C(1)-Pd(1)	72.1(1)
C(1)-Pd(1)-P(1)	102.73(3)	S(2)-C(1)-Pd(1)	114.3(2)
S(1)-Pd(1)-P(1)	108.54(3)	C(3)-C(2)-C(7)	117.5(3)
P(2)-Pd(1)-P(1)	61.8(1)	C(3)-C(2)-C(1)	122.9(3)
C(1)-S(1)-Pd(1)	101.8(2)	C(7)-C(2)-C(1)	119.6(3)
C(8)-S(2)-C(1)	102.4(2)	C(5)-C(4)-C(3)	118.8(3)
C(1A)-P(1)-Pd(1)	112.0(1)	C(4)-C(5)-C(6)	121.7(3)
C(2A)-P(1)-Pd(1)	122.8(1)	C(4)-C(5)-Br(1)	119.3(3)
C(3A)-P(1)-Pd(1)	111.5(1)	C(6)-C(5)-Br(1)	119.0(3)
C(31)-P(2)-Pd(1)	113.4(1)	C(7)-C(6)-C(5)	118.9(3)
C(11)-P(2)-Pd(1)	113.7(1)	C(6)-C(7)-C(2)	12)1.2(3)
C(21)-P(2)-Pd(1)	118.8(1)	C(2)-C(1)-S(2)	112.0(2)
C(2)-C(1)-S(1)	119.8(2)		

The Pd(1)-C(1) bond length of 2.134(3) Å is within the usual range of Pd-C(sp^3) σ bonds and the Pd(1)-S(1) distance, 2.3033(9) Å, is within the normal Pd-S length range (2.23 – 2.31 Å).[18] These distances are also in the range (2.145(8) and 2.278(2) Å respectively) observed for *anti*-$[(Ph_3P)_2Pd[\mu\text{-}\eta^1,\eta^2\text{-}(CS_2Me)PPh_2]W(CO)_5]$.[8] The geometry around the P atom is distorted tetrahedral with the average value of Pd-P-C, 115.4°.

The arrangement of the molecules of **39** in the unit cell viewed along the a-axis is illustrated in Figure 4.2. The lattice consists of alternating layers of the $Pd(PPh_3)_2$ and solvent domains along the a-axis. The molecules are arranged in horizontal rows with the alternating rows varying by inversion. There is only one relatively short intermolecular contact [2.970 Å] observed in the unit cell of **39** between S(2) and a hydrogen atom on the CH_2Cl_2 solvent molecule.

[16] H. Alper, N. D. Silvawe, G. Birnbaum and F. Ahmed, *J. Am. Chem. Soc.,* 1979, **101**, 6582.
[17] M. Pasquali, P. Leoni, C. Floriani, A. Chiesi-Villa and G. Guastini, *Inorg. Chem.,* 1983, **22**, 841.
[18] H. L. Bozec, P. H. Dixneuf, A. J. Carty and N. Taylor, *Inorg. Chem.,* 1978, **17**, 2568.

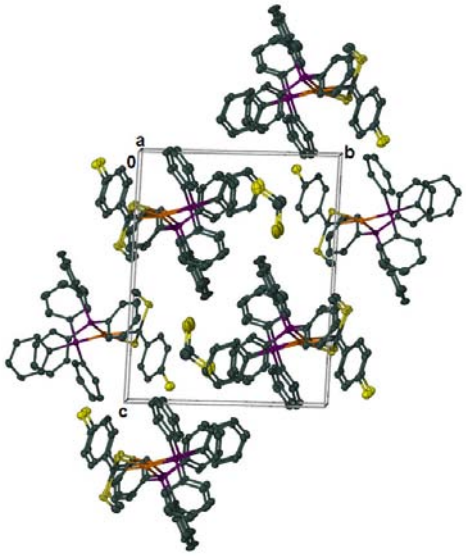

Figure 4.2 Packing diagram of the molecules of **39** viewed along the a-axis; H-atoms omitted for clarity.

4.2.2 Attempting a different route towards the oxidative substitution product

Using an alkylated precursor, it was thought that alkylation prior to reaction with $Pd(PPh_3)_4$ might lead to the oxidative substitution product at C4 with possible carbenic character, since the double bond character between the carbon and sulphur would be diminished. It was attempted to alkylate the sulphur atom with $[Me_3O][BF_4]$ and subsequently reacted the product was with $Pd(PPh_3)_4$. Only di-μ-methylthio-bis[bis(triphenylphosphine-*P*)palladium(II) bis(tetrafluoroborate) (**40** in Scheme 4.2), was isolated as a by-product in very low yield with significant decomposition.

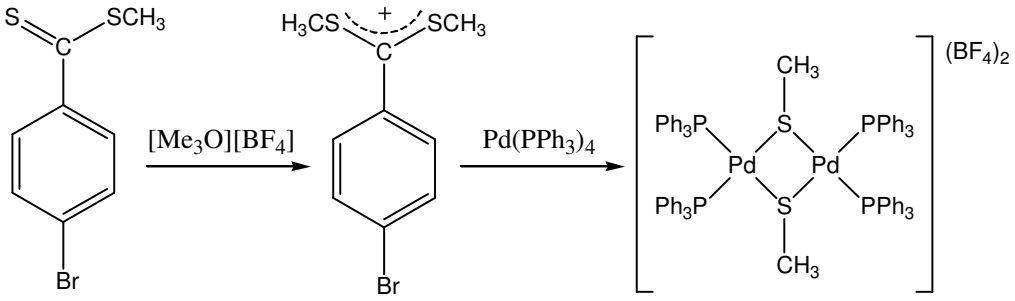

40

Scheme 4.2

Even when this reaction was carried out at room temperature instead of 60 °C, the same products were found. The intermediate might be very unstable and easily loses a SMe^+ group to react with palladium and lead to bridge formation. A similar complex to **40**, namely $[Pt_2(\mu\text{-}SCH_3)_2(PPh_3)_4](PF_6)_2$, has recently been prepared as the first complex obtained by double-

alkylation of $[Pt_2(\mu\text{-}S)_2(PPh_3)_4]$ with dimethyl sulphate.[19] This latter method is a simple solution to a long-standing problem of preparing thiolato substrates such as $Pt_2(\mu\text{-}SR)_2(PPh_3)_4$ which are generally prepared from the repulsively smelling thiols RSH or their respective salts.[20] Complexes of this type with the central metal being Rh have been prepared from the reaction between $(PR_3)_3RhCl$ and the potassium salt of 4-mercaptobenzoic acid and the reaction of allylic aryl sulphides with $RhH(PPh_3)_4$.[21] The complex, $[Pt_2(C_6H_5S)_2(C_6H_{15}P)_4](PF_6)_2$, on the other hand, can be synthesised by the reaction of the cationic hydride complex, *trans*-$[PtH(MeOH)(PEt_3)_4](PF_6)_2$, with $PhSC{\equiv}CSiMe_3$.[22]For Pd as central metal, S-bridged complexes of the type $[Pd(SPh)PPh_3Cl]_2$ have been previously synthesised by reacting polymeric $[Pd(SPh)Cl]_n$ (made by reaction of $Na_2[PdCl_4]$ with diphenyl disulfide in methanol) with a neutral ligand *eg.* PPh_3.[23] Palladium (II) has a great tendency to form thiolato-bridged complexes which are usually very resistant to cleavage by reactions with neutral ligands.[24] Amidst the large array of $[Pt_2S_2]$-based complexes and aggregates known, there are very few doubly bridge thiolato complexes with an R-group on the S-atom and even fewer Pd-containing ones.

4.2.2.1 Physical characterisation of di-μ-methylthiobis[bis(triphenylphosphine-*P*) palladium(II)] bis(tetrafluoroborate), 40

NMR Spectroscopy

The NMR data collected for complex **40** are shown in the following table. All the chemical shifts of the phenyl ligands are in the range expected when bonded to palladium. The chemical shift of SCH_3 in the ^{13}C NMR at δ 22.4 is very similar to that of δ 21.9 observed for μ-methylsulphido-μ-sulphidotetrakis(triphenylphosphine)diplatinum(II) iodide.[25]

The $^{31}P\{^1H\}$ NMR spectrum of **40**, consistent with the symmetrical nature of the molecule, displays a singlet at δ 31.5.

[19] S. H. Chong, W. Henderson and T. S. A. Hor, *Dalton Trans.,* 2007, 4008.
[20] A. Singhal, V. K. Jain, B. Varghese and E. R. T. Tiekink, *Inorg. Chim. Acta,* 1999, **285**, 190.
[21] K. Osakada, K. Matsumoto, T. Yamamoto and A. Yamamoto, *Organometallics,* 1985, **4**, 857.
[22] C. Bruhn, S. Becke and D. Steinborn, *Acta Cryst.C,* 1998, 1102.
[23] T. Boschi, B. Crociani, L. Toniolo and U. Belluco, *Inorg. Chem.,* 1970, **9**, 533.
[24] L. F. Lindoy, *Coord. Chem. Rev.,* 1969, **4**, 41.
[25] C. E. Briant, C. J. Gardner, T. S. A. Nor, N. D. Howells and D. M. P. Mingos, *J. Chem. Soc., Dalton Trans.,* 1984, 2645.

Table 4.4 ^{1}H, ^{13}C and ^{31}P NMR data of complex **40** in CD_2Cl_2

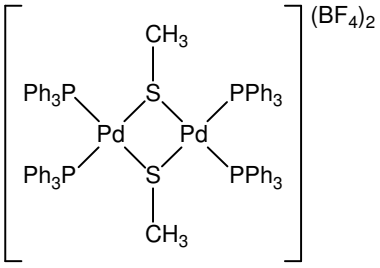

	δ / ppm*
^{1}H NMR	
SMe	2.57 (3H, s)
Ph	7.29 (30H, m)
^{13}C NMR	
SMe	22.4 (s)
Ph^{ipso}	129.2 (d, $^{1}J_{C\text{-}P}$ = 61.2 Hz)
Ph^{ortho}	134.8 (bs)
Ph^{meta}	129.8 (bs)
Ph^{para}	132.6 (s)
^{31}P NMR	
PPh_3	31.5 (s)

Mass spectrometry

The FAB-MS data for complex **40** are given in Table 4.5. The cation of the molecular ion is not observed. The peak with the highest *m/z* (1341.1) can be attributed to the loss of a methyl group, followed by fragments originating from the loss of a methyl and/or PPh_3 groups. The fragment, $[Pd(PPh_3)(PPh)SMe_2]^+$, has the highest intensity (70%) of all the peaks.

Table 4.5 FAB-MS data of complex **40**

m/z	Relative intensity	Fragment ion
1341.1	10	$[M\text{-}2BF_4\text{-}Me]^+$
1171.9	15	$[M\text{-}2BF_4\text{-}2Me\text{-}2Ph]^+$
1112.8	24	$[M\text{-}2BF_4\text{-}Me\text{-}3Ph]^+$
1092.8	26	$[M\text{-}2BF_4\text{-}PPh_3]^+$
830.7	54	$[M\text{-}2BF_4\text{-}2PPh_3]^+$
629.8	41	$[Pd(PPh_3)_2]^+$
568.7	70	$[Pd(PPh_3)(PPh)SMe_2]^+$

4.2.2.2 Crystal and molecular structure of di-μ-methylthiobis[bis(triphenylphosphine)-palladium(II)] bis(tetrafluoroborate), 40

The complex crystallises as discrete cations and anions with no unusual contacts between them. The unit cell contains one formula unit. A view of the dinuclear cation $[Pd_2(MeS)_2(C_6H_{15}P)_4]^{2+}$ is shown in Figure 4.3 and selected bond distances and angles are depicted in Table 4.6.

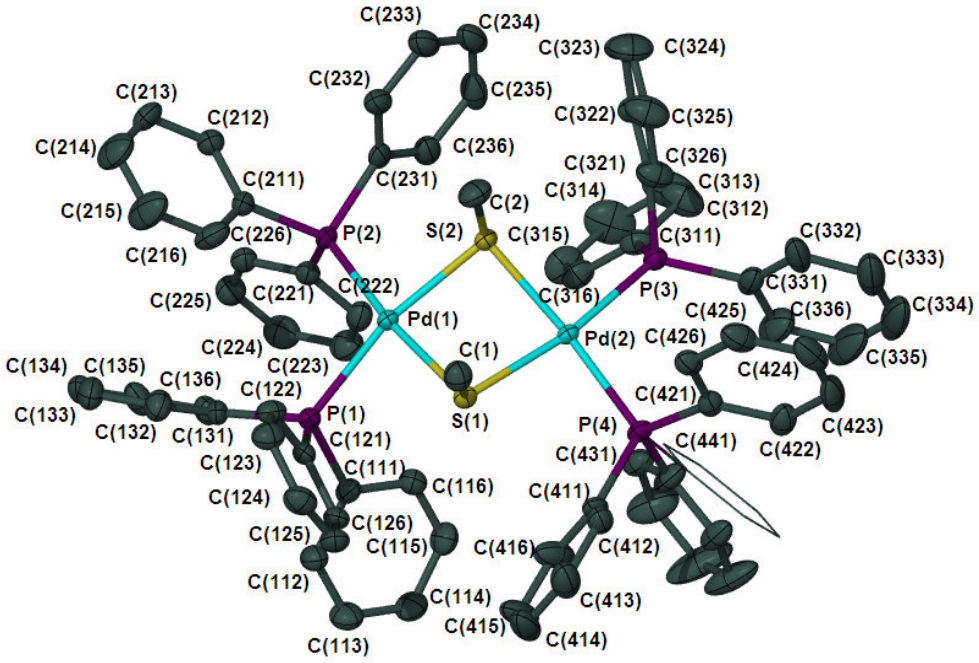

Figure 4.3 Molecular structure of **40**, showing the numbering scheme, generated in POV-Ray; H-atoms and two BF_4^- molecules omitted for clarity; one of the phenyl rings is disordered and showed as a line diagram.

The Pd atoms are hinged square-planar coordinated by two phosphine ligands and two bridging methylthio ligands. The central Pd_2S_2 ring has a distorted rhombic structure with angles S(1)-Pd(1)-S(2) 83.05(3) °, S(1)-Pd(2)-S(1) 83.16(3) °, Pd(1)-S(1)-Pd(2) 93.11(3) ° and Pd(1)-S(2)-Pd(1) 92.45(3)°. The S-S distance is 3.132 Å and lies in the narrow range observed for previous sulphur brigded complexes.[25] The Pd-Pd distance is 3.419 Å, which is slightly longer than the van der Waals distance for Pd and excludes any metal-metal interaction.

Complex **40** may exhibit two different steric configurations:[19] a planar one with all P, Pd and S atoms lying in the same plane (highest symmetry possible D_{2h}) and a nonplanar one in which the Pd and S ring is bent along the line connecting the sulphur atoms (highest symmetry possible C_{2v}). The latter configuration is observed.

Table 4.6 Bond lengths (Å) and angles (º) of complex **40**

Bond lengths (Å)			
Pd(1)-P(2)	2.316(1)	S(1)-Pd(2)	2.357(1)
Pd(1)-S(1)	2.352(1)	Pd(2)-P(4)	2.295(1)
Pd(1)-P(1)	2.354(1)	Pd(2)-P(3)	2.333(1)
Pd(1)-S(2)	2.372(1)	Pd(2)-S(2)	2.3625(9)
S(1)-C(1)	1.771(4)	S(2)-C(2)	1.775(4)
Bond angles (º)			
P(2)-Pd(1)-S(1)	171.68(4)	S(1)-Pd(2)-S(2)	83.16(3)
P(2)-Pd(1)-P(1)	101.51(4)	C(2)-S(2)-Pd(2)	108.3(2)
S(1)-Pd(1)-P(1)	85.13(3)	C(2)-S(2)-Pd(1)	105.5(2)
P(2)-Pd(1)-S(2)	89.93(3)	Pd(2)-S(2)-Pd(1)	92.45(3)
S(1)-Pd(1)-S(2)	83.05(3)	C(431)-P(4)-C(421)	113.7(3)
P(1)-Pd(1)-S(2)	167.47(3)	C(431)-P(4)-C(411)	96.2(3)
C(1)-S(1)-Pd(1)	107.4(2)	C(421)-P(4)-C(411)	106.8(2)
C(1)-S(1)-Pd(2)	103.7(2)	C(431)-P(4)-C(441)	10.4(4)
Pd(1)-S(1)-Pd(2)	93.11(3)	C(421)-P(4)-C(441)	105.6(4)
P(4)-Pd(2)-P(3)	97.47(4)	C(411)-P(4)-C(441)	105.3(4)
P(4)-Pd(2)-S(1)	92.00(4)	C(431)-P(4)-Pd(2)	116.4(2)
P(3)-Pd(2)-S(1)	169.88(3)	C(421)-P(4)-Pd(2)	108.2(1)
P(4)-Pd(2)-S(2)	175.13(4)	C(411)-P(4)-Pd(2)	114.9(1)
P(3)-Pd(2)-S(2)	87.39(3)	C(441)-P(4)-Pd(2)	115.4(3)

Complexes of the general formula, $[Pd_2(\mu\text{-}SR')_2(PR_3)_4]$, with a puckered Pd_2S_2 ring, can also exist as different stereoisomers in solution, in which the thiolates occupy different positions, that is, the *syn* or *anti* conformation. In the *syn* arrangement, the thiolates can occupy the *exo* or *endo* position[26] (Scheme 4.3) In the solid state structure of complex **40** the *syn-exo* conformer is observed.

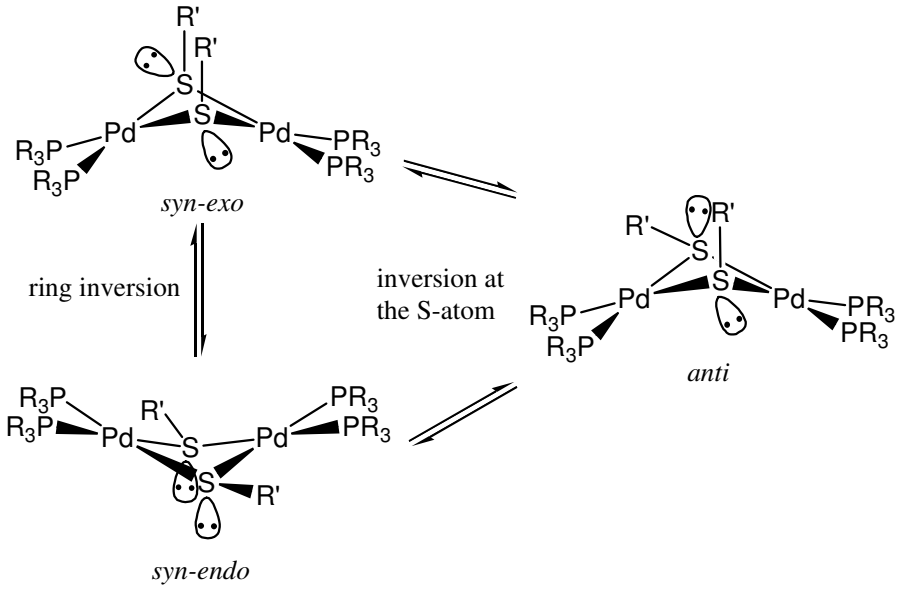

Scheme 4.3

[26] S. S. Oster and W. D. Jones, *Inorg. Chim. Acta,* 2004, **357**, 1836.

The phenyl ring of one of the PPh_3 ligands is disordered in two positions, probably influenced by the highly disordered solvent present in the crystal and two BF_4^- counter ions which could not be modelled properly. This disorder inhibits the crystal structure from having an inversion centre.

The geometry around the P atom is distorted tetrahedral with the average values of Pd-P-C 113.5 º and C-P-C 105.3 °. The disordered phenyl ring makes an angle of 10.4(4) º with the other phenyl plane.

The cations in complex **40** are stacked on top of each other forming layers diagonal to the b-axis (Figure 4.4) that alternate with diagonal layers of the BF_4^- counter ions. Every second column of cations is oriented in the same direction. There are no close spatial interactions between adjacent molecules.

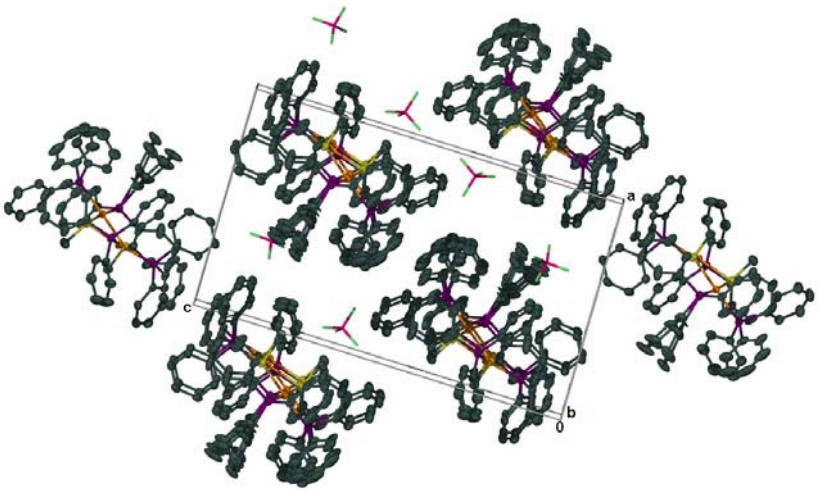

Figure 4.4 Molecular assembly of the molecules of **40** along the b-axis; H-atoms omitted for clarity.

4.2.3 An attempt to synthesise a sulphur-bridged complex that contains carbene ligands: crystal and molecular structure of *trans*-di-iodobis(1,3-dimethyl-imidazoline-2-ylidene)palladium ($PdIm_2I_2$)

The first known binuclear sulphur-bridged carbene complex (**XXXVII**) is the compound obtained from the condensation of thiolate amine chelating carbene precursors with $CODPtCl_2$ (Scheme 4.4).[27]

[27] D. Snellman, W. Prechtel, F. Knoch and M. Moll, *Inorg. Chem.,* 1993, **32**, 538.

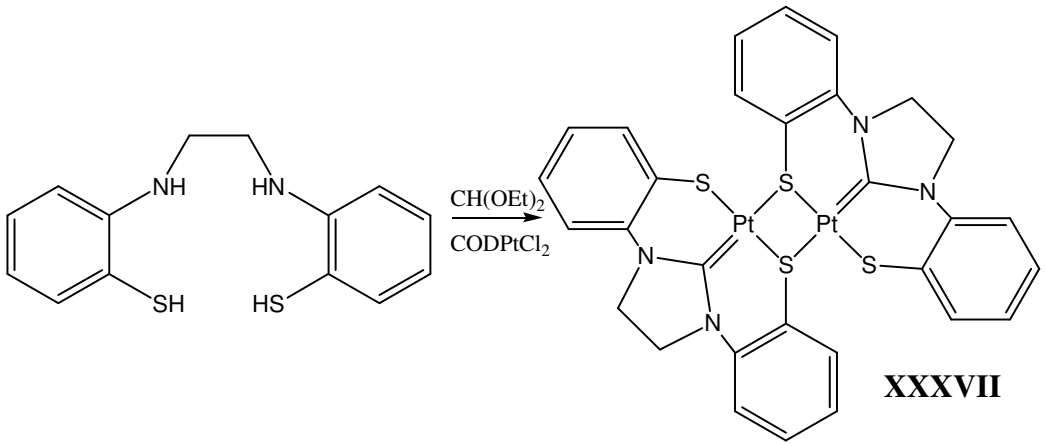

Scheme 4.4

The preparation of a similar complex, bis(μ^2-1-(2-thioethyl)-3-methyl-4-phenylimidazoline-2-ylidene-*C,S,S*)-bis(triphenylphosphine)-di-palladium(II) bis(tetrafluoroborate) [28] (**XXXVIII**), involves the oxidative substitution of the C-S bond of methyl levamisolium triflate (methylated derivative of 2,3,5,6-tetrahydro-6-(*R*)-phenylimidazo[2,1-*b*]thiazole) to Pd(dibenzylidene acetone)$_2$. This reaction represents an easy entry into complexes with chiral NHC ligands.

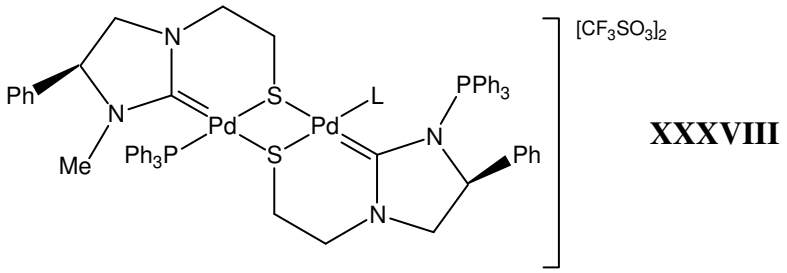

Recently, dipalladium bis(μ-isopropylthiolato) complexes with the Pd_2S_2 core solely supported by classic NHC carbenes (**XXXIX**), were reported.[29] These complexes were obtained by reacting di-iodo-bis(carbene) complexes with AgO_2CCH_3 and subsequently with NaS^iPr (Scheme 4.5).

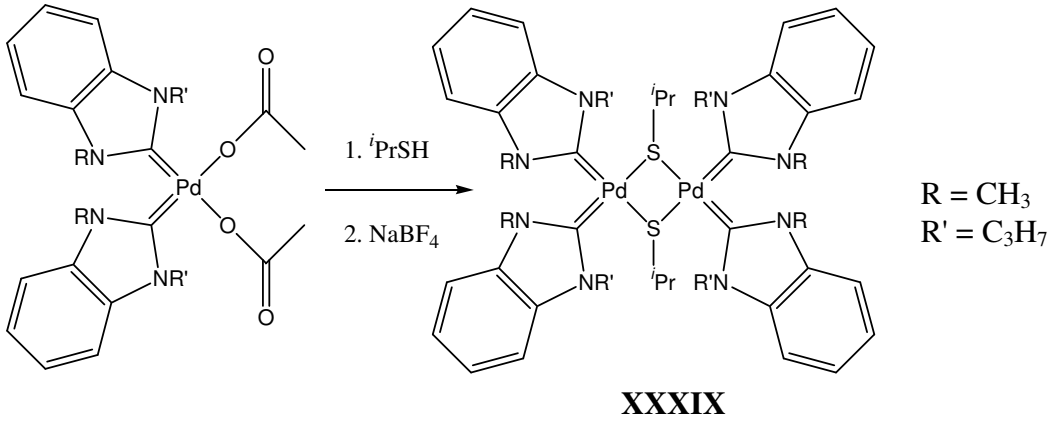

Scheme 4.5

[28] J. A. Cabeza, I. del Rio, M. G. Sanchez-Vega and M. Suarez, *Organometallics,* 2006, **25**, 1831.
[29] H. V. Huynh, R. Jothibasu and L.L. Koh, *Organometallics,* 2007, **26**, 6852.

Just before this last article was published, we endeavoured to also force the formation of such a bridge since no example bearing solely NHCs as supporting ligands was known. In our approach, we reacted di-iodobis(1,3-dimethylimidazoline-2-ylidene)palladium[30] with LiSMe in THF. Only the starting material remained when purification was attempted by crystallisation. Palladium has a very high affinity for iodide, so the reaction was repeated and $AgCF_3SO_3$ was added to assist in the removal of the iodide ligand. This again only led to the isolation of unreacted diidobis(1,3-dimethylimidazoline-2-ylidene)palladium(II) complex that crystallised from the complicated reaction mixture. Since the compound has previously been fully characterised, only the molecular structure of the *trans* isomer determined for the first time is discussed here.

The complex crystallises as yellow crystals of X-ray quality after layering a CH_2Cl_2 solution with pentane. Although the method described by Herrmann *et al.*[30] was used to synthesise *cis*-diiodobis(1,3-dimethylimidazoline-2-ylidene)palladium, the crystals obtained had the *trans* configuration (Figure 4.5) whereas Herrmann *et al.* obtained only the *cis* product. It is important to note that the *trans* complex was obtained when crystallisation was performed at -20 °C and the *cis* at room temperature. Öfele and co-workers[31] have reported a partial rearrangement of *cis* to *trans* (1:6) for di-iodobis(1,4-dimethyl-4,5-hihydro-1*H*-1,2.4-triazol-5-ylidene)palladium(II) when the complex is washed with water to separate it from the unreacted ligand. The same authors also describe a *cis/trans*-isomerisation for carbonylchlorobis(1,3-dimethylimidazoline-2-ylidene)rhodium(I). The *cis*-isomer is accessible from the free carbene and $[Rh(CO)_2Cl]_2$ in kinetically controlled reactions. Selected bond angles and distances for *trans*-di-iodobis(1,3-dimethylimidazoline-2-ylidene)palladium(II) are listed in Table 4.7

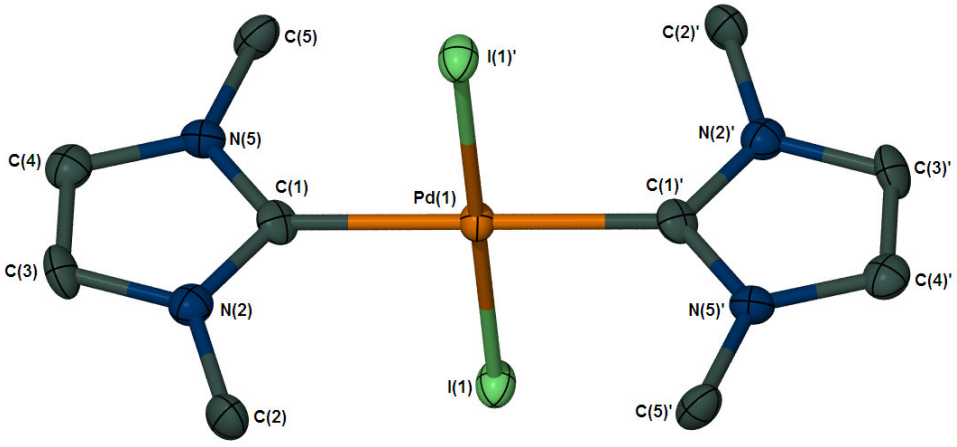

Figure 4.5 POV-Ray representation of the crystal structure of *trans*-di-iodobis(1,3-dimethyl-imidazoline-2-ylidene)palladium ($PdIm_2I_2$). The ellipsoids represent 50% probability; H atoms are omitted for clarity.

[30] W. A. Herrmann, M. Elison, J. Fischer, C. Köcher and G. R. J. Artus, *Chem. Eur. J.,* 1996, **2**, 772. W. A. Herrmann, M. Elison, J. Fischer, C. Köcher and G. R. J. Artus, *Angew. Chem.,* 1995, **34**, 2371.
[31] W. A. Herrmann, J. Fischer, K. Öfele and G. R. J. Artus, *J. Organomet. Chem.,* 1997, **530**, 259.

The compound exhibits the expected square-planar core geometry with the palladium atoms located on a crystallograhic center of inversion. The asymmetric unit contains half of the molecule.

Table 4.7 Selected bond distances (Å) and angles (º) of *trans*-di-iodobis(1,3-dimethyl-imidazoline-2-ylidene)palladium

Bond lengths(Å)			
Pd(1)-C(1)	2.030(7)	C(1)-N(2)	1.345(9)
Pd(1)-I(1)	2.6067(7)	N(2)-C(3)	1.386(9)
N(5)-C(1)	1.335(9)	C(3)-C(4)	1.35(1)
N(5)-C(4)	1.393(9)		
Bond angles (º)			
C(1)-Pd(1)-C(1)'	180.000(1)	N(5)-C(1)-Pd(1)	127.7(5)
C(1)-Pd(1)-I(1)'	90.3(2)	N(2) C(1)-Pd(1)	127.0(5)
C(1)-Pd(1)-I(1)	89.7(2)	C(1)-N(2)-C(3)	110.7(6)
C(1)-N(5)-C(4)	111.3(6)	C(1)-N(2)-C(2)	124.9(6)
C(1)-N(5)-C(5)	123.9(6)	C(3)-N(2)-C(2)	124.3(6)
C(4)-N(5)-C(5)	124.6(6)	N(5)-C(1)-N(2)	105.2(6)

Despite also having the expected square planar core geometry, $[Pd(PR_3)_2X_2]$ (X = halogen) all such complexes with monodendate phosphine ligands that have been previously characterised by crystal structure analyses only have *trans* configurations. Herrmann and co-workers[30] relate this to the greater steric demand of the phosphine ligand. In contrast to the planar carbene ligands, the phosphine ligands cannot relieve the steric congestion by rotation about the metal-ligand bond. Even though the carbene compound has a *trans* configuration, the imidazole rings are tilted in such a way as to minimise the steric interaction between the iodine atoms and substituents on the heterocycles. Comparing the two isomers, the Pd-C bond lengths for the *cis*-isomer [1.990(3) and 1.997(3) Å] and the *trans*-isomer [2.030(7) Å] all lie in the range of known carbene complexes[32] - true Pd-C single bonds [Pd-C(alkyl), Pd-C(benzyl)] are, however, hardly longer.[33] The complex *trans*-$[PdCl_2(EtMeIm)_2$ synthesised by carbene transfer from $[Ag(carbene)_2][AgBr_2]$, has a similar Pd-C bond distance than the *trans* isomer.[34]

The Pd-I distances for *cis*-Im_2PdI_2 [2.6479(3) and 2.6572(3) Å] are significantly longer than those in its *trans*-isomer [2.6067 Å]. This can be ascribed to the influence of the ligand *trans* to the I, with the carbene ligand exerting a larger *trans* influence. Due to different steric demands arising from the

[32] H. C. Clark, C. R. C. Milne, N. C. Payne, *J. Am. Chem. Soc.,* 1978, **100**, 1164.
[33] W. de Graaf, J. Boersma, W. J. J. Smeets, A. L. Spek and G. van Koten, *Organometallics,* 1989, **8**, 2907; W. A. Herrmann, C. Broßmer, K. Öfele, C.-P. Reisinger, T. Priermeier, M. Beller and H. Fischer, *Angew. Chem. Int. Ed. Engl.,* 1995, **34**, 1844.
[34] D. Li and D. Liu, *J. Chem. Cryst.,* 2003, **33**, 989.

ligand arrangement around the Pd center, angles in the *cis*-isomer are between 88.97(4) – 93.60(1) ° and between 89.7(2) – 90.3(2) ° for the *trans*-isomer.

A search performed in the CCSD database, has provided various examples of N^2HC^5 carbene complexes with a $M_2L_2X_2$ (L = NHC, M = Pd, Pt, Ni, X = Cl, Br, I) coordination sphere of which only seven contain a *trans*-$Pd(NHC)_2I_2$ backbone. In these complexes the Pd-I bond distances are 2.595 and 2.629 Å and Pd-C distances between 2.010 and 2.038 Å, showing that the new *trans*-di-iodobis(1,3-dimethyl-imidazoline-2-ylidene)palladium has very typical characteristics.

The molecules of *trans*-di-iodobis(1,3-dimethyl-imidazoline-2-ylidene)palladium are arranged in columns along the *c*-axis (Figure 4.6) with diagonal orientation on the *ab*-plane. No short distance interactions are observed between the respective molecules.

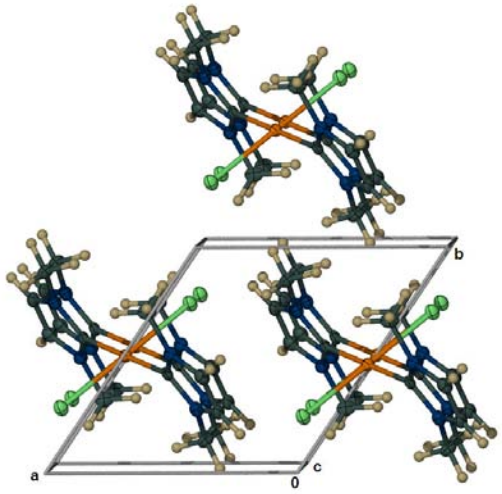

Figure 4.6 Molecular assembly of *trans*-Im_2PdI_2 along the c-axis.

4.2.4 Functionalisation of the Cl-atom in pyridylidene complexes

It is well-known that Cl-ligands in $PdCl_2$(dppe) can be displaced by LiR compounds (transmetallation reaction) to afford PdR_2(dppe) complexes, which can then be converted into mono(phenylalkyl) complexes, [PdR(SPh)(dppe)]. The latter type of complex is regarded as a key intermediate in a Heck reaction in the arylation or vinylation of olefins.[35] Cl-ligands on related metal halides can also be displaced by reaction with NaSH.[36,37]

In an attempt to functionalise the Cl ligand of *trans*-chloro-(*N*-methyl-1,2-dihydro-pyrid-2-ylidene)bis(triphenylphosphine)palladium(II) tetrafluoroborate prepared previously in our

[35] T.Spaniel, H. Schmidt, C. Wagner, K. Merzweiler and D. Steinborn, *Eur. J. Inorg. Chem.,* 2002, 2868.
[36] D. Barañano and J. F. Hartwig, *J. Am. Chem. Soc.,* 1995, **117**, 2937.
[37] M. S. Morton, R. J. Lachicotte, D. A. Vivic and W. D. Jones, *Organometallics,* 1999, **18**, 227

laboratory,[38] the thiolato complex, **41**, with two pyridine-derived carbene ligands attached (Scheme 4.6) was obtained. Although we have been unable as yet to isolate this new compound on a preparative scale, yellow crystals were picked out from a co-precipitate and were analysed by X-ray crystallography. In this manner we found a member of the NHC family (with a *normal* carbene!) that we previously attempted to prepare (Section 4.2.3).

The two pyridylidene ligands have a *trans* arrangement, similar to the thiolato-bridged complexes of Pt(II) of the general formula, $[Pt_2X_2(\mu\text{-}SR')_2(PR_3)_2]$ that have a *trans* arrangement when the R group is aromatic (but *cis* when the R group is aliphatic).[39] Chatt and co-worker have concluded that this preference is not steric at all but that due to electronic effects. No explanation was given. This theory was later corroborated by Jain *et al.*[40] who find that subtle changes in the nature of the ligand *trans* to the chalcogenide group and the nature of the R group on the RS moiety control the thermodynamically preferred configuration. For example, dimeric organochalcogenido-bridged methylpalladium complexes of the type $[Pd_2Me_2(\mu\text{-}SR')_2(PR_3)_2]$ exist as *cis* isomers or as a mixture of *cis* and *trans* forms, with the former predominating.[41]

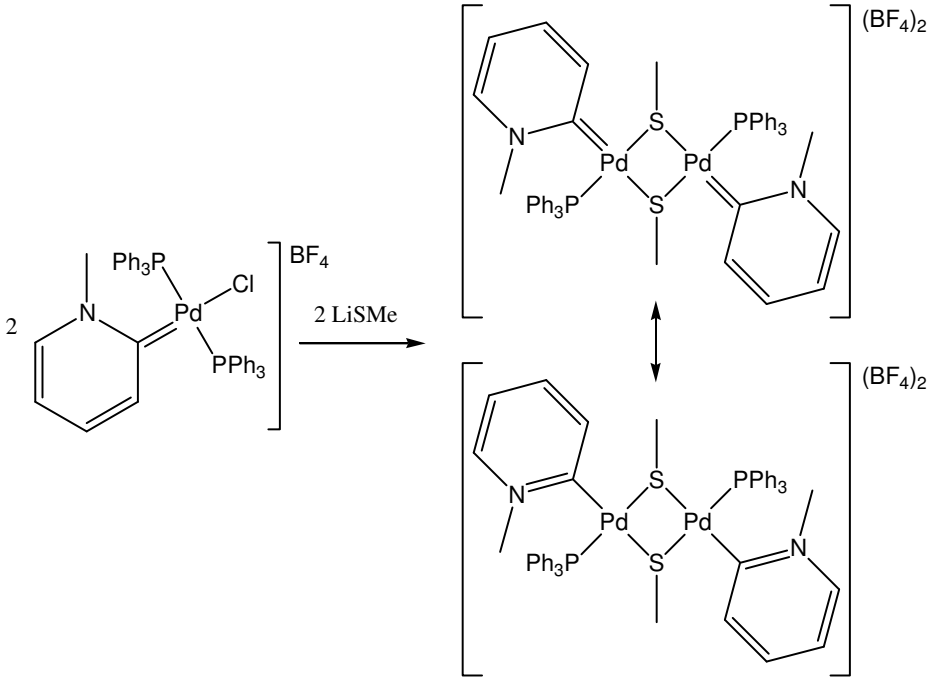

41

Scheme 4.6

Unfortunately a low yield and difficulties in separating crystalline **41** from by-products made it impossible to isolate enough analytically pure product to investigate the complex in detail. The

[38] S. K. Schneider, P. Roembke, G. R. Julius, H. G. Raubenheimer and W. A. Herrmann, *Adv. Synth. Catal.,* 2006, **348**, 1862.
[39] J. Chatt and F. A. Hart, *J. Chem.Soc.,* 1960, 2807.
[40] V. K. Kain, S. Kannan, R. J. Butcher and J. P. Jasinski, *J. Chem. Soc., Dalton Trans.,* 1991, 759.
[41] A. Ainghal and V. K. Jain, *J. Organomet. Chem.,* 1995, **494**, 75.

previously prepared dipalladium bis(μ-isopropylthiolato) complexes with the Pd_2S_2 core that contain imidazole derived carbene ligands have been isolated before.[29]

Mass spectrometric data obtained from a few crystals of complex **41** are listed in Table 4.8. Although the peak representing the cation is not observed, several distinctive fragments are evident *eg.* $[M\text{-}2BF_4\text{-}Me\text{-}PPh_3]^+$ at m/z 738.0, $[M\text{-}2BF_4\text{-}Py\text{-}Me\text{-}PPh_3]^+$ at *m/z* 662.1 and a peak at 508.9 that coincides with half of the molecular mass of the cation ($z = 2$), $[M\text{-}2BF_4]^+/2$.

Table 4.8 FAB-MS data of complex **41**

m/z	Relative intensity	Fragment ion
831.6	11	$[M\text{-}2BF_4\text{-}2Py\text{-}2Me]^+$
756.0	20	$[M\text{-}2BF_4\text{-}Ph]^+$
738.0	16	$[M\text{-}2BF_4\text{-}Me\text{-}PPh_3]^+$
662.1	18	$[M\text{-}2BF_4\text{-}Py\text{-}Me\text{-}PPh_3]^+$
508.9	14	$[M\text{-}2BF_4]^+/2$
262.2	60	$[PPh_3]^+$

An identifiable side product **42** was also observed by X-ray analysis (*vide infra*) of a few darker coloured crystals obtained similar to **41** (see below). Similar compounds of Pt, of the general formula $[(PtL)_3(\mu\text{-}SR)_3]Cl$,[42] have recently been reported and described as trinuclear 44 cve (cluster valence electrons) clusters. Related clusters may contain bridging ligands like CO in $[\{Pt(PR_3)\}_3(\mu\text{-}CO)_3]$[43] and SO_2 in $[\{Pt(PR_3)\}_3(\mu\text{-}SO_2)_3]$.[44] Theoretical studies, using the quantum theory of atoms in molecules, revealed that such complexes (R = Me, Et, Pr) have to be regarded as triangular platinum clusters with Pt-Pt bonds. The triangular M_3 unit represents the smallest cluster of all and can be regarded as the smallest representation of metal surfaces or crystallites. The M_3 clusters may build a bridge between molecular chemistry, solid state chemistry, and nano science and, therefore, the electronic situation and structural variety of triangular clusters - especially of the late transition metal clusters - are of major and fundamental importance. Indications are that dinuclear complexes (such as **41**) may be intermediates in the formation of triangular clusters.[42]

[42] C. Albrecht, S. Schwieger, C. Bruhn, C. Wagner, R. Kluge, H. Schmidt and D. Steinborn, *J. Am. Chem. Soc.,* 2007, **129**, 4551.
[43] A. Moor, P. S. Pregosin and L. M. Venanzi, *Inorg. Chim. Acta,* 1981, **48**, 153.
[44] R. Ros, A. Tassan, G. Laurenczy and R. Roulet, *Inorg. Chim. Acta,* 2000, **303**, 94.

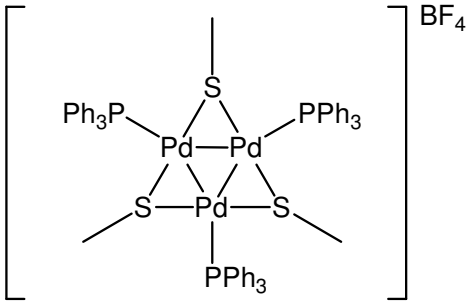

42

4.2.4.1 Molecular structures of complexes 41 and tris-[(μ²-methylthiolato)-(triphenylphosphine)palladium] tris(tetrafluoroborate), 42

Selected bond distances and angles of complex **41** are presented in Table 4.9. Figure 4.7 shows the POV-Ray drawing with atom labelling. Because of the marginal precision of the crystal structure of **41**, only the undeniably clear features that are apparent will be discussed.

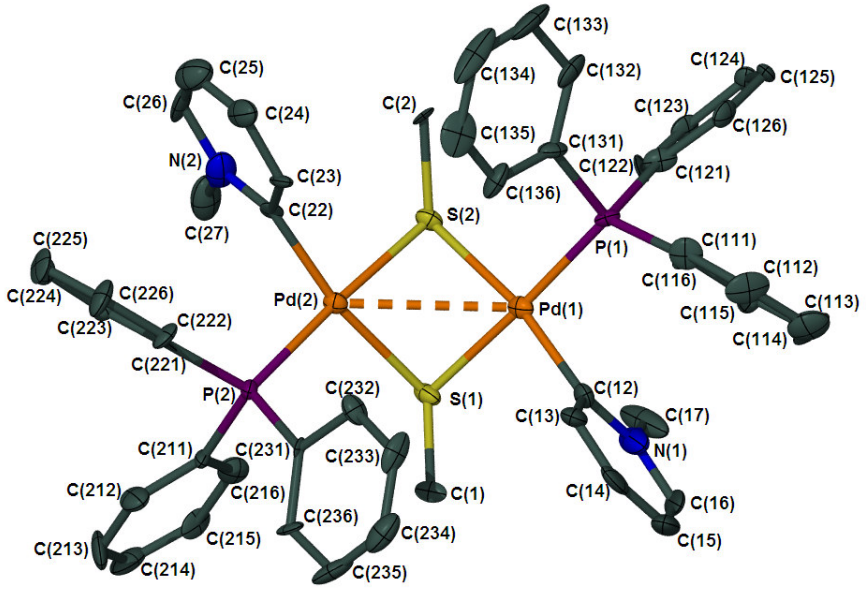

Figure 4.7 Molecular structure of complex **41**, also illustrating the atom numbering scheme; counterions and hydrogen atoms are omitted for clarity.

After establishing the connectivity within **41**, additional diffuse electron density which belongs to one of the two co-crystallised BF_4^- counter-ions was located on the difference map and was removed by using the Squeeze routine in the Platon programme package.[45]

Considering the arrangement of the thiolates in the puckered Pd_2S_2 ring of complex **41**, the *syn-endo* conformer is observed, compared to the *syn-exo* for complex **40** (Scheme 4.3). The complex, **XXXVIII** [bis(μ²-1-(2-thioethyl)-3-methyl-4-phenylimidazolidin-2-ylidene-*C,S,S*)bis(triphenyl-

[45] A. L. Apek, *J. Appl. Crystallogr.,* 2003, **36**, 7.

phosphine)dipalladium(II) bis(tetrafluoroborate)][28] mentioned earlier, also adopts the *syn-endo* arrangement. The pyridylidene ring planes are orientated almost perpendicularly to the PdC_2S_2 coordination planes.

Table 4.9 Bond lengths (Å) and angles (º) of complex **41**

Bond lengths (Å)			
Pd(1)-C(12)	2.000(9)	C(16)-N(1)	1.36(2)
Pd(1)-P(1)	2.267(2)	C(13)-C(14)	1.38(1)
Pd(1)-S(1)	2.353(2)	C(14)-C(15)	1.38(2)
Pd(1)-S(2)	2.380(2)	N(1)-C(16)	1.46(2)
Pd(1)-Pd(2)	3.127(1)	S(1)-C(1)	1.811(8)
Pd(2)-C(21)	2.009(9)	N(2)-C(21)	1.35(1)
Pd(2)-P(2)	2.283(2)	N(2)-C(25)	1.39(2)
Pd(2)-S(2)	2.341(2)	N(2)-C(26)	1.46(1)
Pd(2)-S(1)	2.371(2)	C(21)-C(22)	1.39(1)
S(2)-C(2)	1.841(8)	C(25)-C(24)	1.36(2)
C(12)-N(1)	1.36(1)	C(23)-C(24)	1.32(1)
C(12)-C(13)	1.39(2)	C(23)-C(22)	1.39(1)
C(15)-C(14)	1.35(2)		
Bond angles (º)			
C(12)-Pd(1)-P(1)	89.8(3)	N(1)-C(12)-C(13)	116.6(9)
C(12)-Pd(1)-S(1)	93.3(3)	N(1)-C(12)-Pd(1)	122.3(7)
P(1)-Pd(1)-S(1)	176.93(8)	C(13)-C(12)-Pd(1)	120.9(7)
C(12)-Pd(1)-S(2)	170.2(3)	C(15)-C(16)-N(1)	122.7(11)
P(1)-Pd(1)-S(2)	99.78(8)	C(14)-C(13)-C(12)	121.6(10)
S(1)-Pd(1)-S(2)	77.15(8)	C(15)-C(14)-C(13)	120.3(12)
C(12)-Pd(1)-Pd(2)	123.8(3)	C(12)-N(1)-C(15)	121.5(11)
P(1)-Pd(1)-Pd(2)	129.13(6)	C(12)-N(1)-C(17)	118.3(10)
S(1)-Pd(1)-Pd(2)	48.80(5)	C(16)-N(1)-C(17)	120.2(10)
S(2)-Pd(1)-Pd(2)	47.98(6)	C(1)-S(1)-Pd(1)	111.9(3)
C(21)-Pd(2)-P(2)	90.7(2)	C(1)-S(1)-Pd(2)	116.6(3)
C(21)-Pd(2)-S(2)	92.1(2)	Pd(1)-S(1)-Pd(2)	82.89(7)
P(2)-Pd(2)-S(2)	176.83(8)	C(21)-N(2)-C(25)	121.6(9)
C(21)-Pd(2)-S(1)	169.6(2)	C(21)-N(2)-C(26)	119.1(9)
P(2)-Pd(2)-S(1)	99.57(8)	C(25)-N(2)-C(26)	119.3(9)
S(2)-Pd(2)-S(1)	77.57(8)	N(2)-C(21)-C(22)	115.7(8)
C(21)-Pd(2)-Pd(1)	123.2(2)	N(2)-C(21)-Pd(2)	122.7(7)
P(2)-Pd(2)-Pd(1)	127.93(6)	C(22)-C(21)-Pd(2)	121.4(6)
S(2)-Pd(2)-Pd(1)	49.06(6)	C(15)-C(14)-C(13)	117.2(11)
S(1)-Pd(2)-Pd(1)	48.31(6)	C(24)-C(25)-N(2)	120.9(10)
C(2)-S(2)-Pd(2)	113.8(3)	C(24)-C(23)-C(22)	119.6(10)
C(2)-S(2)-Pd(1)	119.3(3)	C(23)-C(24)-C(25)	119.6(10)
Pd(2)-S(2)-Pd(1)	82.96(7)	C(21)-C(22)-C(23)	122.6(9)

It is known that Pd-S bond lengths are very sensitive to the *trans* influence of the *trans* ligands.[46] When the thiolato-ligands are *trans* to PPh_3, the Pd-S bond lengths lie in the range of 2.341(2) to 2.353(2) Å, whereas they are between 2.371(2) and 2.380(2) Å when *trans* to the pyridine derived

[46] F. R. Hartley, *Chemistry of Palladium and Platinum,* Applied Science, London, 1973.

ligand, clearly demonstrating the smaller *trans influence* of the PPh_3 ligands. The intramolecular Pd-Pd distance of 3.1270(13) Å is much shorter than the Pd···Pd distance in the di-μ^2-isopropylthiolatotetrakis(1,3-dibenzylbenzimidazol-2-ylidene)palladium(II) [3.5026(14) Å] and di-μ^2-isopropylthiolatotetrakis(1-propyl-3-methylbenzimidazol-2-ylidene)palladium(II) [3.4423(6) Å] complexes.[29]

The Pd-C bond distances of 2.000(9) and 2.009(9) Å respectively appears slightly shorter than those reported for the carbene complex, di-μ^2-isopropylthiolatotetrakis(1,3-dibenzylbenzimidazolin-2-ylidene)palladium(II),[29] with bond distances of 2.040(11) and 2.045(11) Å. On the other hand, the Pd-C bond lengths are very similar, but at the longer end, when compared to those of the previously reported palladium(II) carbene complexes carrying either a 2-methoxy-*N*-methylquinol-4-ylidene ligand [1.986(3) Å], [47] a 2-methyl-*N*-methylquinol-4-ylidene ligand [1.986(2) Å][38] or a *N*-methylquinol-4-ylidene ligand [1.999(4) Å].[48]

The molecular arrangement of complex **41** as viewed along the b-axis is portrayed in Figure 4.8. The cations are stacked on top of one another in columns along the b-axis with all the corresponding atoms aligned. Since one of the counter-ions has been removed by using the Squeeze routine, only one of the counter-ions is observed in the spaces in-between the cations.

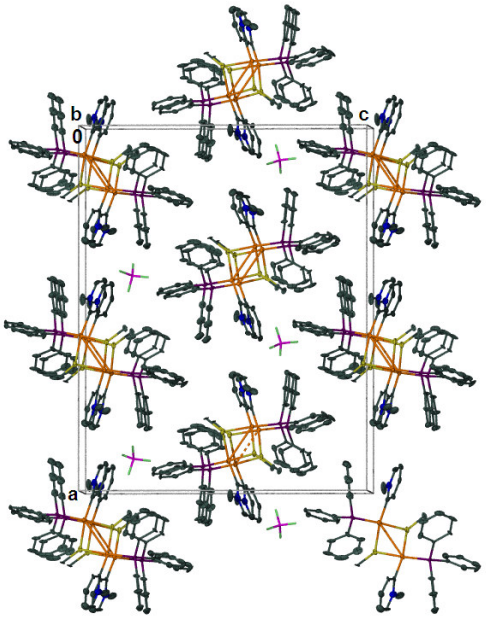

Figure 4.8 Molecular assembly of complex **41** as viewed along the b-axis.

Selected bond distances and angles of complex **42** are listed in Table 4.9. Figure 4.9 show the POV-Ray drawing with atom labelling.

[47] W. H. Meyer, M. Deetlefs, M. Pohlmann, R. Scholz, M. W. Esterhuysen, G. R. Julius and H. G. Raubenheimer, *Dalton Trans.,* 2004, 413.
[48] A. Krüger, *MSc Thesis,* University of Stellenbosch, 2007, p. 44.

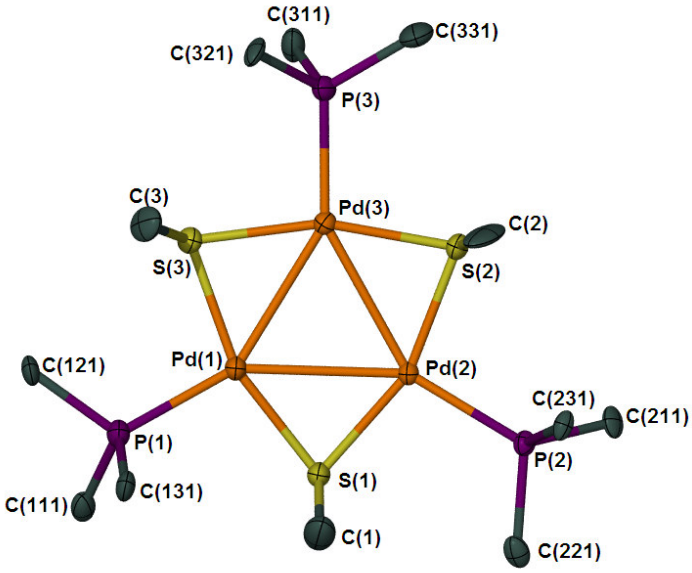

Figure 4.9 Molecular structure of the cation of compound **42** with its atom-labelling scheme; phenyl carbons, hydrogens and the counter-ion omitted are for clarity.

Table 4.10 Bond lengths (Å) and angles (º) of complex **42**

Bond lengths (Å)			
Pd(1)-P(1)	2.275(2)	Pd(2)-Pd(3)	2.8917(9)
Pd(1)-S(1)	2.276(2)	Pd(3)-S(2)	2.260(2)
Pd(1)-S(3)	2.281(2)	Pd(3)-P(3)	2.262(2)
Pd(1)-Pd(3)	2.8658(9)	Pd(3)-S(3)	2.288(2)
Pd(1)-Pd(2)	2.9002(9)	S(3)-C(3)	1.833(8)
Pd(2)-S(1)	2.281(2)	S(2)-C(2)	1.83(1)
Pd(2)-P(2)	2.285(2)	S(1)-C(1)	1.83(1)
Pd(2)-S(2)	2.289(2)		
Bond angles (º)			
P(1)-Pd(1)-S(1)	99.52(8)	S(2)-Pd(2)-Pd(1)	109.38(6)
P(1)-Pd(1)-S(3)	99.11(8)	Pd(3)-Pd(2)-Pd(1)	59.31(2)
S(1)-Pd(1)-S(3)	161.31(8)	S(2)-Pd(3)-P(3)	100.41(8)
P(1)-Pd(1)-Pd(3)	148.47(6)	S(2)-Pd(3)-S(3)	162.45(8)
S(1)-Pd(1)-Pd(3)	110.68(6)	P(3)-Pd(3)-S(3)	97.09(8)
S(3)-Pd(1)-Pd(3)	51.27(5)	S(2)-Pd(3)-Pd(1)	111.45(6)
P(1)-Pd(1)-Pd(2)-	148.15(6)	P(3)-Pd(3)-Pd(1)	148.13(6)
S(1)-Pd(1)-Pd(2)-	50.55(5)	S(3)-Pd(3)-Pd(1)	51.04(5)
S(3)-Pd(1)-Pd(2)-	111.41(6)	S(2)-Pd(3)-Pd(2)	50.98(5)
Pd(3)-Pd(1)-Pd(2)	60.20(2)	P(3)-Pd(3)-Pd(2)	151.30(6)
S(1)-Pd(2)-P(2)	100.92(7)	S(3)-Pd(3)-Pd(2)	111.48(6)
S(1)-Pd(2)-S(2)	159.72(7)	Pd(1)-Pd(3)-Pd(2)	60.49(2)
P(2)-Pd(2)-S(2)	99.30(7)	C(3)-S(3)-Pd(1)	107.3(3)
S(1)-Pd(2)-Pd(3)	109.65(6)	C(3)-S(3)-Pd(3)	108.9(3)
P(2)-Pd(2)-Pd(3)	148.86(6)	Pd(1)-S(3)-Pd(3)	77.69(7)
S(2)-Pd(2)-Pd(3)	50.09(5)	C(2)-S(2)-Pd(3)	103.9(4)
S(1)-Pd(2)-Pd(1)	50.40(5)	C(2)-S(2)-Pd(2)	105.7(3)
P(2)-Pd(2)-Pd(1)	150.23(6)	Pd(3)-S(2)-Pd(2)	78.93(7)

A disordered CH_2Cl_2 solvent molecule in the structure of complex **42** was removed by using the Squeeze routine in the Platon programme package.[45] The rotating co-crystallised BF_4^- counter-ion was very difficult to model and has large displacement parameters.

The $Pd_3S_3P_3$-skeleton is essentially planar and the largest deviation from the plane amounts to 0.0688(11) Å [Pd(1)]. The arrangement of the palladium atoms approximate to an equilateral triangle [Pd-Pd-Pd, 59.31(2) – 60.49(2) °] with Pd-Pd distances between 2.8658(9) and 2.9002(9) Å. The Pd-Pd distances clearly suggest a bonding interaction when compared with the corresponding distances in the only related complex found when a search was conducted on the CCSD, tris[(μ^2-4-hydroxyphenolthiolato)(triphenylphosphine)palladium chloride dihydroxide, known to contain Pd-Pd bonds [2.884(3) – 2.889(3) Å].[49] They are also shorter than in **41**, which was obtained from the same reaction mixture. The palladium atoms in the former complex are also arranged in a almost equilateral triangle [Pd-Pd-Pd, 59.930 – 60.104 °]. The methyl groups bonded to the sulphur atoms are arranged on the same side of the Pd_3-plane in complex **42**. The molecular structure also compares well to that of the previously reported Pt triangular structure, $[\{Pt(PPh_3)\}_3(\mu\text{-}SMe)_3]$.[42].

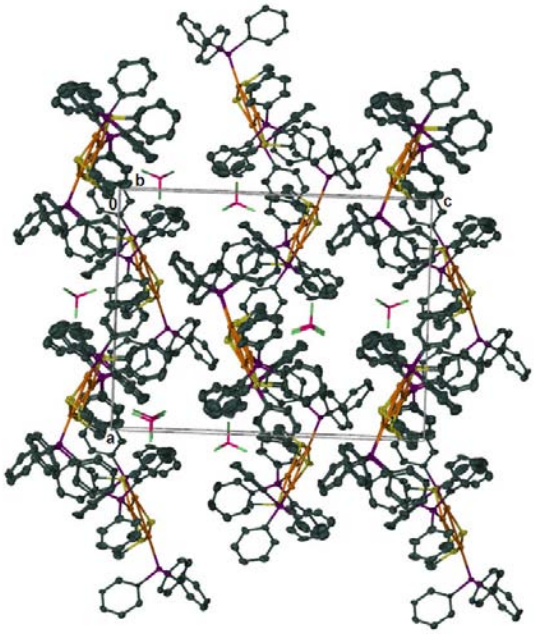

Figure 4.10 The molecular arrangement of the molecules of **42** in the unit cell, viewed along the b-axis

Figure 4.10 illustrates the arrangement of the molecules of complex **42** in the crystal lattice viewed along the b-axis. The molecules are aligned in zigzag rows parallel to the a-axis. The BF_4^- counter ions are located in the spaces amongst the cations. No short intermolecular interactions are observed between the various atoms.

[49] Z. Zhuan-Yun, L. Xing-Ming, M. Jing-Tao, Y. Yuan-Qi and H. L. Ren, *Acta Chim. Sinica,* 1996, **54**, 440.

The same reaction *i.e.* to functionalise the Cl ligand of *trans*-chloro-(*N*-methyl-1,2-dihydro-pyrid-2-ylidene)bis(triphenylphosphine)palladium(II) tetrafluoroborate, was also attempted for the *r*NHC complex, *trans*-chloro(*N*-methyl-1,4-dihydro-pyrid-4-ylidene)bis(triphenylphosphine)palladium(II) tetrafluoroborate. Although the NMR spectra (assigned by ghsqc and ghmqc), data tabulated beneath, of the few crystals obtained give a clear indication of the product formed, the FAB-MS gave no suggestion for the presence of complex **43**. The crystals obtained were not suitable for single crystal X-ray diffraction studies. Again the presence of another product, presumably complex **42**, is detected especially in the ^{31}P NMR.

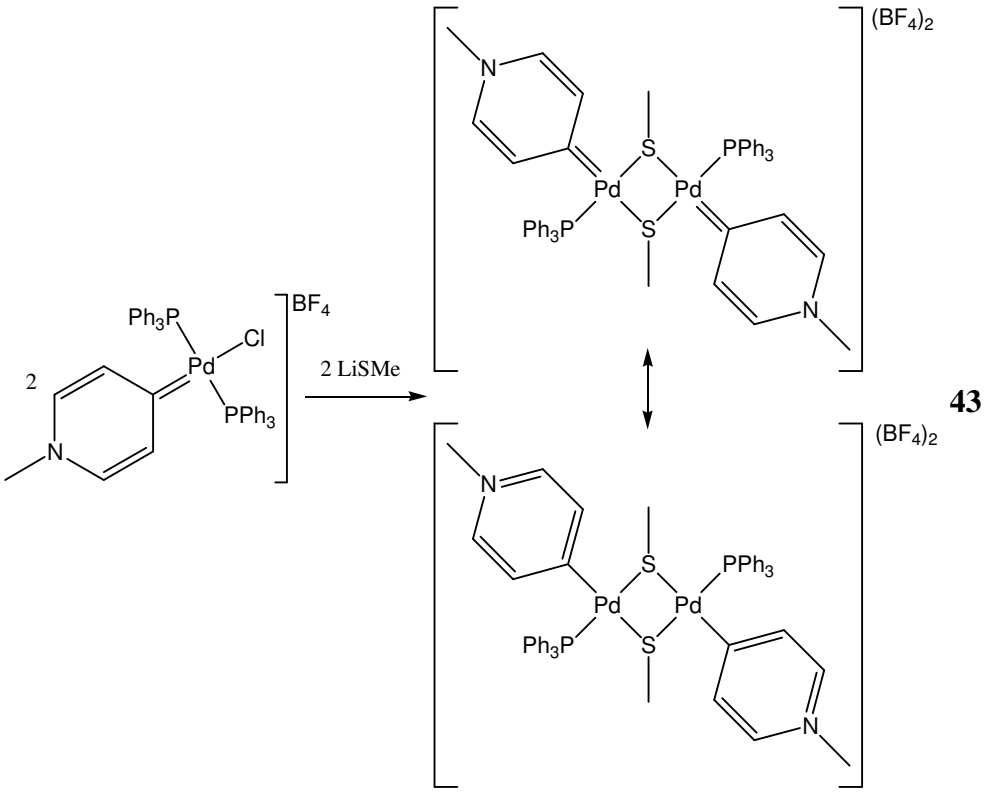

Scheme 4.7

NMR spectroscopic data (Table 4.11) for compound **43** implies that contribution from a carbene structure for this compound could be extremely low and that the palladium-carbon bond has more single bond (thus more pyridinium) than double bond character. Unfortunately FAB mass analysis gave a spectrum that could not be assigned to specific fragments of **43**.

Table 4.11 ^{1}H, ^{13}C and ^{31}P NMR data of complex **43** in CD_2Cl_2

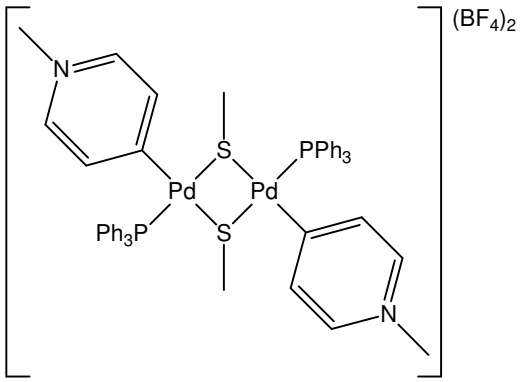

	δ / ppm*
^{1}H NMR	
SMe	2.68 (3H, s)
NMe	4.30 (3H, s)
H^2, H^6	7.67 (2H, d, ^{3}J = 6.9 Hz)
H^3, H^5	8.51 (2H, d, ^{3}J = 6.9 Hz)
Ph	7.33 (30H, m)
^{13}C NMR	
SMe	18.0 (s)
NMe	47.5 (s)
C^2, C^6	122.9 (s)
C^3, C^5	143.0 (s)
C^4	165.2 (2)
Ph^{ipso}	129.9 (bs)
Ph^{ortho}	134.1 (m)
Ph^{meta}	128.8 (m)
Ph^{para}	132.2 (s)
^{31}P NMR	
PPh_3	27.9 (s)

As expected, owing to the symmetric nature of the molecule, and the fact that the *trans*-isomer is observed in the NMR spectra, only a single set of signals is observed for the pyridylidene ligands, SMe-groups (^{1}H and ^{13}C NMR) and then of course a singlet (δ 27.9) in the ^{31}P NMR for the PPh_3 ligands.

The resonances of the protons and carbons of the pyridylidene ligand are in the same range as observed for complex **16a** in Chapter 3 (Section 3.2.4) except those of the carbon donor (C^4) that appear 32.5 ppm upfield (δ 165.2 *vs.* δ 197.7) indicative of the pyridinium character and thus the single bond character of the Pd-C bond. The complex, bis(μ^2-1-(2-thioethyl)-3-methyl-4-phenylimidazolidin-2-ylidene-*C,S,S*)-bis(triphenylphosphine)dipalladium(II) bis(tetrafluoroborate)

(**XXXIII**)[28] mentioned earlier with the same puckered $C_2P_2Pd_2S_2$ backbone, has a chemical shift of δ 195.8, clearly illustrating the carbene character of the Pd-C bond therein.

The signal observed for the SMe protons (δ 2.68) is in the same range than those in previously prepared *trans*-[$Pd_2Me_2(\mu$-$S(R')_2(PR_3)_2$] type complexes – 2.49 ppm for R' = Et and $PR_3 = PMe_2Ph$ and 2.62 ppm for R' = Et and R = PPh_3. Unfortunately the ^{13}C NMR spectrum was not reported for these complexes.[41]

4.2.5 Double oxidative substitution with oxygen as a possible remote heteroatom for carbene stabilisation

Since the investigation with sulphur as a stabilising heteroatom resulted in too many complications using the chosen precursors, the investigation was redirected to compounds with oxygen as a remote hetero-atom. For this purpose, 1,5-dichloroanthraquinone was chosen in order to attain a complex containing two Pd centra attached to carbene ligands. 1,5-Dichloroanthraquinone offers a number of possibilities as a starting material for the synthesis of more complex molecules because of the positioning of the chlorine atoms and the carbonyl groups of the central ring. Double oxidative substitution reactions with $M(PPh_3)_4$ (M = Pd, Pt, Ni) using a range of dihaloaryl organics, have been previously found by Stang and co-workers.[50]

Since alkylation of the oxygen atom with either $[Me_3O][BF_4]$ or $CF_3SO_3CH_3$ was unsuccessful, oxidative substitution was performed first, followed by attempted alkylation (Scheme 4.8).

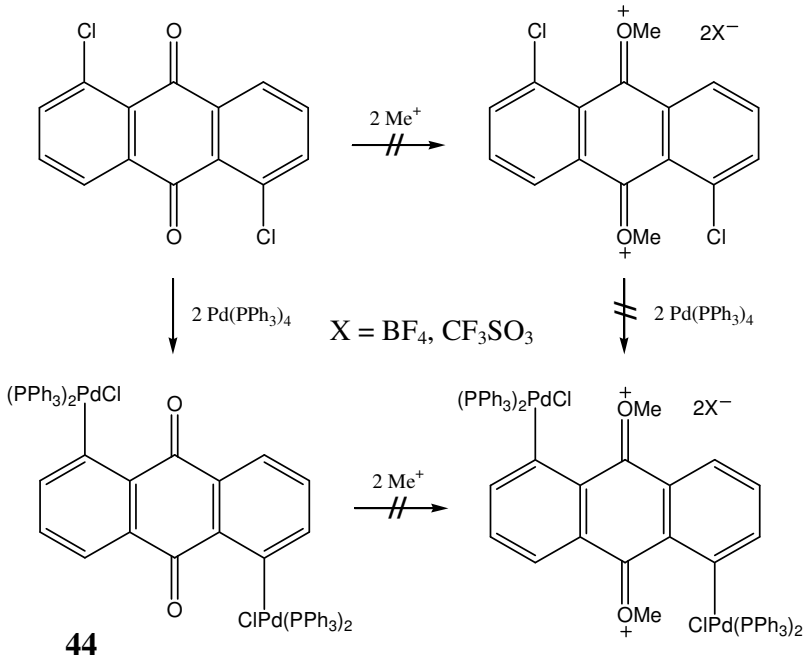

44

Scheme 4.8

[50] J. Manna, C. J. Kuehl, J. A. Whiteford and P. J. Stang, *Organometallics,* 1997, **16**, 1897.

As it turned out, the product from double substitution on two Pd centra could be isolated. Unfortunately, alkylation of the oxygen atom again failed. An attempt to replace the oxygen with sulphur, using Lawson's reagent,[51] did not succeed.

4.2.5.1 Characterisation of 1,5-*trans*-dichloro(anthraquinone)bistriphenylphosphine palladium(II), 44

NMR Spectroscopy

The NMR data (^{1}H, ^{13}C and ^{31}P) of complex **44** are depicted in Table 4.12. There are indications that the product isolated was contaminated with the mono-substituted complex (25 %).

Table 4.12 ^{1}H, ^{13}C and ^{31}P NMR data of complex **44** in CD_2Cl_2

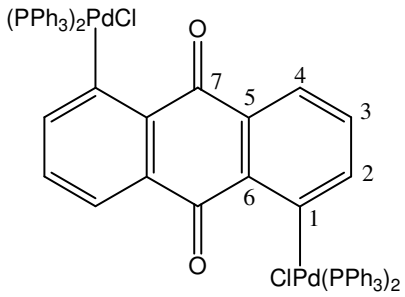

	δ / ppm*
^{1}H NMR	
H^2	8.14 (1H, dd, ^{3}J = 7.8 Hz, ^{4}J = 1.47 Hz)
H^3	7.78 (1H, dm, ^{3}J = 7.8 Hz)
H^4, Ph	7.65 (4H, m)
Ph	7.57, 7.48 (12H, 2 x m)
^{13}C NMR	
C^1	183.1 (s)
C^2	126.4 (s)
C^3	141.0 (t, $^{4}J_{C\text{-}P}$ = 4.3 Hz)
C^4	136.4 (s)
C^5	129.5 (s)
C^6	136.8 (s)
C^7	136.8 (s)
Ph^{ipso}	130.9 (t, $^{1}J_{C\text{-}P}$ = 19.6 Hz)
Ph^{ortho}	134.8 (t, $^{2}J_{C\text{-}P}$ = 6.2 Hz)
Ph^{meta}	128.2 (t, $^{3}J_{C\text{-}P}$ = 4.8 Hz)
Ph^{para}	130.2 (s)
^{31}P NMR	
PPh_3	24.1 (s)

[51] S. Scheibye, R. Shabana, S.-O. Lawesson and C. Rømming, *Tetrahedron*, 1982, **38**(7), 993.

The resonances for the PPh_3 ligands in the $^{13}C\{^1H\}$-NMR spectrum of **44** are akin to those previously reported for PPh_3-containing compounds,[38,52] as are the signals for the protons of PPh_3 and the ligand, anthraquinone in the ^1H NMR spectrum.[53]

The ^{31}P NMR spectrum of complex **44** contains a singlet at δ 24.1 showing the equivalence of all four the phosphine ligands and therefore a *trans* arrangement of the phosphine ligands around the metal centra.

Mass spectrometry

The FAB-MS data for compound **44** is summarised in Table 4.13. The fragment with the highest intensity is that of half the *m/z* of the molecular mass. Other fragments observed can be attributed to the loss of phenyl ligands, oxygen and chlorine ($[M-2Ph-O]^+$ and $[M-6Ph-2Cl]^+$).

Table 4.13 FAB-MS data of complex **44**

m/z	Relative intensity	Fragment ion
1368.8	10	$[M-2Ph-O]^+$
1055.1	11	$[M-PPh_3-2Ph-2O-Cl]^+$
1024.9	21	$[M-6Ph-2Cl]^+$
769.5	40	$[M/2]^+$

4.2.5.2 Crystal and molecular structure of 1,5-*trans*-dichloro(anthraquinone)(bistriphenyl phosphine)palladium(II), 44

The compound crystallised in the triclinic space group P-1 with one half of the molecule in the asymmetric unit. The molecule lies about a crystallographic inversion center with the corresponding atoms denoted by a prime ('). Selected bond angles and distances are listed in Table 4.14.

[52] K. Isobe, K. Nanjo, Y. Nakmura and S. Kawaguchi, *Bull. Chem. Soc. Jpn.,* 1986, **59**, 2141.
[53] E. H. Ruediger, M. L. Kaldas, S. S. Gandhi, C. Fedryna and M. S. Gibson, *J. Org. Chem.,* 1980, **45**, 1974.

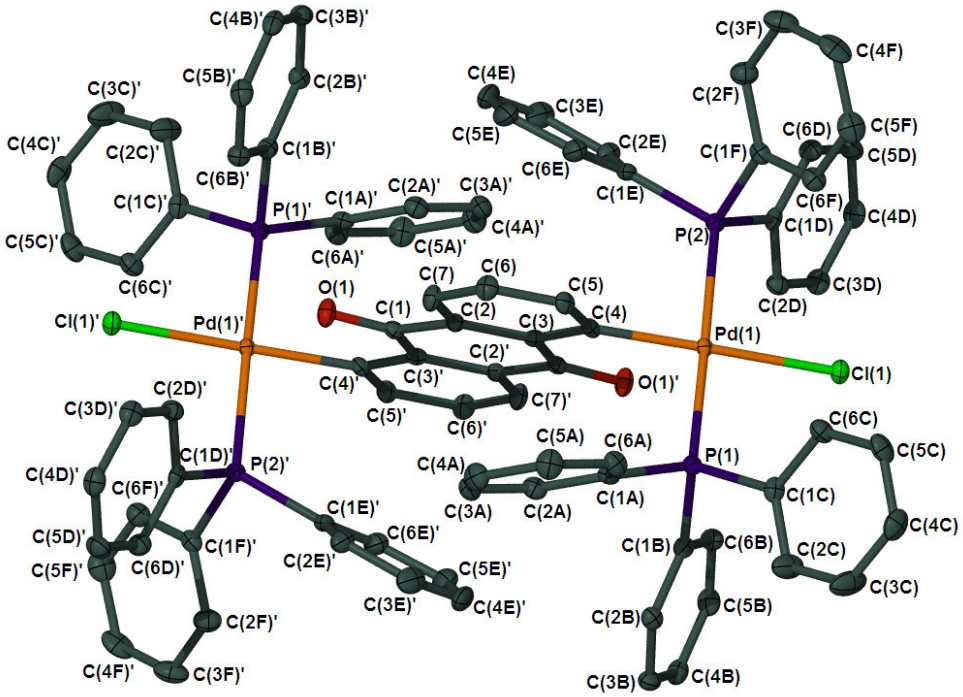

Figure 4.11 Molecular structure of complex **44**; primed and unprimed atoms are related by a centre of inversion; three CH_2Cl_2 molecules and H-atoms are omitted for clarity.

Table 4.14 Bond lengths (Å) and angles (º) of complex **44**

Bond lengths(Å)			
Pd(1)-C(4)	2.002(3)	C(6)-C(7)	1.389(4)
Pd(1)-P(1)	2.3221(7)	C(3)-C(2)	1.417(4)
Pd(1)-P(2)	2.3407(7)	C(3)-C(1)'	1.481(3)
Pd(1)-Cl(1)	2.3970(7)	C(7)-C(2)	1.384(4)
C(4)-C(5)	1.396(4)	C(2)-C(1)	1.493(3)
C(4)-C(3)	1.415(4)	O(1)-C(1)	1.224(3)
C(5)-C(6)	1.383(4)	C(1)-C(3)'	1.481(3)
Bond angles (º)			
C(4)-Pd(1)-P(1)	88.97(7)	C(4)-C(3)-C(2)	120.0(2)
C(4)-Pd(1)-P(2)	89.29(7)	C(4)-C(3)-C(1)'	121.2(2) .
P(1)-Pd(1)-P(2)	174.30(2)	C(2)-C(3)-C(1)'	118.8(2)
C(4)-Pd(1)-Cl(1)	178.81(7)	C(2)-C(7)-C(6)	120.1(2)
P(1)-Pd(1)-Cl(1)	90.92(3)	C(7)-C(2)-C(3)	120.2(2)
P(2)-Pd(1)-Cl(1)	90.93(3)	C(7)-C(2)-C(1)	117.8(2)
C(5)-C(4)-C(3)	117.4(2)	C(3)-C(2)-C(1)	122.0(2)
C(5)-C(4)-Pd(1)	119.8(2)	O(1)-C(1)-C(3)'	121.4(2)
C(3)-C(4)-Pd(1)	122.8(2)	O(1)-C(1)-C(2)	119.4(2)
C(6)-C(5)-C(4)	122.6(2)	C(3)'-C(1)-C(2)	119.2(2)
C(5)-C(6)-C(7)	119.6(2)		

A search in the CCSD database yielded no examples of an anthraquinone ligand with two metals coordinated to it. There is however one example of a monometallic complex of the metal antimony.[54]

Despite the bulk metal groups, there is very little distortion indicated about the anthraquinone O(1) – O(1)' axis and hence the extent that the carbonyl groups is out of plane with the palladium moiety (only by 3.31(18) º).

As portrayed in the POV-Ray diagram (Figure 4.11), the Pd centra display the expected square planar coordination geometry; the four *cis* angles about each palladium are essentially orthogonal [88.97(7) – 90.93(3) °]. The Pd-P bond distances of 2.3221(7) and 2.3407(7) Å are normal compared to the palladium(II) complexes containing PPh_3 ligands described in Chapter 3. The Pd(1)-C(4) bond distance of 2.002(3) Å is typical and is comparable to the Pd-C distance of 1.990(11) Å in the pyridylidene complex, *trans*-chloro(*N*-methyl-1,3-dihydro-pyrid-3-ylidene)bis(triphenylphosphine)palladium(II) triflate (**15a**) discussed in Chapter 3, Section 3.2.4.4 and the previously obtained range [1.979(7) – 2.029(9) Å] for Pd(II) N^1HC^6 complexes.[38]

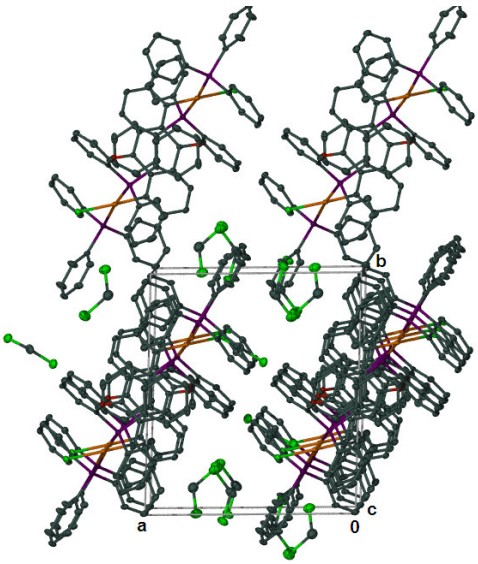

Figure 4.12 The arrangement of the molecules of **44** in the unit cell, viewed along the c-axis

The molecules of complex **44** are arranged with the anthraquinone ligands of the different layers (along the b-axis) aligned on top of each other as viewed along the c-axis (Figure 4.12). The CH_2Cl_2 solvent molecules are located in the spaces amongst the dinuclear complex molecules. No π-π intermolecular interactions, usually so significant in the molecular assemblies of organic bi- and tri-aryl compounds, are observed.

[54] D. W. Allen, S. J. Coles, M. B. Hursthouse and S. M. Khan, *Inorg. Chim. Acta,* 2004, **357**, 265.

4.3 Conclusions

In attempts to synthesise complexes with remote sulphur heteroatoms C-SR bond cleavage occurred more readily than oxidative substitution.

In efforts to synthesise a sulphur-bridged complex that contains carbene ligands, crystals of *trans*-di-iodobis(1,3-dimethyl-imidazoline-2-ylidene)palladium were obtained and crystallographically compared with *cis*-di-iodobis(1,3-dimethyl-imidazoline-2-ylidene)palladium previously reported. These complexes show similar metal-carbon bond distances. Related compounds were unexpectedly found in our attempt to substitute the halogen on pyridinium derived square planar carbene complexes of palladium. The methodology presented here widens the application possibilities of N^1HC^6 ligands in organometallic chemistry beyond that of catalysis. The trinuclear 44 cve cluster $[(PdPPh_3)_3(\mu\text{-}SMe)_3]BF_4$, was isolated as a by-product of these reactions.

Double oxidative substitution on two Pd centra was achieved with 1,5-dichloroanthraquinone. Unfortunately, alkylation of the oxygen atoms failed, and consequently the synthesis of a carbene complex containing oxygen as a remote hetero-atom. The Pd-C bond distances are typical and comparable to the Pd-C distances of previously obtained for Pd(II) N^1HC^6 complexes.

Even though most of the targeted complexes could not be obtained, crystals of interesting and even unique compounds were isolated.

4.4 Experimental

4.4.1 General

The general techniques described in Section 2.4.1 were also applied to the work in this chapter. Starting materials used in the synthesis of the ligands and complexes were purchased from commercial suppliers and used without further purification. The compounds $BrPhCS_2CH_3$, [55] $Pd(PPh_3)$, [56] Di-iodobis(1,3-dimethylimidazol-2-ylidene)palladium[30] *trans*-chloro-(*N*-methyl-1,2-dihydro-pyrid-2-ylidene)bis(triphenylphosphine) palladium(II) tetrafluoroborate and *trans*-chloro-(*N*-methyl-1,4-dihydro-pyrid-4-ylidene)-bis(triethylphosphine)palladium(II) tetrafluroborate[38] were synthesised according to literature procedures.

[55] H. D. Verkruijsse and L. Brandsma, *J. Organomet. Chem.*, 1987, **332**, 95; R. Edler and J. Voß, *Chem. Ber.,* 1989, **122**, 187.
[56] F. Ozawa, *Synthesis of Organometallic Compounds,* Ed. S. Komiya, John Wiley & Sons, Chichester, 1997, p. 286.

4.4.2 Synthetic procedures and physical data

4.4.2.1 Reaction of $BrPhCS_2CH_3$ with $Pd(PPh_3)_4$ to yield complex 39

$BrPhCS_2CH_3$ (0.253 g, 1.03 mmol) and $Pd(PPh_3)_4$ (1.18 g, 1.03 mmol) were dissolved in toluene and stirred overnight at 60 °C. The product mixture was allowed to cool down to room temperature and dried *in vacuo.* The resulting residue was dissolved in CH_2Cl_2 and absorbed unto silica which was transferred to a small filtration column of 5cm long. Unreacted ligand was washed out with hexane and complex **39** was eluated with ether/hexane (1:4) as a yellow fraction, which afforded after solvent evaporation, 0.341 g (0.388 mmol) of **39**.

Table 4.15 Physical data of compound **39**

Yield		37.7 %
Colour		Yellow
Melting point		115 °C with decomposition
Elemental analysis	% calculated for	C 60.18, H 4.25
$C_{44}H_{37}P_2S_2BrPd$	% found	C 60.40, H 4.20

4.4.2.2 The formation of $[(PPh_3)_2PdSMe]_2$, 40

$BrPhCS_2CH_3$ (0.303 g, 1.23 mmol) was alkylated with $[Me_3O][BF_4]$ (0.220 g, 1.49 mmol) by adding the latter (dissolved in CH_2Cl_2/CH_3CN mixture) dropwise to the ligand over a period of 1.5 hours. Work-up was performed as described for similar compounds in literature.[57] The "alkylated" ligand 0.072 g (0.207 mmol) and 0.239 (0.207 mmol) $Pd(PPh_3)_4$ was stirred for 22 hours at 60 °C in toluene. The solution was filtered and pentane added to afford a yellow precipitate that was filtered and dried *in vacuo*. The filtrate contained unreacted $Pd(PPh_3)_4$ and complex **39**. Dissolution of this solid and layering with pentane yielded crystals (0.080 g, 0.052 mmol) of complex **40** suitable for X-ray determinations.

Table 4.16 Physical data of compound **40**

Yield		4.2 %
Colour		Yellow
Melting point		120 °C with decomposition
Elemental analysis	% calculated	C 58.10, H 4.35
$C_{74}H_{66}B_2F_8P_4S_2Pd_2$	% found	C 57.91, H 4.22

[57] H. Boehme and G. Ahrens, *Justus Liebiegs Ann. Chem*., 1982, 1022.

4.4.2.3 An attempt to synthesise a sulphur-bridged complex that contains carbene ligands

Di-iodobis(1,3-dimethylimidazol-2-ylidene)palladium (II) (0.102 g, 0.185 mmol) and 0.020 g (0.370 mmol) LiSMe was suspended in 10 ml THF and stirred for 17 hours at room temperature. The solvent was removed *in vacuo*, the resulting residue dissolved in CH_2Cl_2 and filtered through celite. The filtrate was evaporated to dryness, redissolved in a minimum amount of CH_3CN and layered with pentane to afford yellow crystals of complex **$PdIm_2I_2$** suitable for single crystal X-ray determination.

4.4.2.4 Attempted functionalisation of the chlorine in the complex *trans*-chloro-(*N*-methyl-1,2-dihydro-pyrid-2-ylidene)bis(triphenylphosphine)palladium(II) tetrafluoroborate affording complexes 41 and 42

LiSMe was prepared by adding 3.0 ml (1.58 M, 4.74 mmol) BuLi to 0.447 g (0.42 ml, 4.74 mmol) of MeSSMe in ether. The solution was stirred for 2 hours, filtered and the precipitate washed with 2 x 20 ml ether. A suspension of LiSMe (0.007 g, 0.130 mmol) and *trans*-chloro-(*N*-methyl-1,2-dihydro-pyrid-2-ylidene)bis(triphenylphosphine)palladium(II) tetrafluoroborate in THF was stirred for 20 hours at room temperature. The solvent was removed by evaporation, the resulting residue dissolved in CH_2Cl_2, filtered and the resulting filtrate evaporated to dryness. Dissolution the solid (0.052 g) and layering with pentane afforded yellow crystals of complex **41** and a few red-orange crystals of complex **42**.

Table 4.17 Physical data of compounds **41** and **42**

Compound	**41**	**42**
Colour	Yellow	Orange-red
Melting point	210 °C with decomposition	230 °C with decomposition

4.4.2.5 Functionalisation of the chlorine in the complex *trans*-chloro-(*N*-methyl-1,4-dihydro-pyrid-4-ylidene)bis(triphenylphosphine)palladium(II) tetrafluoroborate affording complex 43

A similar procedure was followed as utilised for the synthesis of complex **41** from 0.008 g (0.148 mmol) LiSMe and 0.046 g (0.054 mmol) *trans*-chloro-(*N*-methyl-1,4-dihydro-pyrid-4-ylidene)bis(triphenylphosphine)palladium(II) tetrafluoroborate to yield a crude mixture of 0.035 g that was analysed by NMR.

4.4.2.6 Synthesis of 1,5-*trans*-dichloro(anthraquinone)bis(triphenylphosphine)palladium(II), 44

The same method as for complex **14a** (Chapter 3) was utilised for the synthesis of complex **44** from 0.004 g (0.0150 mol) 1,5-dichloroanthraquinone and 0.040 g (0.0346 mmol) $Pd(PPh_3)_4$. Instead of

60 °C, the reaction was carried out at 90 °C. Dissolution of the crude solid mixture and layering with pentane afforded orange crystals of complex **44** (0.020g, 0.0130 mmol).

Table 4.18 Physical data of compound **44**

Yield		86.6 %
Colour		Orange
Melting point		204 °C with decomposition
Elemental analysis	% calculated	C 67.11, H 4.32
$C_{86}H_{66}O_2P_4Cl_2Pd_2$	% found	C 66.90, H 4.36

4.4.3 X-ray structure determinations

Data associated with the crystal structures of complexes **39**, **40**, **Im_2PdI_2**, **41**, **42** and **44** are summarised in Tables 4.19 and 4.20. Data sets were collected and processed as described in Section 2.4.4. The structures were solved by direct methods (**40**, **42**, ***trans*-Im_2PdI_2**) or interpretation of a Patterson synthesis (**39**, **41, 44**), yielding the position of the metal atom, and conventional Fourier methods. The positions of the hydrogen atoms were calculated by assuming ideal geometry and their coordinates were refined together with those of the attached carbon atoms as "riding model" for all the complexes. While solving the structure of **40**, the phenyl ring containing C(431) was found to be disordered in two positions related by translation and populated 63 : 37. Additional diffuse electron density which belongs to co-crystallised CH_2Cl_2 solvent was located on the difference map of complexes **40** and **42**, but could not be modelled. It was removed by using the Squeeze routine in the Platon programme package.[45] One of the counter-ions (BF_4^-) of complexes **40** and **41** could not be modelled due to disorder. It was also removed using the Squeeze routine. Restraints were applied in the refinement of complexes **40** – **42** to improve the data quality. Upon application of these restraints, the bond distances and thermal parameters improved and the *R* values decreased. Additional information regarding these crystal structures is available from Prof H. G. Raubenheimer, Department of Chemistry and Polymer Science, University of Stellenbosch.

Table 4.19 Crystal data and structure refinement parameters of complexes **39**, **40** and **$PdIm_2I_2$**

Complex	**$39{\cdot}CH_2Cl_2$**	**40**	**$PdIm_2I_2$**
Empirical formula	$C_{45}H_{39}P_2S_2BrCl_2Pd$	$C_{74}H_{66}B_2F_8P_4S_2Pd_2$	$C_{10}H_{16}N_2I_2Pd$
Formula weight / g.mol^{-1}	963.03	1529.69	552.46
Temperature/ K	100(2)	100(2)	100(2)
Crystal colour and habit	Yellow blocks	orange prisms	yellow blocks
Space group	*P*-1	*P*-1	*P*-1
a / Å	10.757(1)	13.386(2)	8.039(3)
b / Å	12.367(1)	13.792(2)	8.039(3)
c / Å	15.526(2)	22.700(3)	8.133(3)
α / °	92.040(2)	86.577(2)	97.297(5)
β / °	90.174(2)	88.253(2)	115.870(4)
γ / °	93.764(2)	79.242(2)	115.488(5)
V (Å^3)	2059.7(3)	4108.9	393.6(2)
Z	2	2	1
$D_{calc.}$ / g.cm^{-3}	1.553	1.236	2.331
Adsorption coefficient / mm^{-1}	1.762	0.620	5.088
F(000)	972	1552	256
θ (min – max) / °	1.65 – 25.68	0.90 – 26.45	3.02 – 26.34
Reflections collected	15796	36573	2243
Independent reflections	6843	13031	1419
Data/restraints/parameters	7741/0/479	15783/73/862	1511/0/81
Final *R* indices [$I>2\sigma(I)$]	$R_1 = 0.0367$, $wR_2 = 0.0963$	$R_1 = 0.0494$, $wR_2 = 0.1298$	$R_1 = 0.0351$, $wR_2 = 0.0748$
R indices (all data)	$R_1 = 0.0427$, $wR_2 = 0.01002$	$R_1 = 0.0586$, $wR_2 = 0.1352$	$R_1 = 0.0398$, $wR_2 = 0.0845$
Goodness-of-fit on F^2	1.039	1.065	1.135
Largest peak / e Å^{-3}	1.189	1.964	1.239

Table 4.20 Crystal data and structure refinement parameters of complexes **41**, **42** and **44**

Complex	**41**	**42**	**44·3CH_2Cl_2**
Empirical formula	$C_{50}H_{50}BN_2P_2S_2F_4Pd_2$	$C_{57}H_{54}BF_4P_3S_3Pd_3$	$C_{46}H_{39}OP_2Cl_7Pd$
Formula weight / g.mol^{-1}	1104.59	1334.10	1024.33
Temperature/ K	100(2)	100(2)	373(2)
Crystal colour and habit	yellow blocks	red-orange blocks	orange blocks
Space group	*Pna*2$_1$	*P*2$_1$2$_1$2$_1$	*P*-1
a / Å	27.86(1)	15.962(3)	12.909(2)
b / Å	8.253(3)	18.360(3)	13.549(2)
c / Å	21.921(9)	20.720(4)	13.775(2)
α / °	90.0	90.0	82.650(2)
β / °	90.0	90.0	66.581(2)
γ / °	90.0	90.0	89.249(2)
V (Å^3)	5040(4)	6072(2)	2190.7(6)
Z	4	4	2
$D_{calc.}$ / g.cm^{-3}	1.456	1.459	1.553
Adsorption coefficient / mm^{-1}	0.910	1.107	0.960
F(000)	2236	2672	1036
θ (min – max) / °	1.46 – 26.57	1.61 – 26.41	1.63 – 26.39
Reflections collected	24767	33516	23548
Independent reflections	8815	11166	7715
Data/restraints/parameters	9785/56/573	12233/6/643	8864/0/514
Final *R* indices [$I>2\sigma(I)$]	$R_1 = 0.0696$, $wR_2 = 0.1400$	$R_1 = 0.0539$, $wR_2 = 0.1162$	$R_1 = 0.0374$, $wR_2 = 0.0900$
R indices (all data)	$R_1 = 0.0776$, $wR_2 = 0.1437$	$R_1 = 0.0621$, $wR_2 = 0.1271$	$R_1 = 0.0444$, $wR_2 = 0.0933$
Goodness-of-fit on F^2	1.123	1.125	1041
Largest peak / e Å^{-3}	1.018	1.635	1.323

5 *n*NHC and *a*NHC CARBENE COMPLEXES AS POTENTIAL CATALYST PRECURSORS

5.1 Introduction and Aims

5.1.1 Background

Although NHCs have attracted a growing interest as possible alternatives to phosphine ligands in homogeneous catalysis, the isolation of thiazolium and benzothiazolium free carbenes has been unsuccessful.[1] This can be ascribed to their particularly fast dimerization and thus instability.[2] Although chemists have struggled with their isolation, nature has been using them since the beginning of time. Breslow[3] has shown, in the context of ylidene-catalysed benzoin condensations, that the vitamin B_1 enzyme cofactor thiamin (**XL**), a naturally occurring thiazolium salt, plays a key role in biochemistry. In basic aqueous buffers the active catalyst in nature is a 2,3-dihydrothiazol-2-ylidene of the form **XLI**.

XL

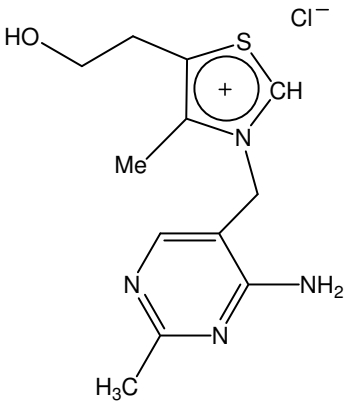

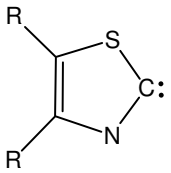

XLI

The first palladium complex with a benzothiazole carbene and a phosphine as ligands was reported by Lappert and synthesised *via* metal insertion into the electron-rich 3,3'-dimethyl-2,2'-dibenzothiazolinylidene. It had, however, no application in catalysis.[4]

---

[1] H. Stetter, *Angew. Chem. Int. Ed. Engl.,* 1976, **15**, 639; R. Kluger, *Chem. Rev.,* 1987, **87**, 863.
[2] H.-W. Wanzlick, H.-J. Kleiner, I. Lasch, H. U. Fuldner and H. Steinmaus, *Liebigs Ann. Chem.,* 1967, **708**, 155; A. J. Arduengo III, J R. Goerlich and W. J. Marshall, *Liebigs Ann. Chem./Recueil,* 1997, 365.
[3] R. Breslow, *J. Am. Chem. Soc.,* 1958, **80**, 3719.
[4] D. J. Cardin, B. Cetinkaya, E. Cetinkaya and M. F. Lappert, *J. Chem. Soc., Dalton Trans.,* 1973, 514.

Cationic carbene complexes of Mn(I) containing thiazolylidene and benzothiazolylidene ligands was prepared by Stone and co-workers with halide displacement reactions.[5] This success was followed by others involving cationic complexes of Ir(I) and Rh(I) (by reacting anionic metal starting materials with borofluoride salts) and neutral complexes of Cr(0) (by reacting $[Cr(CO)_5]^{2-}$ with the respective borofluoride salts).[6] An interesting but difficult method to prepare thiazole containing carbene complexes is by reacting aziridine with thiocarbonyl metal complexes that are not readily synthetically accessible (Scheme 5.1).[7] Similarly, thiirane could be reacted with isocyanide complexes of Pd(II).[8]

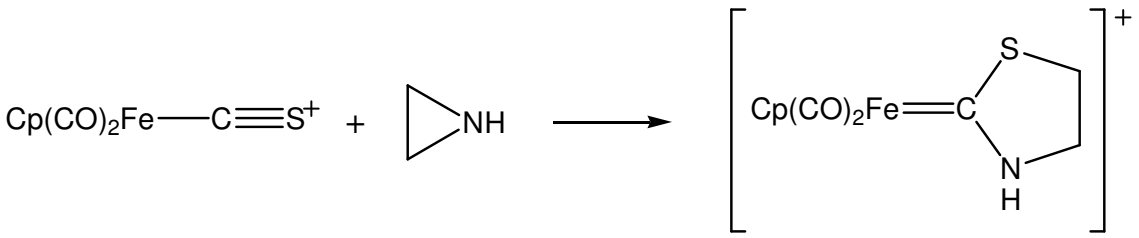

Scheme 5.1

Nacci and co-workers[9] have synthesised complex **XLII** which efficiently catalyses the Heck reaction.[10] Since then, the synthesis of other benzothiazolin-2-ylidene complexes has been successful and these complexes show even better activity in Heck catalysis.[11]

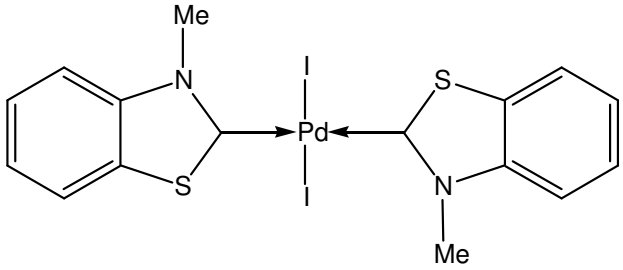

XLII

Thiazole carbene complexes of Au(I),[12] Cu(I),[13] Mn(0)[14] and W(0)[15] can be easily prepared by addition of thiazol-2-yllithium compounds to neutral metal halides and the subsequent protonation or alkylation.[16]

---

[5] P. J. Fraser, W. R. Roper and F. G. A. Stone, *J. Organomet. Chem.,* 1973, **50**, C54.
[6] P. J. Fraser, W. R. Roper and F. G. A. Stone, *J. Chem. Soc., Dalton Trans.,* 1974, 760.
[7] M. M. Singh and R. J. Angelici, *Inorg. Chem.,* 1984, **23**, 2691.
[8] R. Bertani, M. Mozzon and R. A. Michelin, *Inorg. Chem.,* 1988, **27**, 2809.
[9] V. Caló, R. Del Sole, A. Nacci, E. Schingaro and F. Scordari, *Eur. J. Org. Chem.,* 2000, 869; V. Caló, A. Nacci, L. Lopez and N. Mannarini, *Tetrahedron Lett.,* 2000, **41**, 8973; V. Caló, A. Nacci, A. Monopoli, L. Lopez and A. di Cosmo, *Tetrahedron,* 2001, **57**, 6071.
[10] S. A. Forsyth, H. Q. N. Gunaratne, C. Hardacre, A. McKeown, D. W. Rooney and K. R. Seddon, *J. Mol. Cat. A Chem.,* 2005, **231**, 61.
[11] S. K. Yen, L. L. Koh, F. E. Hahn, H. V. Huynh and T. S. A. Hor, *Organometallics,* 2006, **25**, 5105.
[12] H. G. Raubenheimer, F. Scott, G. J. Kruger, J. G. Toerien, R. Otte, W. van Zyl, I. Taljaard, P. Olivier and L. Linford, *J. Chem. Soc., Dalton Trans.,* 1994, 2091.

As mentioned previously, typical transition-metal N^2HC^5 complexes show *normal* carbene bonding at C2. *Abnormal* metalation at C5 of the NHC ring for pyridyl- and picolyl-NHC dihydride complexes of Ir(III)[17] was first reported in elegant studies by Crabtree and co-workers. These abnormally bonded NHCs could potentially offer a useful variant in electronic and steric properties compared to the usual C2 form. An infrared spectroscopic study indicated that the C5-bonded NHC's are significantly more electron-donating than their C2-bonded counterparts. Blocking C2 with a substituent or the fact that a lower steric strain can be felt by the metal centre should encourage bonding at C5.[18] In 2004, Nolan *et al.* reported the structure and interesting catalytic activity of $[PdCl_2(NHC)_2]$ complexes containing NHC ligands derived from imidazolium salts and bonded the "wrong way".[19] The carbene bonded at C4/5 was generated through deprotonation by a base or the use of basic ligands attached to the metal. It has since been shown that C5-bonding in complexes may lead to increased activity in Suzuki-Miyaura (S-M) and Mizoroki-Heck (M-H) reactions. Calculations[18] at the B3LYP/6-31G(d) level of theory, have indicated that the activation barrier for the oxidative addition for the C2-NHC system is slightly lower than that for the C5-NHC system, but that the catalytic capacity of the Pd^0L_2 involving the *abnormal* C5-NHC ligand is similar to the regular C2-NHC ligand.

The same bonding modes can be achieved with thiazolium ligands where the coordinated carbon can be situated at C2, C4 or C5. As is shown schematically for the possible resonance structures for a deprotonated thiazolium precursor in Scheme 5.2, standard carbene formation is only possible after deprotonation at C2, whereas C4 and C5 are situated at positions where such formation (according to a valence bond approach) is not logically possible. Hence the description as *abnormal* carbene when a metal is coordinated at these positions. Carbene formation is still allowed according to a molecular orbital approach.

---

[13] H. G. Raubenheimer, S. Cronje, P. H. van Rooyen, P. J. Olivier and J. G. Toerien, *Angew. Chem. Int. Ed. Engl.,* 1994, **33**, 672.
[14] H. G. Raubenheimer, A. Neveling, S. Cronje and D. G. Billing, *Polyhedron,* 2001, **20**, 1089.
[15] H. G. Raubenheimer and M. Desmet, *J. Chem. Research (S),* 1995, 30.
[16] H. G. Raubenheimer and S. Cronje, *J. Organomet. Chem.,* 2001, **617**, 170.
[17] S. Gründemann, A. Kovacevic, M. Albrecht, J. W. Faller and R. H. Crabtree, *J. Am. Chem. Soc.,* 2002, **124**, 10473.
[18] A. R. Chianese, A. Kovacevic, B. M. Zeglis, J. W. Faller and R. H. Crabtree, *Organometallics,* 2004, **23**, 2461.
[19] H. Lebel, M. K. Janes, A. B. Charette and S. P. Nolan, *J. Am. Chem. Soc.,* 2004, **126**, 5046.

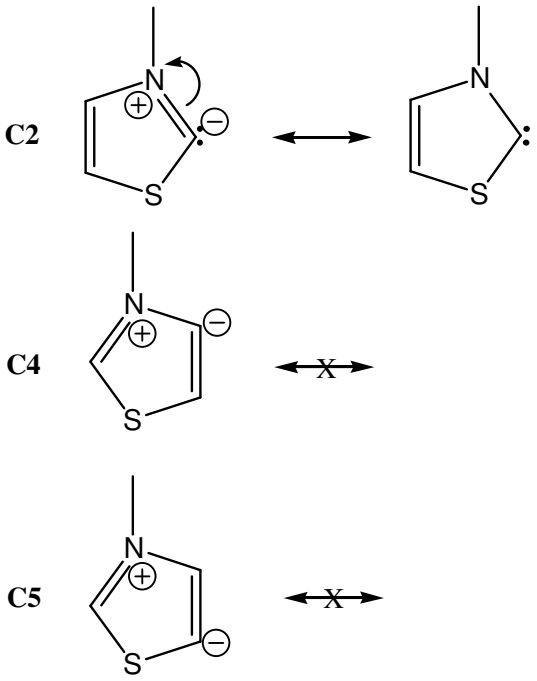

Scheme 5.2

Desmet and co-workers have described the synthesis of carbene complexes of iron which consists of the addition of isothiazolyl-lithium[20] and pyrazole-lithium[21] to $[Fe(Cp)(CO)_2Cl]$ (Cp = η-cyclopentadienyl) and the subsequent alkylation or protonation of the products. Such isothiazolylidene and pyrazolylidene compounds are prepared from precursors in which the nucleophilic heteroatom is situated γ to the coordinated carbon atom and they may be classified as *abnormal* carbene complexes.

5.1.2 Aims

In this investigation directed towards homogeneous catalysis we set out to:

1. prepare and fully characterise, by oxidative substitution of $M(PPh_3)_4$ (M = Pd or Ni), thiazole derived carbene complexes bonded at C2 (*n*NHC), C4 (*a*NHC) and C5 (*a*NHC);

2. determine their (Pd complexes) potential – alongside the Pd pyridinium derived carbene complexes **14a** – **16a** (discussed in Chapter 3) – as precatalysts in Suzuki-Miyaura coupling reactions;

3. test the *r*NHC[6] complex, *trans*-chloro(*N*-methyl-1,2,4-trihydro-2-dimethylaminepyrid-4-ylidene)bis(triphenylphosphine)palladium(II) triflate as a precatalyst in the Suzuki-Miyaura coupling of hindered substrates.

[20] J. G. Toerien, M. Desmet, G. J. Kruger and H. G. Raubenheimer, *J. Organomet. Chem.,* 1994, **479**, C12.
[21] H. G. Raubenheimer, M. Desmet, P. Olivier and G. J. Kruger, *J. Chem. Soc., Dalton Trans.,* 1996, 4431.

5.2 Results and discussion

5.2.1 Synthesis of the thiazolium precursors, 45 – 47, and complexes 48a, 48b, 49a, 49b and 50

The necessary thiazolium triflate precursors (Scheme 5.3) were obtained by utilising similar procedures followed for the synthesis of the pyridinium ligand precursors described in Chapter 3. *N*-methyl-2-bromothiazolium triflate (**45**) was obtained as a white microcrystalline material in 99 % yield and *N*-methyl-5-bromothiazolium triflate (**47**) as an off-white microcrystalline material in 97 % yield. Both are soluble in CH_2Cl_2 and insoluble in diethyl ether and paraffins. *N*-methyl-4-bromothiazolium triflate (**46**) was obtained 96 % yield. It is soluble in acetone, less soluble in CH_2Cl_2 and insoluble in diethyl ether and paraffins.

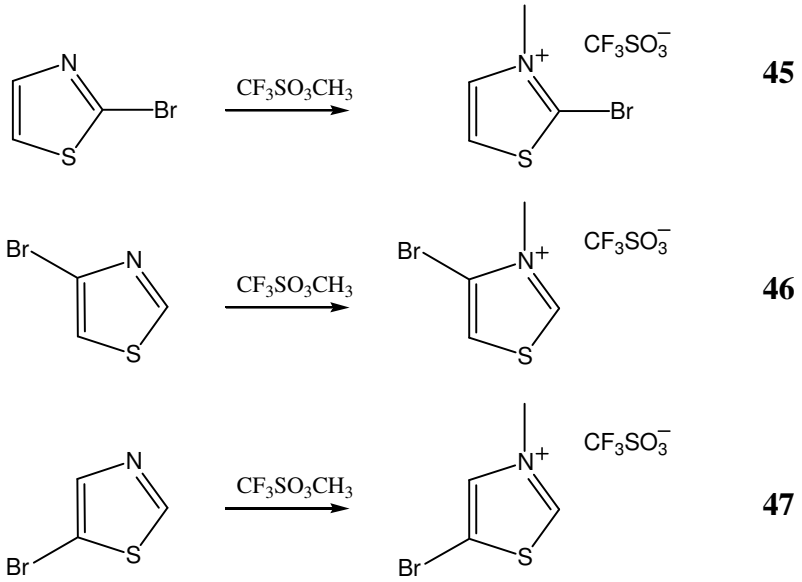

Scheme 5.3

Similar salts of **46**[22]and **47**[23] have previously been prepared with a methyl group at position 2 and an I- instead of a Br-atom at position 4 or 5.

Compounds **45** – **47** reacted with $M(PPh_3)_4$ (M = Pd, Ni) (Scheme 5.4) in the same fashion as during the formation of complexes **14a** (Pd) and **14b** (Ni). *Trans*-bromo(*N*-methyl-thiazol-2-ylidene)bis(triphenylphosphine)palladium(II) triflate, **48a**, was obtained as an off-white microcrystalline material in 8 % yield and *trans*-bromo(*N*-methyl-thiazol-4-

[22] M. Robba and R. C. Moreau, *Ann. Pharm. Franc*., 1964, **22**(3), 201.
[23] A. Cormans, D. Bouin and A. Friedmann, *Compt. Rend. Seances Acad. Sciences, Serie C: Sciences Chim.*, 1971, **272**(1), 5.

ium)bis(triphenylphosphine)-palladium(II) triflate, **49a**, as a white microcrystalline material in 97 % yield. Both are soluble in CH_2Cl_2, slightly soluble in THF and toluene and insoluble in ether and hexanes. The nickel analogues, **48b** and **49b**, were obtained as yellow powders in 36.3 and 45.9 % yield respectively. These latter two complexes are soluble in CH_2Cl_2, slightly soluble in THF, and insoluble in ether and hexanes. Only the Pd-complex (**50**) could be obtained as a slightly off-white powder (87 % yield) from the reaction of *N*-methyl-5-bromothiazolium triflate with $M(PPh_3)_4$ (M = Pd, Ni).

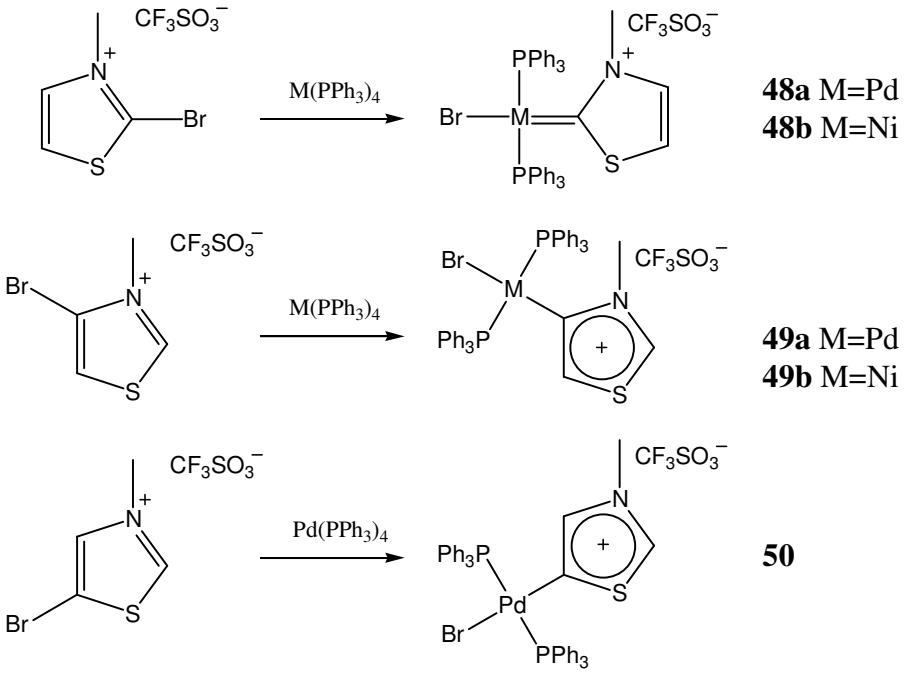

Scheme 5.4

Fehlhammer and co-workers have reported the only other examples of thiazol-2-ylidene complexes of palladium.[24] 1,3-Thiazol-2-ylidene complexes of Cr and W can be synthesized by reacting metal-coordinated α-deprotonated ethyl isocyanoacetate with CS_2 in a [3 + 2] cycloaddition. On reacting the chromium(0) complex with $CODPdCl_2$, carbene transfer (as discussed in Chapter 3) occurs to give the corresponding Pd-thiazol-2-ylidene complex. Unfortunately the NMR data of this latter complex is not documented for comparison.

[24] W. P. Fehlhammer, D. Achatz, U. Plaia and A. Völkl, *Z. Naturforsch. Teil B,* 1987, **42**, 720.

5.2.1.1 Characterisation of the thiazolium precursors, 45 – 47 and complexes 48a, 48b, 49a, 49b and 50

The new complexes will be compared to previously prepared abnormal NHC carbenes **A** (C5) and **B** (C4)[25] derived from imidazolin derivatives and isothiazol complexes with the metal bond at position γ (remote) to the stabilising heteroatom (**C**)[20,26] (Scheme 5.5). The fact that different metals are involved in all the reactions should be considered, as well as the possible formation of the complex bis[μ^2-thiazole-2,3-diyl)bromo(triphenylphosphine)palladium(II)] (**D**)[27]

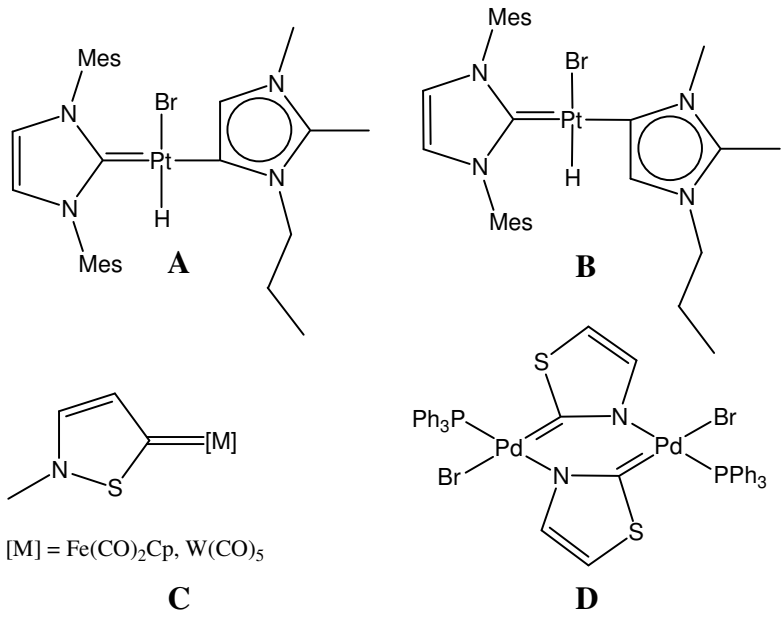

Scheme 5.5

NMR spectroscopy

The signals and their assignments, observed for compounds **45** - **47**, and complexes **48a, 48b**, **49a**, **49b** and **50,** are listed in Tables 5.1, 5.2 and 5.3. All the complexes display a single signal in the ^{31}P NMR spectra, indicating two symmetric *trans* PPh_3 groups. The NMR resonances of all the phenyl rings occur in the range (7.41 – 7.64 ppm, ^{1}H; 129.2 – 134.8 ppm, ^{13}C) - similar to those observed for bis[μ^2-thiazole-2,3-diyl)bromo(triphenylphosphine)-palladium(II)] (**D**) and the complexes (**14** – **16**) discussed in Chapter 3.

[25] D. Bacciu, K. J. Cavell, I. A. Fallis and L.-L. Ooi, *Angew. Chem. Int. Ed. Engl.,* 2005, **44**, 5282.
[26] H. G. Raubenheimer and M. Desmet, *J. Chem. Research (S),* 1995, 30.
[27] Y. Xie, G. K. Tan, Y. K. Yan, J. J. Vittal, S. C. Ng and T. S. A. Hor, *J. Chem. Soc., Dalton Trans.,* 1999, 773.

The chemical shifts of the ligand precursors are similar to those reported previously for thiazolium salts, with C^2 and H^2 appearing the most downfield (159.1 – 160.5 ppm for C^2 and 10.20 – 10.36 ppm for H^2), followed by H^4 (8.58 – 8.70 ppm) and C^4 (136.9 – 137.0 ppm). H^5 (8.35 – 8.43 ppm) and C^5 (126.9 – 127.1 ppm) were observed the most upfield.[28] A similar trend also holds for the complexes.

Table 5.1 NMR data of compound **45** and complexes **48a** and **48b** in CD_2Cl_2

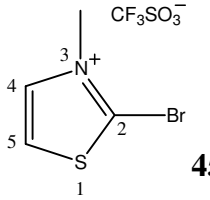

45

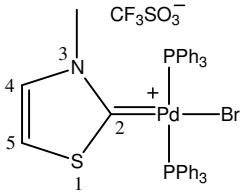

48a

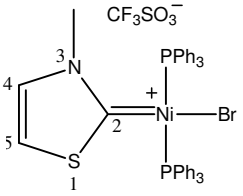

48b

Assignment	δ / ppm		
	45	**48a**	**48b**
^{1}H NMR			
NMe	4.28 (3H, s)	3.55 (3H, s)	3.58 (3H, s)
H^4	8.43 (1H, d, ^{3}J = 4.3 Hz)	n.o	7.26 (1H, d, ^{3}J = 3.4 Hz)
H^5	8.23 (1H, d, ^{3}J = 4.3 Hz)	7.29 (1H, d, ^{3}J = 3.8 Hz)	7.21 (1H, d, ^{3}J = 3.4 Hz)
Ph, H^4	n.a.	7.57, 7.45 (31H, 2 x m)	n.a.
Ph	n.a.	n.o.	7.64, 7.54, 7.45 (30H, 3 x m)
^{13}C NMR			
NMe	43.1 (s)	44.1 (s)	43.8 (s)
C^2	163.0 (s)	197.8 (s)	200.9 (t, $^2J_{C\text{-}P}$ = 32.2 Hz)
C^4	140.6 (s)	169.1 (s)	139.7 (bs)
C^5	127.3 (s)	138.8 (s)	125.2 (s)
Ph^{ipso}, Ph^{meta}	n.a.	129.5 (bs)	129.2 (m)
Ph^{ortho}	n.a.	134.7 (bs)	134.4 (m)
Ph^{para}	n.a.	132.3 (s)	131.9 (s)
^{31}P NMR			
PPh_3	n.a.	22.6 (s)	22.3 (s)

Allylic couplings are observed in the ^{1}H NMR spectra of **45**, **48a** and **48b** ($J_{H\text{-}H}$ = 4.3, 3.8 and 3.4 Hz respectively) in the signals for the H^4 and H^5 protons. The signals appear at a higher field in complexes **48a** and **48b** than in thiazol-2-ylidene manganese complexes[29] compared to that of Pd and Ni. This influence is less pronounced in the ^{13}C NMR spectra.

The ^{13}C NMR of **48a** and **48b** show characteristic signals at δ 197.8 and 200.9 for metal carbene carbons, but at a somewhat higher field than for the C^2 bonded NHC complexes **A** (δ

[28] H.-J. Federsel, G. Glasare, C. Högstrom, J. Wiestål, B. Zinko and C. Ödman, *J. Org. Chem.,* 1995, **60**, 2597.
[29] H. G. Raubenheimer, A. Neveling, S. Cronje and D. G. Billing, *Polyhedron,* 2001*,* **20**, 1089.

180.9) and **B** (δ 180.7) bonded to Pt (Scheme 5.5). These carbene signals also appear much more downfield when compared to chemical shifts of the same signals in *trans*-chloro(1,3-dimethyl-2,3-dihydro-1H-imidazol-2-ylidene)bis(triphenylphosphine)palladium(II) tetrafluoroborate (δ 161.2) and *trans*-chloro(1,3-dimethyl-2,3-dihydro-1H-imidazol-2-ylidene)bis(triphenylphosphine)nickel(II) tetrafluoroborate (δ 158.6). This indicates that this difference is rather due to the presence of the S-atom instead of an NR-group. The same trend has previously been reported for Au and Fe carbene complexes.[30] However, the signal is at a lower field strength than the signal for C^2 in bis[μ^2-thiazole-2,3-diyl)bromotriphenylphosphine palladium(II)] (**D**) which resonates at δ 183.8.

Table 5.2 NMR data of compound **46** and complexes **49a** and **49b** in CD_2Cl_2

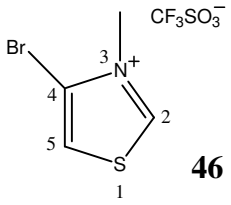

46

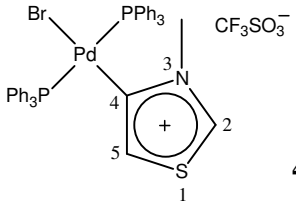

49a

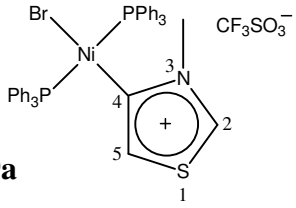

49b

Assignment	δ / ppm		
	46	**49a**	**49b**
^{1}H NMR			
NMe	4.30 (3H, s)	3.72 (3H, bs)	3.92 (3H, bs)
H^2	10.51 (1H, d, ^4J = 2.5 Hz)	9.33 (1H, dd, $^4J_{H-H}$ = 2.5 Hz, $^5J_{H-P}$ = 0.6 Hz)	9.22 (1H, d, ^4J = 2.3 Hz)
H^5	8.06 (1H, d, ^4J = 2.5 Hz)	6.52 (1H, m)	6.69 (1H, m)
Ph	n.a.	7.54, 7.42 (30 H, 2 x m)	7.64, 7.53, 7.43 (30H, 3 x m)
^{13}C NMR			
NMe	43.3 (s)	44.2 (s)	44.0 (s)
C^2	162.5 (bs)	156.6 (s)	157.8 (s)
C^4	125.1 (s)	165.1 (t, $^2J_{C-P}$ = 9.1 Hz)	163.6 (t, $^3J_{C-P}$ = 35.4 Hz)
C^5	121.4 (s)	120.3 (t, $^4J_{C-P}$ = 5.2 Hz)	119.7 (bs)
Ph^{ipso}	n.a.	129.6 (t, $^1J_{C-P}$ = 24.9 Hz)	130.2 (t, $^1J_{C-P}$ = 24.0 Hz)
Ph^{ortho}	n.a.	134.4 (t, $^2J_{C-P}$ = 6.5 Hz)	134.6 (t, $^2J_{C-P}$ = 5.7 Hz)
Ph^{meta}	n.a.	129.2 (t, $^3J_{C-P}$ = 5.2 Hz)	129.3 (t, $^3J_{C-P}$ = 5.0 Hz)
Ph^{para}	n.a.	131.7 (s)	131.7 (s)
^{31}P NMR			
PPh_3	n.a.	22.6 (s)	21.6 (s)

The ^{13}C NMR signals for the C^4 bonded complexes, **49a** and **49b**, occur at a much lower chemical shift than the C^2 bonded complexes, **48a** and **48b**, with the signal for C^4 in complex **49a** appearing upfield by 32.7 ppm to the signal of the metal bonded carbon in **48a**, clearly indicating the larger typical carbene character of the latter complex. However, the signal for

[30] H. G. Raubenheimer and S. Cronje, *J. Organomet. Chem.*, 2001, **617**, 170.

C^4 in complex **49a** still exhibits a downfield shift of 40.0 ppm compared to the ligand precursor, **46**. The corresponding signals for complex **49b** show an upfield shift of 37.3 ppm when compared to **48b** and a downfield shift of 38.5 ppm when compared to the precursor compound. The ^{13}C NMR resonances for C^4 and C^5 are comparable with that of **B** in Scheme 5.4 (δ 151.6 and 124.4 respectively).[25]

In complex **49a**, the coupling of H^2 with H^5 (2.5 Hz) and the P-atoms (0.6 Hz) in the PPh_3 ligands are observed. Only the coupling of H^2 with H^5 (2.3 Hz) is observed in complex **49b**.

Table 5.3 NMR data of compound **47** and complex **50** CD_2Cl_2

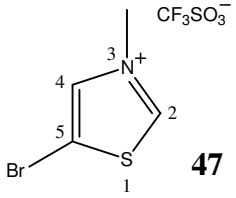

47

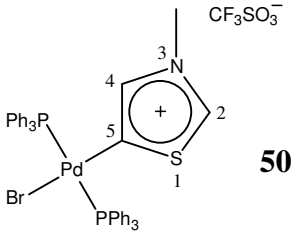

50

Assignment	δ / ppm	
	47	**50**
^{1}H NMR		
NMe	4.33 (3H, s)	3.59 (3H, d, ^4J = 0.6 Hz)
H^2	10.20 (1H, s)	9.28 (1H, m)
H^4	8.18 (1H, s)	6.30 (1H, m)
Ph	n.a.	7.56, 7.51, 7.41 (30H, 3 x m)
^{13}C NMR		
NMe	43.6 (s)	41.0 (s)
C^2	162.1 (s)	158.7 (bs)
C^4	139.0 (s)	154.3 (s)
C^5	115.8 (s)	135.7 (t, $^3J_{C\text{-}P}$ = 4.3 Hz)
Ph^{ipso}	n.a.	129.6 (t, $^1J_{C\text{-}P}$ = 25.4 Hz)
Ph^{ortho}	n.a.	134.8 (t, $^2J_{C\text{-}P}$ = 6.1 Hz)
Ph^{meta}	n.a.	128.8 (t, $^3J_{C\text{-}P}$ = 5.2 Hz)
Ph^{para}	n.a.	131.6 (s)
^{31}P NMR		
PPh_3	n.a.	24.3 (s)

Although a downfield change in chemical shift of 19.9 ppm is observed for C^5 in **50** when compared to the corresponding signal of **47**, the metal bonded carbon resonates more upfield when compared to the metal bonded carbon in **48a** (Δδ 62.1, C^2) and **49a** (Δδ 29.4, C^4). These results for the signals of the metal bonded carbons may be understood in terms of the fact that

carbene carbons are carbo-cationic and therefore, the more carbene character, the bigger the chemical shift.

The ^{13}C NMR resonances are characteristic of C5 ligand bonding and the ^{1}H NMR spectrum is also informative. The C4-bonded proton proximal to the palladium atom is significantly shielded, appearing at δ 6.30 in the ^{1}H NMR spectrum.

The resonance for C5 in the ^{13}C NMR is also very much upfield compared to the metal bonded carbon, α to the S-atom in the Fe- and W-containing abnormal carbene complexes, **C** in Scheme 5.5, which have chemical shifts of δ 189.9 (Δδ 25.9 downfield from the same carbon in the ligand precursor)[20] and δ 197.8[15] respectively.

Mass spectrometry

EI-MS data of **45** - **47** are summarized in Table 5.4 and the FAB-MS data of complexes **48a**, **48b**, **49a**, **49b** and **50** are collected in Table 5.5. Peaks due to the many isotopes of the metal atoms, are observed in the spectra of complexes **48a**, **48b**, **49a**, **49b** and **50**, whereas the two main isotopes of Br are observed in ligands **45** - **47** at respectively *m/z* 180.0 and 178.0.

Table 5.4 EI-MS data of **45** - **47**

Complex	*m/z*	Relative intensity	Fragment ion
45	180.0	100	$[M\text{-}CF_3SO_3]^+$ $[^{81}Br]$
	178.0	98	$[M\text{-}CF_3SO_3]^+$ $[^{79}Br]$
46	180.0	100	$[M\text{-}CF_3SO_3]^+$ $[^{81}Br]$
	178.0	98	$[M\text{-}CF_3SO_3]^+$ $[^{79}Br]$
47	180.0	100	$[M\text{-}CF_3SO_3]^+$ $[^{81}Br]$
	178.0	98	$[M\text{-}CF_3SO_3]^+$ $[^{79}Br]$

The fragments for the cationic parts of the molecules are observed for all the complexes and the calculated isotopic distributions of these fragments are in good agreement with the observed spectra for all the complexes. The fragments due the loss of a PPh_3 ligand, followed by the loss of Br, are observed for **48b**, **49a**, **49b** and **50**. On the other hand, for complex **48a**, the fragments $[Pd(PPh_3)_2]^+$ and $[M\text{-}PPh_3\text{-}Ph\text{+}H\text{-}CF_3SO_3]^+$ are detected.

Table 5.5 FAB-MS data of complexes **48** - **50**

Complex	*m/z*	Relative intensity	Fragment ion
48a	733.0	10	$[M\text{-}Br\text{-}CF_3SO_3]^+$ (^{81}Br, ^{106}Pd)
	630.1	6	$[Pd(PPh_3)_2]^+$
	471.0	25	$[M\text{-}PPh_3\text{-}Ph\text{+}H\text{-}CF_3SO_3]^+$
48b	761.9	15	$[M\text{-}CF_3SO_3]^+$ (^{81}Br, ^{58}Ni)
	499.9	43	$[M\text{-}PPh_3\text{-}CF_3SO_3]^+$
	419.0	21	$[M\text{-}Br\text{-}PPh_3\text{-}CF_3SO_3]^+$
49a	810.2	15	$[M\text{-}CF_3SO_3]^+$ (^{81}Br, ^{106}Pd)
	548.0	19	$[M\text{-}PPh_3\text{-}CF_3SO_3]^+$
	466.1	6	$[M\text{-}Br\text{-}PPh_3\text{-}CF_3SO_3]^+$
49b	762.3	10	$[M\text{-}CF_3SO_3]^+$ (^{81}Br, ^{58}Ni)
	500.0	75	$[M\text{-}PPh_3\text{-}CF_3SO_3]^+$
	419.1	33	$[M\text{-}Br\text{-}PPh_3\text{-}CF_3SO_3]^+$
50	810.3	16	$[M\text{-}CF_3SO_3]^+$ (^{81}Br, ^{106}Pd)
	548.1	14	$[M\text{-}PPh_3\text{-}CF_3SO_3]^+$
	466.1	6	$[M\text{-}Br\text{-}PPh_3\text{-}CF_3SO_3]^+$

5.2.1.2 Crystal and molecular structures of *trans*-bromo(*N*-methyl-2,3-dihydro-thiazol-2-ylidene)bis(triphenylphosphine)nickel(II) triflate, 48b, *trans*-bromo(*N*-methyl-3,4-dihydro-thiazol-4-ylidene)bis(triphenylphosphine)palladium(II) triflate, 49a, and *trans*-bromo(*N*-methyl-thiazol-5-ylidene)bis(triphenylphosphine)palladium(II) triflate 50

Crystals of complexes **48b** and **50** suitable for X-ray structure determinations were grown by solvent diffusion of pentane into a CH_2Cl_2 solution of the respective compound. The crystals obtained for **49a** by the same method, yielded very poor data and, because of the marginal precision of the crystal structure of **49a**, only the undeniable features that are apparent will be discussed. The bond angles and lengths are depicted in Tables 5.6 (**48b**), 5.7 (**49a**) and 5.8 (**50**). These analyses (see also Figures 5.1, 5.3 and 5.4) show that the metal centres exhibit distorted square planar core geometry. The planes of the carbene ligands are twisted by 89.13(10) ° (**48b**), 84.30(31) ° (**49a**) and 76.77(9) ° (**50**) relative to the plane defined by P(1), P(2), M(1) and Br(1). This is typical behaviour for carbene ligands in square planar group 10

complexes – as mentioned in Chapter 3 – which adopt a twisted orientation to minimise steric interactions with other ligands in the metal coordination sphere.[31]

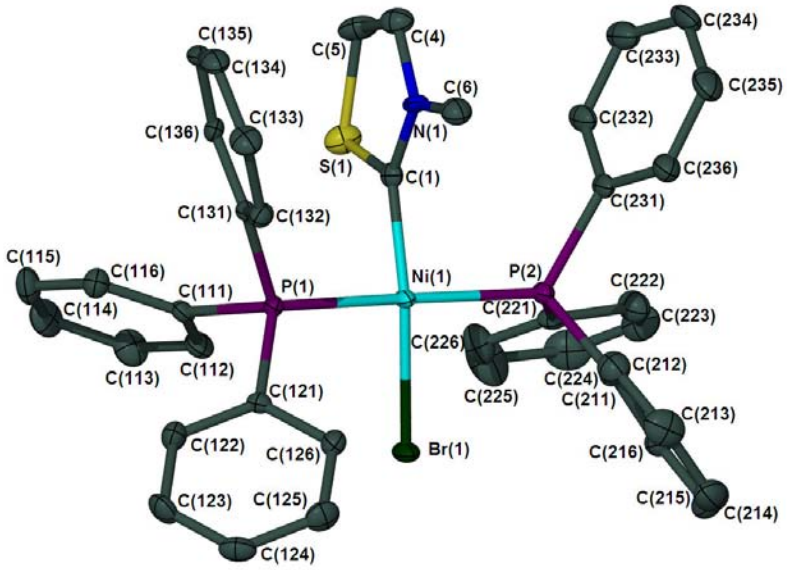

Figure 5.1 Molecular structure of **48b**, indicating the atom numbering scheme, generated in POV Ray; hydrogens, the counter ion and a CH_2Cl_2 solvent molecule are omitted for clarity.

After establishing the connectivity of **48b**, additional diffuse electron density belonging to the $CF_3SO_3^-$ counterion was located on the difference map and was then removed using the Squeeze routine in the Platon programme package.[32]

Table 5.6 Selected bond distances (Å) and angles (º) of complex **48b**

Bond lengths (Å)			
Br(1)-Ni(1)	2.3098(6)	S(1)-C(5)	1.727(4)
Ni(1)-C(1)	1.859(4)	N(1)-C(1)	1.346(5)
Ni(1)-P(2)	2.223(1)	N(1)-C(4)	1.395(5)
Ni(1)-P(1)	2.224(1)	N(1)-C(6)	1.431(6)
S(1)-C(1)	1.714(4)	C(4)-C(5)	1.320(6)
Bond angles (º)			
C(1)-Ni(1)-P(2)	91.1(1)	C(1)-N(1)-C(6)	123.1(3)
C(1)-Ni(1)-P(1)	90.8(1)	C(4)-N(1)-C(6)	122.8(3)
P(2)-Ni(1)-P(1)	173.05(4)	N(1)-C(1)-S(1)	109.6(3)
C(1)-Ni(1)-Br(1)	164.1(1)	N(1)-C(1)-Ni(1)	133.4(3)
P(2)-Ni(1)-Br(1)	88.77(3)	S(1)-C(1)-Ni(1)	117.0(2)
P(1)-Ni(1)-Br(1)	91.32(3)	C(5)-C(4)-N(1)	113.7(4)
C(1)-S(1)-C(5)	92.0(2)	C(4)-C(5)-S(1)	110.5(3)
C(1)-N(1)-C(24)	114.1(3)		

[31] A. M. Magill, D. S. McGuinness, K. J. Cavell, G. J. P. Britovsek, V. C. Gibson, A. J. P. White, D. J. Williams, A. H. White and B. W. Skelton, *J. Organomet. Chem.,* 2001, **617-618**, 546.
[32] A. L. Apek, *J. Appl. Crystallogr.,* 2003, **36**, 7.

Fifteen metal-carbene complexes of thiazole derived ligands were found on the CCSD. None contained a nickel metal.

The C(4)-C(5) bond length of 1.320(6) Å is identical to the C=C double bonds [1.329(9) - 1.333(9) Å] in **D** (Scheme 5.5),[27] suggesting that the carbenoid carbon atom interacts strongly with the two α heteroatoms. The Ni(1)-C(1) bond distance of 1.859(4) Å is at the shorter end of the Ni(II) N^1HC^6 complexes previously reported [1.861(5) – 1.874(6) Å[33] and *trans*-chloro(*N*-methyl-1,3-dihydro-pyrid-3-ylidene)bis(triphenylphosphine)palladium(II) triflate [1.879(6) Å]. The "shorter" Ni-C bond could suggest larger π-acceptance by the 2,3-dihydro-thiazol-2-ylidene ligand. The shorter C(carbene)-N [1.346(5) Å] and similar C(carbene)-S bond lengths [1.714(4) Å], when compared to the other C-N [1.395(5) and 1.431(6) Å] and C-S [1.727(4) Å] bonds in the ring system, confirm π-bonding between the C(carbene) carbon and the N-atom.

The Ni-Br bond length of 2.3098(6) Å is significantly shorter than the Ni-Br bond length of 2.3949 Å in 1-(2,6-dimethyl-4-tert-butyl)-3-(α-picolyl)imidazol-2-ylidene]nickel dibromide[34] and is similar to the same bond distance in *trans*-bis[1,3-bis(2-propenyl)benzimidazolin-2-ylidene]nickel(II) dibromide [2.3100(3) Å][35]. This suggests that the *trans* influence of the thiazol-2-ylidene ligand is weaker than that of a pyridyl or imidazol-2-ylidene group and similar to that of Br.

The cations in complex **48b** are stacked on top of each other forming alternate layers with layers of solvent molecules parallel to the c-axis (Figure 5.2). Viewed along the a-axis, the carbene ligand is pointed diagonally upward and, in the next column, diagonally downward.

[33] S. K. Schneider, C. F. Rentzsch, A. Krüger, H. G. Raubenheimer and W. A. Hermann, *J. Mol. Cat. A: Chem.,* 2007, **265**, 50.
[34] S. Winston, N. Stylianides, A. A. D. Tulloch, J. A. Wright and A. A. Danopoulos, *Polyhedron,* 2004, **23**, 2813.
[35] H. V. Huynh, C. Holtgrewe, T. Pape, L. L. Koh and E. Hahn, *Organometallics,* 2006, **25**, 245.

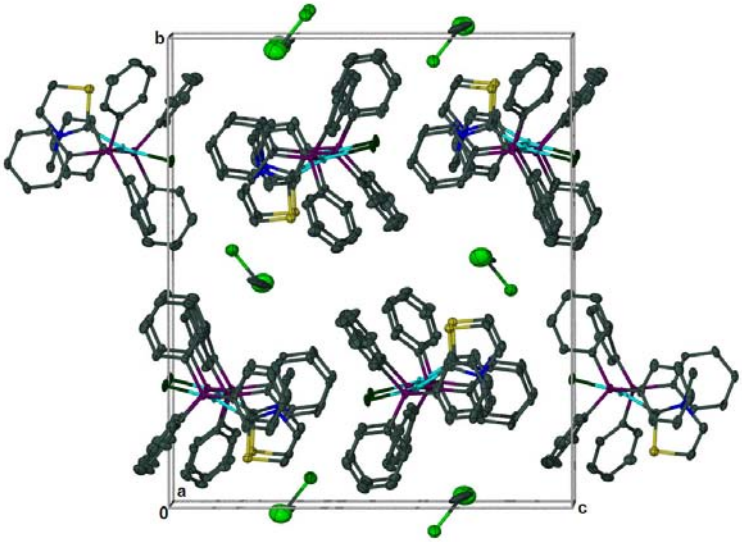

Figure 5.2 The arrangement of the molecules of **48b**, viewed along the a-axis; H-atoms are omitted for clarity.

As mentioned before, the data of complex **49a** is very poor and thus not all the electron densities on the difference maps could be modelled. The asymmetric unit consist of two molecules of complex **49a** (of which one could not be modelled).

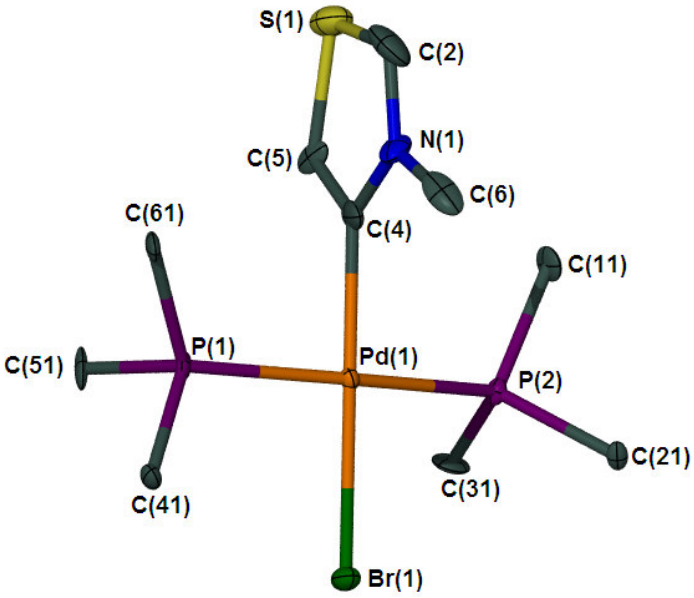

Figure 5.3 The partial molecular structure of **49a**, indicating the atom numbering scheme, generated in POV-Ray; hydrogens, the carbons of the phenyl groups and the counterions are omitted for clarity.

Table 5.7 Selected bond lengths (Å) and angles (°) of complex **49a**

Bond lengths (Å)			
Pd(1)-C(4)	2.03(2)	S(1)-C(5)	1.72(2)
Pd(1)-P(2)	2.315(4)	N(1)-C(2)	1.31(2)
Pd(1)-P(1)	2.321(4)	N(1)-C(4)	1.39(2)
Pd(1)-Br(1)	2.475(2)	N(1)-C(6)	1.47(2)
S(1)-C(2)	1.67(2)	C(4)-C(5)	1.32(2)
Bond angles (°)			
C(4)-Pd(1)-P(2)	90.0(4)	C(2)-N(1)-C(6)	124(1)
C(4)-Pd(1)-P(1)	89.2(4)	C(4)-N(1)-C(6)	122(1)
P(2)-Pd(1)-P(1)	169.5(1)	N(1)-C(2)-S(1)	113(1)
C(4)-Pd(1)-Br(1)	176.3(5)	C(5)-C(4)-N(1)	111(2)
P(2)-Pd(1)-Br(1)	87.8(1)	C(5)-C(4)-Pd(1)	127(1)
P(1)-Pd(1)-Br(1)	92.5(1)	N(1)-C(4)-Pd(1)	122(1)
C(2)-S(1)-C(5)	89.7(8)	C(4)-C(5)-S(1)	113(1)
C(2)-N(1)-C(4)	114(1)		

Although the standard deviations are very large, the undeniable features of the square planar arrangement of the thiazole derived ligand, *trans* PPh_3 groups and Br-atom is apparent.

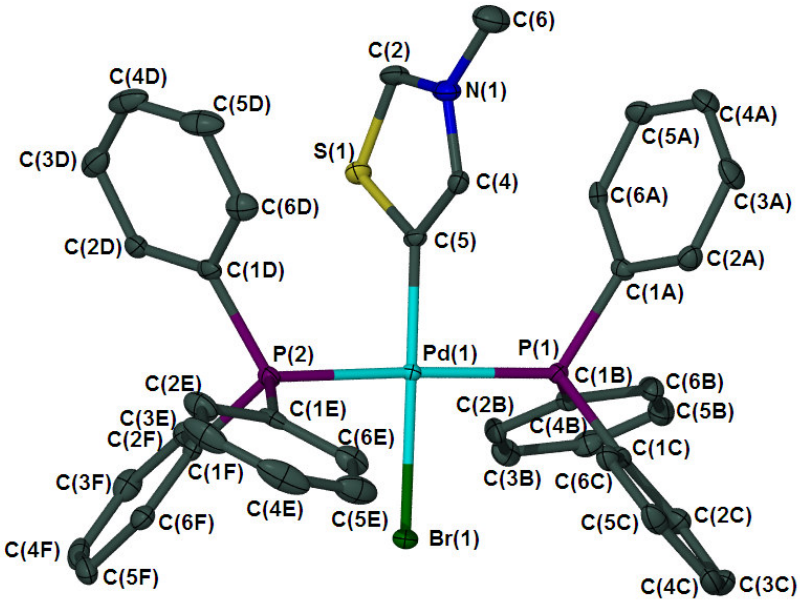

Figure 5.4 Molecular structure of **50**, indicating the atom numbering scheme, generated in POV Ray; hydrogens, a CH_2Cl_2 molecule and the counter ion are omitted for clarity.

A search on the CCSD yielded no examples of complexes with thiazole derived ligands bonded to a metal through C5. Only three examples are however known for imidazole derived complexes, namely bromo(1,3-dimesitylimidazol-2-ylidene)(1,2-dimethyl-3-n-propylimidazol-4-yl)hydridoplatinum(II) (**A**),[25] dichloro(1,3-bis(mesityl)-2-imidazolylidene)-

(1,3-bis(mesityl)-5-imidazolium)palladium(II)[36] and dichloro[1,3-bis(2,6-di-isopropylphenyl)-imidazol-2-ylidene][1,3-bis(2,6-di-isopropylphenyl)imidazolium-5-yl] palladium(II).[37]

Table 5.8 Selected bond lengths (Å) and angles (º) of complex **50**

Bond lengths (Å)			
Pd(1)-C(5)	1.990(4)	S(1)-C(5)	1.732(4)
Pd(1)-P(2)	2.328(1)	N(1)-C(2)	1.316(6)
Pd(1)-P(1)	2.333(1)	N(1)-C(4)	1.392(6)
Pd(1)-Br(1)	2.4753(5)	N(1)-C(6)	1.475(6)
S(1)-C(2)	1.686(5)	C(4)-C(5)	1.348(6)
Bond angles (º)			
C(5)-Pd(1)-P(2)	91.2(1)	C(2)-N(1)-C(6)	124.0(4)
C(5)-Pd(1)-P(1)	90.5(1)	C(4)-N(1)-C(6)	122.2(4)
P(2)-Pd(1)-P(1)	175.66(4)	N(1)-C(2)-S(1)	111.4(3)
C(5)-Pd(1)-Br(1)	179.2(1)	C(5)-C(4)-N(1)	113.9(4)
P(2)-Pd(1)-Br(1)	88.67(3)	C(4)-C(5)-S(1)-	108.4(3)
P(1)-Pd(1)-Br(1)	89.67(3)	C(4)-C(5)-Pd(1)	132.3(3)
C(2)-S(1)-C(5)	92.5(2)	S(1)-C(5)-Pd(1)	119.2(2)
C(2)-N(1)-C(4)	113.8(4)		

The Pd-C(carbene) bond distances of 1.994 – 2.041 Å observed in these complexes compares well with that of complex **50** [1.990(4) Å] bonded at C5 and 2.033(16) Å for **49a** bonded at C4. Similarly to the pyridylidene complex family discussed in Chapter 3, the bond distances of the *abnormal* NHC complexes (**49a** and **50**) do not differ much from the *normal* N^2HC^5 complexes mentioned above and, again, the degree of carbene character can only be roughly estimated from differences in the ^{13}C NMR spectra of the respective compounds.

A view along the c-axis of the unit cell of complex **50** (Figure 5.5) shows that the cations aggregate in columns on top of one another with every alternating molecule's atoms aligned. The solvent molecules and counterions fill up the spaces created by this assembly.

[36] H. Lebel, M.K. Janes, A. B. Charette and S.P. Nolan, *J. Am. Chem. Soc.,* 2004, **126**, 5046.
[37] L. C. Campeau, P. Thansandole and K. Fagnou, *Org. Lett.,* 2005, **7**, 1857.

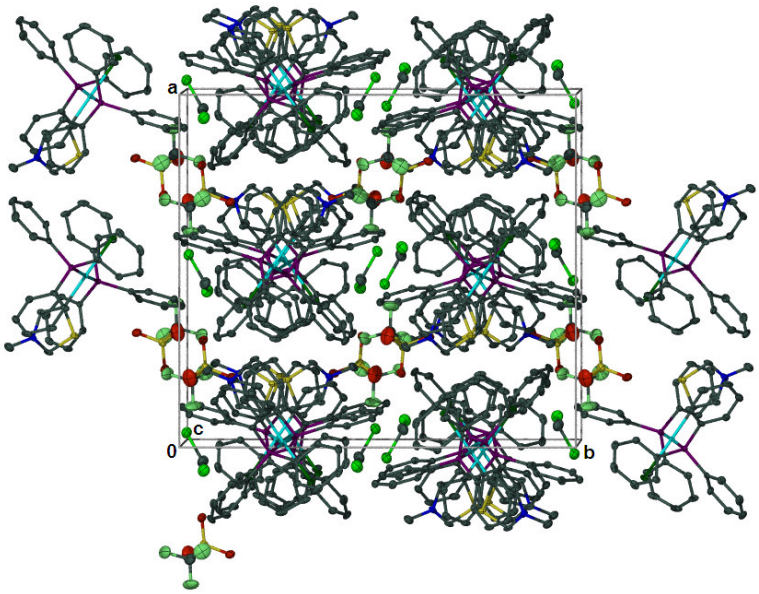

Figure 5.5 The molecular assembly of the molecules of **50**, viewed along the c-axis of the unit-cell; H-atoms are omitted for clarity.

5.3 Catalysis

5.3.1 Introduction

Oxidative addition and reductive elimination are ubiquitous as elementary reaction steps in homogeneous catalysis[38] and have been intensively investigated both experimentally[39] and theoretically.[40] Stabilized nanoparticles,[41] originating from carbene insertion and subsequent reductive elimination, could also constitute catalytically active centra, albeit of a heterogeneous nature. Thus, the divide between homogeneous and heterogeneous catalysis may not be that large after all.

Key questions in all catalytic processes refer to the activity, stereoselectivity and effectivity of the catalyst under the process conditions, as well as the improvement of the lifetime of the catalyst. It is known that tetraalkylammonium salts have been highly successful in enhancing the reactivity and selectivity for Heck-type reactions.[42,43] The presence of water has a crucial

[38] J. P. Collman, L. S. Hegedus, J. R. Norton and R. G. Finke, *Principles and Applications of Organotransition Metal Chemsitry,* University Science Books, Mill Valley, CA, 1987; T. Y. Luh, M.-K. Leung and K. T. Wong, *Chem. Rev.,* 2000, **100**, 3187.
[39] M. Lersch and M. Tilset, *Chem. Rev.,* 2005, **105**, 2471.
[40] M. Torrent, M. Sóla and G. Frenking, *Chem. Rev.,* 2000, **100**, 439.
[41] J. Dupont, R. F. de Souza and P. A. Z. Suarez, *Chem. Rev*., 2002, **102**, 3667.
[42] A. de Meijere and F. E. Meyer, *Angew.Chem. Int. Ed. Engl.,* 1994, **33**, 2379, and references cited therein.

influence (which can be highly detrimental or beneficial) when a tetraalkylammonium salt is used in combination with an inorganic base depending, of course, on the nature of the base. On the other hand, the beneficial effect of tetraalkylammonium salts is more dependent upon its onium cation than upon its anion.[44]

5.3.2 Catalytic C-C coupling reactions

The Suzuki-Miyaura (S-M)[45] reaction is perhaps the most widely used transition metal-mediated cross-coupling reaction today, owing to: the ready availability of reactants that are non-toxic, air- and water-stable; the ease of waste disposal; and, of course, most importantly, its extreme versatility and high regio- and stereo- selectivity.[46] Some of the substrates are attractive for cross-coupling methodology because they are biologically active.[47]

The coupling reaction proceeds *via* transmetallation in the presence of bases. As illustrated in Scheme 5.6, the role of the base is interpreted as activation of either Pd or the boranes. The formation of alkoxo(palladium) species Ar-Pd-OR (**XLIV**) from Ar-Pd-X facilitates the transmetallation with organoboranes. Alternatively, the nucleophilicity of the R-group on the boron is enhanced by quaternization of the boron with a base, generating the corresponding 'ate' complexes (**XLIII**), which undergo facile transmetallation.[48]

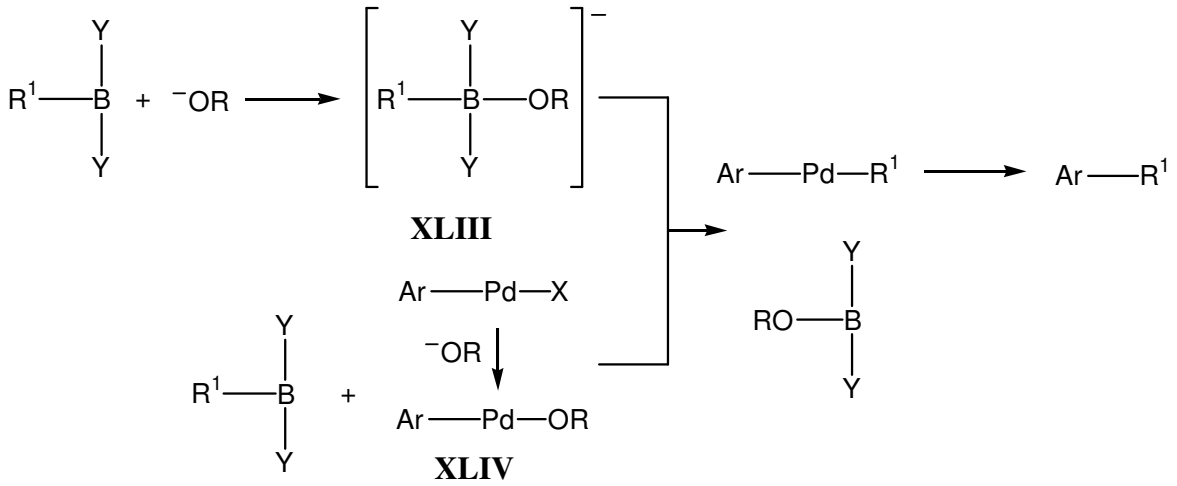

Scheme 5.6

[43] T. Jeffrey, in *Advances in Metal-Organic Chemistry, Vol. 5,* L. S. Liebeskind, JAI Press, Greenwich CT, 1996, pp. 149 – 256.
[44] T. Jeffery, *Tetrahedron*, 1996, **52**, 10113
[45] N. Miyaura, K. Yamada and A. Suzuki, *Tetrahedron Lett.,* 1979, **36**, 3437.
[46] A. Suzuki, *Chem. Commun.,* 2005, 4759.
[47] *Heterocyclic Chemistry*, J. A. Joule and K. Mills, Eds., Blackwell Science, Malden, MA, 2000.
[48] J. Tsuji, *Palladium Reagents and Catalysts New Perspectives for the 21st Century,* John Wiley & Sons, Chichester, 2004, p 289.

A number of papers claiming highly active catalysts for S-M have been published. These catalysts seem in some instances only to be active for a limited number of substrates. In mechanistic considerations of this reaction, it is generally believed that a 14ē Pd(0) complex is the catalytically active species.

The use of aryl chlorides as chemical feedstock has proven difficult but, if successful, would economically benefit a number of industrial processes.[49] The problem with aryl chlorides is the strength of the C-Cl bond, which impedes oxidative addition to the 14ē Pd(0) phosphine complexes.[50] Activated aryl chlorides are less of a problem, but various attempts towards solving this problem have been undertaken in the past of which only a limited number could claim some success. One of these methods uses 1,3-bis-(2,4,6-trimethylphenyl)imidazol-2-ylidene as a ligand on Pd(II) and Cs_2CO_3 as the base to successfully couple aryl chlorides with both electron-donating and electron-withdrawing substituents and arylboronic acids.[51] Another success story is the use of homoleptic Pd(0) NHC complexes, where the more sterically encumbered complexes are more effective. The latter complexes have also proven to be active in amination reactions.[52]

It has been noted that the catalysis is actually preformed by a highly active ligand free system and that the complex only acts as a precatalyst. Tests to confirm this method of action include TEM observations, reusability attempts and Hg poisoning tests.[53]

Various approaches have been followed for the Pd-NHC complexes to enhance their activity in various different processes. They have even been immobilised on amorphous silica, but seem to be more stable when used under typical homogeneous reaction conditions. The tests have indicated that the complex only acts as a precatalyst for highly active, ligand free Pd species.[54] Since Pd is very important in the pharmaceutical industry but also very expensive and toxic, it is important to reduce the amount of Pd in the product solution, hence the advantage of immobilisation.

---

[49] B. Cornils and W. A. Herrmann, EDS., *Applied Homogeneous Catalysis with Organometallic Compounds,* VCH, Weinheim, 1996.
[50] W. A. Herrmann, C. Broßmer, T. Priermeier and K. Öfele, *J. Organomet. Chem.,* 1994, **481**, 97.
[51] C. Zhang, J. Huang, M. L. Trudell and S.P. Nolan, *J. Org. Chem.,* 1999, **64**, 3804.
[52] K. Arentsen, S. Caddick and F. G. N. Cloke, *Tetrahedron,* 2005, **61**, 9710.
[53] M.Scholl, S. Ding, C. W. Lee and R. H. Grubbs, *Org. Lett.,* 1999, **1**, 953.
[54] Ö. Aksin, H. Türkmen, L. Artok, B. Çetinkaya, C. Ni, O. Büyükgüngör, E. Özkal, *J. Organomet. Chem.,* 2006, **691**, 3027.

Tailoring of the already existing pyrid- and quinolylidene complexes, especially by increasing steric bulk and replacing the aromatic phosphines with aliphatic or more sterically hindered ones, could increase their activity even further.

5.3.3 Results and discussion for the preliminary catalytic investigation

The catalyst precursors, shown in Scheme 5.7 (preparation and characterisation discussed earlier in this chapter and in Chapter 3), were tested for their activity in standard S-M reactions and the results obtained are collected in Table 5.9. The respective complexes were not screened against a benchmark, since it is known that complexes **1** and **3** are active in S-M reactions and Heck-type coupling[55] and we only wanted to compare the respective relative activities. It is worth noting that the counterion in these complexes is triflate, where the previously reported examples contained BF_4^-. Although there is little evidence that the counterion plays a significant role in the activity of catalyst, it has been illustrated that the nature of the counterion of the complexes (NHC)ML (M = Au, Cu) has a significant effect on the overall yield and regioselectivity of insertion reactions.[56] It is remarkable that complexes of the pyridylidene type are highly active and selective in both S-M and M-H couplings, as the standard mixed imidazole-2-ylidenes (C4 and C5 bonded imidazolylidene ligands) described earlier, are known rather for their good performance in Suzuki reactions and comparative lack of activity in Heck conversions.[57] Since these carbene ligands are unstable when not coordinated, these results would seem to suggest that a strong association with palladium during the catalytic process is essential. This also explains why no palladium black is formed during the processes that have been studied. Even if soluble Pd(0) colloids are formed, the ligands still maintain their all important individual steering and activating function in subsequent steps.[58]

[55] S. K. Schneider, P. Roembke, G. R. Julius, H. G. Raubenheimer and W. A. Hermann, *Adv. Synth. Catal.,* 2006, **348**, 1862
[56] M. R. Fructos, P. de Frémont, S. P. Nolan, M. M. Díaz-Requejo and P. J. Pérez, *Organometallics,* 2006, **25**, 2237.
[57] W. A. Herrmann, V. P. W. Böhm, C. W. K. Gstöttmayr, M. Grosche, C.-P. Reisinger and T. Weskamp, *J. Organomet. Chem.,* 2001, **617-618**, 616.
[58] J.G. de Vries, *Dalton Trans.,* 2006, 421.

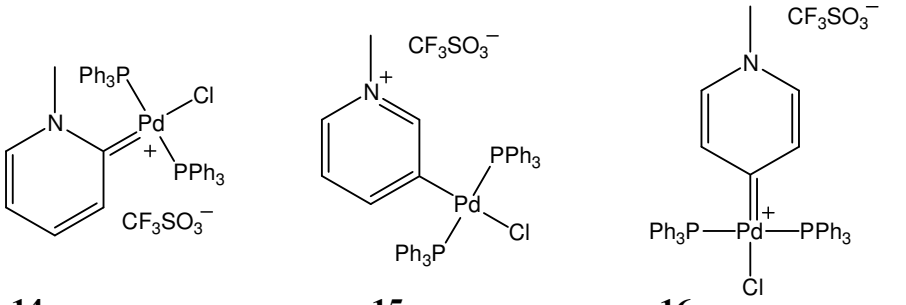

14a **15a** **16a**

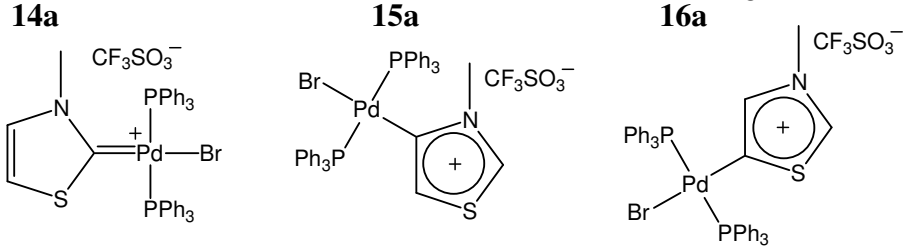

48a **49a** **50**

Scheme 5.7

To obtain a good comparison, we used standard conditions, simple substrates and activated compounds. As shown in Table 5.9, a procedure employing the various pre-catalysts in Scheme 5.7, phenyl boronic acid and bromo acetophenone as substrates, potassium carbonate as the base and DMAc as the solvent, was effective in C-C coupling.

Table 5.9 Catalytic results for S-M coupling of phenyl boronic acid and bromo acetophenone

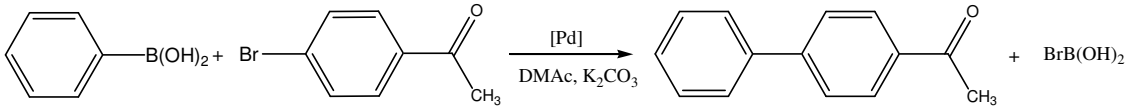

Entry*	Catalyst$	Conditions	Time [h]	Conversion [%]#
1	**14a**	130°, Air	24	86.4
2	**16a**	130°, Air	24	82.4
3	**15a**	130°, Air	25	77.8
4	**50**	130°, Air	25	78.2
5	**49a**	130°, Air	24	81.7
6	**48a**	130°, Air	24	81.4
7	**16a**	130°, Inert	24	92.8
8	**16a**	70°, Air	24	62.3
9	$Pd(PPh_3)_4$	70°, Air	24	68.9
10	$Pd(PPh_3)_4$	130°, Air	24	70.9

*Ratio of aryl halide/phenylboronic acid/base = 2:3:4, Base is K_2CO_3; # ^{1}H-NMR yield using diethyleneglycol-di-*n*-butylether as internal standard; $catalyst loading 0.1 mol %

Under the reported conditions and with relatively low catalyst loading (0.1 mol %), all the catalysts show activity. It is highly likely that the reactions performed in the air may have colloidal Pd involved in the catalysis, although no Pd-black could be observed. Also, no significant induction periods were observed indicating that nanoparticles might not be responsible for catalysis.[10] When open to air, $Ph_3P=O$ may form and subsequently quench the conversions. The conversions are between 62.3 and 92.8 % effective, with the *r*NHC pyridylidene complex, **16a**, showing the highest conversion in an inert environment. For the pyridine derived complexes, somewhat decreased effectivity is observed in the sequence *r* > *a* > *n*. There is little variation in conversion among the different thiazole derived complexes but effectivity decreased somewhat in the series *a* (N next to carbon donor) > *n* > *a* (S next to carbon donor). In general, these conversions all failed to proceed to completion and produced moderate to good yields. $Pd(PPh_3)_4$ performed the worst under the same conditions.

Some screening of the catalyst activity was done by testing complex **14a** in the presence of either K_2CO_3 or Cs_2CO_3 as the base and with or without $[Bu_4N]Br$. The temperature was also lowered to 70 °C and the catalysis was performed under inert conditions to avoid possible Pd-black formation. The rest of the conditions were unchanged. Throughout the reactions, samples of the reaction mixture were removed and analysed by ^1H NMR. The data compiled in Table 5.10 is further extended in Figure 5.6.

Table 5.10 Effect of tetra-alkylammonium salt, $[Bu_4N]Br$, and different bases on Suzuki-Miyaura coupling utilising catalyst **14a** under inert conditions

Entry*	Base	$[Bu_4N]Br$ (0.4 mmol)	Conversion [%]#
1	K_2CO_3	No	61.5
2	K_2CO_3	Yes	72.7
3	Cs_2CO_3	No	79.0
4	Cs_2CO_3	Yes	86.3

*Ratio of aryl halide/phenylboronic acid/base = 2:3:4,; All reactions were performed at 70 °C and under inert conditions; #After 24 hours

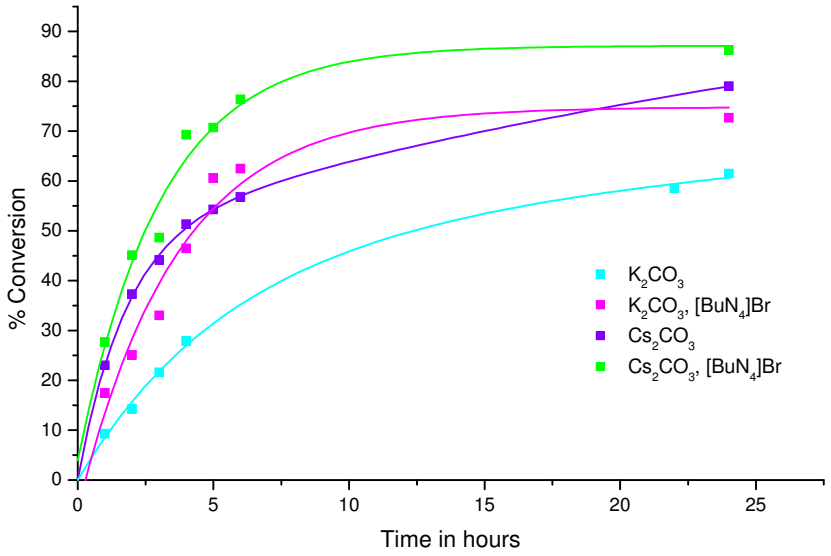

Figure 5.6 Time conversion curves for catalyst **14a** to show the effect of Cs *vs.* K containing carbonate base and $[Bu_4N]Br$

No induction period is observed from the curves, thus indicating a quick formation of the catalytically active Pd species. The lower temperature compared to the initial runs presumably slows the decomposition, although it also lowers the conversion (as also seen for the runs reported in Table 5.9) over the course of the procedure. The beneficial effect of Cs_2CO_3 used in combination with the ammonium salt $[Bu_4N]Br$ on the efficiency of the catalyst precursor **14a** is clearly shown in Table 5.9 and Figure 5.5. It is important to notice that the addition of a co-catalyst *eg*. $[Bu_4N]Br$ does not always improve catalytic results.[59] The lower solubility of sodium carbonate in DMAc compared to ceasium carbonate might be responsible for longer reaction times with this base.

The various pre-catalysts shown in Scheme 5.7 were used again with the better-optimised system under inert conditions. The results are depicted in Table 5.11 and the new time conversion curves are shown in Figure 5.7.

[59] M. A. Taige, A. Zeller, S. Ahrens, S. Goutal, E. Herdtweck and T. Strassner, *J. Organomet. Chem.,* 2007, **692**, 1519.

Table 5.11 Catalytic results after 24 hours for S-M coupling reactions with Cs_2CO_3 as base and $[Bu_4N]Br$ as co-catalyst with various pre-catalysts

Entry*	Catalyst	Conversion [%]
1	**14a**	86.3
2	**15a**	91.4
3	**16a**	98.7
4	$Pd(PPh_3)_4$	75.1
5	**14a** (Air)	78.9
6	**50**	65.3
7	**49a**	72.4
8	**48a**	82.5

*Ratio of aryl halide/phenylboronic acid/base = 2:3:4, All reactions were performed at 70 °C and under inert conditions except entry 5.

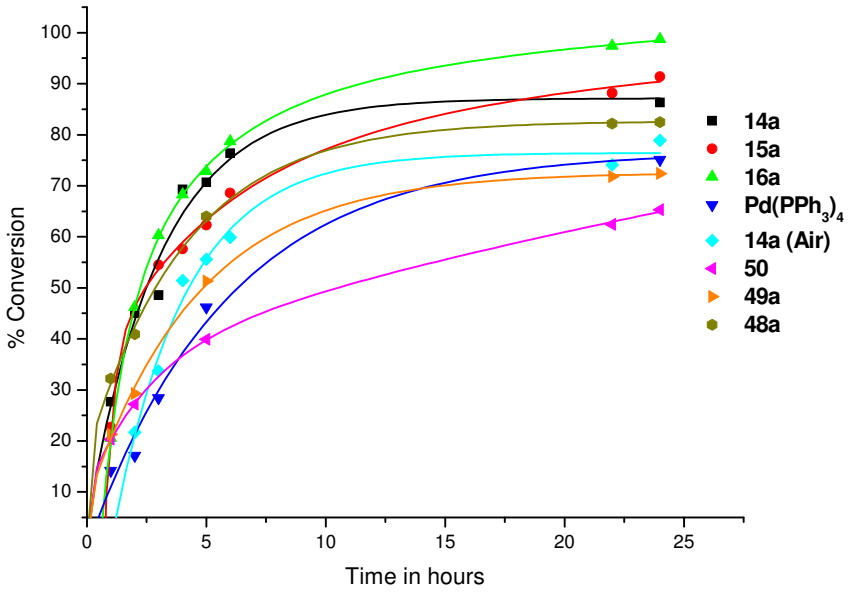

Figure 5.7 Time conversion curves for various pre-catalysts in Scheme 5.7 using Cs_2CO_3 and $[NBu_4]Br$.

From the above data it is clear that the pyridine derived carbene complexes are superior to the thiazole ones and $Pd(PPh_3)_4$ as they show higher conversions after the same time period. This was also found for the reactions performed in air using K_2CO_3 as a base.

Importantly, a decreased activity is again observed in the sequence $r > a > n$ for the N^1HC^6 complexes, whereas the $n N^2HC^5$ precatalysts show higher activity than their *abnormal* carbene counterparts.

5.3.4 Utilisation of a *r*NHC[6] ligand in S-M coupling reactions with hindered substrates

Recent work by Buchwald *et al.* on Pd-catalysed S-M reactions has been directed toward the development of new catalyst systems that efficiently process challenging substrates such as aryl chlorides and hindered aryl boronic acids while still using relatively mild reaction conditions and low catalyst loadings. Success with substrates which are even slightly more hindered or functionalised seldom translates to similar levels of activity.[60]

The catalyst system consisting of $Pd(OAc)_2$, dicyclohexyl-(2',6'-dimethoxy-biphenyl-2-yl)phosphine and K_3PO_4 in toluene was successfully used to catalyse the S-M cross-coupling of unactivated and sterically unactivated aryl chlorides, and sterically hindered boronic acids (*e.g.* 97% conversion at 100°C after 20 hours with 0.02% catalyst loading).[61]

We tested the *r*NHC[6] palladium complex, **28a** (Chapter 3, Section 3.2.8) in similar reactions and compare the activity to that of the well-known *trans*-chloro[(1,3-dimethyl-imidazol-2-ylidene)triphenylphosphine] palladium(II) triflate (N^2HC^5) under inert conditions. The results obtained are summarised in Table 5.12.

Conversions were generally lower in toluene than in THF (entries 5 and 6 *vs*. 3 and 4). Most conversions were efficient at 65 ºC. Under these (0.1 mol % at 65 °C and 0.01 mol % at 130 °C) specific reaction conditions, the classic *trans*-chloro[(1,3-dimethyl-imidazol-2-ylidene)triphenylphosphine] palladium(II) triflate complex outperforms the *r*NHC[6] pre-catalyst.

[60] R. Hoogenboom, M. A. R. Meier and U. S. Schubert, *J. Chem. Educ.,* 2005, **82**, 1693.
[61] S. D. Walker, T. E. Barder, J. R. Martinelli and S. L. Buchwald, *Angew. Chem. Int. Ed.,* 2004, **43**, 1871.

Table 5.12 S-M coupling of an aryl halide and standard boronic acid for a comparison of complex **26a** and a standard N^2HC^5 complex

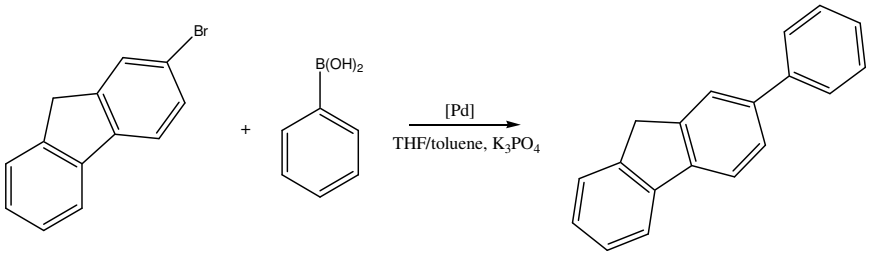

Entry	Pre-catalyst	[mol%]	Conditions	Conversion (%)
1	**28a**	0.01	22 °C, 19h	20
2	**28a**	0.1	22 °C, 19h	33
3	**28a**	0.01	65 °C, 19h	57
4	**28a**	0.1	65 °C, 19h	82
5	**28a**[a]	0.01	65 °C, 19h	45
6	**28a**[a]	0.1	65 °C, 19h	51
7	**28a**	0.01	130 °C, 19h	93
8	**28a**	0.1	130 °C, 19h	93
9	**N^2HC^5**	0.01	65 °C, 19h	88
10	**N^2HC^5**	0.1	65 °C, 19h	100
11	**N^2HC^5**	0.01	130 °C, 19h	100

Ratio of aryl halide/phenylboronic acid/base = 2:3:4; [a]toluene/THF

We were able to achieve S-M couplings of more than 98% of sterically hindered unactivated aryl bromides and sterically hindered boronic acids at lower catalyst concentrations (0.01%) and temperatures (65°C) with the catalysts **28a** within 19 hours (Table 5.13). These are comparable to the Buchwald results with the advantage that our air-stable pre-catalyst complexes can be easily prepared from commercially available starting materials, whereas the synthesis of the phosphine ligand used by Buchwald and co-workers is far more complicated.

Table 5.13 S-M coupling of sterically hindered aryl halide and standard boronic acid using complex **28a**

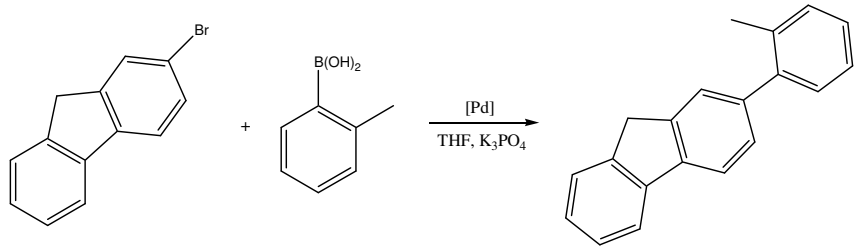

Entry	[mol%]	Conditions	Conversion (%)
1	0.01	65 °C, 19h	> 99
2	0.1	65 °C, 19h	> 99

Ratio of aryl halide/phenylboronic acid/base = 2:3:4

The *r*NHC pre-catalyst (**28a**) was also tested for the S-M coupling of sterically hindered substrates against the standard NHC carbene pre-catalyst, *trans*-chloro[(1,3-dimethyl-imidazol-2-ylidene)triphenylphosphine] palladium(II) triflate (Table 5.14). In this instance the *r*NHC[6] showed a slightly better performance than the classical *n*N^{2}HC[5]. The performance is comparable to previously reported results.[61]

Table 5.14 S-M coupling of sterically hindered substrates

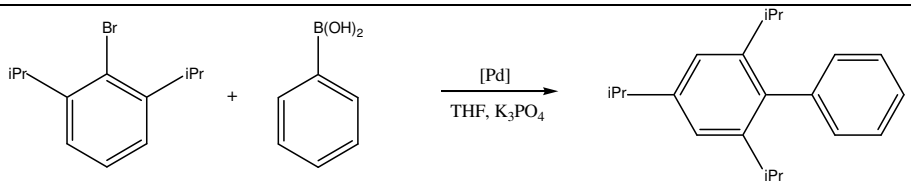

Entry	Pre-catalyst	[mol%]	Conditions	Conversion (%)
1	**28a**	0.01	130 °C, 19h	81
2	**N^{2}HC^5**	0.01	130 °C, 19h	79

Reaction conditions: Ratio of aryl halide/phenylboronic acid/base = 2:3:4

Only the desired biaryl products were formed in all the above-mentioned C-C coupling reactions.

5.4 Conclusions

A series of *normal* and *abnormal* thiazolylidene complexes of nickel and palladium were prepared and unambiguously characterised.

All these complexes as well as members of previously prepared pyridylidene complexes showed activity. An *r*NHC pyridylidene complex was the most active with the activity decreasing in the sequence $r > a > n$. Little variation was observed in conversion amongst the different thiazole derived complexes, with decreased activity in the series *a* (N next to carbon donor) > *n* > *a* (S next to carbon donor).

A beneficial effect is observed when Cs_2CO_3 is used in combination with the ammonium salt, $[Bu_4N]Br$. The pyridine derived complexes are superior to the thiazole ones and show higher conversions after the same time period.

The *r*NHC complex, *trans*-chloro(*N*-methyl-1,2,4-trihydro-2-dimethylaminepyrid-4-ylidene)bis(triphenylphosphine)palladium(II) triflate was successful at coupling sterically hindered substrates in S-M reactions and showed comparable activity to a standard NHC carbene pre-catalyst.

These results do not clearly define superiority between *n*, *a* and *r* N^1HC^6 or between NHC^6 with a NR_2 substituent and N^2HC^5 families of complexes. Reaction conditions, reactants, temperature and co-catalysts probably could be deciding factors. In future work, precatalyst tailoring should receive attention.

5.5 Experimental

5.5.1 General

The general techniques described in Section 2.4.1, Chapter 2, were also applied to the work in this chapter. The starting materials 2-bromo-thiazole, 4-bromo-thiazole, 5-bromo-thiazole, $CF_3SO_3CH_3$, $Ni(PPh_3)_4$ and the substrates for the catalytic testing were purchased from either Aldrich or Merck and used without further purification. $Pd(PPh_3)_4$[62] was synthesised using a previously reported protocol.

[62] F. Ozawa, *Synthesis of Organometallic Compounds,* Ed. S. Komiya, John Wiley & Sons, Chichester, 1997, p. 286.

5.5.2 Synthetic procedures and physical data

5.5.2.1 The synthesis of *N*-methyl-2-bromothiazolium triflate, 45

Methyl triflate (4.43 g, 3.05 ml, 27.0 mmol) was added drop-wise to 2-bromothiazole (4.02 g, 24.5 mmol) in 20 ml of CH_2Cl_2 and stirred at room temperature for 17 hours. The solvent was removed *via* a cannula and the resulting off-white precipitate was washed with THF (1 x 10 ml) and ether (2 x 10 ml) to yield 7.96 g (24. 3 mmol) of compound **45**.

Table 5.15 Physical data of compound **45**

Yield		99.0 %
Colour		Off-white
Melting point		240.6 – 242.9 °C
Elemental analysis	% calculated	C 18.30, H 1.54, N 4.27
$C_5H_5NO_3S_2BrF_3$	% found	C 17.23, H 1.42, N 4.13

5.5.2.2 The synthesis of *N*-methyl-4-bromothiazolium triflate, 46

The same procedure was followed as described for **45** with 0.677 g (4.13 mmol) 4-bromothiazole and 0.745 g (0.514 ml, 4.54 mmol) methyl triflate to yield 1.30 g (3.96 mmol) of **46**.

Table 5.16 Physical data of compound **46**

Yield		95.9 %
Colour		White
Melting point		145.3 – 147.7 °C
Elemental analysis	% calculated	C 18.30, H 1.54, N 4.27
$C_5H_5NO_3S_2BrF_3$	% found	C 17.92, H 1.80, N 4.35

5.5.2.3 The synthesis of *N*-methyl-5-bromothiazolium triflate, 47

The same method was utilised as for **45** with 0.585 g (3.57 mmol) 5-bromothiazole and 0.644 g (0.44 ml, 3.92 mmol) methyl triflate to yield 1.14 g (3.47 mmol) of **47**.

Table 5.17 Physical data of compound **47**

Yield		97.3 %
Colour		Slightly off-white
Melting point		78.1 – 82.2 °C
Elemental analysis	% calculated	C 18.30, H 1.54, N 4.27
$C_5H_5NO_3S_2BrF_3$	% found	C 18.81, H 1.67, N 4.11

5.5.2.4 The synthesis of *trans*-bromo(*N*-methyl-2,3-dihydro-thiazol-2-ylidene)bis(triphenylphosphine)palladium(II) triflate, 48a

Complex **48a** was synthesised in THF at room temperature from 0.219 g (0.669 mmol) **45** and 0.781 g (0.676 mmol) $Pd(PPh_3)_4$ by stirring the mixture for 16 hours. Work-up was performed as described for complex **14b** (Chapter 3). The resulting product had a pinkish colour which was removed by crystallising the product from CH_2Cl_2 layered with pentane at -20 °C to yield 0.050 g (0.052 mmol) of complex **48a**. The use of toluene as solvent and heating the mixture resulted in a brown residue which did not contain **48a**.

Table 5.18 Physical data of compound **48a**

Yield		7.8 %
Colour		Off-white
Melting point		225 °C with decomposition
Elemental analysis	% calculated	C 51.34, H 3.68, N 1.46
$C_{41}H_{35}NO_3P_2S_2BrF_3Pd$	% found	C 52.02, H 3.51, N 1.30

5.5.2.5 The synthesis of *trans*-bromo(*N*-methyl-2,3-dihydro-thiazol-2-ylidene)bis(triphenylphosphine)nickel(II) triflate, 48b

A suspension of $Ni(PPh_3)_4$ (0.667 g, 0.602 mmol) and **45** (0.195 g, 0.596 mmol) in 20 ml THF was stirred for 18 hours at room temperature. The yellow precipitate in a brownish solution was filtered through celite and washed with 2 x 10 ml of toluene and 1 x 5 ml of THF. The product was washed through the filter with CH_2Cl_2 to yield, after solvent evaporation, 0.197 g (0.216 mmol) of complex **48b**.

Table 5.19 Physical data of compound **48b**

Yield		36.3 %
Colour		Mustard yellow
Melting point		150 °C with decomposition
Elemental analysis	% calculated	C 54.03, H 3.87, N 1.54
$C_{41}H_{35}NO_3P_2S_2BrF_3Ni$	% found	C 53.79, H 3.98, N 1.63

5.5.2.6 The synthesis of *trans*-bromo(*N*-methyl-3,4-dihydro-thiazol-4-ylidene)bis(triphenylphosphine)palladium(II) triflate, 49a

Compound **46** (0.105 g, 0.320 mmol) and $Pd(PPh_3)_4$ (0.37 g, 0.320 mmol) were suspended in 20 ml of toluene and stirred at 60 °C for 17 hours. The resulting white suspension in a light yellow solution was filtered over celite and washed with 2 x 5 ml of toluene. The product was washed through the filter with CH_2Cl_2 and the solvent removed under reduced pressure to yield 0.287 g (0.299 mmol) of complex **49a**.

Table 5.20 Physical data of compound **49a**

Yield		93.5 %
Colour		White
Melting point		239 °C with decomposition
Elemental analysis	% calculated	C 51.34, H 3.68, N 1.46
$C_{41}H_{35}NO_3P_2S_2BrF_3Pd$	% found	C 51.02, H 3.71, N 1.54

5.5.2.7 The synthesis of *trans*-bromo(*N*-methyl-3,4-dihydro-thiazol-4-ylidene)bis(triphenylphosphine)nickel(II) triflate, 49b

Complex **49b** (0.207 g, 0.227 mmol) was obtained in a similar fashion as complex **14b** (Chapter 3) from **46** (0.162 g, 0.495 mmol) and $Ni(PPh_3)_4$ (0.576 g, 0.520 mmol).

Table 5.21 Physical data of compound **49b**

Yield		45.9 %
Colour		White
Melting point		172 °C with decomposition
Elemental analysis	% calculated	C 54.03, H 3.87, N 1.54
$C_{41}H_{35}NO_3P_2S_2BrF_3Ni$	% found	C 52.88, H 3.98, N 1.71

5.5.2.8 The synthesis of *trans*-bromo(*N*-methyl-3,5-dihydro-thiazol-5-ylidene)bis(triphenylphosphine)palladium(II) triflate, 50

The same procedure was followed as described for the synthesis of complex **49a** with 0.054 g (0.165 mmol) of **46** and 0.191 g (0.165 mmol) of $Pd(PPh_3)_4$ to produce 0.138 g (0.144 mmol) of complex **50**.

Table 5.22 Physical data of compound **50**

Yield		87.2 %
Colour		Slightly off-white
Melting point		189 °C with decomposition
Elemental analysis	% calculated	C 51.34, H 3.68, N 1.46
$C_{41}H_{35}NO_3P_2S_2BrF_3Pd$	% found	C 51.98, H 3.52, N 1.53

5.5.3 Representative Procedure for the Suzuki-Miyaura coupling[63]

Phenylboronic acid (3 mmol, 0.3658 g), bromo acetophenone (2 mmol, 0.3981 g), potassium carbonate/cesium carbonate (4 mmol, 0.5528/1.303 g), diethyleneglycol-di-*n*-butylether (2 mmol, 0.4367 g, 0.5 ml) and dimethylacetamide (5 ml) were placed in a 25 ml two-neck round bottom flask. The flask was equipped with a reflux condenser and a septum and placed into an oil bath pre-heated to 130°C. The catalyst solution was added after thermostating for 5 min. Aliquots (0.2 ml) were removed at regular intervals from the reaction mixture and added to 5ml of CH_2Cl_2. The organic layer was washed with 3 x 5 ml of water, dried over $MgSO_4$ and filtered. The solvent was removed *in vacuo* and the residue was analysed by ^1H NMR spectroscopy.

For inert conditions, the dry chemicals were placed in a three-neck round bottom flask (equipped with a reflux condenser) that was evacuated and flushed with N_2. Degassed dimethylacetamide and diethyleneglycol-di-*n*-butylether were added under a positive stream of N_2. The condenser and the open neck on the round bottom flask were equipped with septa. The nitrogen atmosphere was maintained by a balloon filled with nitrogen that was connected through the septa on the condenser *via* a needle. The catalyst solution was added after thermostating for 5 min. Work up was performed as described for open air reactions.

[63] The Suzuki-Miyaura reactions for the hindered substrates were executed by Xia Sheng as part of her BSc Honours project with the pre-catalyst, **26a**, synthesised by the author.

5.5.4 X-ray structure determinations

Data associated with the crystal structures of complexes **48b**, **49a** and **50** is summarised in Table 5.19. Data sets were collected and processed as described in Section 2.4.3. The structures were solved by direct methods (**49a** and **50**) or through the interpretation of Patterson synthesis (**48b**) and conventional Fourier methods. The positions of the hydrogen atoms were calculated by assuming ideal geometry and their coordinates were refined together with those of the attached carbon atoms as a "riding model" for all the complexes. The counter ion, $CF_3SO_3^-$, of complex **48b** could not be modelled since it was spinning around its axis. It was removed using the Squeeze routine in the Platon programme package.[64] Additional information regarding these crystal structures is available from Prof H. G. Raubenheimer, Department of Chemistry and Polymer Science, University of Stellenbosch.

[64] A. L. Apek, *J. Appl. Crystallogr.,* 2003, **36**, 7.

Table 5.19 Crystal data and structure refinement parameters of complexes **48b**, **49a** and **50**

Complex	**48b·CH_2Cl_2**	**49a**[*]	**50**
Empirical formula	$C_{41}H_{37}NP_2SBrCl_2Ni$	-	$C_{42}H_{37}NP_2S_2O_3F_3BrCl_2Pd$
Formula weight / g.mol^{-1}	847.24	-	1044.00
Temperature/ K	100(2)	100(2)	100(2)
Crystal colour and habit	yellow plates	white needles	white needles
Space group	$P2_1/c$	$P2_1/n$	Pbca
a / Å	11.486(1)	16.807(2)	18.268(2)
b / Å	20.791(2)	20.895(3)	20.577(2)
c / Å	17.998(2)	22.801(3)	22.679(2)
α / °	90.0	90.0	90.0
β / °	94.595(2)	96.256(3)	90.0
γ / °	90.0	90.0	90.0
V (Å^3)	4284.2(6)	7959.6(19)	8524.8(14)
Z	4	4	8
$D_{calc.}$ / g.cm^{-3}	1.314	1.536	1.627
Adsorption coefficient / mm^{-1}	1.661	1.701	1.725
F(000)	1732	3716	4192
θ (min – max) / °	1.50 – 26.43	1.33 – 26.44	1.74 – 28.27
Reflections collected	25100	45940	52584
Independent reflections	6910	9945	7978
Data/restraints/parameters	8786/0/437	16333/0/844	10282/0/515
Final R indices [$I>2\sigma(I)$]	$R_1 = 0.0566$, $wR_2 = 0.1368$	$R_1 = 0.1408$, $wR_2 = 0.3978$	$R_1 = 0.0617$, $wR_2 = 0.1139$
R indices (all data)	$R_1 = 0.0700$, $wR_2 = 0.1437$	$R_1 = 0.1962$, $wR_2 = 0.4466$	$R_1 = 0.0862$, $wR_2 = 0.1222$
Goodness-of-fit on F^2	1.049	1.561	1.169
Largest peak / e Å^{-3}	2.176	18.372	0.962

[*] could not be determined due to a weak data set; some values omitted due to uncertainty